An Evaluation of HTV-SR Insulators with Different Creepage Lengths under AC and Bipolar DC in Marine Polluted Service Conditions

by

Andreas Iyambo Elombo

Thesis presented in partial fulfilment of the requirements for the degree Master of Science in Engineering at the University of Stellenbosch

Supervisor:

Prof. HJ Vermeulen

Co-supervisor:

Dr. JP Holtzhausen

Faculty of Engineering
Department of Electrical and Electronics Engineering

-March 2012-

Declaration

By submitting this thesis electronically, I declare that the entirety of the work contained therein is my own, original work, that I am the sole author thereof (save to the extent explicitly otherwise stated), that reproduction and publication thereof by Stellenbosch University will not infringe any third party rights and that I have not previously in its entirety or in part submitted it for obtaining any qualification.

March 2012

Abstract

The use of high voltage direct current (HVDC) applications has gained enormous popularity for long distance power transmission. This is due to the lucrative benefits offered by this type of power transmission technology when compared to the traditional high voltage alternative current (HVAC). This new shift in the paradigm of power system design has led to the increased interest in the research that focuses on issues relating to the reliability of power supply associated with HVDC. Amongst such issues, insulation coordination has increasingly become a challenging task that continues to receive renewed research focus. It has been convincingly demonstrated, both from field experience and laboratory research, that insulator contamination constitutes a multifaceted phenomenon, especially when transmission voltages ramp up into high operating voltage levels. More so, this is particularly interesting with reference to the increasing applications of high voltage direct current (HVDC).

The recently commissioned HVDC power-line in Namibia is one of the major motivations upon which NamPower (Namibia's national power utility) has committed financial resources to research on insulator pollution performance. This project was a part of NamPower's research initiative – seeking to investigate the phenomena associated with insulator pollution performance under natural pollution environments when energized under both AC and DC excitation voltage types. The significance of this research is especially crucial for HVDC applications given the paucity of research conducted on the DC performance of insulators, under natural pollution environments.

This study was conducted at the Koeberg Insulator Pollution Test Station (KIPTS) on the west coast of Cape Town in the Western Cape province of South Africa. KIPTS is an internationally recognized insulator pollution test facility, which is widely used by both insulator manufacturers and academic researchers from many parts of the world. STRI and ABB, both Swedish-based companies, are good examples of international subscribers to the KIPTS research facility. The first objective of this research was to design a suitable DC excitation voltage system for both DC+ and DC- to be used at KIPTS. This apparatus was designed and built at the University of Stellenbosch. The second objective was to conduct a comparative evaluation of the performance of high temperature vulcanized silicone rubber (HTV-SR) power line insulators under AC, DC+

and DC- when subjected to natural pollution conditions at KIPTS. All test insulators were made from the same material and sourced from the same manufacturer – having different creepage lengths. Five different creepage lengths were considered for each excitation voltage – summing up to fifteen HTV-SR test samples. A standard DC glass disc insulator was also installed on each excitation voltage as a control sample. It was therefore envisaged that this study would give rise to new research questions, leading to future explorations on the subject.

With reference to weather monitoring and leakage current measurements (using an online leakage current monitoring device - OLCA), a correlation was found to exist between the variations in climatic conditions and the corresponding occurrence of leakage current on the insulator surfaces. High leakage current levels were recorded in summer due to the high pollution levels that were measured in that season (using the equivalent salt deposit density (ESDD) approach). Winter, in contrast, had lower levels of leakage current recorded. This corresponds to a high prevalence of rainfall in winter, which caused occasional natural washing of the insulator surfaces. The leakage current levels for the HTV-SR insulators were of a similar order of magnitude for AC and DC+ and lower for DC-.

The harshest pollutants (with high conductivities, as measured with the directional dust deposit gauges (DDDG)) were found to have emanated largely from the south. As a result, most instances of erosion were observed in the southward direction on the test insulators. The electrical discharge activity observations, conducted at night, had revealed that dryband corona (DBC) and dryband discharge (DBD) prominently occurred on the terminating sheaths (both live and ground ends) and bottom side of HTV-SR and glass disc insulators, respectively. This justifies the dominance of erosion that was observed on the terminating sheaths and bottom side of HTV-SR and glass disc insulators, respectively. Flashover events were recorded on the shortest HTV-SR insulator installed on DC+ and the glass disc insulator installed on DC-. All flashover events occurred in summer (the harshest season at KIPTS). Two interesting observations, albeit unexplained, were observed: *star-shaped erosion on the shed bottoms of the HTV-SR insulators installed on DC+* and *material peel-off at the shed-to-sheath bonding interface of the HTV-SR insulators installed on DC-*. These observations therefore require further investigation in order to establish possible explanations.

Opsomming

Die gebruik van hoë gelykspanning (HSGS) het baie gewild geword vir kragtransmissie oor lang afstande. Dit is as gevolg van die uitstekende voordele wat hierdie tipe tegnologie teenoor die tradisionele hoë wisselspanning (HSWS) bied. Hierdie paradigmaskuif in die ontwerp van kragstelsels het tot verhoogde belangstelling in navorsing gelei wat betrekking het op aspekte wat verband hou met die betroubaarheid van kragvoorsiening deur HSGS. Van hierdie aspekte word isolasiekoördinasie toenemend ŉ uitdagende taak en navorsing word tans daarop toegespits. Daar bestaan oortuigende bewyse, gebaseer op laboratorium- en veldtoetse dat isolatorbesoedeling ŉ verskynsel met vele fasette is, veral wanneer hoër spannings gebruik word. Dit is in ‘n meerdere mate van belang met verwysing na toepassings van HSGS.

Die onlangs inbedryfgestelde HSGS kraglyn in Namibië is een van die hoofmotiverings vir die verskaffing van geldelike steun deur NamPower (Namibië se nasionale kragvoorsiener) vir navorsing oor die besoedelingsprestasie van isolators. Hierdie projek is deel van NamPower se navorsingsinisiatief om verskynsels betreffende die besoedelingsprestasie van isolators in natuurlik-besoedelde omgewings te ondersoek, onder WS en GS-bekragtiging. Die betekenis van hierdie navorsing is veral belangrik vir die HSGS-toepassings in die lig van die skaarsheid van navorsing oor die GS-prestasie van isolators in natuurlik-besoedelde omgewings.

Hierdie studie is gedoen by die Koeberg isolatorbesoedelingstoetsstasie (KIPTS) aan die weskus van die Wes-Kaap. KIPTS is 'n internasionaal-erkende toetsfasiliteit en word algemeen gebruik deur beide isolatorvervaardigers en akademiese navorsers uit baie dele van die wêreld. STRI en ABB, albei Sweeds-gebaseerde maatskappye, is die goeie voorbeelde van die internasionale gebruikers van die KIPTS navorsingsfasiliteit.

Die oogmerk van hierdie navorsing was om eerstens 'n geskikte GS-kragbron vir beide die GS+ en die GS- vir gebruik by KIPTS te ontwerp. Hierdie apparaat is ontwerp en gebou deur die Universiteit van Stellenbosch. Tweedens is 'n vergelykende evaluering van die prestasie hoë temperatuur gevulkaniseerde silikoon (HTV-SR) kraglynisolators onder WS, GS+ en GS– onder natuurlike besoedeling by die KIPTS uitgevoer. Alle toetsisolators is van dieselfde materiaal gemaak en is afkomstig van dieselfde vervaardiger, maar het verskillende kruipafstande. Vyf verskillende kruipafstande is gebruik vir elke tipe spanning – 'n totaal van vyftien HTV-SR toets

monsters. 'n Standaard GS glasisolatorskyf is ook vir elke spanning as' n kontrolemonster geïnstalleer. Dit kan dus verwag word dat hierdie studie aanleiding sal gee tot nuwe navorsingsvrae, wat kan lei tot verdere toekomstige ondersoeke oor die onderwerp.

Met verwysing na die monitering van die weer en die lekstroommetings (met behulp van 'n aanlyn-lekstroommoniteringstoestel - OLCA), is 'n korrelasie gevind tussen die variasie in klimaatstoestande en die ooreenstemmende voorkoms van lekstroom op die isolator-oppervlaktes. Hoë lekstroomvlakke is waargeneem in die somer, as gevolg van die hoë besoedelingsvlakke wat in daardie seisoen gemeet is (met behulp van die ekwivalente soutneerslag-digtheid (ESDD) metode). In die winter, in teenstelling, is die laagste vlakke van lekstroom aangeteken. Dit stem ooreen met 'n hoë voorkoms van reënval in die winter, wat die isolatoroppervlaktes van tyd tot tyd natuurlik gewas het. Die lekstroomvlakke op die HTV-SR isolators was van soortgelyke ordegrootte vir WS en GS+ maar laer vir GS-.

Dit is bevind dat die ergste besoedelingstowwe, met 'n hoë geleiding, soos gemeet met die rigtingsensitiewe stofneerslagsmeters (DDDG), hoofsaaklik uit ’n suidelike rigting kom. As gevolg hiervan, is die meeste gevalle van erosie aan die suidekant van die toetsisolators waargeneem. Die waarneming van elektriese ontladingsaktiwiteit in die nag, het aan die lig gebring dat droëbandkorona (DBC) en droëbandontladings (DBD) prominent voorgekom het op die skedes aan die uiteindes (beide lewende en grond kante) en onderste kant van HTV-SR en glasskywe, onderskeidelik.

Oorvonkings is waargeneem op die kortste HTV-SR isolator op GS+ en op die glasisolator op GS-. Al die oorvonkings het in die somer (die ergste seisoen by KIPTS) voorgekom. Twee interessante, dog onverklaarbare, verskynsels is waargeneem: *stervormige erosie aan die onderkante van die skerms van die HTV-SR isolators op GS+ en material-afskilfering by die skerm-skede tussenvlak van die HTV-SR isolators op GS-*. Hierdie verskynsels vereis verdere ondersoek ten einde moontlike verklarings vas te stel.

Table of Contents

Declaration .... **i**
Abstract .... **ii**
Opsomming .... **iv**
Table of Contents .... **vi**
List of Figures .... **xviii**
List of Tables .... **xxvi**
Nomenclature .... **xxx**
Acknowledgements .... **xxxi**
1. Chapter 1: Introduction **1**
1.1 Overview 1
1.1.1 Interconnection of HVAC power networks *3*
1.1.2 Power transfer over long distances *4*
1.1.3 Economic considerations *4*
1.1.4 Environmental considerations *5*
1.1.5 Demerits of HVDC *6*
1.2 Project motivation 7
1.3 Project description 9
1.3.1 Introduction *9*
1.3.2 Research objectives *10*
1.4 Thesis outline 12
2. CHAPTER 2: Literature review **14**
2.1 Overview 14
2.2 The Role of Insulators in a Power System 14
2.3 Characteristics of Insulators 19
2.3.1 Insulator types *19*
2.3.2 Common insulator materials *20*
2.3.2.1 Introduction *20*
2.3.2.2 Porcelain *21*
2.3.2.3 Glass *21*
2.3.2.4 Resins *21*
2.3.2.5 Composite polymers *22*
2.3.3 Physical design parameters *23*
2.3.3.1 Introduction *23*
2.3.3.2 Arcing distance *23*
2.3.3.3 Creepage distance *23*
2.3.3.4 Connecting length *24*

2.3.3.5 *Puncture distance*......24

2.4 Environmental and Climatic Effects on Insulator Performance...... 25

2.4.1 *Overview* 25

2.4.2 *Pollution*...... 25

2.4.3 *Humidity and Rain* 26

2.4.4 *Solar radiation* 26

2.4.5 *Wind speed and direction*...... 27

2.4.6 *Bird droppings and streamers*...... 27

2.4.7 *Physical damage and human vandalism* 28

2.5 Indicators of Insulator Failures 28

2.5.1 *Introductory remarks* 28

2.5.2 *Porcelain insulators*...... 30

2.5.3 *Glass insulators* 30

2.5.4 *Resin insulators*...... 30

2.5.5 *Polymeric insulators* 30

2.6 Basic theory on Insulator Pollution Flashover 31

2.6.1 *Introductory remarks* 31

2.6.2 *Pollution flashover process*...... 32

2.6.3 *Important aspects for insulator pollution studies* 34

2.6.4 *Prediction of insulator pollution flashover*...... 36

3. CHAPTER 3: Design and choice of test apparatus 38

3.1 Overview 38

3.2 The Koeberg Insulator Pollution Test Station (KIPTS)...... 38

3.2.1 *Introduction*...... 38

3.2.2 *Details on KIPTS* 39

3.2.3 *Excitation voltage system: AC, DC+ and DC-* 42

3.3 Test insulator samples 44

3.4 Video camera equipment...... 47

3.4.1 *Introduction*...... 47

3.4.2 *Corocam Mark I*...... 47

3.4.3 *0-lux Sony camcorder* 49

3.5 Data logging system 50

3.6 Current sensor calibrations...... 54

3.6.1 *Introduction*...... 54

3.6.2 *AC sensors* 55

3.6.3 *DC sensors*...... 56

4. Chapter 4: Research procedures and methodology 59

4.1 Overview on insulator monitoring procedures...... 59

4.1.1.1 *Climatic and environmental conditions* 62

4.1.1.2 *Leakage current data* 62

4.1.1.3 *Electrical discharge activity observations* 62

4.1.1.4 *Surface condition inspections* 62

4.2 Environmental and climatic condition monitoring.. 62
4.2.1 Overview 62
4.2.2 What is the pollution severity at KIPTS? 63
4.2.2.1 Introduction.. 63
4.2.2.2 Equivalent salt deposit density (ESDD) 63
4.2.2.3 Non-soluble deposit density (NSDD) 65
4.2.2.4 Directional dust deposit gauge (DDDG) 66
4.2.2.5 Pollution severity classification 67
4.2.3 What combination of climatic conditions plays a determining role in the insulator pollution process at KIPTS? 68
4.3 Leakage current monitoring 69
4.3.1 Introduction.. 69
4.3.2 Positive and negative peak leakage currents 70
4.3.3 Absolute peak leakage current 70
4.3.4 Accumulative coulomb-ampere 70
4.4 Night observations: Electrical discharge activities 71
4.5 Daytime observations: Insulator surface conditions 73
5. CHAPTER 5: Results and interpretations 76
5.1 Overview 76
5.2 Results for the climatic and environmental conditions at KIPTS 77
5.2.1 Climatic conditions 77
5.2.1.1 Introduction.. 77
5.2.1.2 Rainfall.. 78
5.2.1.3 Relative humidity.. 79
5.2.1.4 Ambient and dewpoint temperatures.. 81
5.2.1.5 Wind speed and direction.. 84
5.2.1.6 UV-B radiation.. 87
5.2.2 Environmental considerations: site pollution severity results 89
5.2.2.1 Introduction.. 89
5.2.2.2 Equivalent salt deposit density (ESDD) 89
5.2.2.3 Non-soluble deposit density (NSDD) 92
5.2.2.4 Directional dust deposit gauge (DDDG) 93
5.3 Leakage current performance... 96
5.3.1 Overview 96
5.3.2 Results for individual test insulators... 97
5.3.2.1 Introduction.. 97
5.3.2.2 Leakage current performance for the HTV-SR 84 insulators 101
5.3.2.3 Leakage current performance for the HTV-SR 72 insulators 104
5.3.2.4 Leakage current performance for the HTV-SR 56 insulators 107

5.3.2.5 *Leakage current performance for the HTV-SR 44 insulators* 110
5.3.2.6 *Leakage current performance for the HTV-SR 29 insulators* 113
5.3.2.7 *Leakage current performance for the Glass disc 42 insulators* 116
5.3.3 *An overview of the results on accumulative coulomb-ampere* 119
5.3.3.1 *Introduction* 119
5.3.3.2 *AC excitation voltage* 120
5.3.3.3 *DC+ excitation voltage* 121
5.3.3.4 *DC- excitation voltage* 122
5.3.4 *General comments* 123
5.3.4.1 *Introductory remarks* 123
5.3.4.2 *Statistical approach using time of day bin count analysis* 123
5.3.4.3 *Comparisons of leakage current performance for summer and winter periods* 123
5.3.4.4 *Correlation of leakage current performance with climatic conditions* 124
5.3.4.5 *Peak leakage current and flashover events* 125
5.3.4.6 *The optimal creepage length considerations* 125
5.3.4.7 *Accumulative coulomb-ampere* 126
5.4 Electrical discharge activity monitoring results 127
5.4.1 *Overview* 127
5.4.2 *Observations specific to individual insulators* 128
5.4.2.1 *Electrical discharge activities for the HTV-SR 84 insulators* 128
5.4.2.2 *Electrical discharge activities for the HTV-SR 72 insulators* 129
5.4.2.3 *Electrical discharge activities for the HTV-SR 56 insulators* 130
5.4.2.4 *Electrical discharge activities for the HTV-SR 44 insulators* 131
5.4.2.5 *Electrical discharge activities for the HTV-SR 29 insulators* 132
5.4.2.6 *Electrical discharge activities for the Glass disc 42 insulators* 133
5.4.3 *Overall comparisons* 134
5.4.3.1 *General discussions* 134
5.4.3.2 *Frequency of occurrence of electrical discharge activities* 135
5.4.3.3 *First occurrence of electrical discharge activities* 138
5.4.3.4 *The relevance of a 0-lux camcorder in electrical discharge observations* 140
5.5 Surface condition inspections: Ageing performance 141
5.5.1 *Overview* 141
5.5.2 *Results for individual test insulators* 142
5.5.2.1 *Surface conditions for the HTV-SR 84 insulators* 142
5.5.2.2 *Surface conditions for the HTV-SR 72 insulators* 145
5.5.2.3 *Surface conditions for the HTV-SR 56 insulators* 148
5.5.2.4 *Surface conditions for the HTV-SR 44 insulators* 150

5.5.2.5 Surface conditions for the HTV-SR 29 insulators 152
5.5.2.1 Surface conditions for the Glass disc 42 insulators 155
5.5.3 Overall comparisons 158
5.5.3.1 Introductory remarks 158
5.5.3.2 Discussion on specific observations 158
5.6 Results on wettability (hydrophobicity) classification tests 163
5.6.1 Overview 163
5.6.2 Wettability classifications for individual insulators 164
5.6.2.1 Introduction 164
5.6.2.2 Wettability classifications for the HTV-SR 84 insulators 166
5.6.2.3 Wettability classifications for the HTV-SR 72 insulators 167
5.6.2.4 Wettability classifications for the HTV-SR 56 insulators 168
5.6.2.5 Wettability classifications for the HTV-SR 44 insulators 169
5.6.2.6 Wettability classifications for the HTV-SR 29 insulators 170
5.6.3 Overall comparisons 171
6. CHAPTER 6: Conclusions and recommendations 172
6.1 Overview 172
6.2 Conclusions 173
6.2.1 Introductory remarks 173
6.2.1.1 Concluding remarks on the climatic and environmental conditions at KIPTS 174
6.2.1.2 Concluding remarks on leakage current performance of test insulators 175
6.2.1.3 Concluding remarks on electrical discharge activity observations 177
6.2.1.4 Concluding remarks on surface condition inspections: ageing performance 178
6.2.1.5 Concluding remarks on wettability (hydrophobicity) classification tests 180
6.3 Recommendations 181
6.3.1 The use of the energized test insulator for ESDD pollution sampling 181
6.3.2 Statistical approach to leakage current performance analysis 181
6.3.3 A fundamental study on the mechanism of electrical discharge activity developments for DC excitation voltages versus AC excitation voltage 182
6.3.4 The use of corona and arcing mitigation techniques 182
REFERENCES 183
APPENDICES 188
A. APPENDIX A: Samples of record sheets for surface condition inspections, wettability (hydrophobicity) classification tests and electrical discharge activity observations 188
A.1 Surface condition inspection record sheet 188
A.2 Wettability (hydrophobicity) classification sheet 189
A.3 Electrical discharge observation record sheets 190

A.3.1 Corocam Mark I ... 190
A.3.2 0-lux Sony Camcorder ... 190
B. APPENDIX B: The monthly climatic conditions that were recorded at KIPTS during the entire test period ... 191
B.1 Overview ... 191
B.2 Rainfall profile for the first six months of the test period ... 192
B.3 Relative humidity profile for the first six months of the test period ... 193
B.4 Ambient temperature profile for the first six months of the test period ... 194
B.5 Wind speed and direction profiles for the first six months of the test period ... 195
B.5.1 Wind speed profile ... 195
B.5.2 Wind direction profile ... 196
B.5.2.1 Introduction ... 196
B.5.2.2 Conventional compass directions ... 196
B.5.2.3 The actual wind direction profile in degrees ... 197
B.6 UV-B radiation profile for the first six months of the test period ... 198
C. APPENDIX C: Leakage current performance for individual test insulators 199
C.1 Overview ... 199
C.2 Leakage current performance for high temperature vulcanized, silicone rubber insulators with a unified specific creepage length of 84 mm/kV – HTV-SR 84 ... 200
C.2.1 Leakage current bin count analysis ... 200
C.2.1.1 Monthly leakage current bin counts ... 200
C.2.1.2 Total bin counts for the entire test period ... 200
C.2.2 Average and maximum values of the recorded leakage current ... 202
C.3 Leakage current performance for high temperature vulcanized, silicone rubber insulators with a unified specific creepage length of 72 mm/kV – HTV-SR 72 ... 203
C.3.1 Leakage current bin count analysis ... 203
C.3.1.1 Monthly leakage current bin counts ... 203
C.3.1.2 Total bin counts for the entire test period ... 203
C.3.2 Average and maximum values of the recorded leakage current ... 205
C.4 Leakage current performance for high temperature vulcanized, silicone rubber insulators with a unified specific creepage length of 56 mm/kV – HTV-SR 56 ... 206
C.4.1 Leakage current bin count analysis ... 206
C.4.1.1 Monthly leakage current bin counts ... 206
C.4.1.2 Total bin counts for the entire test period ... 206
C.4.1.3 Average and maximum values of the recorded leakage current ... 208
C.5 Leakage current performance for high temperature vulcanized, silicone rubber insulators with a unified specific creepage length of 44 mm/kV – HTV-SR 44 ... 209
C.5.1 Leakage current bin count analysis ... 209
C.5.1.1 Monthly leakage current bin counts ... 209

C.5.1.2 Total bin counts for the entire test period 209

C.5.2 Average and maximum values of the recorded leakage current 211

C.6 Leakage current performance for high temperature vulcanized, silicone rubber insulators with a unified specific creepage length of 29 mm/kV – HTV-SR 29 212

C.6.1 Leakage current bin count analysis 212

C.6.1.1 Monthly leakage current bin counts......212

C.6.1.2 Total bin counts for the entire test period 212

C.6.2 Average and maximum values of the recorded leakage current 214

C.7 Leakage current performance for glass disc insulators with a unified specific creepage length of 42 mm/kV – Glass disc 42 215

C.7.1 Leakage current bin count analysis 215

C.7.1.1 Monthly leakage current bin counts......215

C.7.1.2 Total bin counts for the entire test period 215

C.7.2 Average and maximum values of the recorded leakage current 217

D. APPENDIX D: Detailed observations of electrical discharge activities for individual test insulators 218

D.1 Overview 218

D.2 Electrical discharge activity observations for high temperature vulcanized, silicone rubber insulators with a unified specific creepage length of 84 mm/kV – HTV-SR 84 219

D.2.1 Corocam Mark I......219

D.2.1.1 Frequency of occurrence 219

D.2.1.2 Locations of electrical discharge activities......220

D.2.2 0-lux Sony Camcorder 221

D.2.2.1 Frequency of occurrence 221

D.2.2.2 Location of electrical discharge activity......222

D.3 Electrical discharge activity observations for high temperature vulcanized, silicone rubber insulators with a unified specific creepage length of 72 mm/kV – HTV-SR 72 223

D.3.1 Corocam Mark I......223

D.3.1.1 Frequency of occurrence 223

D.3.1.2 Location of electrical discharge activity......224

D.3.2 0-lux Sony Camcorder 225

D.3.2.1 Frequency of occurrence 225

D.3.2.2 Location of electrical discharge activity......226

D.4 Electrical discharge activity observations for high temperature vulcanized, silicone rubber insulators with a unified specific creepage length of 56 mm/kV – HTV-SR 56 227

D.4.1 Corocam Mark I......227

D.4.1.1 Frequency of occurrence 227

D.4.1.2 Location of electrical discharge activity......228

D.4.2 0-lux Sony Camcorder 229

D.4.2.1 Frequency of occurrence 229
D.4.2.2 Location of electrical discharge activity 230
D.5 Electrical discharge activity observations for high temperature vulcanized, silicone rubber insulators with a unified specific creepage length of 44 mm/kV – HTV-SR 44 231
D.5.1 Corocam Mark I 231
D.5.1.1 Frequency of occurrence 231
D.5.1.2 Locations of electrical discharge activities 232
D.5.2 0-lux Sony Camcorder 233
D.5.2.1 Frequency of occurrence 233
D.5.2.2 Location of electrical discharge activity 234
D.6 Electrical discharge activity observations for high temperature vulcanized, silicone rubber insulators with a unified specific creepage length of 29 mm/kV – HTV-SR 29 235
D.6.1 Corocam Mark I 235
D.6.1.1 Frequency of occurrence 235
D.6.1.2 Location of electrical discharge activity 236
D.6.2 0-lux Sony Camcorder 237
D.6.2.1 Frequency of occurrence 237
D.6.2.2 Location of electrical discharge activity 238
D.7 Electrical discharge activity observations for glass disc insulators with a unified specific creepage length of 42 mm/kV – Glass disc 42 239
D.7.1 Corocam Mark I 239
D.7.1.1 Frequency of occurrence 239
D.7.1.2 Location of electrical discharge activity 240
D.7.2 0-lux Sony Camcorder 241
D.7.2.1 Frequency of occurrence 241
D.7.2.2 Location of electrical discharge activity 242
E. APPENDIX E: A summary of detailed observations of insulator surface conditions per test cycle 243
E.1 Overview 243
E.2 Surface conditions for high temperature vulcanized, silicone rubber insulators with a unified specific creepage length of 84 mm/kV – HTV-SR 84 244
E.2.1 Test cycle 1 244
E.2.1.1 HTV-SR 84 AC (Week 5) 244
E.2.1.2 HTV-SR 84 DC+ (Week 3) 244
E.2.1.3 HTV-SR 84 DC- (Week 2) 245
E.2.2 Test cycle 2 246
E.2.2.1 HTV-SR 84 AC (Week 9) 246
E.2.2.2 HTV-SR 84 DC+ (Week 8) 247

E.2.2.3 HTV-SR 84 DC- (Week 6) *248*
E.2.3 Test cycle 3 .... *248*
E.2.3.1 HTV-SR 84 AC (Week 13) *248*
E.2.3.2 HTV-SR 84 DC+ (Week 11) *249*
E.2.3.3 HTV-SR 84 DC- (Week 10) *250*
E.2.4 Test cycle 4 .... *251*
E.2.4.1 HTV-SR 84 AC (Week 22) *251*
E.2.4.2 HTV-SR 84 DC+ (Week 18) *252*
E.2.4.3 HTV-SR 84 DC- (Week 16) *253*
E.3 Surface conditions for high temperature vulcanized, silicone rubber insulators with a unified specific creepage length of 72 mm/kV – HTV-SR 72 255
E.3.1 Test cycle 1 .... *255*
E.3.1.1 HTV-SR 72 AC (Week 5) *255*
E.3.1.2 HTV-SR 72 DC+ (Week 3) *255*
E.3.1.3 HTV-SR 72 DC- (Week 2) *256*
E.3.2 Test cycle 2 .... *256*
E.3.2.1 HTV-SR 72 AC (Week 9) *256*
E.3.2.2 HTV-SR 72 DC+ (Week 8) *257*
E.3.2.3 HTV-SR 72 DC- (Week 6) *258*
E.3.3 Test cycle 3 .... *259*
E.3.3.1 HTV-SR 72 AC (Week 13) *259*
E.3.3.2 HTV-SR 72 DC+ (Week 11) *260*
E.3.3.3 HTV-SR 72 DC- (Week 10) *261*
E.3.4 Test cycle 4 .... *262*
E.3.4.1 HTV-SR 72 AC (Week 22) *262*
E.3.4.2 HTV-SR 72 DC+ (Week 18) *264*
E.3.4.3 HTV-SR 72 DC- (Week 16) *265*
E.4 Surface conditions for high temperature vulcanized, silicone rubber insulators with a unified specific creepage length of 56 mm/kV – HTV-SR 56 266
E.4.1 Test cycle 1 .... *266*
E.4.1.1 HTV-SR 56 AC (Week 5) *266*
E.4.1.2 HTV-SR 56 DC+ (Week 3) *267*
E.4.1.3 HTV-SR 56 DC- (Week 2) *267*
E.4.2 Test cycle 2 .... *267*
E.4.2.1 HTV-SR 56 AC (Week 9) *267*
E.4.2.2 HTV-SR 56 DC+ (Week 8) *268*
E.4.2.3 HTV-SR 56 DC- (Week 6) *269*

E.4.3 Test cycle 3 .... *269*
E.4.3.1 HTV-SR 56 AC (Week 13) *269*
E.4.3.2 HTV-SR 56 DC+ (Week 11) *270*
E.4.3.3 HTV-SR 56 DC- (Week 10) *271*
E.4.4 Test cycle 4 .... *272*
E.4.4.1 HTV-SR 56 AC (Week 22) *272*
E.4.4.2 HTV-SR 56 DC+ (Week 18) *273*
E.4.4.3 HTV-SR 56 DC- (Week 16) *274*
E.5 Surface conditions for high temperature vulcanized, silicone rubber insulators with a unified specific creepage length of 44 mm/kV – HTV-SR 44 276
E.5.1 Test cycle 1 .... *276*
E.5.1.1 HTV-SR 44 AC (Week 5) *276*
E.5.1.2 HTV-SR 44 DC+ (Week 3) *277*
E.5.1.3 HTV-SR 44 DC- (Week 2) *277*
E.5.2 Test cycle 2 .... *277*
E.5.2.1 HTV-SR 44 AC (Week 9) *277*
E.5.2.2 HTV-SR 44 DC+ (Week 8) *278*
E.5.2.3 HTV-SR 44 DC- (Week 6) *278*
E.5.3 Test cycle 3 .... *279*
E.5.3.1 HTV-SR 44 AC (Week 13) *279*
E.5.3.2 HTV-SR 44 DC+ (Week 11) *280*
E.5.3.3 HTV-SR 44 DC- (Week 10) *280*
E.5.4 Test cycle 4 .... *281*
E.5.4.1 HTV-SR 44 AC (Week 22) *281*
E.5.4.2 HTV-SR 44 DC+ (Week 18) *282*
E.5.4.3 HTV-SR 44 DC- (Week 16) *283*
E.6 Surface conditions for high temperature vulcanized, silicone rubber insulators with a unified specific creepage length of 29 mm/kV – HTV-SR 29 285
E.6.1 Test cycle 1 .... *285*
E.6.1.1 HTV-SR 29 AC (Week 5) *285*
E.6.1.2 HTV-SR 29 DC+ (Week 3) *285*
E.6.1.3 HTV-SR 29 DC- (Week 2) *286*
E.6.2 Test cycle 2 .... *286*
E.6.2.1 HTV-SR 29 AC (Week 9) *286*
E.6.2.2 HTV-SR 29 DC+ (Week 8) *286*
E.6.2.3 HTV-SR 29 DC- (Week 6) *287*
E.6.3 Test cycle 3 .... *288*
E.6.3.1 HTV-SR 29 AC (Week 13) *288*

E.6.3.2 HTV-SR 29 DC+ (Week 11)...288
E.6.3.3 HTV-SR 29 DC- (Week 10)...289
E.6.4 Test cycle 4...289
E.6.4.1 HTV-SR 29 AC (Week 22)...289
E.6.4.2 HTV-SR 29 DC+ (Week 18)...290
E.6.4.3 HTV-SR 29 DC- (Week 16)...291
E.7 Surface conditions for glass disc insulators with a unified specific creepage length of 42 mm/kV – Glass disc 42 ... 292
E.7.1 Test cycle 1...292
E.7.1.1 Glass disc 42 AC (Week 5)...292
E.7.1.2 Glass disc 42 DC+ (Week 3)...292
E.7.1.3 Glass disc 42 DC- (Week 2)...293
E.7.2 Test cycle 2...293
E.7.2.1 Glass 42 AC (Week 9)...293
E.7.2.2 Glass disc 42 DC+ (Week 8)...294
E.7.2.3 Glass disc 42 DC- (Week 6)...295
E.7.3 Test cycle 3...295
E.7.3.1 Glass disc 42 AC (Week 13)...295
E.7.3.2 Glass disc 42 DC+ (Week 11)...296
E.7.3.3 Glass disc 42 DC- (Week 10)...296
E.7.4 Test cycle 4...297
E.7.4.1 Glass disc 42 AC (Week 22)...297
E.7.4.2 Glass disc 42 DC+ (Week 18)...298
E.7.4.3 Glass disc 42 DC- (Week 16)...299
F. APPENDIX F: Wettability (hydrophobicity) classifications for the respective high temperature vulcanized, silicone rubber (HTV-SR) insulators301
F.1 Overview ... 301
F.2 Wettability classifications for high temperature vulcanized, silicone rubber insulators with a unified specific creepage length of 84 mm/kV – HTV-SR 84 ... 302
F.2.1 Live-end insulator section...302
F.2.2 Ground-end insulator section...302
F.3 Wettability classifications for high temperature vulcanized, silicone rubber insulators with a unified specific creepage length of 72 mm/kV –HTV-SR 72 ... 303
F.3.1 Live-end insulator section...303
F.3.2 Ground-end insulator section...303
F.4 Wettability classifications for high temperature vulcanized, silicone rubber insulators with a unified specific creepage length of 56 mm/kV –HTV-SR 56 ... 304
F.4.1 Live-end insulator section...304
F.4.2 Ground-end insulator section...304

F.5 Wettability classifications for high temperature vulcanized, silicone rubber insulators with a unified specific creepage length of 44 mm/kV –HTV-SR 44 305
F.5.1 Live-end insulator section 305
F.5.2 Ground-end insulator section 305
F.6 Wettability classifications for high temperature vulcanized, silicone rubber insulators with a unified specific creepage length of 29 mm/kV –HTV-SR 29 306
F.6.1 Live-end insulator section 306
F.6.2 Ground-end insulator section 306

List of Figures

Figure 1-1: Circuit diagram of the Caprivi link interconnector HVDC transmission line [38, 39] 2
Figure 1-2: Cost considerations for HVDC when compared to HVAC in relation to the length of transmission line [39, 40] 5
Figure 1-3: A combination of factors that can lead to the ageing or failure of a power line insulator (*adapted from reference [30]*) 8
Figure 2-1: Evolution of early insulators [11] 16
Figure 2-2: Arcing distance of an insulator 23
Figure 2-3: Creepage distance of an insulator 24
Figure 2-4: Common insulating material ageing modes [7, 28] 29
Figure 2-5: Basic insulator pollution flashover process 34
Figure 2-6: Typical fused-insulator testing circuit for pollution studies 36
Figure 3-1: Complete configuration of the AC/DC test rig at KIPTS 39
Figure 3-2: Topographical representation of prominent pollution sources in the surroundings of KIPTS [7, 16] 41
Figure 3-3: Electrical configuration of the test rig at KIPTS 43
Figure 3-4: A set of HTV-SR test sinsulators with different creepage lengths installed on the test rig at KIPTS 45
Figure 3-5: Pig-tail connection of test insulators onto the busbar and the incorporation of an explosive fuse (Mace fuse) 46
Figure 3-6: UV-sensitive, image intensified night observation camera - Corocam Mark I 48
Figure 3-7: Sony GV-HD700 external video recorder 48
Figure 3-8: 0-lux (HDR XR550) Sony camcorder used for the night observations and photo capturing during surface inspections 50
Figure 3-9: Front view of the online leakage current analyzer (OLCA) for current and weather data logging 51
Figure 3-10: Components of the leakage current and weather data logging system used at KIPTS 53
Figure 3-11: Block diagram for the linearity tests of the AC leakage current sensors 55
Figure 3-12: Typical calibration curve for the AC leakage current sensors 55
Figure 3-13: Block diagram for the linearity tests of the DC leakage current sensors 57
Figure 3-14: Typical calibration curve for the DC leakage current sensors 57
Figure 4-1: An aerial view of the installation layout of test insulators on the test rig at KIPTS.. 60
Figure 4-2: ESDD measurements, considering the top and bottom pollutions separately [27].... 64
Figure 4-3: Design and installation specifications for directional dust deposit gauges [26, 27] .. 67
Figure 4-4: Typical partial electrical discharge activities on insulator surfaces [7, 26] 72
Figure 4-5: Hydrophobicity classification indices [26] 74
Figure 4-6: Insulator sections considered for wettability (hydrophobicity) classification tests ... 75

Figure 5-1: Time-of-day average rainfall recorded at KIPTS for the entire test period, February - July 2011 78
Figure 5-2: Monthly total rainfall recorded at KIPTS for the entire test period, February – July 2011 79
Figure 5-3: Time-of-day average relative humidity recorded at KIPTS for the entire test period, February through July 2011 80
Figure 5-4: Monthly average of the relative humidity recorded at KIPTS for the entire test period, February through July 2011 81
Figure 5-5: Inverse relationship between temperature (ambient and dewpoint) and relative humidity 82
Figure 5-6: Time-of-day average ambient temperature recorded at KIPTS for the entire test period, February through July 2011 83
Figure 5-7: Monthly average of the ambient temperature recorded at KIPTS for the entire test period, February through July 2011 84
Figure 5-8: Time-of-day average wind speed recorded at KIPTS for summer and winter periods 85
Figure 5-9: Time-of-day average wind direction recorded at KIPTS for summer and winter periods 86
Figure 5-10: Monthly average wind speed recorded at KIPTS for the entire test period, February through July 2011 86
Figure 5-11: Time-of-day average UV-B radiation recorded at KIPTS for summer and winter periods 87
Figure 5-12: Monthly average UV-B radiation recorded at KIPTS for the entire test period, February through July 2011 88
Figure 5-13: Equivalent salt deposit density (ESDD) measurements performed at KIPTS 91
Figure 5-14: Non-soluble deposit density (NSDD) measurements performed at KIPTS 93
Figure 5-15: Directional dust deposit gauge (DDDG) measurements performed at KIPTS 95
Figure 5-16: A graphical representation of bin count analysis of the leakage current recorded for all test insulators 99
Figure 5-17: The highest absolute peak leakage currents recorded for all the test insulators 100
Figure 5-18: The time-of-day average absolute peak leakage current profile recorded for all the HTV-SR 84 insulators 102
Figure 5-19: The time-of-day maximum absolute peak leakage current profile recorded for all the HTV-SR 84 insulators 103
Figure 5-20: The time-of-day average absolute peak leakage current profile recorded for all the HTV-SR 72 insulators 106
Figure 5-21: The time-of-day maximum absolute peak leakage current profile recorded for all the HTV-SR 72 insulators 106
Figure 5-22: The time-of-day average absolute peak leakage current profile recorded for all the HTV-SR 56 insulators 108

Figure 5-23: The time-of-day maximum absolute peak leakage current profile recorded for all the HTV-SR 56 insulators 109
Figure 5-24: The time-of-day average absolute peak leakage current profile recorded for all the HTV-SR 44 insulators 111
Figure 5-25: The time-of-day maximum absolute peak leakage current profile recorded for all the HTV-SR 44 insulators 112
Figure 5-26: The time-of-day average absolute peak leakage current profile recorded for all the HTV-SR 29 insulators 114
Figure 5-27: The time-of-day maximum absolute peak leakage current profile recorded for all the HTV-SR 29 insulators 115
Figure 5-28: The time-of-day average absolute peak leakage current profile recorded for all the glass disc insulators 117
Figure 5-29: The time-of-day maximum absolute peak leakage current profile recorded for all glass disc insulators 118
Figure 5-30: Accumulative coulomb-ampere for all the HTV-SR insulators installed on the AC excitation voltage 120
Figure 5-31: Accumulative coulomb-ampere for all the HTV-SR insulators installed on the DC+ excitation voltage 121
Figure 5-32: Accumulative coulomb-ampere for all the HTV-SR insulators installed on the DC- excitation voltage 122
Figure 5-33: Frequency of occurrence of electrical discharge activities on the test insulators, given in terms of the number of times that they were observed out of the total observation nights 136
Figure 5-34: First occurrence of electrical discharge activities on the test insulators, given in terms of the N’th night on which they were first observed 139
Figure 5-35: Two instances of material erosion on the sheath interfacing with the live end-fitting in the (a) southward direction and (b) northward direction, week 22 143
Figure 5-36: The bottom view of Glass disc 42 AC, week 22 156
Figure 5-37: Material erosion on the bottom of Glass disc 42 DC+ around the pin, week 18 156
Figure 5-38: Material erosion on the bottom of Glass disc 42 DC- around the pin, week 16 157
Figure 5-39: Comparisons of the wettability classifications for all the HTV-SR insulators given for the shed tops, shed bottoms and sheaths 165

Figure B-1: Profile of the time-of-day average rainfall for the entire test period, given for the respective months 192
Figure B-2: Profile of the time-of-day average relative humidity for the entire test period, given for the respective months 193
Figure B-3: Profile of the time-of-day average ambient temperature for the entire test period, given for the respective months 194

Figure B-4: Profile of the time-of-day average wind speed for the entire test period, given for the respective months 195
Figure B-5: Compass directions in degrees 196
Figure B-6: Profile of the time-of-day average wind direction for the entire test period, given for the respective months *(please refer to Figure B-5 for corresponding compass directions)* 197
Figure B-7: Profile of the time-of-day average UV-B radiation for the entire test period, given for the respective months 198
Figure C-8: Time of day leakage current bin counts for [0-10] mA, HTV-SR 84 201
Figure C-9: Time of day leakage current bin counts for [10-100] mA, HTV-SR 84 201
Figure C-10: Time of day leakage current bin counts for [100-1000] mA, HTV-SR 84 201
Figure C-11: Time of day leakage current bin counts for [0-10] mA, HTV-SR 72 204
Figure C-12: Time of day leakage current bin counts for [10-100] mA, HTV-SR 72 204
Figure C-13: Time of day leakage current bin counts for [100-1000] mA, HTV-SR 72 204
Figure C-14: Time of day leakage current bin counts for [0-10] mA, HTV-SR 56 207
Figure C-15: Time of day leakage current bin counts for [10-100] mA, HTV-SR 56 207
Figure C-16: Time of day leakage current bin counts for [100-1000] mA, HTV-SR 56 207
Figure C-17: Time of day leakage current bin counts for [0-10] mA, HTV-SR 44 210
Figure C-18: Time of day leakage current bin counts for [10-100] mA, HTV-SR 44 210
Figure C-19: Time of day leakage current bin counts for [100-1000] mA, HTV-SR 44 210
Figure C-20: Time of day leakage current bin counts for [0-10] mA, HTV-SR 29 213
Figure C-21: Time of day leakage current bin counts for [10-100] mA, HTV-SR 29 213
Figure C-22: Time of day leakage current bin counts for [100-1000] mA, HTV-SR 29 213
Figure C-23: Time of day leakage current bin counts for [0-10] mA, Glass disc 42 216
Figure C-24: Time of day leakage current bin counts foor [10-100] mA, Glass disc 42 216
Figure C-25: Time of day leakage current bin counts for [100-1000] mA, Glass disc 42 216
Figure E-26: Heavy pollution on the sheath of HTV-SR 84 AC (Week 5) 244
Figure E-27: Traces of dryband activity visible on the shed bottom of HTV-SR 84 DC+ (Week 3) 245
Figure E-28: (a) Heavy pollution deposits on the sheath and (b) salt crystals on the shed top of HTV-SR 84 DC+ (Week 3) 245
Figure E-29: (a) Light pollution build-up and (b) a close-up view of the salt crystals on HTV-SR 84 DC- (Week 2) 246
Figure E-30: Material erosion on the sheath interfacing with the live end-fitting and (b) light crazing on the sheath interfacing with the ground end-fitting (Week 9) 246
Figure E-31: (a) Dark burns on pollution layer on the sheath interfacing with the ground end-fitting and (b) drybands on the shed bottom of HTV-SR 84 DC+ (Week 8) 247
Figure E-32: A sample of the plant threads that were observed on HTV-SR 84 DC+(Week 8) 248
Figure E-33: Material erosion along the heavy pollution deposit on sheath 4 of HTV-SR 84 DC- (Week 6) 248

Figure E-34: Material erosion on the sheath interfacing with the live end-fitting of HTV-SR 84 AC (Week 13) 249
Figure E-35: Light material erosion, light crazing and drybands on the bottom of shed 3 of HTV-SR 84 DC+ (Week 11) 250
Figure E-36: Samples of (a) the plant threads and (b) the dead insects that were observed on HTV-SR 84 DC+ (Week 11) 250
Figure E-37: Material erosion on the sheath interfacing with the ground end-fitting along the heavy pollution deposit on HTV-SR 84 DC- (Week 10) 251
Figure E-38: Material erosion on the sheath interfacing with the live end-fitting in the (a) southward direction and (b) northward direction (Week 22) 252
Figure E-39: Material erosion on the sheath interfacing with the ground end-fitting (Week 22) 252
Figure E-40: Material erosion on the sheath interfacing with the live end-fitting in the southward direction (Week 18) 253
Figure E-41: Material erosion on the sheath interfacing the the live end-fitting in the westward direction (Week 16) 254
Figure E-42: Blue patches on the shed tops (a form of discoloration) of HTV-SR 84 DC- (Week 16) (*please zoom in*) 254
Figure E-43: Evidence of dryband activity on the sheaths interfacing with the (a) live and (b) ground end-fittings in the southward direction (Week 5) 255
Figure E-44: Traces of dryband activities on the shed bottom and heavy pollution on the sheaths of HTV-SR 72 DC+ (Week 3) 256
Figure E-45: (a) Dark burns on the sheath interfacing with the live end end-fitting and (b) material erosion on sheath 5 in the southward direction (Week 9) 257
Figure E-46: Dead insect (fly) spotted on sheath 3 of HTV-SR 72 AC in the eastward direction (Week 9) 257
Figure E-47: Traces of dryband activities on the shed bottom of HTV-SR 72 DC+ (Week 8).. 258
Figure E-48: A sample of plant threads observed on HTV-SR 72 DC+ (Week 8) 258
Figure E-49: Material erosion on the sheath interfacing with the ground end-fitting in the southward direction (Week 6) 259
Figure E-50: Material erosion on (a) sheath 3 and (b) sheath 5 in the southward direction (Week 13) 260
Figure E-51: Material erosion on the sheath interfacing with the live end-fitting in the (a) southward and (b) northward directions (Week 13) 260
Figure E-52: Material erosion (a) on the bottom of shed 3 in the southward direction and (b) on the sheath interfacing with the ground end-fitting in the northward direction (week 11) 261
Figure E-53: Material erosion on the sheath interfacing with the live end-fitting (Week 10).... 262
Figure E-54: Dead insect on the shed top in the southward direction (Week 10) 262

Figure E-55: Material erosion on (a) sheath 3 and (b) sheath 5 in the southward direction (Week 22) 263
Figure E-56: Material erosion on the sheaths interfacing with the (a) live end-fitting and (b) ground end-fitting (Week 22) 263
Figure E-57: Material erosion on the sheath interfacing with the ground end-fitting (Week 18) 264
Figure E-58: Rust pacthes on the sheath interfacing with the live end-fitting (Week 18) 265
Figure E-59: Some form of discoloration on the shed top in patterns of darker blue (a) spot and (b) radial patches (Week 16) *(please zoom in)* 265
Figure E-60: Traces of dark burns on pollution layer (a) on the sheath interfacing with the ground end-fitting and (b) on sheath 3 in the southward direction (Week 5) 266
Figure E-61: Traces of dryband activities on the shed top of HTV-SR 56 DC+ (Week 3) 267
Figure E-62: Material erosion on the sheath interfacing with the live end-fitting in the southward direction (Week 9) 268
Figure E-63: Material erosion on (a) sheath 3 and (b) sheath 4 in the southward direction (Week 9) 268
Figure E-64: Material erosion observed on the sheath interfacing with the ground end-fitting in the southward direction (Week 8) 269
Figure E-65: Instances of material erosion (a) on sheath 3 and (b) on the sheath interfacing with the live end-fitting in the shouthward direction (Week 13) 270
Figure E-66: Instances of material erosion observed on the sheaths interfacing with both the (a) ground and (b) live end-fittings (Week 11) 271
Figure E-67: Material erosion observed on the sheath interfacing with the live end-fitting (Week 10) 271
Figure E-68: A dead insect observed on the shed top of HTV-SR 56 DC- (Week 10) 272
Figure E-69: Instances of material erosion on the sheaths interfacing with both the (a) live and (b) ground end-fittings (Week 22) 273
Figure E-70: Material erosion observed on the sheaths interfacing with both the (a) live and (b) ground end-fittings (Week 18) 274
Figure E-71: (a) Material erosion on the sheath interfacing with the live end-fitting in the northward direction and (b) material peel-off at the sheath-to-shed bonding interface (Week 16) 275
Figure E-72: Blue patches (a form of discoloration) spotted on the shed top of HTV-SR 56 DC- (Week 16) *(please zoom in)* 275
Figure E-73: A dead insect on the shed top of HTV-SR 56 DC- (Week 16) 276
Figure E-74: The first sign of material erosion on the sheath interfacing with the live end-fitting in the southward direction (Week 5) 276
Figure E-75: Erosion on the sheath interfacing with the live end-fitting in the southward direction (Week 9) 278
Figure E-76: Salt crystals on the shed top of HTV-SR 44 DC- (Week 6) 279

Figure E-77: Instances of material erosion (a) on the sheath interfacing with the live end-fitting and (b) on sheath 2 (Week 13)... 279
Figure E-78: Material erosion on the sheath interfacing with the live end-fitting (Week 11).... 280
Figure E-79: The first instance of material erosion on the sheath interfacing with the ground end-fitting (Week 10).. 281
Figure E-80: Instances of material erosion observed (a) on the sheath interfacing with the live end-fitting, (b) on sheath 2 and (c) on the sheath interfacing with the ground end-fitting.. 282
Figure E-81: Material erosion on the sheaths interfacing with both the (a) live and (b) ground end-fitting (Week 18) 283
Figure E-82: Material peel-off at the sheath-to-shed bonding interface (week 16).................... 284
Figure E-83: Dark burns on pollution on the sheath interfacing with the live end-fitting (Week 5) 285
Figure E-84: The first sign of material erosion on the sheath interfacing with the live end-fitting in the southward direction (Week 9) 286
Figure E-85: The first signs of erosion on the sheaths interfacing with both the (a) live and (b) ground end-fittings in the southward direction (week 8)....................................... 287
Figure E-86: Material erosion on the sheath interfacing with the live end-fitting (week 13) 288
Figure E-87: Rust deposit on the sheath interfacing with the live end-fitting in the westward direction (Week 11) 289
Figure E-88: Material erosion on the sheath interfacing with the live end-fitting (Week 22).... 290
Figure E-89: Rust deposit on the sheath interfacing with the live end-fitting in the westward direction (Week 18) 291
Figure E-90: Material erosion on the sheath interfacing with the ground end-fitting (Week 16) 291
Figure E-91: Pollution conditions on the (a) top and (b) bottom of glass disc (Week 5)........... 292
Figure E-92: Pollution conditions on the top of glass disc (Week 3) 293
Figure E-93: Traces of dryband activity on the bottom of glass disc (Week 9) 294
Figure E-94: Light material erosion on the bottom of glass disc around the pin (Week 8)........ 294
Figure E-95: The first instance of material erosion on the bottom of glass disc around the pin (Week 6) 295
Figure E-96: Traces of dryband activity on the bottom of glass disc around the pin (Week 13) 295
Figure E-97: Material erosion on the bottom of glass disc around the pin (Week 11).............. 296
Figure E-98: Material erosion on the bottom of glass disc around the pin (Week 10).............. 297
Figure E-99: A dead insect on the top of glass disc (Week 10).. 297
Figure E-100: The bottom view of glass disc (Week 22) 298
Figure E-101: (a) Traces of dryband activity on the top of glass disc around the cap and (b) the signs of dryband activity and material erosion on the bottom side around the pin (Week 18) 299

Figure E-102: (a) Traces of dryband activity on the top of glass disc around the cap and (b) the signs of dryband activity and material erosion on the bottom side around the pin (Week 16) 300

List of Tables

Table 1-1: A summary of monitoring activities performed at KIPTS 11
Table 2-1: A summary of the commonly used types of insulators on overhead power lines [3, 6] 20
Table 3-1: Additional pollution sources in the vicinity of KIPTS 42
Table 3-2: Technical specifications of the converter unit used for the DC voltage source 44
Table 3-3: Technical specifications of the test insulators 46
Table 3-4: Technical specifications of Corocam Mark I and the video recorder 49
Table 3-5: Linearity test results for all the AC leakage current sensors 56
Table 3-6: Linearity test results for all the DC+ leakage current sensors 58
Table 3-7: Linearity test results for all the DC- leakage current sensors 58
Table 4-1: Pollution severity classes based on ESDD, NSDD and DDDG [3, 26] 68
Table 5-1: A summary of rainfall data obtained at KIPTS during February through July 2011 .. 79
Table 5-2: A summary of relative humidity recorded at KIPTS during February through July 2011 81
Table 5-3: A summary of ambient temperatures recorded at KIPTS during February through July 2011 84
Table 5-4: A summary of wind speed data recorded at KIPTS during February through July 2011 86
Table 5-5: A summary of UV-B radiation data recorded at KIPTS during February through July 2011 88
Table 5-6: A summary of the equivalent salt deposit density (ESDD) measurements performed on a non-energized glass insulator installed at KIPTS 91
Table 5-7: Comparisons of ESDD values for summer and winter 91
Table 5-8: A summary of the non-soluble deposit density (NSDD) measurements performed on a non-energized glass insulator installed at KIPTS 92
Table 5-9: Comparisons of NSDD values for summer and winter 92
Table 5-10: A summary of the directional dust deposit gauge (DDDG) measurements performed at KIPTS 95
Table 5-11: Comparisons of DDDG values for summer and winter 95
Table 5-12: A summary of bin count analysis of the leakage current recorded for all test insulators 99
Table 5-13: The average and maximum values of the leakage current recorded for all test insulators, given per time of day 100
Table 5-14: Flashover events recorded in the entire test period 100
Table 5-15: Summary of frequency of occurrence of electrical discharge activities observed with Corocam Mark I 135
Table 5-16: Summary of frequency of occurrence of electrical discharge activities observed with 0-lux Sony Camcorder 140

Table 5-17: Surface inspection timelines 142
Table 5-18: A total count of instances of material erosion in week 22, HTV-SR 84 AC 143
Table 5-19: A total count of instances of material erosion in week 18, HTV-SR 84 DC+ 144
Table 5-20: A total count of instances of material erosion in week 16, HTV-SR 84 DC- 145
Table 5-21: A total count of instances of material erosion in week 22, HTV-SR 72 AC 146
Table 5-22: A total count of instances of material erosion in week 18, HTV-SR 72 DC+ 147
Table 5-23: A total count of instances of material erosion in week 16, HTV-SR 72 DC- 147
Table 5-24: A total count of instances of material erosion in week 22, HTV-SR 56 AC 148
Table 5-25: A total count of instances of material erosion in week 18, HTV-SR 56 DC+ 149
Table 5-26: A total count of instances of material erosion in week 16, HTV-SR 56 DC- 150
Table 5-27: A total count of instances of material erosion in week 22, HTV-SR 44 AC 151
Table 5-28: A total count of instances of material erosion in week 18, HTV-SR 44 DC+ 151
Table 5-29: A total count of instances of material erosion in week 16, HTV-SR 44 DC- 152
Table 5-30: A total count of instances of material erosion in week 22, HTV-SR 29 AC 153
Table 5-31: A total count of instances of material erosion in week 18, HTV-SR 29 DC+ 154
Table 5-32: A total count of instances of material erosion in week 16, HTV-SR 29 DC- 155
Table 5-33: A summary of surface conditions observed on all test insulators 160
Table 5-34: An overview of instances of material erosion observed on all the HTV-SR test insualtors per each excitation voltage type 160
Table 5-35: A summary of wettability classifications for all the high temeperature vulcanized, silicone rubber (HTV-SR) test insulators 164

Table A-1: Record sheet for surface condition inspections 188
Table A-2: Record sheet for wettability classification tests 189
Table A-3: Record sheet for electrical discharge activity observations: Corocam Mark I 190
Table A-4: Record sheet for electrical discharge activity observations: 0-lux Sony Camcorder 190
Table C-5: Monthly bin counts of absolute peak leakage currents for the HTV-SR 84 insulators 200
Table C-6: Comparisons between the three excitation voltages, HTV-SR 84 200
Table C-7: The time-of-day average and maximum absolute peak leakage currents 202
Table C-8: Monthly bin counts of absolute peak leakage currents for the HTV-SR 72 insulators 203
Table C-9: Comparisons between the three excitation voltages, HTV-SR 72 203
Table C-10: The time-of-day average and maximum absolute peak leakage currents 205
Table C-11: Monthly bin counts of absolute peak leakage currents for the HTV-SR 56 insulators 206
Table C-12: Comparisons between the three excitation voltages, HTV-SR 56 206
Table C-13: The time-of-day average and maximum absolute peak leakage currents 208
Table C-14: Monthly bin counts of absolute peak leakage currents for the HTV-SR 44 insulators 209

Table C-15: Comparisons between the three excitation voltages, HTV-SR 44 209
Table C-16: The time-of-day average and maximum absolute peak leakage currents 211
Table C-17: Monthly bin counts of absolute peak leakage currents for the HTV-SR 29 insulators 212
Table C-18: Comparisons between the three excitation voltages, HTV-SR 29 212
Table C-19: The time-of-day average and maximum absolute peak leakage currents 214
Table C-20: Monthly bin counts of absolute peak leakage currents for the Glass disc 42 insulators 215
Table C-21: Comparisons between the three excitation voltages, Glass disc 42 215
Table C-22: The time-of-day average and maximum absolute peak leakage currents 217
Table C-23: Flashover events recorded on the glass disc insulator installed on DC- 217
Table D-24: Frequency of occurrence of electrical discharge activity observed with Corocam Mark I, HTV-SR 84 219
Table D-25: Location of electrical discharge activity observed with Corocam Mark I, HTV-SR 84 220
Table D-26: Frequency of occurrence of electrical discharge activity observed with 0-lux Sony Camcorder, HTV-SR 84 221
Table D-27: Location of electrical discharge activity observed with 0-lux Sony Camcorder, HTV-SR 84 222
Table D-28: Frequency of occurrence of electrical discharge activity observed with Corocam Mark I, HTV-SR 72 223
Table D-29: Location of electrical discharge activity observed with Corocam Mark I, HTV-SR 72 224
Table D-30: Frequency of occurrence of electrical discharge activity observed with 0-lux Sony Camcorder, HTV-SR 72 225
Table D-31: Location of electrical discharge activity observed with 0-lux Sony Camcorder, HTV-SR 72 226
Table D-32: Frequency of occurrence of electrical discharge activity observed with Corocam Mark I, HTV-SR 56 227
Table D-33: Location of electrical discharge activity observed with Corocam Mark I, HTV-SR 56 228
Table D-34: Frequency of occurrence of electrical discharge activity observed with 0-lux Sony Camcorder, HTV-SR 56 229
Table D-35: Location of electrical discharge activity observed with 0-lux Sony Camcorder, HTV-SR 56 230
Table D-36: Frequency of occurrence of electrical discharge activity observed with Corocam Mark I, HTV-SR 44 231
Table D-37: Location of electrical discharge activity observed with Corocam Mark I, HTV-SR 44 232

Table D-38: Frequency of occurrence of electrical discharge activity observed with 0-lux Sony Camcorder, HTV-SR 44 233
Table D-39: Location of electrical discharge activity observed with 0-lux Sony Camcorder, HTV-SR 44 234
Table D-40: Frequency of occurrence of electrical discharge activity observed with Corocam Mark I, HTV-SR 29 235
Table D-41: Location of electrical discharge activity observed with Corocam Mark I, HTV-SR 29 236
Table D-42: Frequency of occurrence of electrical discharge activity observed with 0-lux Sony Camcorder, HTV-SR 29 237
Table D-43: Location of electrical discharge activity observed with 0-lux Sony Camcorder, HTV-SR 29 238
Table D-44: Frequency of occurrence of electrical discharge activity observed with Corocam Mark I, Glass disc 42 239
Table D-45: Location of electrical discharge activity observed with Corocam Mark I, Glass disc 42 240
Table D-46: Frequency of occurrence of electrical discharge activity observed with 0-lux Sony Camcorder, Glass disc 42 241
Table D-47: Location of electrical discharge activity observed with 0-lux Sony Camcorder, Glass disc 42 242
Table E-48: Timelines for surface inspection test cycles 243
Table F-49: A summary of wettability classifications for HTV-SR 84, live-end section 302
Table F-50: A summary of wettability classifications for HTV-SR 84, ground-end section 302
Table F-51: A summary of wettability classifications for HTV-SR 72, live-end section 303
Table F-52: A summary of wettability classifications for HTV-SR 72, ground-end section 303
Table F-53: A summary of wettability classifications for HTV-SR 56, live-end section 304
Table F-54: A summary of wettability classifications for HTV-SR 56, ground-end section 304
Table F-55: A summary of wettability classifications for HTV-SR 44, live-end section 305
Table F-56: A summary of wettability classifications for HTV-SR 44, ground-end section 305
Table F-57: A summary of wettability classifications for HTV-SR 29, live-end section 306
Table F-58: A summary of wettability classifications for HTV-SR 29, ground-end section 306

Nomenclature

ABB:	**A**sea **B**rown **B**overi
AC:	**A**lternating **C**urrent
CIGRE:	**C**onseil **I**nternationale des **G**randes **R**eseaux **E**lectriques (*International Council for Large Electric Systems*)
DBC:	**D**ry**b**and **C**orona
DBD:	**D**ry**b**and **D**ischarge
DC:	**D**irect **C**urrent
DDDG:	**D**irectional **D**ust **D**eposit **G**auge
ECB:	**E**lectricity **C**ontrol **B**oard
EPDM:	**E**thylene **P**ropylene **D**iene **M**onomer
ESDD:	**E**quivalent **S**alt **D**eposit **D**ensity
ESKOM:	Formerly "ESCOM" for **E**lectricity **S**upply **Com**mission
HTV-SR:	**H**igh **T**emperature **V**ulcanized **S**ilicone **R**ubber
HVAC:	**H**igh **V**oltage **A**lternating **C**urrent
HVDC:	**H**igh **V**oltage **D**irect **C**urrent
IEC:	**I**nternational **E**lectrotechnical **C**ommission
IGBT:	**I**nsulated **G**ate **B**ipolar **T**ransistor
KIPTS:	**K**oeberg **I**nsulator **P**ollution **T**est **S**tation
NamPower:	**Nam**ibia **Power** Corporation
NSDD:	**N**on-**s**oluble **D**eposit **D**ensity
OLCA:	**O**nline **L**eakage **C**urrent **A**nalyzer
RMS:	**R**oot **M**ean **S**quare
SAPP:	**S**outhern **A**frican **P**ower **P**ool
SCD:	**S**pot **C**orona/**D**ischarge
USCD:	**U**nified **S**pecific **C**reepage **D**istance
UV:	**U**ltra **V**iolet
VSC:	**V**oltage **S**ource **C**ontrolled
WDC:	**W**ater **D**rop **C**orona

Acknowledgements

Herewith recording my acknowledgements:

- I would like to thank my good Lord for all the unspeakable love and care throughout my studies. His words: "*For I know the plans I have for you, plans to prosper you and not to harm you, plans to give you hope and a future.*" [Jeremiah 29: 11]. I deeply appreciate the hope that God has given me during the daunting experiences in my life and I look forward to a future that he promises.

- Special thanks go to my supervisor, Prof. HJ Vermeulen for his exceptional support throughout this project, without which this thesis would not have become a success.

- The invaluable contributions from Dr JP Holtzhausen, Dr WL Vosloo and Mr P Pieterse are sincerely appreciated.

- I wish to record special acknowledgements to Mr D Mvayo, Mr R Watson and Mr R Davey for the technical guidance and assistance received during those long days and nights of observations at KIPTS.

- Tributes to my father: His passing has left me with volatile emotions as it came at the time when I needed to finish up on my work. I dedicate this document to his accolade. "*Omwenyo goye nagu vululukwe nombili, Tate.*"

- To you: Mommy and the entire family, your love and the words of encouragement are deeply appreciated and I am grateful for all the support. Special thanks must go to Tatekulu and Kuku Hango for being my wonderful guardian parents.

- I wish to extend my sincerest acknowledgement to NamPower for providing financial sponsorship for the project.

- All material, spiritual and moral support from all the people of God cannot be overstated.

1. Chapter 1: Introduction

1.1 Overview

The decade that just ended has been marked by a shortage of electrical power due to capacity problems and growth in demand in the Southern African region. Electrical engineers therefore face the challenge to find solutions to the worsening energy crisis. The possible options that may be available to cater to this challenge include the following:

- Expanding the generation capacity of existing power stations in the region;
- Adopting renewable energy resources as a means of providing additional electrical power;
- Importing power from other countries through regional power trading contracts.

Namibia, a member of the Southern African Power Pool (SAPP), is no exception from the crisis-struck countries as it battles to meet the electricity demand of its nation. As a result, the national power utility, NamPower (Pty) Ltd, has undertaken a number of projects in order to seek ways of rescuing the dire electricity demand in the country. Importing power from neighbouring countries such as South Africa has consequently been an option that NamPower resorted to. In fact, a 400kV AC interconnector was constructed from Kenhardt in South Africa to the Auas substation near Windhoek and this line has provided imported power to the Namibian network since 2001 [36, 37]. Additionally, load management programs have been embarked on by the national power utility in the context of encouraging efficient use of the meager available power in the country. To this effect, an energy-saving campaign was thus launched countrywide, culminating in the distribution of compact fluorescent lamps (CFL's) in 2007 by NamPower in conjunction with the Ministry of Mines and Energy (MME) and the Electricity Distribution Board (ECB).

Moreover, one of the most staggering projects that NamPower has embarked on is the design and construction of the high voltage direct current (HVDC) power line, commonly known as the 'Caprivi Link Interconnector' – henceforth referred to as the CLI project. This project is a 970 km, ±350 kV HVDC bipolar power line, which was recently commissioned on November 15 2010 by His Excellency Dr. Hifikepunye Pohamba, Namibia's president. Linking both the

Namibian and Zambian electricity grids, this project offers the first electrical connection between the Caprivi region in the north-eastern part of Namibia and the rest of the country and it also provides a lucrative channel for power trading within the SAPP.

The CLI project was the first of its kind designed using the HVDC Light technology and is especially significant in that it is an overhead transmission line spanning such a long distance (970 km) when compared to the commonly used underground or underwater cable implementation [38]. All technical work was administered by the ABB Group (a Swedish-based company) including the design and installation of the converter stations at the two ends of the HVDC line. The converter stations are situated at the ends of the line, one station at Zambezi near the Zambia-Namibia border and the other at Gerus, some 300 km north of Windhoek in central Namibia. The high voltage alternating current (HVAC) operating voltage levels of the two systems to be interconnected are 330 kV and 400 kV at the Zambezi and Gerus converter stations, respectively. The configuration of the CLI transmission line is shown in the circuit diagram below.

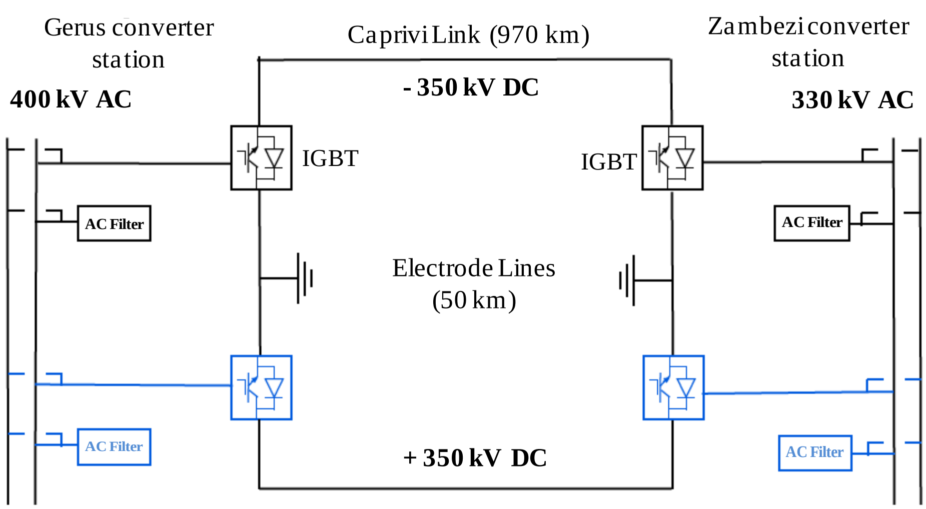

Figure 1-1: Circuit diagram of the Caprivi link interconnector HVDC transmission line [38, 39]

The design of this transmission line allows for two stages:

- Stage 1 – Designing for monopolar operation mode with a capacity of 300 MW. In this mode, the link can be operated with two parallel DC lines and an earth return for minimal losses. The line is currently operating in the monopolar mode since its commissioning.

- Stage 2 – Upgrading to a bipolar operation mode with a capacity of 600 MW. In this mode, the link can be operated as a balanced bipole with zero ground current. This stage is still under development.

As can be seen in Figure 1-1, the two converter stations employ an insulated gate bipolar transistor (IGBT)-based, voltage source controlled (VSC) switching mechanism.

The CLI project could have been implemented using HVAC. However, this would have led to a compromise on the resulting stability of the power network. This is due to the weak networks (330 kV and 400 kV HVAC) that needed to be interconnected over a long line. The use of HVDC was therefore considered a better option owing to the benefits that it can offer, especially in connecting weak HVAC networks by means of powerful voltage control.

The choice of HVDC by NamPower was thus based on the advantages that are inherent to HVDC technology when compared to HVAC, especially where the two networks to be interconnected are electrically weak in terms of network stability. The advantages of HVDC are briefly highlighted below.

1.1.1 Interconnection of HVAC power networks

HVDC applications are ideal for providing a tie line interconnection between separate HVAC networks with dissimilar electrical characteristics. For instance, it may be required that two HVAC networks with different voltage levels and different operating frequencies be interconnected. This cannot easily be achieved with the use of AC applications. However, HVDC provides an appealing solution since the power that it transfers across the two different networks is not frequency dependent. In addition, HVDC power lines can help improve the reliability and controllability of the network's power transfer capacity [41, 42]. This may have an effect of enhancing system protection and a reduction of wide-area system faults.

1.1.2 Power transfer over long distances

HVDC provides two major advantages with regard to the transfer of power over long distances. Firstly, HVDC requires fewer conductors when compared to the HVAC applications. This means that if the same amount of electrical power were to be transferred over certain spans of distance, then more cost would be incurred for HVAC when compared to the HVDC that would require fewer conductors and hence fewer support structures and insulators. This could potentially cut costs quite significantly (refer to section 1.1.3). Secondly, DC power is entirely real power – it is not associated with reactive power. A combination of these two advantages therefore make HVDC a far more economical option for transferring bulk electrical power between distantly separated power networks.

1.1.3 Economic considerations

When planning a new transmission line, cost is often an important factor to consider. Some of the costs that can be considered include: station terminal costs, line costs and the costs incurred due to line losses. Figure 1-2 illustrates how the cost of investment for HVDC compares to that of HVAC.

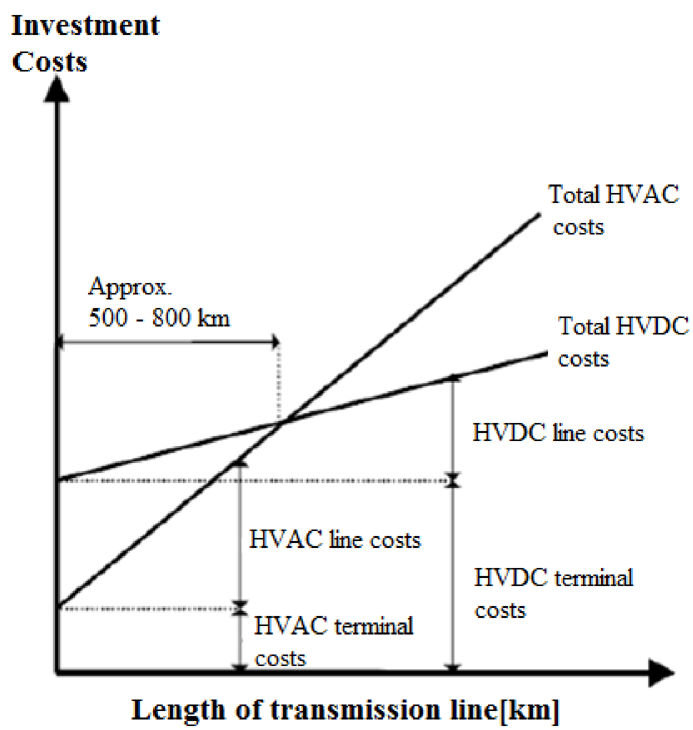

Figure 1-2: Cost considerations for HVDC when compared to HVAC in relation to the length of transmission line [39, 40]

It can be seen that HVDC proves to be a more economical option for transferring power over long distances (typically above 800 km) [39, 40, 42]. This is evident from Figure 1-2, where the HVDC costs become much lower than those associated with HVAC applications above the break-even point and this corresponds with the very long transmission distances. The difference between the costs could be explained by the fact that HVDC requires fewer conductors when compared to HVAC which requires at least three conductors on a three-phase system and consequently results in lower costs for HVDC. In general, it has been found that the line losses associated with HVDC can be as much as a quarter of the losses on an HVAC system [40]. This is a significant cost saving.

1.1.4 Environmental considerations

Safety of the inhabitants near transmission lines is an important consideration when right-of-way is negotiated and it is always desirable that no harmful effects are imposed on the lives of those living nearby. The electromagnetic and electrostatic fields are some of the aspects that one might want to consider. These become less important in HVDC applications due to the non-varying fields that are generated by this type of voltage. The use of HVDC gives an effect that there would be no induced voltages or currents due to alternating fields [39, 42]. In contrast, HVAC produces alternating fields which could create induced voltages or currents in nearby objects and consequently cause interference.

1.1.5 Demerits of HVDC

Besides all the benefits as discussed above, there are some demerits associated with HVDC. These are listed below [39 - 41]:

- The cost of HVDC may be considerably higher than that of HVAC with an equivalent capacity, especially for the construction of a converter station compared to a substation in an HVAC system. HVDC is less economical than HVAC for shorter transmission distances due to the losses that can occur in the static inverters.

- The realization of an HVDC-based multi-terminal system is a complex task. It therefore follows that the control mechanisms for power flow required in a multi-terminal HVDC system will be quite sophisticated - requiring a carefully coordinated communication protocol between all the terminals. This can be a costly consideration.

- An increased number of power electronic devices on the HVDC systems can have the undesirable effect of injecting harmonics into the network, which can be dangerous to the sensitive equipment connected on the system. Filters and smoothing devices are thus needed to reduce harmonics and these devices can incur very high costs.

The new interest in HVDC has not only introduced positive aspects in power system design, but its growing application also means that a different approach to power system design and maintenance is required other than the traditional HVAC approach. This necessitates the need for new research to find an optimal design approach for HVDC-based power systems. In particular, research should find ways of maintaining the integrity of the power system. One such power system aspect is insulation coordination. It is therefore against this background that NamPower has decided to invest in the research that seeks to study the performance of different insulation scenarios. Once obtained, the optimal insulation technology will be used on the newly commissioned CLI HVDC line and also on other existing infrastructure that may need refurbishment in the future. The next section describes the reasons for undertaking the research that is reported in this thesis.

1.2 Project motivation

An insulator bears the dual function of providing electrical isolation between the high voltage and ground potentials as well as providing mechanical support for the high voltage apparatus (and/or conductors). When an insulator fails, a phase (or line) to ground flashover fault can occur on the power system – causing a loss of integrity in the continuity of power supply to the customers. A multitude of factors can lead to the failure of insulators, which may include overvoltages due to power frequency faults, switching or lightning strikes. Refer to Figure 1-3 for the detailed hierarchy of factors affecting the performance of power line insulators.

Another critical factor is insulator pollution, which constitutes a multifaceted phenomenon. Insulator pollution performance has dominated research in the field of power line insulator design, and this has led to the conception of silicone rubber (SR) insulators having a superior performance. It must be mentioned that the performance of most insulator types has been adequately studied in the recent years for AC applications. However, only a limited number of studies have been conducted on HVDC insulator performance under laboratory conditions. No practical studies have been conducted on the performance of insulators under HVDC applications when subjected to harsh pollution environments. NamPower has therefore committed a great deal of financial investment toward insulator performance research as a support project for ensuring adequate insulation of its transmission and distribution infrastructures, especially for the newly commissioned CLI HVDC power line.

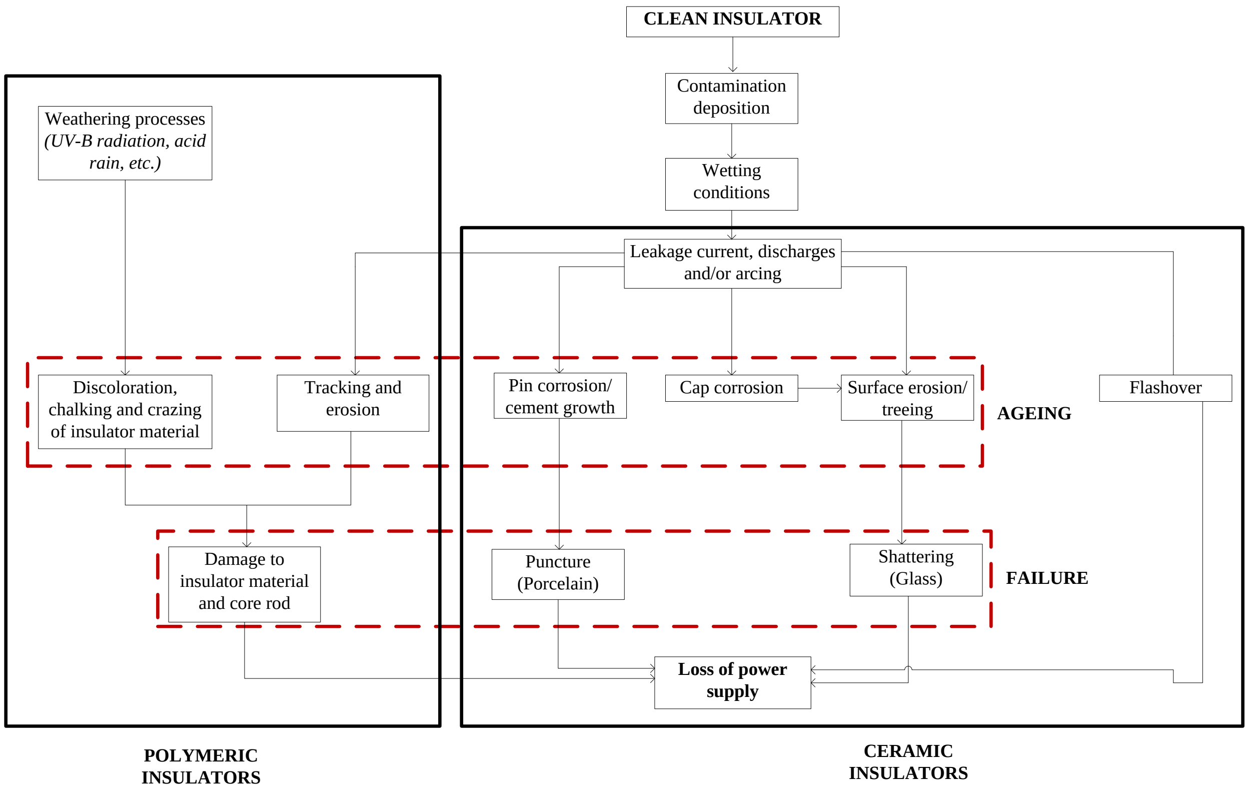

Figure 1-3: A combination of factors that can lead to the ageing or failure of a power line insulator (*adapted from reference [30]*)

The insulator performance research is a three-party synergy project between NamPower, the University of Stellenbosch and ESKOM. The research program was planned in two stages: *firstly to perform laboratory experiments on insulator pollution performance* and then *secondly to perform studies on insulator performance under natural pollution environments*.

The first stage of this research project involved a comparative study of different insulator materials under both AC and DC when subjected to artificial pollution environments. Two different research methods were used: the Inclined Plane Test method (IPT) by Gernot Heger and the Tracking Wheel Test (TWT) method by Beulah Limbo. Both Heger and Limbo did their research at the High Voltage Laboratory of Stellenbosch University under the sponsorship of NamPower. The findings reported in their theses have given interesting revelations on the differences in the performance of different insulator materials when subjected to different excitation voltage types: AC, DC+ and DC-. Details on Gernot and Beulah findings have been published in references [35] and [43], respectively.

The second stage of the project now seeks to build on the insulator pollution studies conducted by Heger and Limbo, focusing on natural ageing performance of insulators with different creepage lengths (the length measured along the contours of the insulator between its two terminating ends) under both AC and bipolar-DC voltages. The author of this thesis has been working on the second stage of this insulator research project since March 2010 under the sponsorship of NamPower. The results presented in this thesis are of particular importance to obtain knowledge of the ageing performance of power line insulators when energized under different excitation voltages under natural pollution conditions. This is especially crucial for the HVDC applications given the paucity of research conducted on the DC performance of insulators. From the perspective of industrial relevance, it is envisaged that the understanding gained from the findings of this research will serve as guidance in designing maintenance procedures and insulation specifications for HVDC power transmission lines. Preliminary results were presented and published at the Southern African Power Engineering Conference (SAUPEC 2011) in Cape Town, July 2011 and also at the International Symposium on High Voltage Engineering (ISH 2011) in Germany, August 2011 [17, 29]. A brief description of this project follows in the next section.

1.3 Project description

1.3.1 Introduction

The aim of this project is to perform an evaluation of the performance of power line insulators when energized under AC, DC+ and DC- under natural pollution conditions. As noted in section 1.2, this research project is a part of the NamPower initiative that seeks to gain an in-depth understanding of the performance of power line insulators with particular emphasis on the relative impacts of both DC+ and DC- when compared to AC. This study was carried out at the Koeberg Insulator Pollution Test Station (KIPTS), which is situated close to ESKOM's Koeberg Nuclear Power Station near Cape Town, some 50 m eastward from the west coast. KIPTS was first designed and constructed in its original form in 1974, with the initial aim to study pollution performance of power line insulators under marine polluted conditions [26].

It may be queried as to why NamPower has decided to perform studies at KIPTS which might not be fully representative of the environmental conditions experienced in Namibia. However, KIPTS had gradually developed into an internationally recognized insulator pollution test facility, which is now widely used by both insulator manufacturers and academic researchers from many parts of the world. STRI and ABB, both Swedish-based companies, are the good examples of international subscribers to the KIPTS research facility. Refer to Figure 3-1 for the pictorial representation of the test rig populated with the test insulators. KIPTS is characterized by hot dry summers, cold and wet winters, mist banks, strong winds and heavy marine pollution from the sea and it is often considered a harshly polluted environment, with a pollution index recorded to a value in the order of 2000 μS/cm [3, 15]. This pollution index is classified as "very heavy" and hence the reference to KIPTS as an accelerated insulator natural pollution test facility [3, 15]. The test rig is fitted with a control room (housing the measuring instruments), and leakage current and weather sensing facilities connected to the online leakage current analyzers (OLCA's) in the control room for data logging purposes. Further, it has been established that the results obtained from KIPTS over a one-year period are far more severe than those obtained from the IEC 5000-hour accelerated ageing test [3, 7]. Therefore, such severe pollution conditions at KIPTS may serve to validate the site as an ideal location that is representative of the harshest service conditions to which insulators may be subjected. It is therefore the ideally severe pollution conditions of KIPTS that formed the basis on which it was chosen for this research. Detailed descriptions of KIPTS are presented in Chapter 3.

1.3.2 Research objectives

The objectives of this study were as follows:

- To design a suitable DC excitation voltage system for both DC+ and DC-. This apparatus was designed and built at the University of Stellenbosch (refer to section 3.2.3).
- To perform a comparative evaluation of the performance of high temperature vulcanized, silicone rubber (HTV-SR) power line insulators under AC, DC+ and DC- when subjected to natural pollution conditions at KIPTS. All test insulators were made from the same

material and sourced from the same manufacturer – having different creepage lengths (refer to section 3.3).

This study was therefore conducted with the view to provide insight into the following research questions:

1st: What is the effect of creepage distance on the *performance* and *ageing* of high temperature vulcanized, silicone rubber (HTV-SR) insulators when energized under AC, DC+ and DC-?

2nd: What would be the recommended creepage distance for use on each of the excitation voltage type with reference to performance and ageing perspective?

The following observations and measurements were executed in order to gather data necessary for analyzing the performance and ageing of the test insulators considered in the study.

Table 1-1: A summary of monitoring activities performed at KIPTS

Monitoring activity	Details
Climatic and environmental conditions	● Climatic conditions were continuously monitored using the on-site weather station coupled to the online leakage current anaylzer (OLCA) device.
	● Equivalent salt deposit density (ESDD), non-soluble deposit density (NSDD) and directional dust deposit gauge (DDDG) readings were collected weekly. A separate glass disc insulator and a set of four directional dust deposit gauges (DDDG) were installed at the rig for this purpose.
Leakage current data	● Continuous leakage current measurements were taken using the OLCA device.
Electrical discharge activity observations	● Electrical surface discharge activity observations were done on all the insulators each night between 22h00 and 02h00, using COROCAM Mark I and a 0-lux Sony Camcorder .
Surface condition inspections	● Visual inspections of insulator surface conditions including wettability (hydrophobicity) classification tests were done; taking particular note of surface degradations.

Since all test insulators were made from the same material (HTV-SR), it was assumed that they all have the same chemical characteristics and only differ in creepage length. Additionally, it was assumed that all test insulators were subjected to the same environmental conditions and the same electrical stress. The DC excitation voltages were designed to an equivalent RMS of the AC voltage to ensure that all insulators were subjected to the same electrical stress (ageing due to electrical stress is dependent on the power dissipated over the insulator surface during electrical discharge activities and hence the choice of RMS equivalence). Thus, two major aspects under investigation are: the effect of creepage length on the performance of test insulators and the impact of the three excitation voltage types.

The results presented in this thesis are expected to serve as a key basis in the analysis of the relative performance of high temperature vulcanized silicone rubber insulators energized under the three respective voltage types: AC, DC+ and DC-. It is also envisaged that new research questions will unfold from this thesis that will lead into future studies, especially in the interest of DC applications.

1.4 Thesis outline

The chapters of this thesis are structured as described below.

- **Chapter 2:** A literature review on the fundamental roles of power line insulators and how the approach to insulator design evolved over the years. The literature review also covers a description of different insulator types that are commonly used on power lines to date, with particular emphasis on the possible deteriorations that may occur due to either environmental or electrical stresses. Finally, a review on the basic pollution flashover process is presented.

- **Chapter 3:** This chapter describes the design and choice of test apparatus used in the study. Such descriptions include details on KIPTS, the design of the bipolar DC excitation system, the video cameras used for observation purposes, as well as the data logging system. The philosophy behind the choice of test insulators is also presented in this chapter.

- **Chapter 4:** A comprehensive description of research procedures and methodology is presented in this chapter.

- **Chapter 5:** All the results obtained in the study are discussed in this chapter. Interpretations are also provided herein. The results are presented in a comparative manner with reference to both the effect of different creepage lengths as well as the different excitation voltage types on the performance of test insulators.

- **Chapter 6**: Finally, conclusions and recommendations are provided in this last chapter with the view of addressing the research questions, as noted in the previous section (refer to section 1.3).

2. CHAPTER 2: Literature review

2.1 Overview

This chapter presents a literature survey on the general aspects that pertain to insulator pollution studies. The following aspects have been explored and are presented in the following sections:

- The importance of insulators on the reliability of a power system and how the approach to insulation evolved over the years;
- Descriptions of insulators that are commonly used on power lines to date;
- An overview of the effect of environmental and climatic conditions on insulator performance;
- A review on the common ageing modes that may serve as indicators on the ageing performance of insulators and;
- A brief review on the theory of insulator pollution flashover

2.2 The Role of Insulators in a Power System

The advent of technological advancements has transformed the approach to power system design into a new paradigm. Unlike in the earliest days, the newer power systems span thousands of kilometers with very high operating voltages. The longer transmission lines and higher operating voltages are necessitated by the need to transmit the generated electrical power to the distant concentrations of customer loads, at minimal power loss [1, 30]. It is therefore the rapidly growing demand for electric power that has made it necessary to construct new transmission lines with increased capacity, which in practice can only be optimally viable at transmission voltages as high as 765kV (p-p) [11, 12].

Power transmission lines constructed in the earliest days covered relatively short distances and this was due to the constraints imposed by the associated power losses due to very low operating voltages [1]. The first transmission line was designed in 1882 by von Miller and Duprez and had an operating voltage of 1.3 kV DC [2]. In 1886, C.E.L. Brown (a son of Charles Brown) built another line 8 kms long, with an operating voltage of 2kV, from Kriegstetten to Solothurn [2, 11]. Then, five years later, Brown designed the first transmission line that used three-phase alternating current, with a 25 kV operating voltage (although originally designed for 15 kV), 175 km in length from Lauffen to Frankfurt. It is interesting to note that the insulation philosophy used by Brown was based on telegraph insulators, the so-called oil-bath insulators [11, 33]. Refer to Figure 2-1 (e). By the year 1910, there was a marked development of higher operating voltage power lines ranging between 50 kV and 66 kV, the trend of which has continued to increase ever since [2-4].

Figure 2-1 shows some of the pioneering insulators that were used in the early years of electrical insulation.

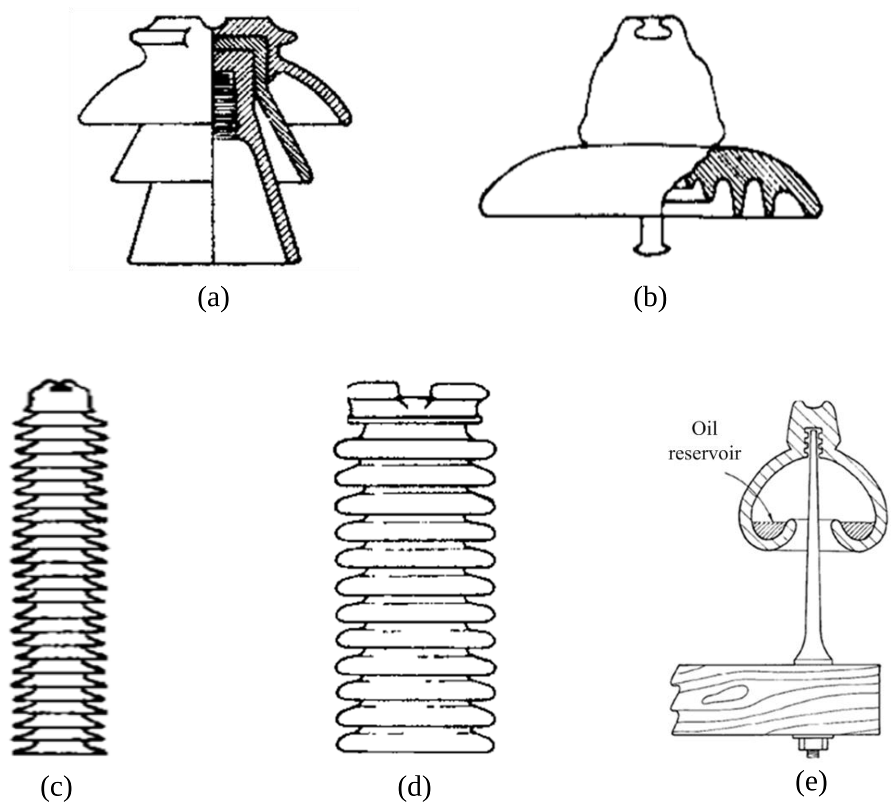

Figure 2-1: Evolution of early insulators [11]

In Figure 2-1, a series of evolutional developments of the early insulators relative to the corresponding increase in the operating voltages can be seen: (a) A 35 kV pin-type insulator designed around 1900, showing three nested porcelain shells [34]. This was the first pin-type insulator that was based on the earlier telegraph insulator; (b) The suspension insulator that was developed in the first decade of the 20th century for use on transmission lines with operating voltages 100 kV and above; (c) A 66 kV porcelain line post insulator and (d) A long rod insulator for use at 110 kV. Figure 2-1(e) shows an anti-contamination insulator that was initially used on the Lauffen-Frankfort 25 kV line in 1891 – the first transmission line that was designed by Brown. This insulator was equipped with annular oil reservoirs which served to inhibit the flow of surface current between the line on top and the iron support pin. The idea was specifically conceived to prevent surface "sparkover" under wet conditions [11]. The use of an anti-contamination insulator in 1891 suggests that the importance of contamination flashover phenomena can be traced back, along with high voltage transmission, to the time of the first electric installations [11, 12].

Amongst other pertinent requirements of a power line affecting reliability of supply, insulation coordination has increasingly become a challenging task. It has also been convincingly demonstrated, both from field experience and laboratory research, that insulator contamination problems become more acute when transmission voltages ramp up into high operating voltage levels for AC applications [11, 31]. So much so, it becomes a more interesting task with reference to the common trend of the increasing applications of high voltage direct current (HVDC) technologies when compared to AC applications [31].

Since the newer power lines span longer distances, it follows that they are subjected to a wide spectrum of varying environmental conditions [3, 4]. Consequently, the performance of insulators to be used on these power lines needs to be studied under polluted conditions in order to gain understanding of the resulting performance of the power lines and also to facilitate informed selection of appropriate insulators for specific areas. It has been stressed in reference [2] that the fallacy that dogged the insulator design in the earlier days was that water is the main enemy. The resistance to flashover of an insulator in polluted environments is determined by the following parameters [2, 30]:

- profile of the dielectric;
- orientation of the insulator, i.e. vertical, inclined or horizontal and;
- properties of the insulator surface, whether hydrophobic or rough/hydrophilic. Reference [3] confirmed that the properties of an insulator surface determine the mechanism of pollution flashover.

The above-listed parameters play a significant role in ensuring that an insulator bears its inherent functional requirement: the provision of adequate insulation with durable dielectric and mechanical strength [13]. This further ensures that the insulator would be able to sustain mechanical loads on the overhead line structure as well as offering an appreciably high resistance to harsh weather conditions throughout its entire service life. Thus, insulators can be defined in general as non-conductive devices that are used to provide electrical isolation between high voltage conductors (or apparatus) and the ground and also to provide mechanical support for the high voltage conductors as regards their mounting structures.

At normal atmospheric pressure, air is regarded as an ideal form of insulator [1-3]. However, the insulation properties of air are degraded by the presence of excessive electric stresses, typically over 30kV/cm [1]. Excessive electric fields may cause the air particles to ionize, thereby resulting in the breakdown of the air separation. Under these circumstances, air cannot satisfy the dual requirements of insulators: providing both electrical isolation and mechanical support. Thus, solid materials that have high strength dielectric properties and hydrophobic surfaces are the preferred option, especially in adverse environmental conditions where pollution is imminent [3, 30].

The role of insulators is to ensure power system reliability. A power system is comprised of a variety of equipment and machinery, some of which may be relatively expensive such as transformers, generators and circuit breakers [14]. For good system integrity, it is desirable that these apparatus be protected from conditions that could be harmful, for example lightning and power frequency overvoltages. During these conditions, it is therefore necessary that insulator flashovers due to dryband arcing may be minimized hence curbing power interruptions to customers. In this modernized era, industrial customers have begun to demand higher quality of electrical services, whereby not only does it become more difficult for to power utilities to provide stable voltage and frequency profiles, but where it becomes so pressing that the entire continuity of service reaches a renewed plateau [13]. It therefore becomes imperative that insulators be able to withstand sizeable magnitudes of system overvoltages. This would ensure that interruptions are minimized and that adequate protection/insulation is warranted. Power interruptions cost industrial customers dearly due to lost production or loss of process control [13, 14]. More so, power interruptions could lead to fatalities especially in critical hospital operations such as surgery [14].

2.3 Characteristics of Insulators

The performance of an insulator is predetermined by its electrical and mechanical properties. This section will therefore discuss the characteristics of the commonly used insulators, including popular types of insulators used to date.

2.3.1 Insulator types

There are a variety of insulator technologies that are used on power transmission lines to date. These insulators take on different shapes and are composed of different materials, hence providing different insulation capabilities. This section therefore presents a summary of some of the commonly used types of insulators for overhead power lines. The summary is presented in Table 2-1, detailing the type of insulator, description, materials used, insulator class and the installation orientation. All insulators for use on overhead power lines are categorized into two major insulator classes, viz. Class A and Class B [3]. Class A consists of insulators whose puncture distance is at least half their arcing distance and these insulators are regarded as unpuncturable. In contrast, Class B consists of insulators whose puncture distance is less than half their arcing distance and they are considered to be puncturable due to a short puncture distance. Refer to section 2.3.3 for the definition of puncture distance.

Table 2-1: A summary of the commonly used types of insulators on overhead power lines [3, 6]

High Voltage Overhead Power Line Insulators				
Insulator type	*Description*	*Materials used*	*Insulator class*	*Installation orientation*
PIN	Consists of an insulating component that is firmly mounted on a support structure, using a pin passing up inside the insulator. The insulating component is either separable from the pin or permanently affixed.	Porcelain, glass and resins.	Class B	Suspension positions
LINE POST	Comprises of one or more pieces of insulating material that are permanently assembled, with a metal base and sometimes with a cap. It is affixed to the support structure using a central stud or bolts.	Porcelain, glass and resins.	Class A	Suspension positions
COMPOSITE LINE POST	Consists of three main parts: load-bearing cylindrical insulating core, housing and terminating end-fittings attached to the central insulating core.	Composites: Fibreglass core, Silicone Rubber (SR) or Ethylene Propylene Rubber	Class A	Suspension positions
CAP-AND-PIN	Consists of a bell-shaped or disc-shaped insulating part, which can be affixed to the support structure using a cap with an inside axial pin.	Porcelain and glass.	Class B	Suspension and strain positions.
LONG ROD	Consists of a cylindrically cored insulating part fitted with sheds and terminated with external or internal metal end-fittings.	Porcelain and resins.	Class A	Suspension and strain positions.
COMPOSITE LONG ROD	Comprising of at least two insulating parts, viz. a core and housing, and terminated with metal end-fittings. This insulator is suited for use under tension.	Composites: Fibreglass core, Silicone Rubber (SR) or Ethylene Propylene Rubber	Class A	Suspension and strain positions.

2.3.2 Common insulator materials

2.3.2.1 Introduction

The properties of an insulating material are a key consideration in the design of an insulator [3]. Owing to the dual functions of an insulator (electrical insulation and mechanical support), it is critical that the material to be used is both dielectrically and mechanically sound. This ensures that the insulator will be capable of sustaining prolonged exposures to harsh electrical stresses without resulting in flashover failures. It also ensures the insulator is able to bear the tensile forces and other mechanical loads associated with the installation of the insulator [2-3, 13].

The principal insulating materials that are in common use today are ceramics and polymers [2]. The latter have gained popularity due their robust performance. Ceramic insulators include porcelain and glass insulators, whereas the polymeric insulators include composite polymers and epoxy resins. These four common insulating materials are discussed below.

2.3.2.2 Porcelain

These insulator materials were first introduced in the mid 1880's and they are still widely used today. The overall performance of porcelain is primarily determined by the manufacturing process and the quality of the raw materials used [2, 3, 5]. Porcelains usually have a finishing glaze which serves to provide a smooth surface [3, 5]. This glazed, smooth surface helps to inhibit the adherence of pollutants and also facilitates natural washing by rain. In addition, the glazing of the porcelain surface forms a compressive outer layer, with characteristic resistance to cracking and high mechanical (compressive) strength [3].

However, porcelains have low tensile and cantilever strength-to-weight ratios [3]. Also, they are susceptible to chipping due to poor resistance to thermal effects such as those experienced during power arcs [3, 5].

2.3.2.3 Glass

Glass insulators can either be made of 'toughened glass' or 'annealed glass' [3]. The former employs a differential rate of solidification, whereby the insulator surface is cooled in an accelerated manner whilst the interior is cooled slowly. This gives toughened glass insulators their high compressive strength features, which aid in preventing the formation of surface micro-cracks and also inhibit the propagation of cracks due to the highly compressed surface [2, 3, 5]. Toughened glass insulators have high dielectric strength and are resistant to electrical punctures and environmental effects such as ultraviolet (UV) radiation [2]. In contrast, annealed glass insulators have poor mechanical strength due to the imminent surface micro-cracks which tend to propagate through the volume of the insulator [3]. Toughened glass insulators do however have a tendency to shatter. They are also prone to leakage current erosion [2, 3].

2.3.2.4 Resins

These insulating materials have improved over the years, especially their resistance to UV radiation exposure [2]. Resins are strengthened by the incorporation of fibrous fillers. There is therefore a matrix resin that protects the fibres against invasions which would otherwise lead to the formation of micro-cracks [3]. The matrix resins can either be based on polyesters or epoxies [5].

Resin insulators can be made into a variety of shapes, and this makes them suitable for a number of applications. Epoxy resins are made of organic materials, which make them vulnerable to the effects of surface partial discharge activities [2]. They also suffer from leakage current erosion [2, 5].

2.3.2.5 Composite polymers

A composite insulator consists of a central fibre glass core for mechanical support. The core is usually enclosed with a housing to guard the core against adverse environmental attacks and also to provide the required electrical characteristics [2, 3]. At both ends of a composite insulator, the central core is bonded in some way to the high voltage conductor and the adjacent ground potential using metal end-fittings. The integrity of a composite insulator can therefore be viewed to be dependent on the resulting performance of these three elements: central core, insulating material and end-fittings. Housing materials are commonly made of ethylene propylene diene monomer (EPDM) or Silicone rubber [3]. EPDM enhances the mechanical strength and the resistance to tracking of the housing material, whereas silicone rubber allows for a high resistance to UV degradations and also maintains a hydrophobic (water repellent) surface. Silicone rubbers are gaining popularity due to their unique hydrophobicity characteristics and it has been established that they offer the best electric performance under contaminated environments when compared to other subordinate non-ceramics as well as porcelain and glass insulators [14]. The central core of a composite insulator comprises of continuous, uni-directional glass fibres in a matrix resin. The matrix resin could be based on epoxy, polyester or vinyl-ester types [5]. In addition, the two types of glass that are used for the fibres are the normal electric ‘E’ glass or the special acid-resistant ‘E-CR’ glass [3].

Polymeric composite insulators possess quite high tensile strength-to-weight ratio and attractive performance characteristics in polluted environmental conditions [2, 33]. However, care should be exercised during the design process to ensure that correct material and dimensioning are considered. This minimizes the susceptibility to leakage current erosion.

2.3.3 Physical design parameters

2.3.3.1 Introduction

In addition to the material properties of an insulator, the physical profiles and dimensions influence the resulting electrical and mechanical performance of an insulator [3]. The major design parameters that are commonly considered are the arcing distance, creepage distance and connecting length as well as the puncture distance. The definitions of these parameters are therefore given below and their significance to insulator performance is also briefly discussed.

2.3.3.2 Arcing distance

Arcing distance is the shortest distance between the insulator's metalwares at the two terminating end-fittings across which the operating voltage is usually applied [3-4, 6]. This parameter could be readily measured with a tightly pulled string across the two terminating end-fittings of the insulator [6], as depicted in Figure 2-2.

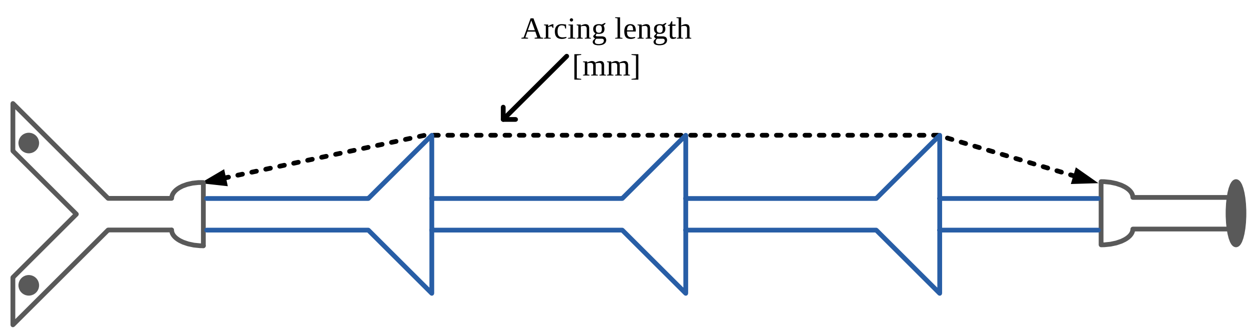

Figure 2-2: Arcing distance of an insulator

At a specified voltage level, the arcing distance of an insulator determines the type of insulator with a sufficient arcing distance to be used, in order to achieve electrical insulation requirements of the system. It is vital to ensure sufficient arcing distance since a failure to do so will render the system prone to power frequency and impulse flashover voltages even under non-polluted conditions [3].

2.3.3.3 Creepage distance

Creepage distance is the shortest distance traceable along the contours of the external surface of the insulator [3-4], between the metalwares at the two terminating end-fittings. This distance could be readily measured by sticking masking tape along the insulator surface [6], as depicted in Figure 2-3. This parameter is sometimes referred to as leakage distance [3].

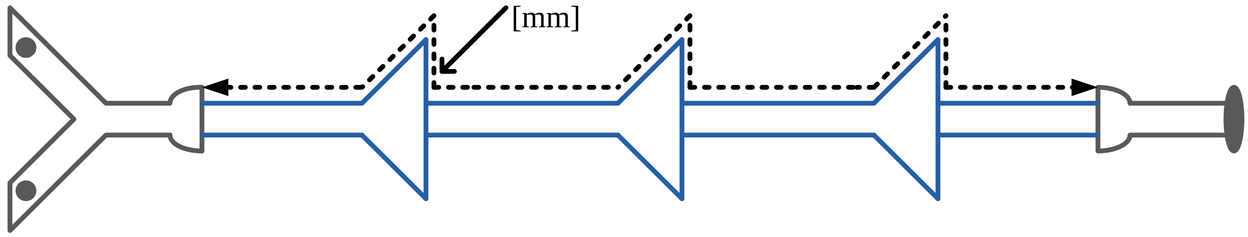

Figure 2-3: Creepage distance of an insulator

Creepage distance plays a critical role in determining the power frequency flashover voltage under polluted conditions [3-4, 6]. It is usually expressed in terms of *unified specific creepage distance [USCD]*, which is a quotient of the total creepage distance of the insulator in [mm] and the highest phase-to-ground voltage of the system in [kV] [6] – the actual voltage applied across the insulator. The units of USCD are therefore [mm/kV (U_m)].

2.3.3.4 Connecting length

This is the axial length of an insulator between the terminating end-fittings [6], usually considered for any two insulators of the same profile.

2.3.3.5 Puncture distance

Puncture distance refers to the shortest distance through the insulating material between the terminating end-fittings across which the operating voltage is usually applied [3].

A sufficient puncture distance ensures that the insulator does not become too susceptible to permanent damages that may be caused by overvoltages, especially those resulting from steep-fronted lightning impulses [3]. This parameter therefore plays a role in determining the puncture strength of the insulator [6].

2.4 Environmental and Climatic Effects on Insulator Performance

2.4.1 Overview

The previous sections have dealt with the effects of choice of insulator material and the consideration of insulator design techniques. Although these material and design aspects may be well coordinated, insulator performance is still found to be affected significantly by a number of environmental and climatic conditions [3, 6]. Some effects instantaneously lead to insulation failure, while others may cause a gradual degradation in the insulating properties of the insulator (often referred to as ageing), thereby eventually leading to insulation failure [6].

A major factor that affects insulator performance is the deposition of contaminants or pollutants that may render the insulator surface to be conductive. Other factors include precipitation, wind speed and direction, bird droppings and streamers and physical surface damages and human vandalism [3-5]. These factors are discussed below.

2.4.2 Pollution

The exposure of insulators to the environment subjects them to the deposition of pollutants onto their external surfaces [6]. The collection of deposits can either immediately cause a leakage current to flow along the insulator surface or it would require some form of wetting to become conductive [3-5] on an energized insulator. Therefore, there are two insulator pollution mechanisms: *pre-deposited pollution and instantaneous pollution* processes [3]. The former collects over a certain time stretch and it requires wetting to form an electrolytic layer depending on the solubility of the pollutants. Pre-deposited pollution can be either *active*, which contains soluble pollutants that can form a conductive layer when wetted or *inert*, which contains non-soluble pollutants and no conductive layer may be formed even in the presence of wetting. In contrast, instantaneous pollution contains pollutants that are readily electrically conductive even in the absence of any wetting mechanisms.

Common pre-deposited pollutions include salts, chemical deposits, fertilizers, bird excrements and many others [3-4]. Alongside, instantaneous pollution constitutes electrolytic pollutants such as salt fogs, coastal fogs, acid fogs or acid rains, crop sprayings and bird streamers [3, 5].

Moreover, there are other rare forms of pollution that may lead to insulator flashover [2]. These usually take on the form of electrically conductive pollutants which include carbon, metallic oxides and metals in dusty or powdery forms. These types of pollutants are commonly found close to railway lines, resulting from wheel brakes or the ablation of carbon or copper from conductors or panto graphs [2].

2.4.3 Humidity and Rain

Both humidity and rain can lead to the formation of an electrolytic layer on a polluted insulator surface [2-6]. Humidity is a measure of the extent of moisture content in the atmosphere. High levels of humidity, in excess of 75%, can lead to the wetting of the pollution deposits on the insulator surface [3, 5, 18]. This wetted pollution layer may cause leakage currents to flow along the electrolytic pollution layer of an energized insulator, thereby leading to the formation of dry-bands. The formation of dry-bands usually precedes electrical discharge activities such as arcing. These electrical discharge activities can pose detrimental ageing threats to the insulator surface. Excessive levels of humidity may however lead to the washing off of the pollution layer, thereby preventing the occurrence of insulator flashover [2, 5, 18].

In addition, rain can also cause the wetting of a pollution layer on the insulator surface leading to similar effects as those of humidity [4-6]. Rains in excess of 10 mm/h can cause the washing off of pollution, which can serve as a favorable effect [3]. However, acid rains can cause instantaneous pollution – causing rapid insulator flashover.

2.4.4 Solar radiation

Solar radiation is a spectrum of different types of radiation with different wavelengths and hence different energy levels, including high-energy UV-B photons [3, 5]. In particular, UV-B photons can cause ageing on polymeric insulator materials such as EPDM's and Silicon rubbers [5]. The heating effect of solar radiation can also cause wetting of insulator pollution deposits, when the insulator surface is heated to below the ambient dew point [3].

2.4.5 Wind speed and direction

Wind is one of the principal and most predominant carriers of pollutant materials onto insulator surfaces [2-6]. Other carriers include gravitational forces and electrostatic attractions of electrically charged particles [2]. The speed and direction of wind are critical in determining the quantity and nature of the pollution deposit onto the insulator surface. It has been found that there is a close relationship between the salt deposit density (SDD) and wind, exhibiting a cubic relationship, i.e. pollution deposit tends to increase with the increase in the wind speed to the power of three [3, 5]. Depending on the direction of wind, different types of pollutants may be deposited onto the insulator surface [2].

However, when strong winds containing suspended particles blow over an insulator, pollution deposits may be removed from the insulator surface. Additionally, the efficiency with which an insulator may catch pollutants is dependent on the insulator profile, as well as on the size and density of the particles contained in the wind and also the speed of wind thereof [2, 4].

2.4.6 Bird droppings and streamers

In areas where birds are commonly found, there is a likelihood of finding bird droppings on insulator surfaces. These are organic in nature and can be conductive when wetted, thereby causing leakage currents to flow, leading to insulator flashover [32]. Another isolated case is the instantaneous flashover that can result from the presence of bird streamers, which are highly conductive strings of bird excrements with 20-40 kΩ/m conductivities called streamers [3, 5]. These streamers can reduce the air gap, resulting in air break down and then causing the air gap to flashover [1]. Insulator characteristics do not however have any direct role to play in this type of flashover, but the high energy power electrical discharges that may occur could greatly damage the insulators [3, 32].

2.4.7 Physical damage and human vandalism

Animals such as birds, rodents and termites are found to cause physical damage to insulator surfaces, especially on polymeric insulators [3, 5]. This physical damage aggravates the ageing process of insulators.

Owing to the enticing glazed appearances of ceramic insulators, it is found that they tend to fall victim to human vandalism as well as being easily tampered with by animals due to their brittleness [3]. Once the glazing of a ceramic insulator is damaged, pollutants can easily gain access to the core material of the insulator and thereby aggravate material ageing [5].

2.5 Indicators of Insulator Failures

2.5.1 Introductory remarks

Reliable operation of an insulator requires that both its electrical and mechanical strengths are reasonably sound. This highlights the importance of constant monitoring of an insulator's performance in order to ensure that the insulator does not exceed the limits of its electrical and mechanical integrity; thereby reducing insulator failures. The types of insulator failure mechanisms are material and design specific [3]. Therefore, adequate knowledge on the possible modes of failure and their likely causes is required for specific types of insulators. This will greatly facilitate informed decisions on the choice of insulators for given service conditions, as well as devising appropriate maintenance and inspection procedures. Remedies for any degradation conditions affecting insulators may thus be identified and counteracted.

The circumstances that lead to insulator failure/degradation may be systemic or random in nature [2]. Some conditions can lead to abrupt insulator failure, while others may first lead to the degradation of one or several material insulating properties and then eventually cause total insulator failure [5].

Before discussing the common failure modes of the different types of insulators, as discussed in section 2.3.2, a brief introduction to common types of insulating material ageing modes are presented below. These ageing modes would usually be discovered through visual inspections of the insulator surface, and they are often irreparable [6]. The common ageing modes include discoloration, chalking, crazing, dry-bands, tracking and erosion [6-7, 28]. Each of these ageing modes is explained below, with their typical visual appearance depicted in Figure 2-4 . Some of the photographs used here have been adapted from references [7] & [28].

Discoloration: a change in the base color of the housing material of the composite insulator.

Chalking: appearance of rough and powdery surface, due to some filler particles of the housing material that have been exposed.

Crazing: comprises of surface micro-fractures of depths approximately 0.01 to 0.1 mm.

Dryband: a trace that is left on the insulator surface after a dryband activity had occurred.

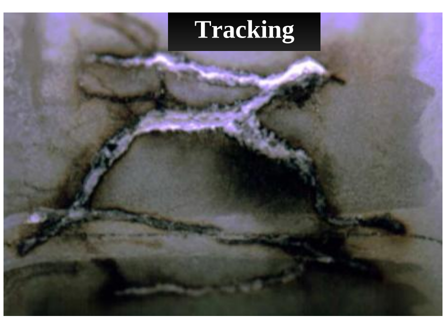

Tracking: irreversible degradation by the formation of conductive (even in dry conditions) paths starting and developing on the insulating material surface due to arcing. Tracking is only typical for carbon-based polymers.

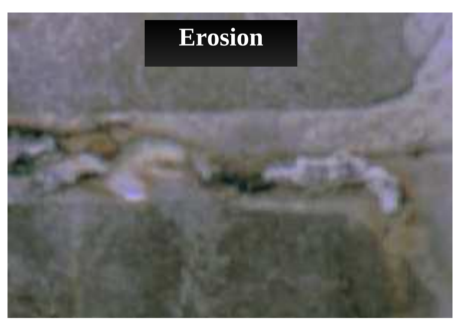

Material erosion: a visible evidence of the loss of material on the insulator surface. It may be uniform, localized or tree-shaped, and it may appear like tracking. However, the eroded area is not electrically conductive.

Figure 2-4: Common insulating material ageing modes [7, 28]

2.5.2 Porcelain insulators

Class B types of porcelain insulators are prone to electrical puncturing that is caused by steep-fronted lightning impulses [3, 6, 34]. Cracking is however the most dominant form of failure that is found in porcelain insulators. This may result from rough handling or vandalism or can also be caused by the effects of rapid thermal changes and uneven heating. High-energy electrical discharge activities (with uneven heating effects) such as power arcs can therefore potentially cause porcelain insulators to form cracks, which can lead to mechanical failure.

2.5.3 Glass insulators

The dominant failure mode for glass insulators is shattering, caused by the presence of inclusions of impurities of raw materials that might have escaped weeding out during thermal shock tests or particles that may have been leached out from the wall of the glass furnace [3-5]. Steep-fronted impulse activities also tend to aggravate this type of shattering [6].

Under HVDC applications, ionic currents tend to cause a buildup of electrical stresses, which further lead to ionic migrations within impurity inclusions [3, 31]. These ionic migrations can lead to the buildup of excessive internal mechanical stresses, thereby causing the insulator to shatter. Shattering can also be caused by physically tampering with the insulator.

2.5.4 Resin insulators

Epoxy resin insulators are found to be dominantly affected by UV radiation, which causes them to be prone to chalking [3]. This may render the insulator electrically incompetent, especially in harshly polluted service conditions.

2.5.5 Polymeric insulators

The aggregate failures of composite insulators emanate from problems within the insulator housing, the core or the terminating end-fitting metalwares [3]. Housing materials of composite insulators are prone to erosion and tracking caused by high-energy electrical discharge activities [6]. Tracking causes a reduction in creepage distance [3], leading to escalated probabilities of insulator flashover. Additionally, erosion can be deep enough to expose the core and it can also cause puncturing to occur on insulator shed [5] - leading to the reduction of creepage distance. Erosion and tracking are very particular to specific housing materials. It should be noted that UV radiation has been found to exacerbate the effects of tracking and erosion [3]. Effects of UV radiation can also cause crazing and cracking on insulators that are not sufficiently UV stabilized. However, modern as well as silicone-based housing materials have been made with UV stabilizer capabilities [3, 6].

Further, the degradation of the core can either be caused by direct or induced effects. Direct effects usually result from electrical discharge activities. Alternatively, a core may be exposed due to damaged insulator housing materials. This leads to the occurrence of electrical discharge activities, thereby rendering the core surface susceptible to tracking and erosion. If a sizeable portion of the core is eroded away, it may lead to a loss of mechanical strength or deterioration thereof [6]. Composite insulator cores may also be prone to mechanical failure called *brittle fracture*, which occurs when the insulator is subjected to loads that may be well below the damage limit level [3, 5-6], usually under combined effects of acid and tensile forces.

Damages to the terminating end-fitting metalwares seldom occur [3]. However, if not equipped with some means of arc protection, power arcs may cause end-fittings of the insulator to melt or evaporate, rendering the insulator incapable of supporting the core. Aluminium alloy end-fitting metalwares are known to be the most susceptible in this regard [3].

2.6 Basic theory on Insulator Pollution Flashover

2.6.1 Introductory remarks

As highlighted in the previous section, it is important that an insulator be constantly monitored to keep track of the probabilities of flashover. It is therefore good practice to keep a constant check on insulators' performance indicators and service conditions [3, 6, 8] in order to devise informed maintenance procedures and to employ proactive measures as remedies for insulator ageing. This necessitates a thorough understanding of the physics of the insulator pollution flashover process. This section will therefore provide a discussion of the mechanics of a typical pollution flashover process and the general antecedent activities that are generally found to prevail before flashover.

The important aspects to consider in insulator pollution studies will also be reviewed in this section. Additionally, existing methods for predicting insulator pollution flashover will be discussed.

2.6.2 Pollution flashover process

The apparent catastrophe of pollution flashover is that electrical discharges are produced, which can be harsh enough to cause significant deterioration of the insulator housing material [2]. The underlying cause of flashover stems from the flow of leakage current that causes the drying out of the pollution electrolytic film on the insulator surface [2, 7], leading to the formation of dry bands. For energized insulators, the operating voltage that is applied across these dry bands can create sizeable electric stresses that may lead to the ionization of the air separation across the dry band (gap) [2-4, 6-8]. This therefore gives rise to the inception of electrical discharges, with a pronounced probability of arcing – thereby causing total flashover as long as the enticing pollution conditions persist [7, 30].

The formation of electrolytic film on an insulator surface is dependent on the adhesive properties of the insulating material [3, 9]. There are two major classifications of surface conditions [3, 6]: *hydrophobic and hydrophilic.* These two surface conditions define how easily an electrolytic film can form on the surface of a polluted insulator. Polymeric insulators are generally hydrophobic, which means that an electrolyte beads up into separate droplets inhibiting the formation of a continuous electrolytic film [3, 7-6]. In contrast, ceramic insulators have enticing surface properties that render them susceptible to the formation of a continuous electrolytic film and hence are referred to as hydrophilic.

The list below presents some of the common precursors of pollution flashover for hydrophilic insulators [2]:

- “Arrival of nearly pure water, as dew, rain or mist, at an insulator which carries a burden of pollution comprising soluble ionic components like common salt

- Deposition of droplets from marine or industrial fogs, or of other combinations of water and electrolyte

- Build up of hoar frost, freezing fog or ice on the fouled surface of an insulator, the ionic components of the fouling then proceeding to depress the freezing point of the water and allow solution at the interface

- Switching in of a circuit containing insulators which are wet and fouled

- Arrival of a temporary overvoltage, or of a switching surge, at an insulator which is wet, fouled and possibly already energized."

The first two conditions lead to the formation of a conducting pollution layer – hence a leakage current will flow on the insulator surface, whereas the last two conditions aggravate flashover probability on a wet and polluted insulator. Due to the heating effect associated with leakage currents, a portion of the pollution layer (the conducting portion) will be dried out to form a dry band (usually very narrow, few centimeters wide) [7]. The operating voltage is then applied across the dry band, causing the breakdown of the insulating properties of the separating air across the dry band [8, 9]. The dry band may therefore be bridged by arcs, leading to a complete flashover event.

The flashover process is summarized on the flowchart below,

Figure 2-5. It should be noted that the pollution flashover process is a result of the interaction between the insulator surface and its surrounding environmental conditions.

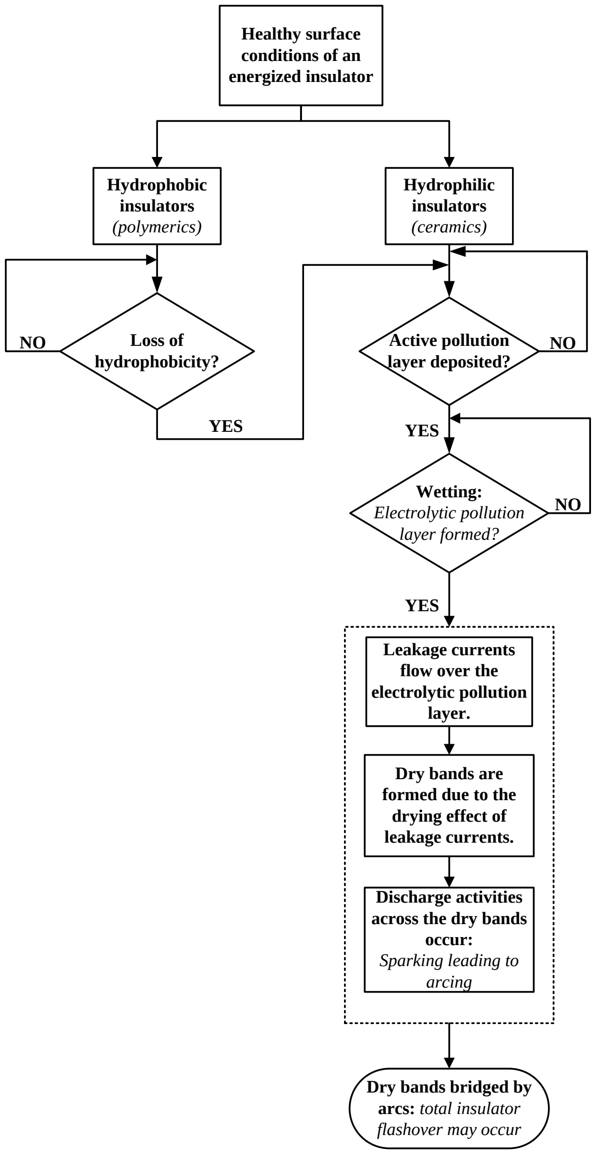

Figure 2-5: Basic insulator pollution flashover process

2.6.3 Important aspects for insulator pollution studies

The significance of insulator pollution studies is to understand the performance of insulators under certain polluted service conditions. This could help with the identification of imminent insulator failure. The resulting performance is a consequence of the interaction between the insulator housing material, pollution deposits, environmental and climatic conditions for an energized insulator [2-3, 33].

It therefore follows that the major aspects that play a defining role in pollution deposition process will include:

- Insulating material properties

- Insulator physical design properties
- Nature of pollutant deposits
- Environmental and climatic conditions
- Operating voltage

Noting that insulators would normally be subjected to a variety of service conditions, it should be understood that each insulator test environment would yield unique observations [10]. Therefore, it makes sense to study the interaction of insulators in relation to their service environmental and climatic conditions. This allows for general trends to be conceptualized, irrespective of test location or conditions. As a result, it was decided by the CIGRE Task Force 33.04.03 that all parties involved in insulator pollution studies share their experience in order to gain deeper insights into the science of field performance of insulators [7, 10]. The *Round Robin Pollution Monitor Study Test Protocol* was thus conceived by the CIGRE Task Force 33.04.03 to serve as a platform for this exchange of information [7, 10]. This protocol monitors the measurements of the following aspects [10]:

- Equivalent Salt Deposit Density (ESDD) in mg/cm^2
- Non-soluble Deposit Density (NSDD) in mg/cm^2
- Leakage current in Amps
- DDDG readings in µS/cm

Additionally, it is recommended in other literature that the following be studied in order to understand the insulator pollution flashover process [2-3, 7-8, 30]:

- Local climatic and environmental conditions surrounding the insulator
- Pollution deposition and wetting processes
- Visual inspections of the insulator surface conditions
- Electrical surface discharge activities on the insulator surface
- Electrical surface conductivity of the insulator

It is understood that it is the flow of leakage current over the electrolytic layer that usually leads to the formation of dry bands, causing flashover under high electric stresses. Therefore, it has been conventionally accepted that leakage current monitoring adequately defines the performance of the insulator under polluted conditions [3].

The figure below, Figure 2-6, depicts a typical fused-insulator testing circuit [2] that is typically used in insulator pollution studies.

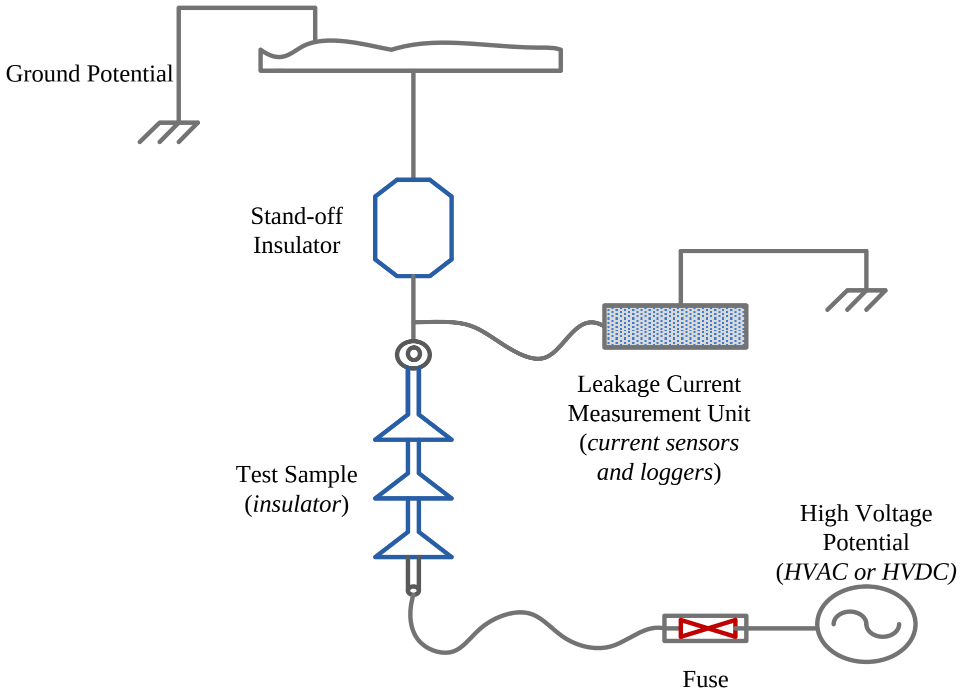

Figure 2-6: Typical fused-insulator testing circuit for pollution studies

2.6.4 Prediction of insulator pollution flashover

Leakage current is considered the key factor that leads to the degradation of insulators housing materials that in turn may cause electrical and/or mechanical breakdown of the insulating material. It is therefore crucial to monitor the current that flows over the pollution layer on the insulator surface. This section presents a brief summary of the well-known empirical reignition model referred to as the Verma I_{max} theory. The I_{max} theory postulates that the probability of insulator flashover reaches a critical value when the leakage current approaches a certain threshold [2-3]. This threshold, as defined in Equation(1), is considered to be the peak leakage current just a cycle before the insulator flashes over.

$$I_{max} = \left(\frac{S_{cd}}{15.32} \right)^2 \tag{1}$$

where S_{cd} is the specific creepage distance of the insulator, recorded in mm/kV (ph-ph rms). The parameter S_{cd} is the quotient of the total creepage distance of the insulator (in mm) and the system's highest phase-to-phase voltage in kV.

This helps in determining the risks of insulator flashover, by comparing all the measured leakage current values to the I_{max} of an insulator with a given specific creepage distance [7]. It has also been further proposed that there is a maximum permissible limit of leakage current. This permissible leakage current is defined by Holtzhausen as below [4, 7]:

$$I_{perm} = 0.25 \text{ x } I_{max} \tag{2}$$

where I_{perm} is the highest permissible peak value of the leakage current in Amps.

3. CHAPTER 3: Design and choice of test apparatus

3.1 Overview

This chapter describes the setup of the apparatus used in this research. The aspects listed below are discussed in the following sections:

- Design of the Koeberg Insulator Pollution Test Station (KIPTS) and the excitation voltage system;
- The choice of test insulators in relation to the research objectives;
- Brief details on the equipment used in the study: cameras (Corocam Mark I and 0-lux Sony camcorder) and the data monitoring devices for both leakage current and weather data.
- Calibration of the leakage current sensors

3.2 The Koeberg Insulator Pollution Test Station (KIPTS)

3.2.1 Introduction

A longstanding history of insulator pollution studies has provided insightful knowledge on the pollution flashover process of insulators over the years. Albeit, no definite theory has yet been fully conceived and all of the knowledge gathered so far seems to be continually undergoing research [11]. However, it can be appreciated that a judicious combination of the knowledge obtained from laboratory experiments and field work studies has made it possible to drive the design of power line insulators into a much improved plateau. It must be mentioned that the performance of insulators is heavily determined by the service conditions in which the insulator operates. Thus, laboratory experiments and field work studies cannot be expected to yield results that may be fully comparable due to the different test environments in which the studies have been conducted. This further means that the findings procured from laboratory experiments may not serve as a direct extrapolation for field work applications [34].

In order to gain firsthand understanding of the pollution performance of power line insulators under harsh pollution conditions, it was decided that this study be conducted at a natural marine polluted facility. This would provide a real observation on the pollution performance of an insulator when subjected to harsh natural pollution environments as opposed to artificial pollution studies which may sometimes have exaggerated or underrated pollution conditions. This study is particularly important for HVDC applications, given the fact that no comprehensive practical study on insulator pollution had been conducted under this type of excitation voltage [30, 35]. In contrast, the AC performance of most insulators has been amply explored using both the artificial and natural pollution approach [30].

3.2.2 Details on KIPTS

KIPTS was first designed and constructed in its original form in 1974, with the initial aim to study pollution performance of insulators under marine polluted conditions [26].

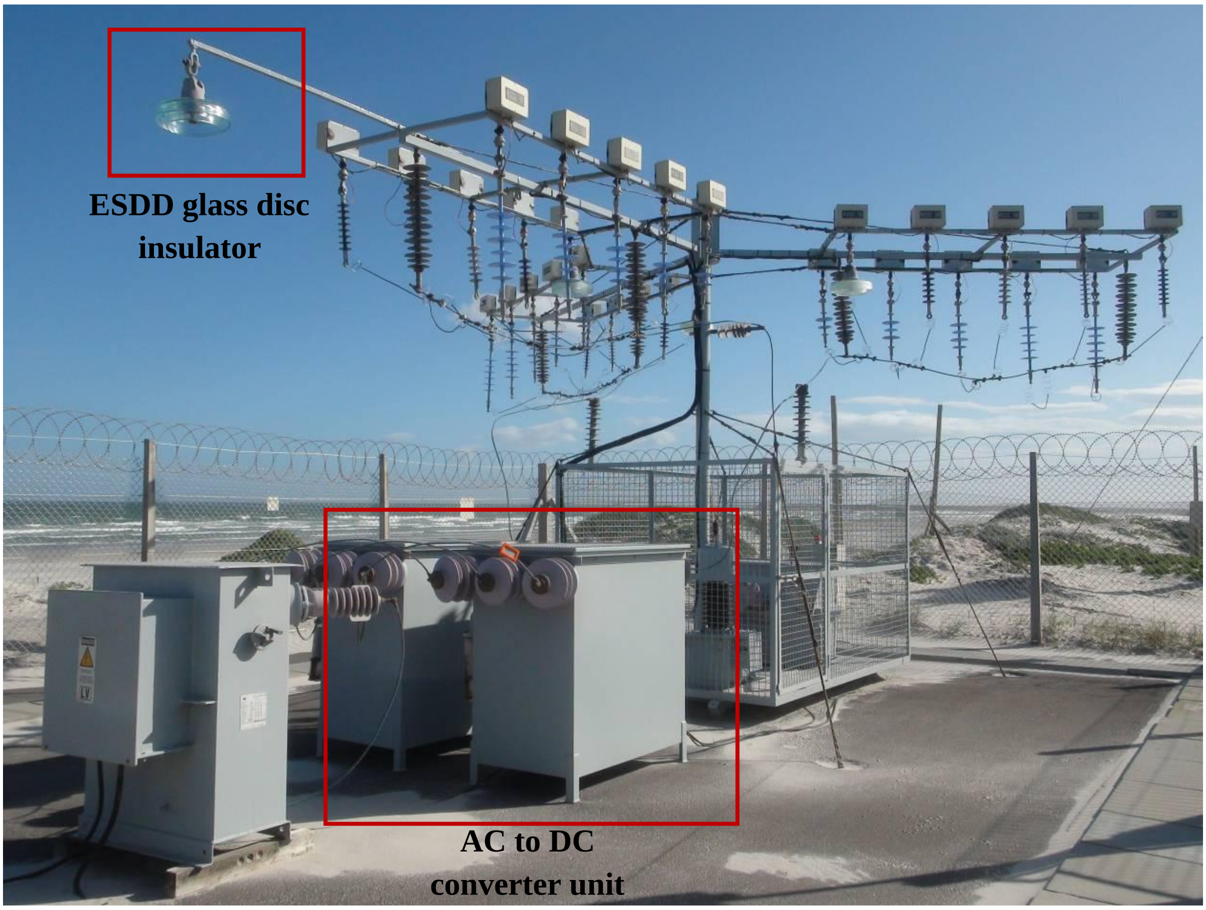

Figure 3-1: Complete configuration of the AC/DC test rig at KIPTS

Over the past years, KIPTS had gradually developed into an internationally recognized insulator pollution test facility, which is now widely used by both insulator manufacturers and academic researchers. Situated some 50 m in the east of the west coast of Cape Town near the Koeberg nuclear power station, KIPTS is a natural insulator ageing test facility, designed with the view to study pollution performance of insulators under marine polluted conditions. The pictorial representation of this test rig is depicted in Figure 3-1. KIPTS is characterized by hot dry summers, cold and wet winters, mist banks, strong winds and heavy marine pollution from the sea and it is often considered a harshly polluted environment, with a pollution index recorded to a value in the order of 2000 µS/cm [3, 15]. This pollution index is classified as "very heavy" and hence the reference to KIPTS as an accelerated insulator natural pollution test facility [3, 15]. The test rig is fitted with a control room (housing the measuring instruments), and leakage current and weather sensing facilities connected to the online leakage current analyzers (OLCA's) in the control room for data logging purposes. Further, it has been established that the results obtained from KIPTS over a one-year period are far more severe than those obtained from the IEC 5000-hour accelerated ageing test [3, 7]. Therefore, such severe pollution conditions at KIPTS may serve to validate the site as an ideal location that is representative of the harshest service conditions to which insulators may be subjected.

In addition to the environmental conditions, climatic conditions play a role in determining the type of pollutants that would be deposited onto the insulator surfaces. Figure 3-2 depicts a topographical representation of prominent sources of pollution that can be found in the surrounding of KIPTS [7, 16]. It must be stressed here that wind has been found to be the main carrier of pollution, causing directional deposition of pollution [17]. Industrial and marine pollutions are the dominant types of pollution experienced at KIPTS [15]. Thus, a variation in the wind direction determines the type of pollutants which may be deposited onto the insulators and this, in turn, varies with season changes. At KIPTS, wind blows in a dominant north-easterly direction in winter and south-westerly in summer [7]. As shown in Figure 3-2, the ocean lies to the west, whereas industrial areas lie to the south-east of the test site. Westerly winds will therefore tend to cause gusts of marine pollution, whilst the south-easterly winds give rise to the deposition of industrial pollutants.

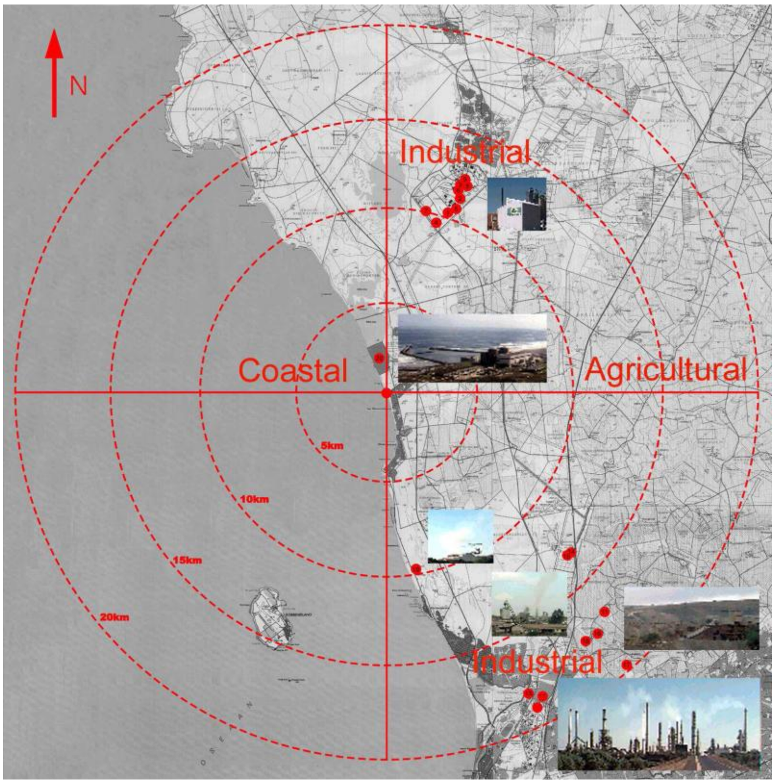

Figure 3-2: Topographical representation of prominent pollution sources in the surroundings of KIPTS [7, 16]

In summary, the following list gives an overview of the possible forms of pollution that emanate from the four compass directions in the surrounding of KIPS [3, 16 -15]:

- WEST: The wave action, sea breezes and misty banks generate enticing wetting conditions that cause an influx of moist conditions and salt particles. Westerly winds may also carry plankton toward the vicinity of the test site.

- NORTH: The breakwater wall at the Koeberg nuclear plant northward of KIPTS causes local salt mist banks to occur.

- EAST: The eastward direction is predominated by occasional veld fires, ploughing, harvesting and crop spraying on the agricultural area that lies to the east of KIPTS. On the north-east direction lies an industrial area within 10 - 13 km from KIPTS, emitting burnt diesel, coal and heavy fuel oil particles into the atmosphere which could be transported by south-easterly winds.

- SOUTH: There is a lime plant (Kilson) some 10 km southward of the test site, which is operational. To the south-south-east, heavy industries such as Kynoch Fertiliser Plant and Caltex Oil Refineries are the main causes of severe particle emissions.

The following table, Table 3-1, provides details on the additional pollution sources surrounding KIPTS.

Table 3-1: Additional pollution sources in the vicinity of KIPTS

Area	Source of pollution	Direction from KIPTS	Distance from KIPTS [km]	Type of pollution
Atlantis	Atlantis Diesel Engines	NNE	10	Burn diesel and coal
	Aries Packing	NNE	12	Burn diesel
	Baja Industries	NNE	12	Burn HFO
	Barbican Investments	NNE	10	Burn coal
	Biopolymers	NNE	11	Burn HFO
	Unita	NNE	12.5	Burn scrapwood
	Promeal	NNE	10	Burn diesel and coal
	Rotex	NNE	12.5	Burn coal and HFO
	SA Fine Worsteds	NNE	13	Burn coal and HFO
Duinefontein	Koeberg Nuclear	N	2	Burn diesel
Bloubergrand	Kilson Lime Works	SSE	10	Lime
Milnerton	Caltex Refinery	SSE	18	SOx, Nox, burn gas and oil
	Kynoch Fertilizer	SSE	18	Nox, CO2 and Particulate
	Fertilizer Producers	SSE	18	Nox, CO2 and Particulate
	Alpha Stone and	SE	17	Particulate
	FFS Refiners	SE	13	SO2, NO2 and burn HFO
	Wastetech	SE	13	Burn diesel
	CBS Ciolli Brothers	SE	17	Particulate
	Tygerberg Quarries	SE	20	Particulate
	More Asphalt	SE	17	Burn HFC

3.2.3 Excitation voltage system: AC, DC+ and DC-

The worldwide increase in the applications of high voltage direct current (HVDC) power lines has led to a shift in the paradigm of power system design, introducing new challenges that are not directly akin to those experienced on the traditional AC applications. For example, the issue of insulator pollution performance on AC applications cannot be directly extrapolated to the expected performance of certain insulators on HVDC power lines under the same climatic and environmental conditions. The best insulator on AC might be the worst on HVDC. The converse might also be true. This study therefore seeks to investigate the performance of the commonly used insulators under both AC and HVDC (bipolar) voltages when subjected to the same operating climatic and environmental conditions. Performance of most insulator types has been adequately studied in the past years for AC applications, whereas a limited number of studies have been conducted on HVDC insulator performance under laboratory conditions. No practical studies have been conducted on the performance of insulators under HVDC applications when subjected to harsh pollution environments. Thus, the need to study insulator performance under HVDC applications had necessitated that KIPTS be re-designed to accommodate HVDC energization with both positive and negative polarities. As a result, the test rig was revamped to support a total of thirty (30) test samples, i.e. ten (10) identical test samples for the three respective voltage types: AC, DC+ and DC-. All test insulators are exposed to the same pollution environment and all voltage sources (AC & DC) were tapped from a common supply transformer to ensure that all samples were subjected to the same electrical stress. The electrical configuration of the test rig is depicted in the circuit diagram below, Figure 3-3 [17].

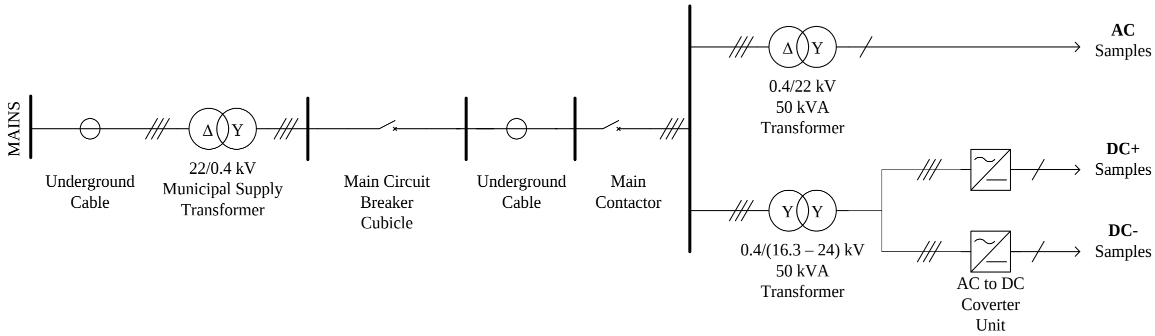

Figure 3-3: Electrical configuration of the test rig at KIPTS

The AC operating voltage is 22 kV (line-to-line RMS), whereas the DC voltage (both positive and negative) was designed to an equivalent line-to-neutral RMS voltage of 12.7 kV. Hence, all the voltage sources (i.e. AC, DC+ & DC-) were set to an effective energization level of 12.7 kV (line-to-neutral RMS) since the ageing performance of insulators is dependent on the electrical power dissipated across the insulator during surface electrical discharge activities. All the AC test samples were energized from a 50 kVA, 0.4/22 kV Δ/Y (Delta/Star) transformer, using only Phase A for all the ten AC test samples. The star point of this transformer was solidly connected to the station earth.

The DC system was designed and manufactured at the University of Stellenbosch. This system comprises of two separate converter units, each of which is suited with a three-phase pulse rectifier and a smoothing capacitor. The two units: DC+ and DC- are both fed from a

50 kVA, 0.4/(16.3 - 24) kV three-phase transformer, using an offline tap-changer. Technical specifications of the converter unit are shown in Table 3-2 [17].

Table 3-2: Technical specifications of the converter unit used for the DC voltage source

Developer & Manufacturer	University of Stellenbosch, Department of Electrical and Electronics Engineering, High Voltage Engineering Group
Rectifier type	3-pulse, with a grounded star point
Smoothing technique	Capacitor bank, with a ripple factor of 3% at 2A
Input voltage	16.3 - 24 kV, 3ϕ AC
Output voltage	13.3 - 19.6 kV, Bipolar DC
Primary phase current	1.2 - 1.8 A
Secondary maximum continuous current	2 Amps
Peak stored energy at 19.6 kV	3.3 kJ
Insulating/cooling medium	Main tank: **Air**, Diodes and capacitors: **Mineral oil**

3.3 Test insulator samples

In order to achieve the objectives of this study, as stated in section 1.3, a set of test insulators was chosen accordingly. The project dealt with two comparative studies: the analysis of the relative performance of different insulator materials and the evaluation of the impact of creepage distance on the resulting performance of insulators under harsh marine polluted conditions. It should, however, be mentioned that this thesis will only report on the aspect of creepage distance. Details on the analysis of the various insulator materials considered will be published in a separate report.

Factors that prominently influence the performance of insulators form a complex set of variables such as the climatic and environmental conditions (pollution deposits, wetting conditions, UV, etc), insulator's physical design parameters (insulating material, profile and dimensions), as well as the operating electrical conditions (power-frequency overvoltages, lightning, switching overvoltages, etc) [7, 18, 30]. The effects of creepage distance and the type of excitation voltage form the basis of this study. Thus, in order to assess the impact of creepage distance, a set of five high temperature vulcanized, silicone rubber (HTV-SR) insulators from the same manufacturer - with identical design profiles were used as test insulators. These insulators all had different creepage lengths. This was to ensure that the only variable under investigation was creepage length, whilst keeping other aforesaid factors common to all insulators. For compliance purposes, the insulators were chosen in accordance with the IEC 60815-3:2008 standard [19] – allowing for heavy pollution areas such as KIPTS. The test insulator with the shortest electrical length was therefore set to a minimum unified specific creepage distance (USCD) of 29 mm/kV (rms). Figure 3-4 shows the set of test insulators considered in this study. A similar set of these test insulators was installed on each of the excitation voltages: AC, DC+ and DC-.

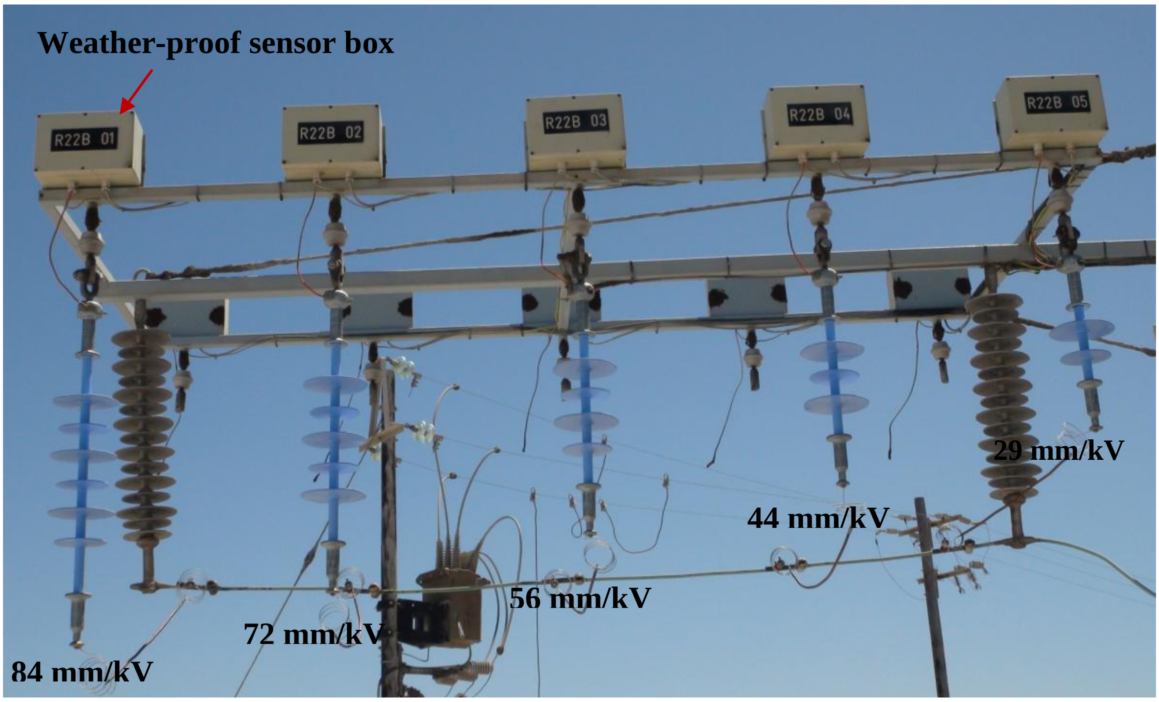

Figure 3-4: A set of HTV-SR test sinsulators with different creepage lengths installed on the test rig at KIPTS

The technical specifications of all the test insulators are detailed below.

Table 3-3: Technical specifications of the test insulators

Long-rod HTV-SR test insulators		
Creepage length [mm]	*Unified specific creepage distance - USCD [mm/kV]*	*Form factor*
1175	84	9.79
1010	72	8.71
780	56	6.40
615	44	5.48
400	29	3.26
Cap-and-pin DC glass disc insulator (reference)		
USCD = 42 mm/kV		

It should be mentioned that an explosive fuse, commonly referred to as a 'Mace fuse' was used as a means of over-current protection mechanism. This fuse was specifically designed to electrically isolate the test insulators from the busbar from which they are connected for all leakage currents exceeding 750 mA. The connection of test insulators to the busbar was designed in such a way that when the fuse explodes, the insulators should be able to be physically disconnected from the busbar. This was achieved by using a 'pig-tail' configuration as shown below.

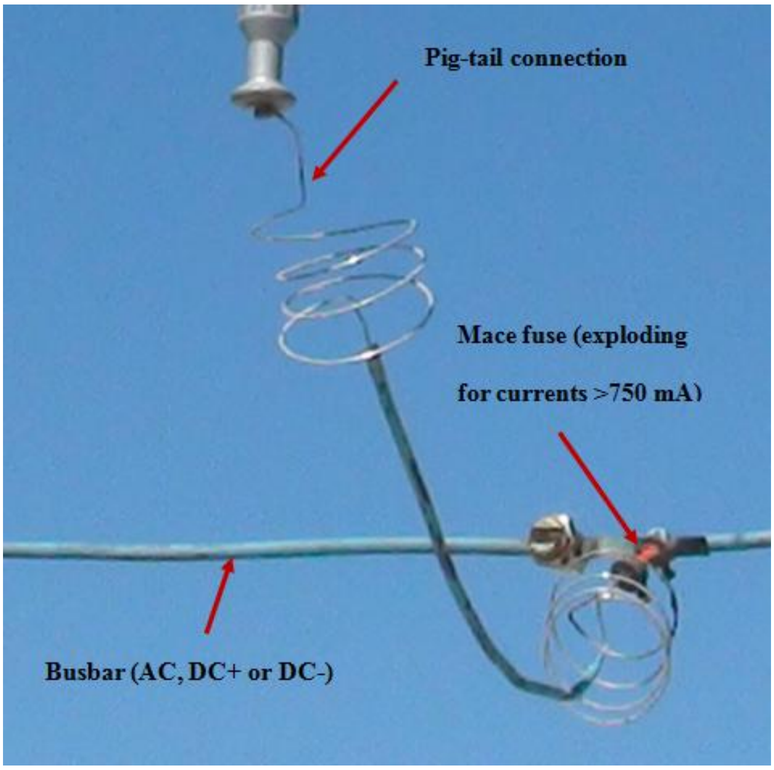

Figure 3-5: Pig-tail connection of test insulators onto the busbar and the incorporation of an explosive fuse (Mace fuse)

3.4 Video camera equipment

3.4.1 Introduction

Research has shown that the amount of power dissipation and the chemical processes that arise as a result of dryband activities significantly contribute to the ageing of insulators [11, 20, 30]. It was therefore crucial that, beside leakage current measurements and visual observations, the type and location of electrical discharge activities be observed. This helps to ascertain traces of any dryband activities that may be observed on insulator surfaces. It is unfortunate, however, that such electrical discharge activities (especially corona) that exhibit during dryband activities cannot be observed with a naked eye – their emissions fall within the ultra-violet (UV) spectral range, which is not visible to a human eye [20]. Thus, some means of UV-sensitive image intensive approach becomes necessary and this has led to the use of UV-sensitive, image intensifying cameras usually used at night [3]. Daytime UV cameras are also increasingly gaining use [20].

3.4.2 Corocam Mark I

The UV-sensitive, image-intensified camera commonly referred to as CoroCam Mark I (see Figure 3-6) has been used in this study. This camera was originally designed for use at the salt/clean fog chamber at the University of Stellenbosch and the Elandsbaai insulator test site in South Africa [3]. CoroCam Mark I is suitably equipped with a quartz lens and adjustable optical filters within a wide UV spectrum [3, 21-23]. Video footages of the observed electrical discharge activities can be captured using an external Sony video recorder and stored on MiniDV cassettes. A photograph of this recorder is shown in Figure 3-7.

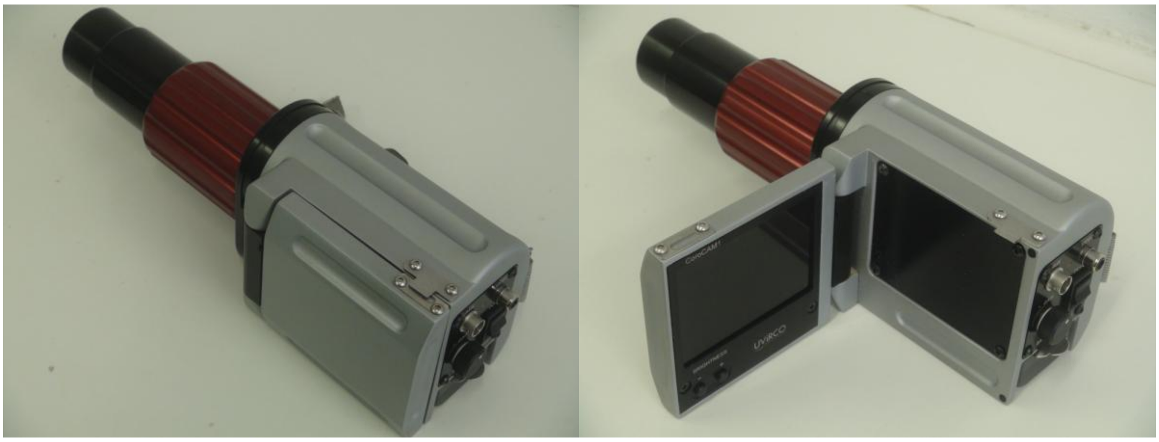

Figure 3-6: UV-sensitive, image intensified night observation camera - Corocam Mark I

Figure 3-7: Sony GV-HD700 external video recorder

Highlights of the technical specifications of CoroCam Mark I and the video recorder are given in Table 3-4 [21, 22].

Table 3-4: Technical specifications of Corocam Mark I and the video recorder

Parameter	Details
Optics	• A minimum focal range of 0.5 m with a focal length of 10 mm.
	• Adjustable filters having a wide range within the UV spectrum. These filters are useful to distinguish between the actual electrical discharge activities and
	• Producing a video output of both the electrical discharge activity and the actual object onto which the discharges are incident.
	• The sensitivity of the detector can be controlled using a built-in gain control mechanism.
Video display and capturing	• An adjustable LCD display is fitted on the side of the camera for real-time display.
	• Videos can be captured using an external recorder: Sony GV-HD700 and stored onto a standard MiniDV cassette.
Battery technology	• Camera uses rechargeable Li-Ion cells with a runtime of approximately three (3) hours.
	• Recorder uses rechargeable InfoLithium batteries and it displays the remaining battery life.

3.4.3 0-lux Sony camcorder

An additional camera was used for both the night observations and for capturing photographs during surface inspections of test insulators. Figure 3-8 shows a picture of the 0-lux Sony camcorder that has been used. This camera was used with the view of identifying a better camera that would be more successful in ascertaining the location of electrical discharge activities. Although Corocam Mark I is well suited for the detection of electrical discharge activities, it was not possible to obtain a clearly focused view of the intense electrical discharge activities such as dryband discharges due to saturation limitations. This limitation therefore makes Corocam Mark I inadequate in ascertaining the precise location of the electrical discharge activity.

Figure 3-8: 0-lux (HDR XR550) Sony camcorder used for the night observations and photo capturing during surface inspections

3.5 Data logging system

A correlation between the actual leakage current that flows on an insulator surface and the prevailing environmental and climatic conditions has been established in the literature on insulator pollution studies [3, 7, 33]. As commonly understood, a leakage current can flow over the surface of an energized insulator when the pollution deposits which may be existent on the surface of the insulator form a conductive electrolyte during wetting conditions. This indicates that it is the type of pollutants (environmental aspect) that would determine the conductivity of the conductive electrolyte that forms during enticing wetting conditions such as high humid conditions, fogs and mists. It was therefore decided that both leakage current and the environmental and climatic parameters be monitored in order to obtain full details on the operating conditions that affect insulator pollution performance. A commercially available real-time logging system was adopted for purposes of leakage current and weather data recording. Environmental conditions were monitored using procedures detailed in section 4.2.2.

The data logging system used in this study comprises of a complete set of leakage current and weather sensors for leakage current and weather monitoring respectively. This logging system is a South African product, designed by CT Lab (Pty) Ltd and it has gained international applications in insulator pollution studies. It is commonly known as the Online Leakage Current Analyzer (OLCA) as it was mainly designed to perform online monitoring of live insulators installed in the field [5, 7]. A front view of the OLCA is shown in Figure 3-9.

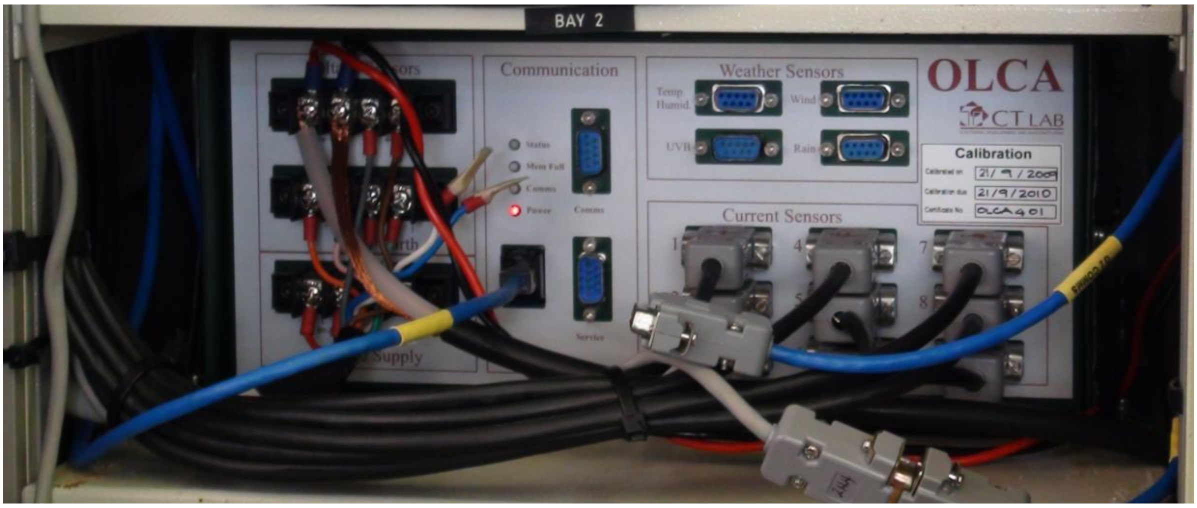

Figure 3-9: Front view of the online leakage current analyzer (OLCA) for current and weather data logging

A complete installation of a single logging system unit consists of the following:

- One (1) OLCA
- Nine (9) hall-effect current sensors
- One (1) combination temperature and humidity probes
- One (1) combination wind speed and direction sensor
- Tipping bucket rain gauge
- UV-B sensor
- Cabling connection of sensors to the OLCA

Figure 3-10 depicts the sensing devices for both leakage current and weather monitoring.

All the logged data is stored on an onboard storage space and can be retrieved via a high speed RS232 communications port onto a dedicated workstation computer.

The OLCA records leakage current parameters that are either measured directly by the sensors or those that have been derived from the measured values. The leakage current sensors have been contained in a weather-proof box in order to guard them against inclement weather. Refer to Figure 3-4.The leakage current acquisition system has a sampling accuracy of 0.5 % of full scale at a sampling rate of 2 kHz, which yields 40 samples/cycle in a 50 Hz system. Data is sampled continuously and all desirable parameters are stored every 10 minutes. The retrievable leakage current parameters include:

- Positive and negative peak leakage current values [mA]
- Absolute peak leakage current [mA]
- Positive and negative average leakage current [mA]
- RMS leakage current [mA]
- Daily peak leakage current and supply voltage waveforms
- Average dissipated power [W]
- Positive and negative integrated charge [C]
- Integrated leakage current squared or accumulative coulomb-ampere [CA]
- True power dissipation [W]
- Energy [J]

Figure 3-10: Components of the leakage current and weather data logging system used at KIPTS

The following climatic parameters can be retrieved from the OLCA, which may have been directly recorded or calculated at 1 % accuracy. All monitored parameters are continuously sampled at 1 Hz continuously, and stored every 10 minutes.

- Wind speed from 0 to 60 m/s and direction from -0.5 ° to 357.5 °
- Relative humidity [%]
- Ambient and Dewpoint temperatures from -50 °C to 50 °C

- Vapour pressure [hPa]
- Precipitation (rain) in steps of 0.1 mm
- UV-B radiation from 0 to 400 mW/cm^2, within the wavelength range of 280 to 315 nm

3.6 Current sensor calibrations

3.6.1 Introduction

For purposes of accurate leakage current measurements, it was crucial to ensure that the measurement instruments were accurately calibrated. The major components of the leakage current measurement system comprises of the leakage current sensors (both AC and DC) and the online-leakage current analyzers (OLCA's). The latter were calibrated by the manufacturer (CTLab (Pty) Ltd), whereas a comprehensive calibration test on all the installed leakage current sensors was done by the author along with the technical assistance from the personnel at KIPTS.

A predetermined current was injected through the sensors and a corresponding value was recorded from the OLCA and then the two values were compared against each other to establish the linearity of the current sensors. In addition, an assessment was done to determine the dynamic linearity range of the sensors.

3.6.2 AC sensors

The block diagram shown in Figure 3-11 depicts the circuit configuration that was used to run the linearity test for the AC leakage current sensors. All components used for the linearity test are illustrated on the block diagram. The input current to the sensor is labeled as I_{input}, whereas the current that was measured from the OLCA is labeled as I_{output}.

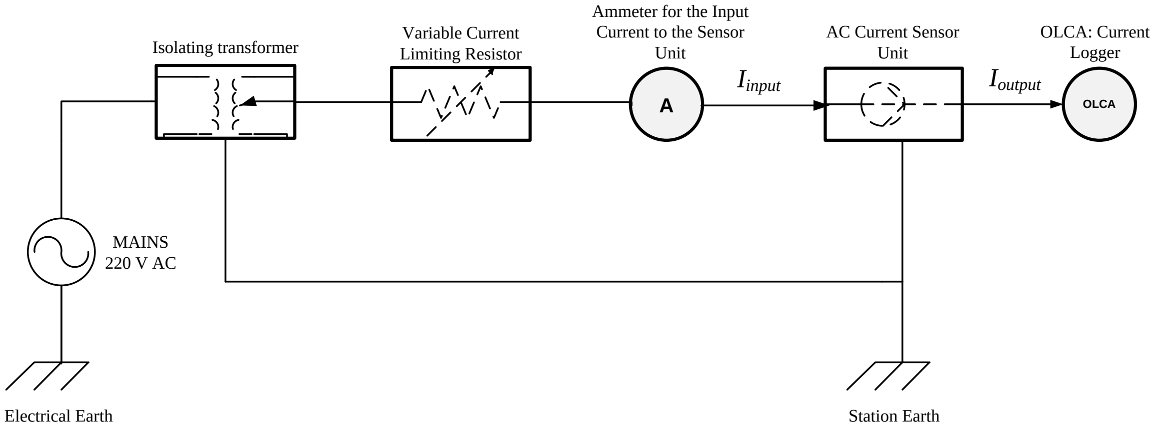

Figure 3-11: Block diagram for the linearity tests of the AC leakage current sensors

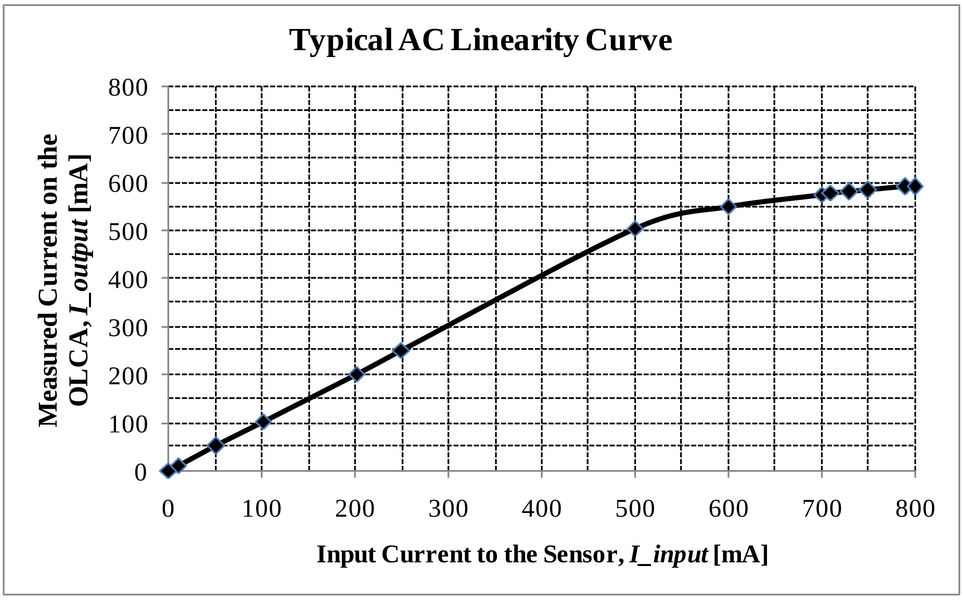

Figure 3-12: Typical calibration curve for the AC leakage current sensors

From Figure 3-12, we can see that the AC measuring system has a dynamic linear range of up to about 500 mA. The average ratio of I_{output} to I_{input} was found to be approximately 1.00 within this range, which indicates a good degree of linearity of the current sensors. As evident from the graph in Figure 3-12, it can be observed that the linearity deteriorates for input current values exceeding 500 mA (saturation point). This would thus mean that even if a value of 800 mA were to flow on the insulator surface, only a maximum value of about 600 mA would be recorded – equivalent to 849 mA (peak). Please note that the AC current measurements were recorded in root mean squares (rms).

It must be mentioned that the OLCA has a measuring range of 500 mA (rms) and this might have been the factor that has led to the limitation of the measured values.

The linearity results for all the AC sensors are presented in Table 3-5. Note that the reference to the sensors bears the name of the respective test insulators to which they are associated. Refer to section 4.1 for details on the naming convention used.

Table 3-5: Linearity test results for all the AC leakage current sensors

HTV-SR 84 AC		HTV-SR 72 AC		HTV-SR 56 AC		HTV-SR 44 AC		HTV-SR 29 AC		Glass disc 42 AC	
I_{input} *Sensor* [mA]	I_{output} *OLCA* [mA]	I_{input} *Sensor* [mA]	I_{output} *OLCA* [mA]	I_{input} *Sensor* [mA]	I_{output} *OLCA* [mA]	I_{input} *Sensor* [mA]	I_{output} *OLCA* [mA]	I_{input} *Sensor* [mA]	I_{output} *OLCA* [mA]	I_{input} *Sensor* [mA]	I_{output} *OLCA* [mA]
0	0	0	0	0	0	0	0	0	0	0	0
10	10	11	11	10	10	10	11	12	12	10	10
51	51	50	50	51	51	48	48	52	52	50	51
101	102	100	101	99	99	99	100	99	100	102	103
201	201	202	203	202	202	200	201	200	201	202	203
249	250	250	251	250	251	251	252	250	251	250	251
500	505	500	503	500	509	500	502	500	508	500	510
600	549	510	511	520	520	520	520	510	509	510	512
700	575	530	526	530	526	530	524	520	517	530	526
710	578	550	534	550	536	540	530	530	522	540	533
730	580	600	558	600	559	550	536	540	531	550	537
750	584	700	584	690	585	600	558	550	533	600	557
790	590	800	602	800	605	700	584	600	554	700	586
800	591					800	603	700	580	800	605
								800	598		

3.6.3 DC sensors

The circuit confirguration for the linearity tests performed on the DC leakage current sensors was slightly different from the arrangement employed for AC. The components for the test arrangement are illustrated on the block diagram in Figure 3-13. The current that was injected through the sensors is denoted as I_{input} on the block diagram, whereas the current that was measured from the OLCA is labeled as I_{output}.

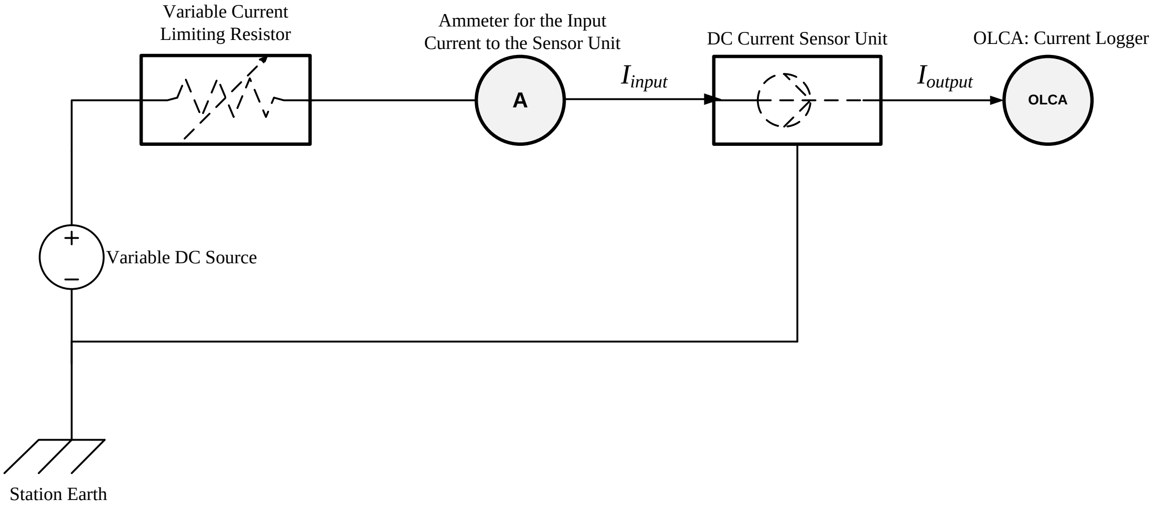

Figure 3-13: Block diagram for the linearity tests of the DC leakage current sensors

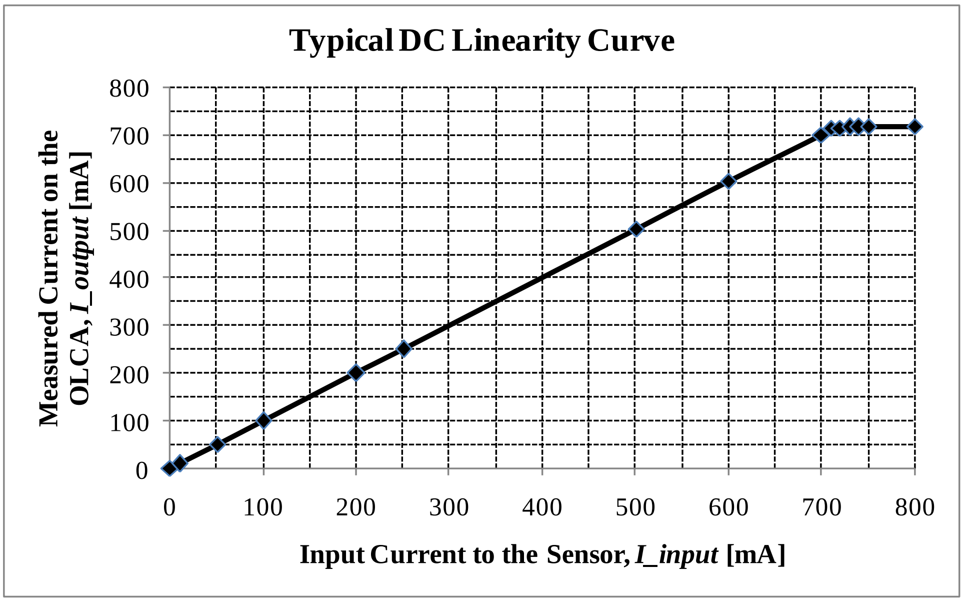

Figure 3-14: Typical calibration curve for the DC leakage current sensors

A typical linearity curve for all the DC leakage current sensors is shown in Figure 3-14. This is representative of both DC+ and DC- sensors. It should be indicated that the DC measurements were recorded in peak values, which means that the DC values were $\sqrt{2}$ higher than the AC values. We can see that the dynamic linear range for the DC measuring system is between 0 and 700 mA (an equivalent of a range between 0 and 495 mA in rms values). As noted for the AC measurements, it appears again that the OLCA measuring range had imposed a clipping effect on the measured values beyond 500 mA (equivalent to 707 mA). This is evident from Figure 3-14, where the dynamic linear range only goes up to about 700 mA.

All sensors (both AC and DC) have been found to be linear within the range between 0 and 500 mA (rms). This translates to an observation that the leakage current measuring system would be capable of measuring peak current values up to 707 mA within the dynamic linear range. All input values exceeding 707 mA (peak) would be clipped to a saturation level of 720 mA.

A summary of all the linearity test results for both DC+ and DC- leakage current sensors is given in Table 3-6 and Table 3-7, respectively. Again, all sensors are annotated with reference to their associated test insulators.

Table 3-6: Linearity test results for all the DC+ leakage current sensors

HTV-SR 84 DC+		**HTV-SR 72 DC+**		**HTV-SR 56 DC+**		**HTV-SR 44 DC+**		**HTV-SR 29 DC+**		**Glass disc 42 DC+**	
I_{input} *Sensor* [mA]	I_{output} *OLCA* [mA]	I_{input} *Sensor* [mA]	I_{output} *OLCA* [mA]	I_{input} *Sensor* [mA]	I_{output} *OLCA* [mA]	I_{input} *Sensor* [mA]	I_{output} *OLCA* [mA]	I_{input} *Sensor* [mA]	I_{output} *OLCA* [mA]	I_{input} *Sensor* [mA]	I_{output} *OLCA* [mA]
0	0	0	0	0	0	0	0	0	0	0	0
10	10	10	9	10	11	10	10	10	10	10	10
51	51	50	49	50	51	51	51	51	50	50	50
100	100	101	100	100	100	101	101	100	99	100	99
200	200	201	200	201	201	201	201	200	199	200	199
251	250	250	249	250	251	250	250	250	248	251	248
500	503	500	501	500	502	500	508	500	499	500	488
600	603	600	605	600	607	600	605	600	597	600	588
700	700	700	704	700	705	700	707	700	702	700	696
710	714	710	710	710	709	710	716	710	707	710	708
720	716	720	715	720	713	720	717	720	714	720	713
730	717	730	715	730	713	730	718	730	715	730	719
740	717	740	716	740	714	740	718	740	715	740	719
750	717	750	716	750	714	750	718	750	716	750	719
800	717	800	716	800	714	800	719	800	716	800	719

Table 3-7: Linearity test results for all the DC- leakage current sensors

HTV-SR 84 DC-		**HTV-SR 72 DC-**		**HTV-SR 56 DC-**		**HTV-SR 44 DC-**		**HTV-SR 29 DC-**		**Glass disc 42 DC-**	
I_{input} *Sensor* [mA]	I_{output} *OLCA* [mA]	I_{input} *Sensor* [mA]	I_{output} *OLCA* [mA]	I_{input} *Sensor* [mA]	I_{output} *OLCA* [mA]	I_{input} *Sensor* [mA]	I_{output} *OLCA* [mA]	I_{input} *Sensor* [mA]	I_{output} *OLCA* [mA]	I_{input} *Sensor* [mA]	I_{output} *OLCA* [mA]
0	0	0	0	0	0	0	0	0	0	0	0
10	10	10	12	11	10	10	9	10	9	11	10
50	50	50	52	51	50	51	49	50	49	50	50
100	100	100	102	101	99	100	99	101	99	100	99
201	200	201	202	200	197	201	200	201	199	201	199
250	249	250	251	250	247	251	249	251	249	250	249
500	487	500	497	500	488	500	494	500	493	500	490
600	590	600	598	600	592	600	592	600	594	600	600
700	689	700	695	700	686	700	694	700	693	700	696
710	700	710	703	710	699	710	706	710	702	710	705
720	712	720	709	720	703	720	712	720	708	720	714
730	712	730	708	730	709	730	713	730	710	730	714
740	714	740	706	740	710	740	714	740	711	740	714
750	714	750	705	750	711	750	715	750	711	750	714
800	715	800	700	800	712	800	715	800	712	800	714

4. Chapter 4: Research procedures and methodology

4.1 Overview on insulator monitoring procedures

This chapter presents descriptions of all test procedures and methodology used in this research. With reference to the research objectives, as outlined in section 1.3, it was necessary that the choice of the approach to insulator monitoring was carefully tackled in order that the objectives are adequately addressed. As mentioned in section 3.3, this research encompassed two major focal points: (1) a study on the relative ageing performance of different insulating materials and also (2) a study on the relative ageing performance of insulators with different creepage lengths. This thesis however only reports on the latter. The research work reported in this thesis was conducted at KIPTS, under natural pollution environments on the west coast of Cape Town. A common set of five HTV-SR insulators with different creepage lengths were installed on the test rig under three voltage types, namely AC, DC+ and DC- each with an effective phase voltage of 12.7 kV rms. All insulators have been supplied from a common manufacturer. Figure 4-1 shows the aerial layout of the positioning of test insulators on the test rig.

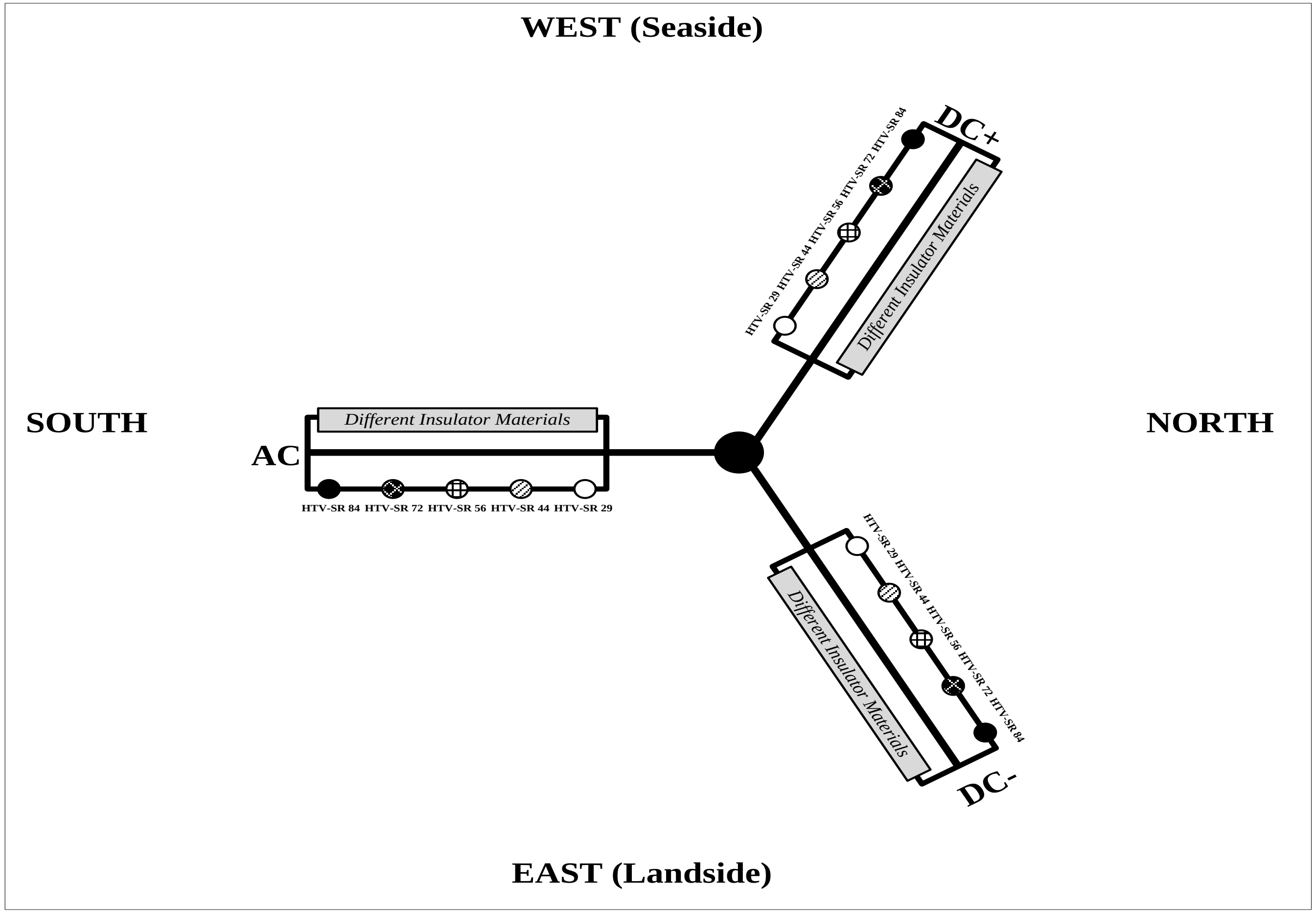

Figure 4-1: An aerial view of the installation layout of test insulators on the test rig at KIPTS

Note that the naming convention of the test insulators depicts the type of insulator material, the unified specific creepage length and the excitation voltage type. For instance, a test insulator with a unified specific creepage distance of 84 mm/kV installed on AC would have the name: HTV-SR 84 AC, where the following denotes:

HTV-SR → High temperature vulcanized silicone rubber

84 → Specific creepage distance in mm/kV

AC → Excitation voltage type

Since the study focuses on the effect of creepage length on the performance of the test insulators, it was ensured that the insulators were all made from the same material (HTV-SR) having the same profile and that the only variables under investigation were the creepage length parameters and the excitation voltage types.

All human factors related to the monitoring procedures (for example, interfering with insulator pollution layers) that could affect the ageing performance of the test insulators were avoided. This was achieved by ensuring that there was no physical interference with the insulator surfaces in order to minimize disturbances on the ageing process of the test insulators. The test rig was only switched off once a week for all the offline observations and measurements. Offline observations and measurements are those that were done whilst the test rig was switched off.

A secure means of data storage was ensured in order to avoid data loss. Data was therefore stored on an external drive and also backed up on a server at Stellenbosch University.

A trial-run through the monitoring procedures was done before the actual test-run began. This was to ensure that a smooth monitoring routine was established upfront.

The following observations and measurements were done in order to gather data that would be useful to carry out analyses on the ageing performance of the test insulators considered in the study.

4.1.1.1 Climatic and environmental conditions

- Climatic conditions were continuously monitored using the on-site weather station coupled to the OLCA device.

- ESDD and DDDG readings were collected weekly. A separate glass disc insulator and a set of four directional dust deposit gauges (DDDG) were installed at the rig for this purpose.

4.1.1.2 Leakage current data

- Continuous leakage current measurements were taken using the OLCA device.

4.1.1.3 Electrical discharge activity observations

- Electrical surface discharge activity observations were done on all the insulators each night between 22h00 and 02h00, using Corocam Mark I and a 0-lux Sony Camcorder for the first six weeks of the test program and then on an ad hoc basis thereafter.

4.1.1.4 Surface condition inspections

- Visual observations on insulator surface conditions including wettability (hydrophobicity) classification tests were done on a weekly basis.

All OLCA data for both leakage current and weather was downloaded and stored on the external drive and then a backup was done on the server at Stellenbosch University. This exercise was done weekly.

4.2 Environmental and climatic condition monitoring

4.2.1 Overview

Both the performance of insulators and the likelihood of insulator flashover bear direct relations to the interaction between prevailing weather conditions and the nature of pollutants deposited on the insulator surface. The environmental and climatic conditions at KIPTS were thus studied in order to understand the insulators operating conditions and be able to explain the insulator pollution process for all the test insulators. The approach to environmental and climatic condition monitoring used for this research was adopted from the information and techniques detailed in the CIGRE document titled “Guide for the establishment of naturally polluted insulator testing stations CIGRE Working Group B2.03" [26]. These techniques are also akin to those detailed in the Round Robin Pollution Monitoring Study Test Protocol CIGRE Task Force 33.04.03 as used in the previous studies performed at KIPTS by Dr. Vosloo [7].

The main aim of environmental and climatic condition monitoring was to adequately study all factors that contribute either directly or indirectly to the insulator pollution flashover process. It was therefore necessary to find answers to the following key questions:

4.2.2 What is the pollution severity at KIPTS?

4.2.2.1 Introduction

Here it was desirable to know the type of pollution deposits with which insulators may be contaminated. It was therefore necessary to understand the possible sources of pollution in the surrounding of KIPTS such as industrial plants, agricultural areas and marine pollutions and, most importantly, to establish the locations of these pollution sources. An overview of the predominant pollution sources has been presented in section 3.2.2, which is a summary of the survey that was conducted within some 20 km radius around KIPTS.

In order to obtain answers to the above question, pollution severity parameters of KIPTS were monitored using standard methods, viz. Equivalent Salt Deposit Density (ESDD), Non-Soluble Deposit Density (NSDD) and Directional Dust Deposit Gauge (DDDG) measurements, as detailed in reference [26]. These pollution severity monitoring methods were used to provide information about the state (nature and source) of pollutants that prevailed at KIPTS. The following sections provide details on the procedures that have been employed.

4.2.2.2 Equivalent salt deposit density (ESDD)

Definition: ESDD refers to the equivalent amount of Sodium Chloride (NaCl) deposits on the surface area of an insulator that will have an electrical conductivity equal to that of the actual deposit dissolved in the same amount of water [3, 7, 26-27]. This value is measured in mg/cm^2. A non-energized standard glass disc insulator was installed on the rig for purposes of ESDD measurements. The glass disc insulator identical to the reference glass disc insulators installed on the three voltage types was used and it was installed at exactly the same elevation as all the energized test insulators.

Procedure: Firstly, it was crucial that the pollution deposits on the glass disc insulator surfaces were not interfered with during the measurement process and also that the deposits on all end-fitting metalwares were curbed from being included in the measurements. This was ensured by covering all metalwares with sellotape before the pollution deposits were washed off the surfaces. Secondly, considering the bottom and top sides separately, the pollution deposits were washed off using 1 litre of de-ionized water and then the solution was transferred into the measuring jar. Refer to Figure 4-2 below.

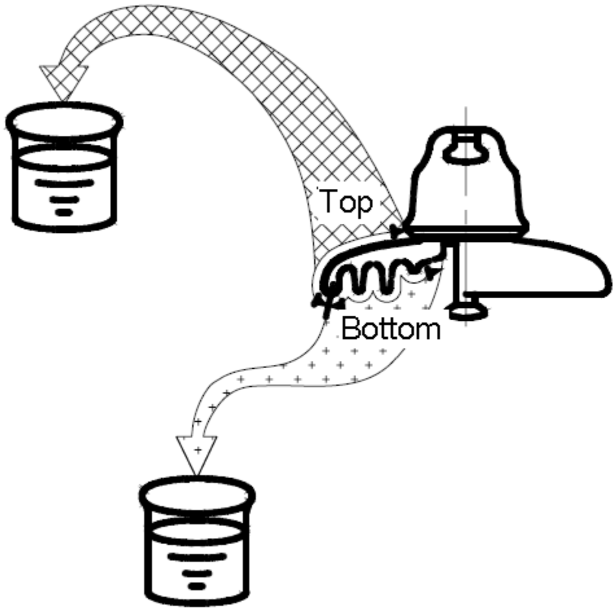

Figure 4-2: ESDD measurements, considering the top and bottom pollutions separately [27]

Finally, the conductivity and temperature of the solution were then measured using a conductivity meter probe. The solutions were secured for purposes of NSDD measurements. The glass disc would then be reinstalled to the rig once all pollution deposits have been washed off. The ESDD value was calculated using Equation(3)

$$\text{ESDD} = \frac{(S_a \cdot V_d)}{A_{ins}} \tag{3}$$

where:

S_a : Salinity of the solution [kg/cm^3]

V_d : Volume of the distilled water used [cm^3]

A_{ins} : Area of insulator surface washed [cm^2]

Salinity of the solution was obtained as follows:

$$S_a = (5.7^{-4} \,.\, \sigma_{20})^{1.03} \tag{4}$$

where σ_{20} [µS/cm] denotes the conductivity measurements corrected to 20 °C. See Equation(5). This was necessary because the conductivity meter probe would only measure conductivities at the solution temperature, whereas the ESDD calculations were derived for salinities at 20 °C [3, 26].

Temperature correction for the measured conductivities was calculated as below:

$$\sigma_{20} = \sigma_t \,.\, \left[1 - k_t\left(t_s - 20\right)\right] \tag{5}$$

where:

σ_t : Measured solution conductivity [µS/cm]

t_s : Solution temperature [°C]

k_t : Temperature constant

The temperature constant can be calculated using Equation(6):

$$k_t = -3.200.10^{-8}.t_s^{\,3} + 1.032.10^{-5}.t_s^{\,2} - 8.272.10^{-4}.t_s + 3.544.10^{-2} \tag{6}$$

It is important to note that all equations pertaining to the calculations of the ESDD measurements are only valid for solution temperatures between 5 and 30 °C and volume conductivities between 40 and 4000 µS/cm [10]. The ESDD measurements were done weekly for the duration of the test period.

4.2.2.3 Non-soluble deposit density (NSDD)

Definition: NSDD is defined as the amount of non-soluble (inert) pollution deposits over a given unit area of the insulator surface [3, 7, 26-27]. This value is measured in mg/cm^2.

Procedure: The NSDD measurements were done from the solutions used for ESDD measurements. Firstly, the solutions were filtered through a GF/A 1,6 µm filter paper to sift out all non-soluble materials suspended in the solution. Prior to NSDD measurements the clean filter paper to be used for filtering was pre-dried and its mass was then measured. Once the filtering was complete, the contaminated filter paper was then re-dried and weighed to obtain the combined mass of the filter paper and the non-soluble materials. Thus, the difference between the mass of the contaminated filter paper and the clean filter paper yields the mass of the non-soluble materials. The NSDD measurements were done weekly for the duration of the test period.

NSDD can be evaluated as follows:

$$NSDD = \frac{M_2 - M_1}{A_{ins}} \qquad (7)$$

where:

NSDD	: Non-soluble deposit density [mg/cm^2]
M_1	: Mass of the dry, clean filter paper [mg]
M_2	: Mass of the contaminated filter paper [mg]

4.2.2.4 Directional dust deposit gauge (DDDG)

Definition: Directional dust deposit gauge (DDDG) approach provides a pollution severity assessment method that quantifies the amount of pollution deposits that emanate from all four cardinal directions at the test site. The setup comprises of four vertical tubes with removable containers fastened to the bottom of each tube to contain the collected pollution deposits. The four gauges are placed such that they face in all four respective cardinal directions. Figure 4-3 depicts the design of a complete DDDG installation. Note that the gauges are installed at an elevation of 3 m above ground level and that all tubes have open slots on the sides through which the pollution deposits may be blown.

Procedure: The removable containers at the bottom of each gauge were removed every week in order to sample the collected pollution deposits. It was important that the walls of the collection tubes were thoroughly rinsed with distilled water to ensure that all pollution deposits were sampled. De-ionized water was then added to the contents of the removable containers in order to dissolve the collected pollution deposits. Here, precautions were taken such that the total amount of water used to dissolve the collected deposits does not exceed 500 ml. Thus, no additional water was added if the containers had already contained an amount of water exceeding 500 ml [7, 26-27]. This may happen due to heavy rainfall. In such cases, the total water volume was measured and noted. The conductivities of the solutions were then measured using the conductivity meter probe. Again, all conductivity values were corrected to 20 °C using Equation(5). The results were normalized to a 30-day month period in order to obtain a month-equivalent data. This is because these tests are usually done at a 30-day interval.

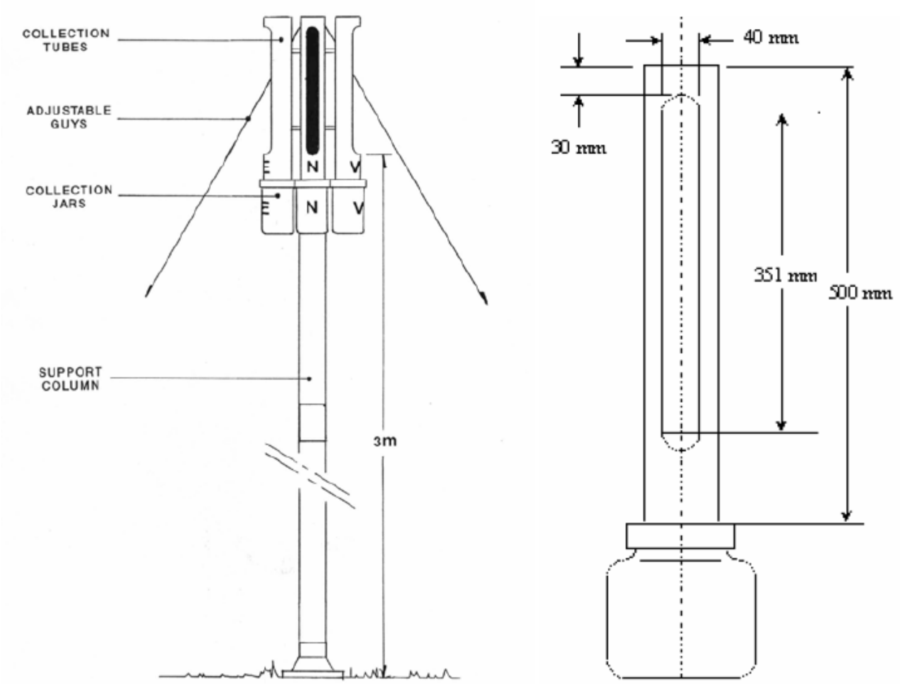

Figure 4-3: Design and installation specifications for directional dust deposit gauges [26, 27]

The following formula can be used to convert the measured DDDG conductivity values for the respective cardinal directions to a 30-day month equivalent data:

$$DDDG = \sigma_{20} \cdot \frac{V_d}{500} \cdot \frac{30}{D} \qquad (8)$$

where:

DDDG : Directional deposit gauge conductivity [µS/cm]

σ_{20} : Measured conductivity corrected to 20 °C [µS/cm]

V_d : Volume of water used [ml]

D : Length of exposure in days

4.2.2.5 Pollution severity classification

The pollution indices of the site, based on the ESDD, NSDD and DDDG measurements, were categorized according to the classification table below.

Table 4-1: Pollution severity classes based on ESDD, NSDD and DDDG [3, 26]

Pollution Severity Class		ESDD [mg/cm²], Monthly maximum	NSDD [mg/cm²], Proposed by Riquel	DDDG [µS/cm], Monthly average
Light	I	< 0.06	0.15 – 0.44	0 - 75
Medium	II	0.06 - 0.12	0.45 – 0.85	76 - 200
Heavy	III	> 0.12 - 0.24	0.90 – 1.95	201 - 350
Very heavy	IV	> 0.24	> 1.95	> 350

As a rule, it should be noted that the site severity class would need to be increased by one level if the measured NSDD value is above 2 mg/cm^2 (in the case of ESDD), or if a high NSDD is expected such as encountered in the vicinity of a cement factory [3, 26-27].

For DDDG-based site pollution severity, the indices could be modified to incorporate climatic influences depending on the availability of weather data for the site [3, 26-27]. The indices are modified by multiplying them with the climatic factor, C_f, which can be calculated as follows:

$$C_f = \sqrt{\frac{\frac{F_d}{20} + \frac{D_m}{3}}{2}} \qquad (9)$$

where:

C_f : Climatic factor

F_d : Number of foggy days (visibility less than 1000 m for some part of the day) per year

D_m : Number of dry months (< 20 mm of precipitation) per year

4.2.3 What combination of climatic conditions plays a determining role in the insulator pollution process at KIPTS?

A literature survey was conducted (and reported in section 2.4) on the interaction of insulators with climatic conditions that may lead to the insulator pollution flashover phenomenon. These factors include relative humidity, rainfall, ambient and dew point temperatures, and wind speed and direction. Additionally, UV-B radiation plays a role in the wetting process of the insulator, as well imposing direct ageing effects on insulators due to its heating effects.

A set of weather sensors (refer to Figure 3-10) was installed at KIPTS to monitor climatic parameters to correlate the observed insulator performance with the measured operating climatic conditions. As discussed in section 2.4, climate can have an impact on the performance of insulators, especially such factors that cause wetting conditions (e.g. relative humidity, rainfall, temperature) as well as those that determine the deposition of pollutants (e.g. wind speed and direction) onto the insulator surfaces. These climatic parameters were therefore monitored continuously and then sampled at 10 minute intervals using the OCLA device.

4.3 Leakage current monitoring

4.3.1 Introduction

Leakage current is internationally recognized as a sensible indicator of insulator performance [3, 26]. Leakage current parameters were therefore monitored for all the test insulators. As described in section 3.5, a full logging system was installed at KIPTS in order to provide real-time monitoring of all measurable leakage current parameters that would help with the understanding of insulator performance. It has been established that peak leakage current magnitude provides a measure of the probability of insulator flashover when it reaches a certain threshold value, usually referred to as I_{max} [3, 7, 26]. Thus, the magnitude of peak leakage currents was the major parameter considered in this study. In addition, the accumulative coulomb-ampere was recorded for each test insulator in order to evaluate the test insulator in relation to the continuous exhibition of leakage current on their surfaces. This parameter was used for purposes of comparing the relative electrical performance of the test insulators under the three voltage types and also between the different creepage lengths.

A dedicated current sensor was installed for each test insulator and coupled through to the OLCA for logging purposes (refer to section 3.5, Figure 3-10 for details). The measured parameters are explained below [26].

4.3.2 Positive and negative peak leakage currents

The OLCA device continuously samples both positive and negative peak leakage current values at 2 kHz and then it compares each sampled value with the previous positive and negative peak leakage current values stored in registers. Each time a higher peak value is detected, an old register value is replaced with the new peak value. Then, at the end of each 10 minute interval, both the positive and negative register values are stored onto memory. Once the maximum peak current value is stored onto memory, the registers are then zeroed and the next 10 minute measuring interval begins.

4.3.3 Absolute peak leakage current

The OLCA evaluates the mathematical absolute values of both the positive and negative peak leakage current values for each 10 minute interval. The maximum of the two absolute peak values is then stored as the absolute peak leakage current value for a given measuring interval.

4.3.4 Accumulative coulomb-ampere

The accumulative coulomb-ampere is a parameter that is representative of the accumulated power (or energy) that gets dissipated on the surfaces of test insulators as a result of leakage currents. In addition, this parameter also resembles the accumulative electrical charge which can be used as a measure of the continuous interaction of an insulator surface with leakage current. The squared values of the accumulated absolute peak leakage current (as explained in section 4.3.3) are then multiplied with the sampling interval Δt to calculate the accumulative coulomb-ampere values. Accumulative coulomb-ampere can be calculated according to Equation(10):

$$CA\ (i(n)) = \sum_{n=0}^{N} \left(i(n) \right)^2 .\ \Delta t \qquad (10)$$

where:

CA (i(n)) : Accumulative coulomb-ampere [CA]

i(n) : Absolute peak leakage current [A]

Δt : Sampling interval, $\frac{1}{2\ \text{kHz}} = 0.5$ ms

N : f . T = 1 200 000, where f = 2 kHz & T = 10 minutes x 60 seconds = 600 s

4.4 Night observations: Electrical discharge activities

The amount of electrical power dissipated during electrical discharge activities over an insulator can have direct impact on the ageing process of polymeric insulators. This had therefore warranted the decision that all test insulators be monitored to observe all electrical discharge activities that may exhibit on the insulator surfaces. It was particularly important to observe the locations of such electrical discharge activities and to note the type of these electrical discharge activities. The knowledge about the location and type of electrical discharge activities would help to justify whether the visible ageing conditions that may be observed on the insulator surfaces during visual inspections were caused by electrical discharge activities or as a result of other ageing processes such as UV-B radiation. A special, image-intensified, UV-sensitive camera Corocam Mark I was used for the night observations and a one-minute video was taken for each insulator. All videos were stored on MiniDV cassettes, which were specifically labeled. In addition, a 0-lux Sony video camcorder was also used during night observations and a one-minute video footage was taken and stored on the built-in hard drive. The two cameras are described in chapter 3 (refer to section 3.4).

It may be queried why trouble is taken to perform observations at night. This preference is based largely on the philosophy behind insulator pollution mechanisms. It is usually when a polluted insulator is wetted that leakage current flows over an energized insulator – thereby leading to dryband formations and hence to some exhibitions of electrical discharge activities [11, 30, 33]. Thus, it would be expected that suitable times to perform these observations must coincide with enticing wetting conditions such as high humid conditions. So, the choice of doing observations at night was based on capturing the conditions when one would observe pronounced electrical discharge activities (during the times when critical wetting conditions occur) rather than during daytime when wetting conditions are limited. In addition, Corocam Mark I has been designed for night observations only.

The pioneering study conducted by Dr. Vosloo at KIPTS had established that critical wetting tends to occur during the early morning hours when the temperatures at the insulator surface drop to a value lower than the ambient temperature and also at night when high relative humidities are reached (found to be > 90% for winter and > 85% for summer) [7]. The times for observations were therefore chosen to be between 22h00 and 02h00. All the observed electrical discharge activities were documented on the observation sheets. A sample of these observation sheets is included in Appendix A. Typical electrical discharge activities are defined on the illustration below [7, 26].

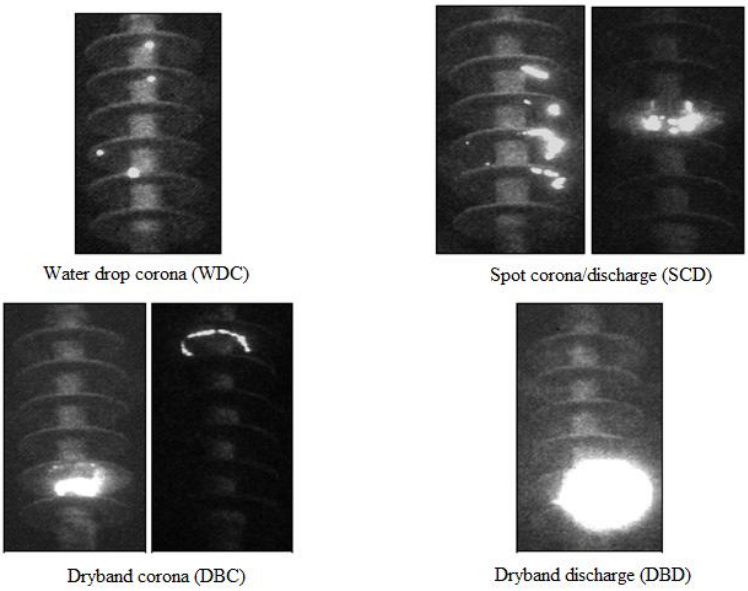

Figure 4-4: Typical partial electrical discharge activities on insulator surfaces [7, 26]

The above partial electrical discharge activities, as depicted in Figure 4-4, are explained below [7, 26]:

- *Water drop corona (WDC):* The electric field strength may intensify around water droplets, which may produce corona. This is referred to as WDC.
- *Spot corona/discharge (SCD):* This is a type of corona that forms around an electrolytic filament or a partial discharge between water droplets or electrolytic filaments.
- *Dryband corona (DBC):* This type of corona exhibits within the dryband zone.
- *Dryband discharge (DBD):* This includes streamers, sparking and arcing activities over the dryband zone.

4.5 Daytime observations: Insulator surface conditions

As referred to earlier, the interaction of insulator surfaces with the operating weather conditions may cause electrical discharge activities to occur whose high electrical power dissipations could cause deteriorations in the insulator surface conditions. Such deteriorations could have negative impacts on the insulating properties of an insulator, thereby leading to reduced electrical performance of the insulator or even irreversible material degradations [15]. Thus, a close-up inspection of insulator surface conditions was regarded as a valuable approach to tracking the ageing performance of insulators.

Visual inspections were done according to the STRI Guide 5, 2005 [24], without touching the insulator surfaces. This was to ensure that the pollution layers were not interfered with. The inspections were done weekly. A close-up inspection was done on each test insulator and all observations were recorded on the observation sheets, noting all visible material deteriorations and damages as defined in the STRI Guide 5: 2005 document (and also discussed in section 2.5). Once the visual inspections were complete, a wettability (hydrophobicity) classification test was then performed on the test insulators. Digital photographs of all observed surface conditions were captured and documented. The results obtained from these observations were then used to analyze the relative performance of different insulators energized under different voltages, noting the development of insulator surface deteriorations. Samples of the surface inspection and wettability classification test record sheets are given in Appendix A.

Wettability classification tests were done in accordance with STRI Guide 1, 92/1 [25]. Please note that the terms ‘wettability” and “hydrophobicity” will be used interchangeably, henceforth. Hydrophobicity is a superior electrical property of most polymeric insulators. However, this property can get worn out over time when insulator surfaces are exposed to harsh weather conditions and electrical discharge activities. A spot check was thus done on all insulators to assess the integrity of this property. The guide provides for six hydrophobicity classes (HC 1 - 6), as shown in Figure 4-5 [25, 26].

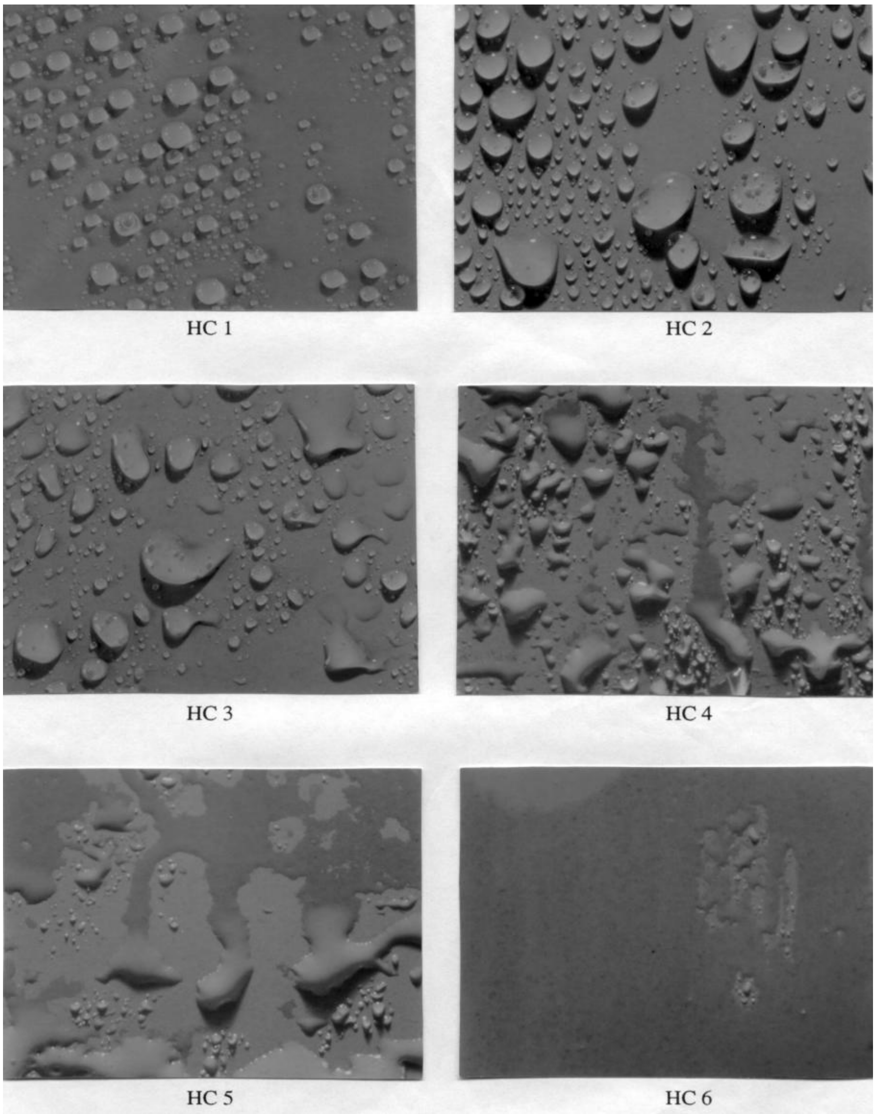

Figure 4-5: Hydrophobicity classification indices [26]

An additional hydrophobicity class has been defined for insulators whose surfaces get completely wetted (forming a continuous film of water). Such insulator surfaces would be classified as hydrophilic and assigned an HC 7 class, whereas a water-repellent insulator surface would be classified as hydrophobic (water beaded into droplets) and assigned an HC 1 class. A small area (approximately 50 – 100 cm^2) of the insulator surface was sprayed with a fine mist of de-ionized water using a standard spray bottle at a distance of 25 ± 10 cm [25]. Since hydrophobicity may be a localized property, a general hydrophobicity test was done at different sections (sheaths, shed bottom and shed top) of the insulator from both sea-side and land-side. The insulator sections considered in the HC tests are shown in Figure 4-6. Once the selected area had been sprayed with a fine mist of water, a decision on the hydrophobicity class was then taken within 10 seconds thereafter.

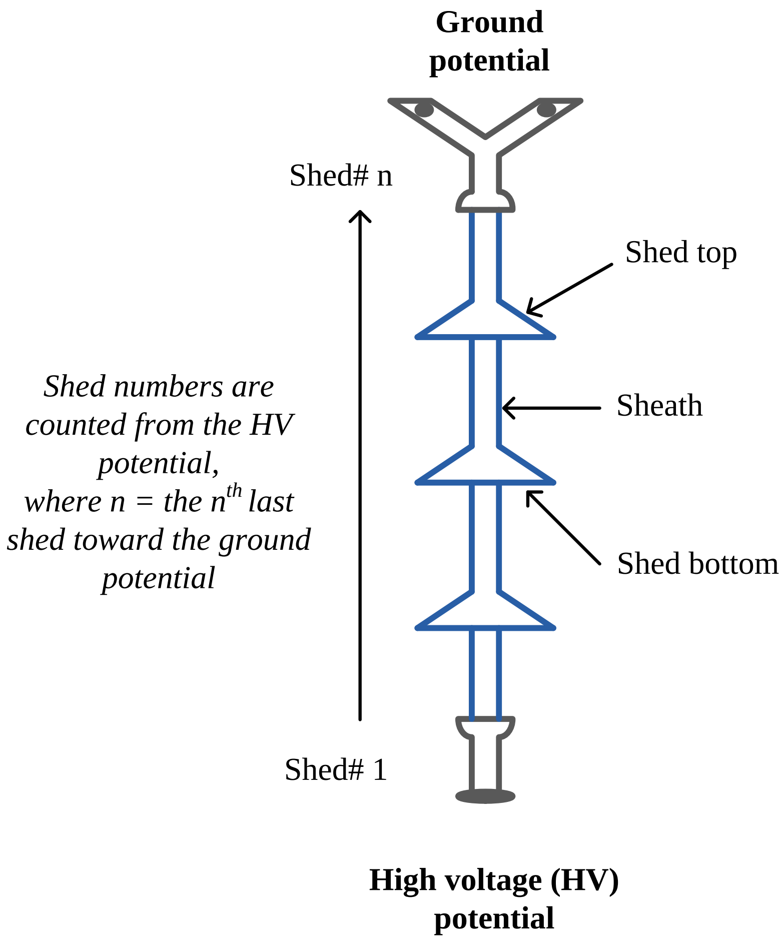

Figure 4-6: Insulator sections considered for wettability (hydrophobicity) classification tests

5. CHAPTER 5: Results and interpretations

5.1 Overview

This chapter presents a discussion on the results obtained in the test program. The results include the following aspects:

- An overview of the environmental and climatic conditions experienced at KIPTS during the entire test period, from February 3rd to July 31st 2011.

- A discussion of leakage current performance of the test insulators, considering the absolute peak values. Leakage current values were categorized into nine different bin categories. In addition, accumulative coulomb-ampere (representative of the dissipated electrical power) was also considered in order to assess the continual electrical performance of the test insulators for the three excitation voltage types - AC, DC+ and DC-.

- A discussion of the electrical discharge performance of the test insulators. The results include observations obtained by using two observation cameras (Corocam Mark I and 0-lux Sony Camcorder), as explained in the previous chapter in section 4.4.

- Detailed descriptions of surface conditions of all test insulators as observed during the daytime surface inspections performed.

- An overview of the wettability (hydrophobicity) classification results for the high temperature vulcanized, silicone rubber (HTV-SR) test insulators..

The environmental conditions encompass the results obtained from the site pollution severity indicators, namely the equivalent salt deposit density (ESDD), the non-soluble deposit density (NSDD) and the directional dust deposit gauge (DDDG). Climatic conditions encompass results from the meteorological data (relative humidity, rainfall, temperature, wind speed and direction and UV-B radiation) that have been recorded using the online leakage current analyzer (OLCA). A careful consideration was made that a profile of environmental and climatic condition would be obtained for each month throughout the entire test period.

A comparison is made for all test insulators with the same creepage length in order to compare their relative performance under the three voltage types: AC, DC+ and DC. The glass disc insulator with a specific creepage distance of 42 mm/kV has also been considered for purposes of performance reference.

5.2 Results for the climatic and environmental conditions at KIPTS

Prior to the presentation of performance results of test insulators, it is important to discuss the climatic and environmental conditions that prevailed at KIPTS during the test program. Sections 5.2.1 and 5.2.2 give an overview of the climatic and pollution conditions, respectively. Climatic conditions include rainfall, relative humidity, ambient and dewpoint temperatures, wind speed and direction and UV-B radiation. These aspects affect the electrical performance of insulators and may sometimes even lead to material ageing, as discussed in section 2.4. After an in-depth cross-study of the obtained weather patterns, it was found that the weather profile varies greatly in accordance to the time of day and a correlation had been found between the variations of weather and the corresponding leakage current performance of the test insulators [29]. Therefore, the average results for the afore-listed climatic parameters are presented per time-of-day for the respective six months. Monthly averages are also presented. These will help explain the pollution deposition and wetting conditions experienced at the test site and hence uncovering justifications for the resulting performance of the test insulators. In addition, the results on pollution condition indicators (ESDD, NSDD and DDDG) are discussed.

5.2.1 Climatic conditions

5.2.1.1 Introduction

It should be noted that the results presented here are for the first six months of the test program, i.e. from February until the end of July. This period has been split into two seasons: summer and winter. The former comprises of February through April, whereas the latter comprises of May through July. The time-of-day average values of all climatic parameters are presented for each respective month of the test program in Appendix B.

5.2.1.2 Rainfall

Rain can yield favorable conditions that may lead to the wash-off of pollution deposits from the insulator surface. However, rain can also be an unfavorable factor that may lead to the formation of conducting electrolytes. This can happen when small drizzles of rain dampen pollution deposits on the insulator surfaces without causing complete wash-offs. Even without any pollution deposits, acidic rain can cause events of instantaneous pollution. The pH level of rainfall at KIPTS has been reported to be slightly acidic. An average of 5.6 was reported in reference [7].

It was found that greater amounts of rain fell during the earliest morning hours of the day. This can be seen in Figure 5-1. In fact, the highest instances of rain were recorded around 04h00. The time-of-day monthly averages of rainfall are given in Figure B-1.

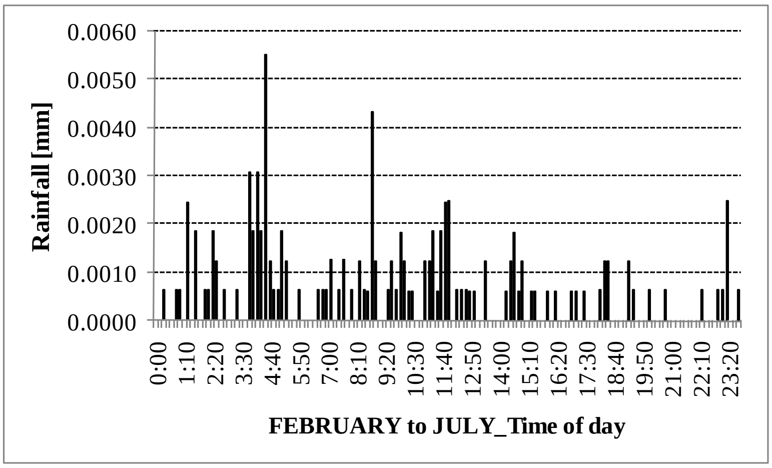

Figure 5-1: Time-of-day average rainfall recorded at KIPTS for the entire test period, February - July 2011

As expected, the highest aggregate rainfall was recorded during the winter months: May through July. A total of 6.1 mm rainfall was recorded for July. This shows that winter is the rain dominant season at KIPTS, whereas summer is the dry season with very little rain. This is evident from Figure 5-2. A total of 14.7 mm was recorded for the entire test program, of which 91% was recorded in winter and the other 9% in summer.

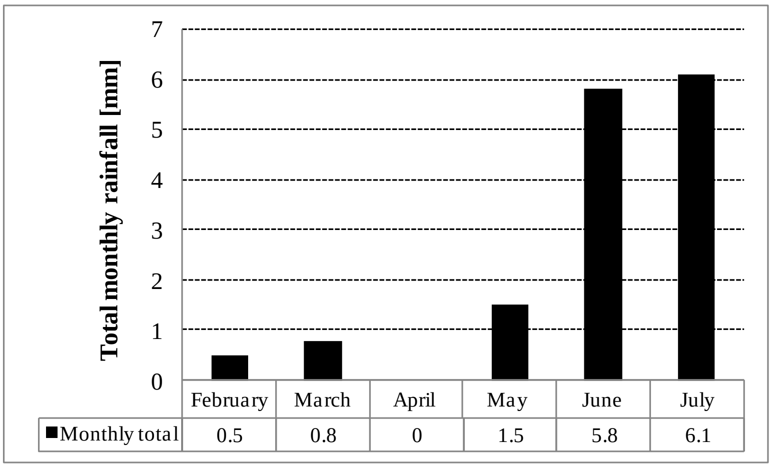

Figure 5-2: Monthly total rainfall recorded at KIPTS for the entire test period, February – July 2011

Table 5-1 shows a summary of the rainfall data obtained at KIPTS for the duration of the test program. Both the minimum and maximum rain recorded for each month are shown in the table. The minimum for all the months was found to be zero. The maxima for May, June and July were 0.1 mm, 0.3 mm and 0.9 mm, respectively; whereas the maxima for February and March were both found to be 0.1 mm. No rainfall was recorded for April.

Table 5-1: A summary of rainfall data obtained at KIPTS during February through July 2011

Rainfall [mm]	February	March	April	May	June	July	Entire test program
Maximum	0.1	0.1	0.0	0.1	0.3	0.9	**0.9**
Minimum	0.0	0.0	0.0	0.0	0.0	0.0	**0.0**
Total	0.5	0.8	0.0	1.5	5.8	6.1	**14.7**

In summary, therefore, summer months (February through April) were found to be dry with a maximum recorded rain of 0.1 mm and a total of 1.38 mm; whereas winter recorded a maximum of 0.9 mm and yielding a total of 13.4 mm. The amount of rain recorded for the entire test program was 14.7 mm.

5.2.1.3 Relative humidity

This climatic factor plays an important role in the performance of insulators. Relative humidities above 75% are found to be the most critical in providing enticing wetting conditions for active pollution deposits to form conducting electrolytes on an energized insulator surface [3, 18], thereby leading to the corresponding flow of leakage currents. It should also be understood that, as with rain, persistent high levels of relative humidity could also cause a wash-off of pollution deposits from the insulator surface. For solid, active pollution deposits, wetting is pre-requisite to the formation of conducting electrolytes and this means that a close correlation between relative humidity and the exhibition of leakage currents on the test insulators can be expected. Thus, it is important to review the relative humidity conditions experienced at KIPTS. The time-of-day monthly averages of relative humidity are given in Figure B-2.

Figure 5-3 and Figure 5-4 show the average relative humidity per time-of-day and also for each month, respectively, throughout the entire test period.

High levels of humidity were experienced during the early morning hours and also in the late evenings. This is evident from Figure 5-3, with levels of relative humidity exceeding 75% from 00h00 to 10h00 (early mornings) and also from 19h00 to 23h00 (late evenings). Low levels of relative humidity were recorded between 10h00 and 19h00, with levels below 75%. This means that on a given day, critical wetting conditions would prevail 67% of the day.

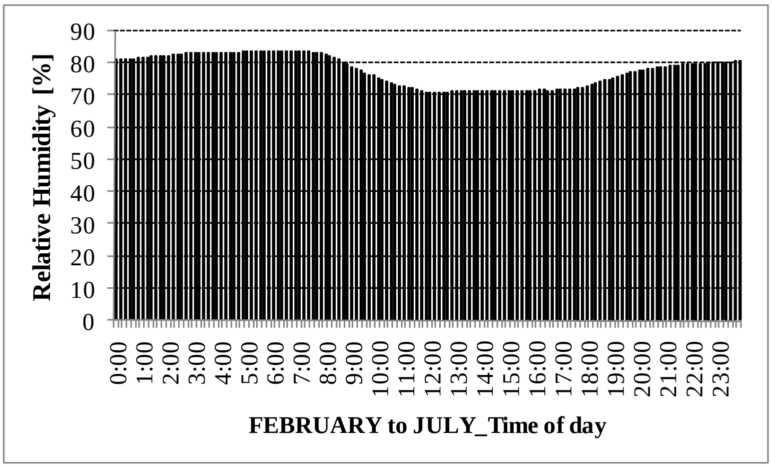

Figure 5-3: Time-of-day average relative humidity recorded at KIPTS for the entire test period, February through July 2011

The monthly averages are shown in Figure 5-4. Relative humidity levels higher than 75% were recorded for February, March, May and June. This indicates that, on average, critical wetting conditions prevailed during the entire test period, except for April and July when levels of relative humidity were lower than 75%. . The highest average relative humidity was recorded in June – 82.8%, whereas the lowest was recorded in July – 74.3%.

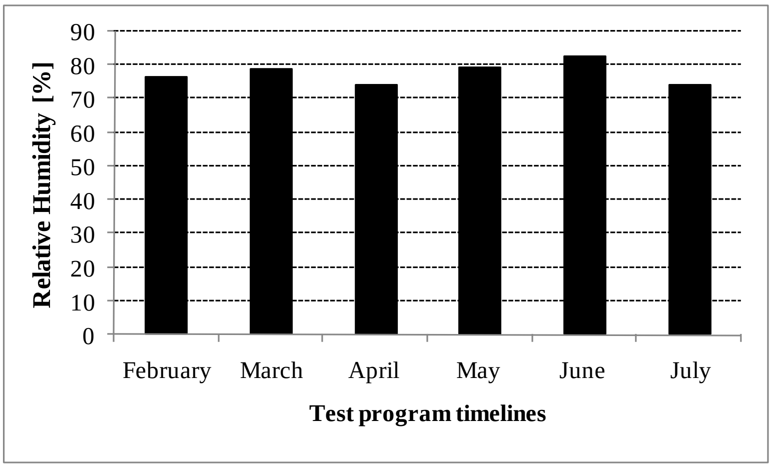

Figure 5-4: Monthly average of the relative humidity recorded at KIPTS for the entire test period, February through July 2011

The maximum relative humidity recorded during the entire test period was 95.6% (in May) and the minimum was recorded to be 13.4% (in May). Both the maximum and minimum relative humidity levels are presented in Table 5-2.

Table 5-2: A summary of relative humidity recorded at KIPTS during February through July 2011

Relative Humidity [%]	February	March	April	May	June	July	Entire test program
Maximum	95.5	95.4	95.1	95.6	95.3	94.6	**95.6**
Minimum	35.8	31.2	23.7	13.4	25.5	24.6	**13.4**
Average	76.7	78.8	74.4	79.2	82.8	74.3	**77.8**

5.2.1.4 Ambient and dewpoint temperatures

The exchange of heat between the ambient air and the surface of the insulator plays a critical role in the wetting process of a contaminated insulator. It is customary that dew may form on the insulator surface when its surface temperature is lower than the ambient and the dewpoint temperature. Ambient temperature indicates the extent of heat of the surrounding air, whereas dewpoint temperature denotes the temperature at which a packet of humid air must be cooled in order to condense into liquid water. The condensation can be termed as a dew and hence the name 'dewpoint temperature'. In literal terms, dewpoint temperature can be defined as the temperature at which dew begins to occur.

The condensation phenomenon introduces wetting effects onto the insulator surface, which may dissolve the pollution deposits that might be present on the insulator – thereby leading to the formation of conducting electrolytes. An interrelation between the ambient and dewpoint temperatures and relative humidity is found to exist, with an effect that high relative humidity levels occur when the difference between the two temperatures decreases. This inverse relationship has been derived as follows [7]:

$$T_{dew} = \left(\frac{2720.(T_a + 273.16)}{\frac{((T_a + 273.16).\log(100/RH))}{2} + 2720} \right) - 273.16 \qquad (11)$$

where:

T_{dew} : Dewpoint temperature [°C]

T_a : Ambient temperature [°C]

RH : Relative humidity [%]

Figure 5-5 shows the inverse relationship between both the ambient and dewpoint temperatures and the relative humidity, displayed per time of day. The difference between the ambient and dewpoint temperatures is smaller than 4.6 °C from 00h00 to 10h00 (early mornings) and also from 19h00 to 23h00 (late evenings). It can be seen that when these instances occur, the relative humidity is correspondingly found to be exceeding 75 %. This would probably mean that one would expect 100% relative humidity when the difference between the ambient and dewpoint temperatures approaches zero. The greater the difference between the two temperatures, the lower the relative humidity. Thus, no critical wetting was experienced during the periods when the difference between the two temperatures exceeded 4.6 °C, between 10h00 and 19h00.

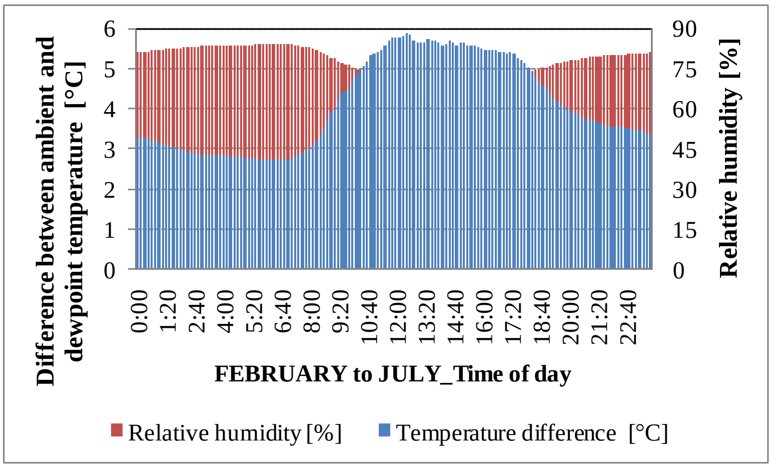

Figure 5-5: Inverse relationship between temperature (ambient and dewpoint) and relative humidity

With reference to Figure 5-6, it can be noted that temperatures averaged between 13.4 °C and 16.8 °C at night (including the early morning hours), whereas temperatures between 13.4 °C and 18.5 °C were recorded during daytime. The maximum temperature of 33.2 °C was recorded during daytime at 17h40 in February, whereas the minimum temperature of 2.1 °C was recorded at 06h40 in July. This shows that extreme, hot temperatures were experienced during the daytime, whilst low temperatures generally occurred around sunrise, as would be expected.

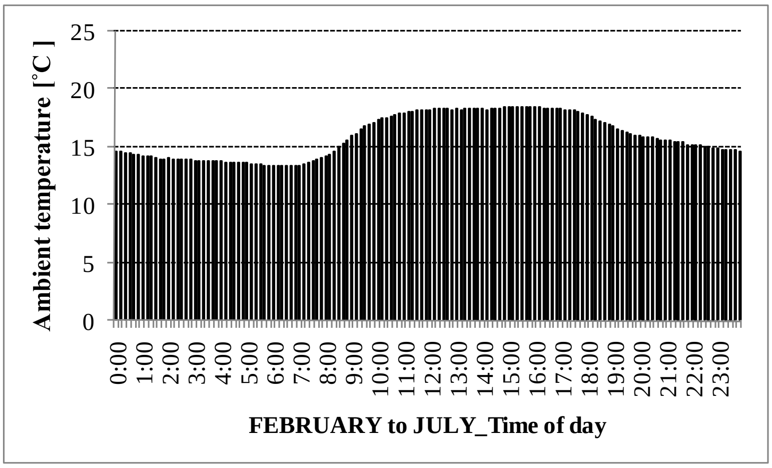

Figure 5-6: Time-of-day average ambient temperature recorded at KIPTS for the entire test period, February through July 2011

The monthly average temperatures are depicted in Figure 5-7. The temperatures averaged between 16.8 °C and 20.4 °C in summer, whereas temperatures for winter averaged between 12.9 °C and 14.8 °C. The hottest month was found to be February and the coldest was found to be July. As would be expected, it can be observed that the average temperatures followed a descending trend as we moved from summer (February) to winter (July). Note that the time-of-day monthly averages of the ambient temperature are given in Figure B-3.

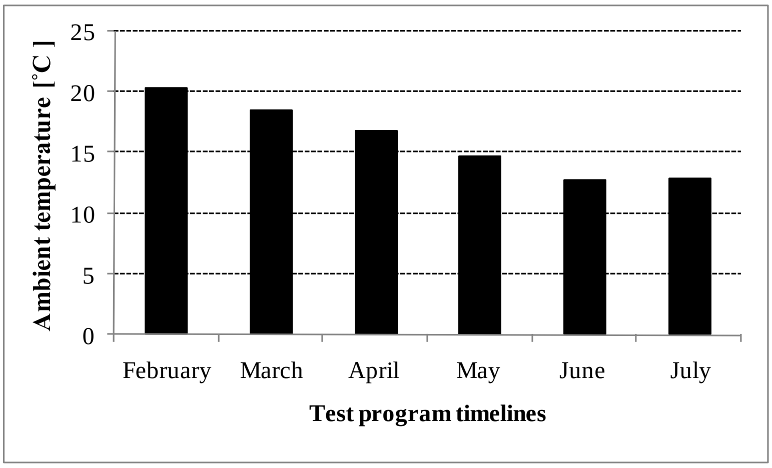

Figure 5-7: Monthly average of the ambient temperature recorded at KIPTS for the entire test period, February through July 2011

All important details of the ambient temperatures recorded at KIPTS are summarized in Table 5-3.

Table 5-3: A summary of ambient temperatures recorded at KIPTS during February through July 2011

Ambient temperature [°C]	February	March	April	May	June	July	Entire test program
Maximum	33.2	32.1	30.1	32.9	28.5	26.5	**33.2**
Minimum	11.1	7.8	5.0	6.2	4.1	2.1	**2.1**
Average	20.4	18.5	16.8	14.8	12.7	12.9	**16.0**

5.2.1.5 Wind speed and direction

Wind does not only play a role in the wetting process of insulators, but it also plays a role in the deposition process of pollution onto the insulator surface. The two aspects of wind, namely speed and direction are key in the determination of the extent of wetting and pollution deposition. Typical wind speeds in excess of 2 m/s have been reported to be a considerable factor in the pollution deposition process and a cubic relationship between ESDD has been observed thereof [3]. Wind direction determines the nature of contaminants that may be deposited onto the insulator surface and this may also depend on the wind strength (speed). For instance, westerly wind directions at KIPTS would carry salt deposits from the sea which lies to the west of the test rig. This causes the phenomenon of directional-dominant deposition of pollutants depending on wind direction. Sand blast cleaning can also occur when strong winds, containing sand particles, blow over an insulator surface.

The time-of-day wind speed and direction conditions for both summer and winter are shown in Figure 5-8 and Figure 5-9, respectively. An average speed of 6 m/s was commonly recorded during the night with a south-easterly direction, gradually rising to a maximum of

8.6 m/s during the afternoon with a south-westerly direction throughout the entire test period. Wind conditions were however found to vary greatly for both summer and winter periods. The average range of wind conditions were recorded as summarized below:

- *Summer*

  Speed: 5.9 – 10.4 m/s

  Direction: South-easterly at night and in the early morning hours; South-westerly during the afternoons

- *Winter*

  Speed: 3.9 – 7.2 m/s

  Direction: South-easterly at night and in the early morning hours; South-westerly during the afternoons

This indicates that strong winds (i.e. high speeds) were often recorded through the afternoons emanating from the south-westerly direction, whereas lighter winds emanated from the south-easterly direction usually experienced at nights and the early morning hours. The variability of wind direction for both summer and winter was however found to be somewhat similar. This is evident from Figure 5-9. As it can be seen in Figure 5-8, summer generally had stronger winds when compared to winter.

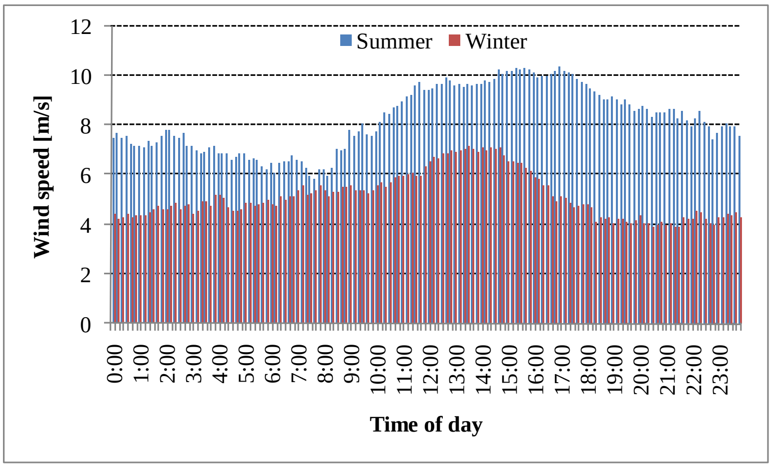

Figure 5-8: Time-of-day average wind speed recorded at KIPTS for summer and winter periods

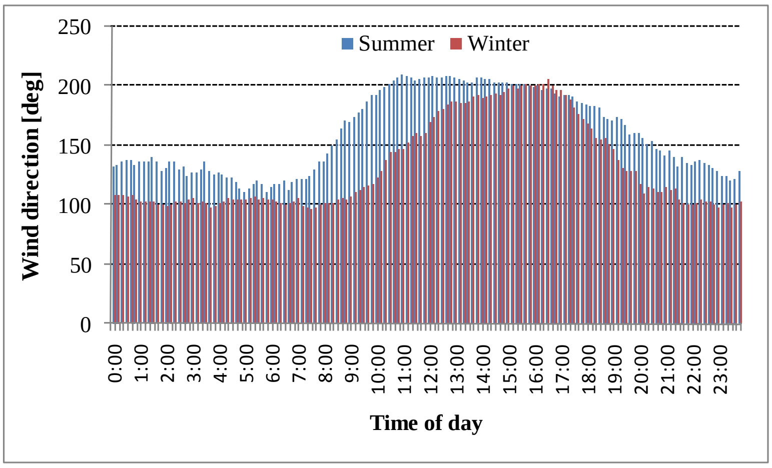

Figure 5-9: Time-of-day average wind direction recorded at KIPTS for summer and winter periods

Figure 5-10 and Table 5-4 present a summary of the monthly wind speed conditions recorded at KIPTS.

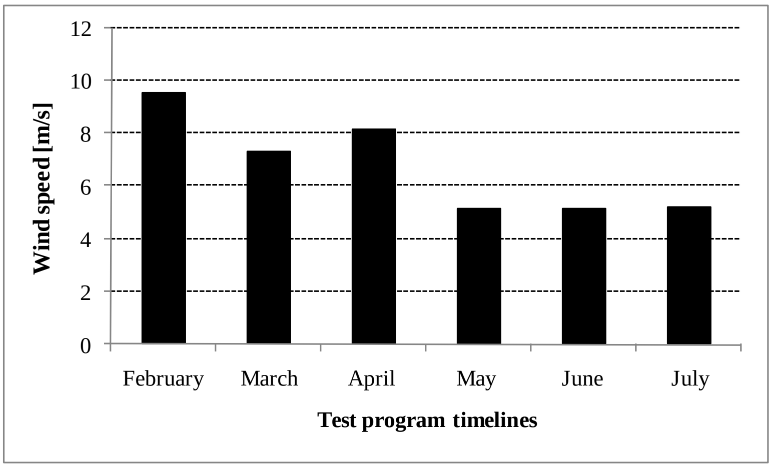

Figure 5-10: Monthly average wind speed recorded at KIPTS for the entire test period, February through July 2011

It can be noted from Table 5-4 that the highest wind speed recorded was 13.6 m/s, occurring in May just before midday at 11h50. Please refer to Figure B-4 and Figure B-6 for the time-of-day monthly averages of wind speed and direction, respectively.

Table 5-4: A summary of wind speed data recorded at KIPTS during February through July 2011

Wind speed [m/s]	February	March	April	May	June	July	Entire test program
Maximum	13.5	13.2	13.5	13.6	13.4	13.2	**13.6**
Minimum	0.0	0.0	0.0	0.0	0.0	0.0	**0.0**
Average	9.6	7.3	8.2	5.2	5.2	5.2	**6.7**

5.2.1.6 UV-B radiation

UV-B radiation forms a part of the electromagnetic spectrum, with shorter wavelengths than those that are visible to a human eye. Typical wavelengths of UV are between 10 nm and 400 nm. The sun is a major source of UV-B emissions. The energy associated with this type of radiation can be particularly high, even strong enough to cause burns on a human skin. Therefore, exposures of non-ceramic insulators to the high-energy intensive UV-B photons can lead to direct ageing of the insulating material [7]. In addition, it would be expected that the heating effects of UV-B radiation on the ambient air can have effects on the relative humidity. This means that the insulator surface may tend to absorb heat during daylight and thus keeping the surface temperature above the temperature of the ambient air. Therefore, relative humidity and dew formation can be expected to be low during daylight.

The time-of-day average UV-B radiation data for both summer and winter is given in Figure 5-11. It is clear that summer had higher levels of UV-B radiation when compared to winter. The highest average UV-B radiation of 154 µW/cm² was recorded in summer at 13h00, whereas 86 µW/cm² was recorded in winter at 12h30. It can also be observed that the test insulators were exposed to UV-B radiation for longer periods in summer than in winter.

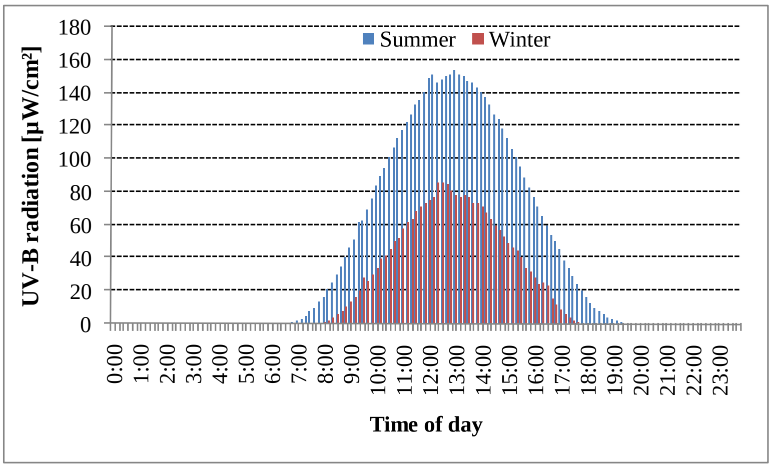

Figure 5-11: Time-of-day average UV-B radiation recorded at KIPTS for summer and winter periods

With reference to Figure 5-12, it can be observed that the highest average UV-B radiation was experienced in February and lower levels were recorded for the winter months (May, June and July). This was an expected observation.

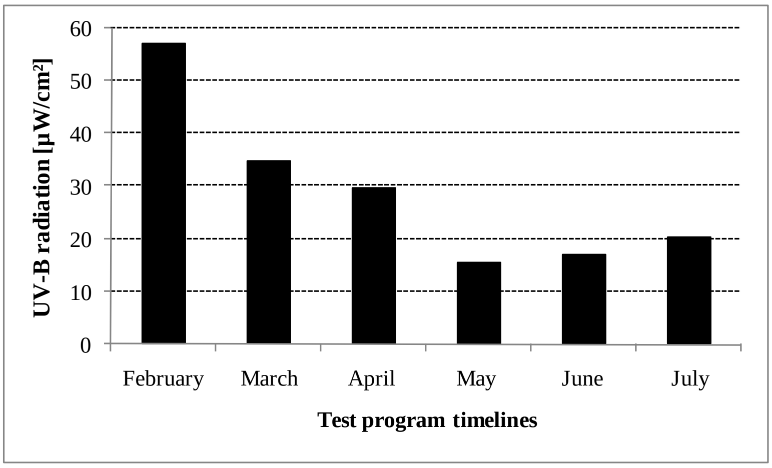

Figure 5-12: Monthly average UV-B radiation recorded at KIPTS for the entire test period, February through July 2011

The following table, Table 5-5, summarizes the UV-B radiation conditions experienced at KIPTS during the entire test period. Note that the time-of-day monthly averages of the UV-B radiation are given in Figure B-7. The following observations can therefore be made:

- *Summer*

  A maximum of 725.7 µW/cm² was recorded in April at noon.

- *Winter*

  A maximum of 703.2 µW/cm² was recorded in July at 12h30.

This means that the peak UV-B radiation occurred at midday.

Table 5-5: A summary of UV-B radiation data recorded at KIPTS during February through July 2011

UV-B radiation [µW/cm²]	February	March	April	May	June	July	Entire test program
Maximum	304.1	182.7	725.7	177.7	102.6	703.2	**725.7**
Average	57.3	34.9	29.6	15.6	17.2	20.3	**28.7**

5.2.2 Environmental considerations: site pollution severity results

5.2.2.1 Introduction

This section gives a brief summary of the pollution measurements conducted at KIPTS. The procedures followed to obtain pollution measurement results have been explained in section 4.2.2. The ESDD and NSDD results provide information about the severity of pollutants that are likely to have been deposited onto the test insulators, whereas the DDG results provide information about the severity of pollutants originating from the four cardinal directions around KIPTS. The latter can therefore indicate the directional likelihood of pollution sources with reference to the topographical representation of prominent pollution sources in the surrounding of KIPTS (refer to Figure 3-2 and Table 3-1).

It should be understood that the ESDD and NSDD measurements were done on a separate non-energized glass disc insulator, similar to the one installed on the test rig. No pollution sampling was done on the energized test insulators.

5.2.2.2 Equivalent salt deposit density (ESDD)

The ESDD measurement results are presented in Table 5-6 and Figure 5-13. As expected, the first measurement performed on February 9th yielded quite low ESDD levels which were rated light. This is because the glass insulator was still relatively clean. However, it can be observed from Figure 5-13 that the ESDD levels continued to increase through the summer months where higher ESDD levels were recorded on the top side when compared to the bottom side. In contrast, higher ESDD levels were recorded on the bottom side when compared to the top side in winter. This was the opposite to the observations made for summer. Rainfall appears to have played a role in the levels of the ESDD values measured on the glass insulator and this is not an unexpected revelation. With reference to the rain conditions presented in section 5.2.1 (refer to Figure 5-2), it is logical that there would be frequent washing of the top side of the glass disc insulator in winter which renders the ESDD values to be lower than the bottom side due to limited washing on the bottom side. This was not true for summer due to limited rain recorded during this season. The average ESDD levels measured on the top side of the glass disc insulator can be classified as medium for summer and light for winter, whereas those measured on the bottom side of the glass insulator can be classified as light for both summer and winter, as shown in Table 5-7.

In addition, we can see that, although the highest total rainfall was recorded on July 7^{th}, a considerable level of ESDD was still recorded. This could be related to the long interval (30 days) that had lapsed since the previous measurement was done on June 7^{th}, which means that the length of measurement interval can affect the level of ESDD values that may be recorded. Therefore, the levels of ESDD values recorded in winter did not have a descending trend as would have been anticipated due to relatively longer and inconsistent measurement intervals compared to the relatively shorter and more consistent measurement intervals in summer. The inconsistency of measurement intervals in winter was a result of the inability to perform measurements on schedule due to inclement weather conditions.

Table 5-6: A summary of the equivalent salt deposit density (ESDD) measurements performed on a non-energized glass insulator installed at KIPTS

Date	ESDD [mg/cm^2]			Severity classification		
	Top side	*Bottom side*	*Average*	*Top side*	*Bottom side*	*Average*
9-Feb	0.05	0.02	0.04	Light	Light	Light
16-Feb	0.05	0.03	0.04	Light	Light	Light
24-Feb	0.07	0.05	0.06	Medium	Light	Medium
3-Mar	0.06	0.06	0.06	Medium	Medium	Medium
11-Mar	0.12	0.06	0.09	Medium	Medium	Medium
16-Mar	0.11	0.07	0.09	Medium	Medium	Medium
25-Mar	0.03	0.06	0.04	Light	Medium	Light
5-Apr	0.06	0.07	0.07	Medium	Medium	Medium
14-Apr	0.09	0.05	0.07	Medium	Light	Medium
4-May	0.01	0.04	0.03	Light	Light	Light
24-May	0.00	0.03	0.02	Light	Light	Light
7-Jun	0.02	0.03	0.02	Light	Light	Light
7-Jul	0.03	0.05	0.04	Light	Light	Light

Table 5-7: Comparisons of ESDD values for summer and winter

ESDD [mg/cm^2]	Summer		Winter	
	Top side	*Bottom side*	*Top side*	*Bottom side*
Maximum	0.12	0.07	0.03	0.05
	Medium	Medium	Light	Light
Minimum	0.03	0.02	0.00	0.03
	Light	Light	Light	Light
Average	0.07	0.05	0.02	0.04
	Medium	Light	Light	Light

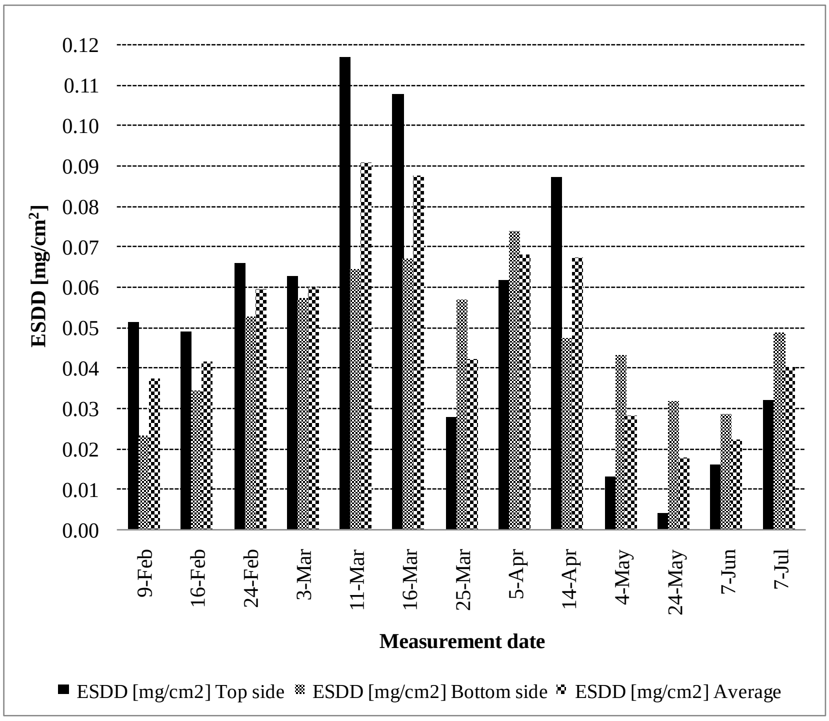

Figure 5-13: Equivalent salt deposit density (ESDD) measurements performed at KIPTS

It should be noted that surface conductivity can be computed from the ESDD data using the following relationship: 0.1 mg/cm^2 (ESDD) ≈ 10 µS (surface conductivity, σ_s) [3].

5.2.2.3 Non-soluble deposit density (NSDD)

Both the ESDD and NSDD measurements were performed on the same non-energized glass insulator. The NSDD measurement results are presented in Table 5-8 and Figure 5-14, detailing the severity results for the top and bottom sides of the glass disc insulator.

Table 5-8: A summary of the non-soluble deposit density (NSDD) measurements performed on a non-energized glass insulator installed at KIPTS

Date	NSDD [mg/cm^2]			Severity classification		
	Top side	*Bottom side*	*Average*	*Top side*	*Bottom side*	*Average*
9-Feb	0.01	0.02	0.02	Light	Light	Light
16-Feb	0.02	0.00	0.01	Light	Light	Light
24-Feb	0.32	0.06	0.19	Light	Light	Light
3-Mar	0.08	0.02	0.05	Light	Light	Light
11-Mar	0.04	0.01	0.02	Light	Light	Light
16-Mar	0.01	0.00	0.01	Light	Light	Light
25-Mar	0.03	0.02	0.02	Light	Light	Light
6-Apr	0.01	0.00	0.00	Light	Light	Light
14-Apr	0.00	0.00	0.00	Light	Light	Light
4-May	0.03	0.01	0.02	Light	Light	Light
24-May	0.01	0.02	0.01	Light	Light	Light
7-Jun	0.09	0.04	0.07	Light	Light	Light
7-Jul	0.05	0.01	0.03	Light	Light	Light

Table 5-9: Comparisons of NSDD values for summer and winter

NSDD [mg/cm^2]	Summer		Winter	
	Top side	*Bottom side*	*Top side*	*Bottom side*
Maximum	0.32	0.06	0.09	0.04
	Light	Light	Light	Light
Minimum	0.00	0.00	0.01	0.01
	Light	Light	Light	Light
Average	0.06	0.01	0.05	0.02
	Light	Light	Light	Light

All NSDD values were classified as light throughout the entire test period for both the top and bottom sides of the glass insulator. Note that NSDD levels were found to be higher on the top side of the glass insulator for both summer and winter periods.

The results for both summer and winter periods are summarized in Table 5-9. It can be seen that the average NSDD levels recorded in summer were higher than those recorded in winter for the top side of glass insulator, whereas the NSDD levels for the bottom side of glass insulator were higher in winter when compared to those measured in summer. The maximum NSDD levels of 0.32 mg/cm^2 and 0.09 mg/cm^2 were recorded on the glass top in summer (February 24th) and winter (June 7th), respectively. The lowest NSDD levels were recorded toward the end of summer (April 14th) for both glass top and bottom sides. See Figure 5-14.

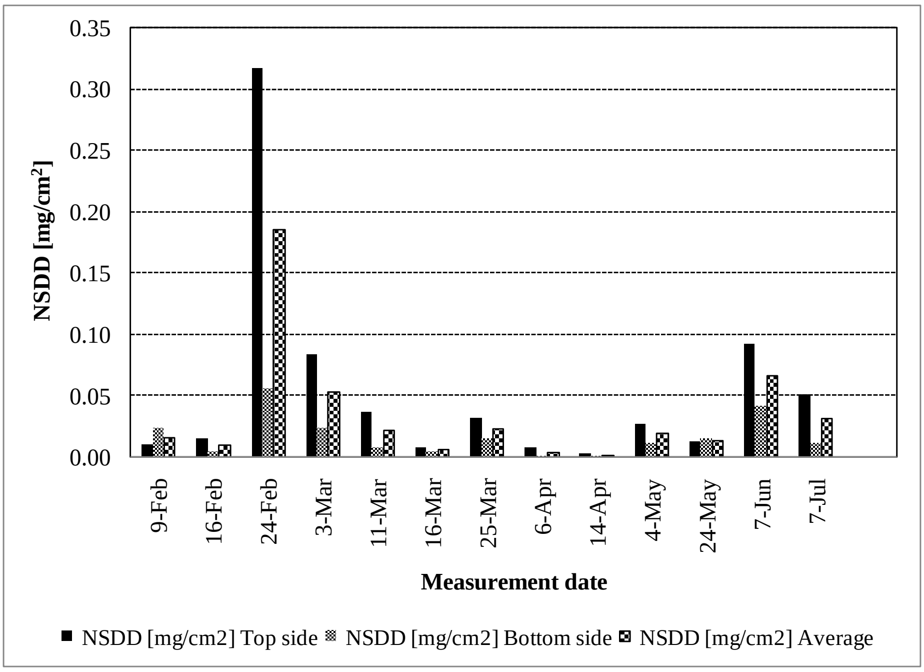

Figure 5-14: Non-soluble deposit density (NSDD) measurements performed at KIPTS

5.2.2.4 Directional dust deposit gauge (DDDG)

The results for DDDG measurements have been normalized to a 30-day month equivalent data, as explained in section 4.2.2. A summary of the obtained results for all the cardinal directions is presented in Table 5-10 and Figure 5-15. In addition, details on the DDDG levels obtained for both summer and winter periods are highlighted in Table 5-11.

It was observed that the highest average conductivities of 1272 µS/cm and 1104 µS/cm were found to have emanated from the southward direction for both summer and winter, respectively. The maximum DDDG value recorded in the entire test period was 2996 µS/cm recorded in summer on February 24th, as it can be clearly seen in Figure 5-15. With reference to the average DDDG values given in Table 5-10 for summer and winter periods, the DDDG conductivity levels recorded in summer were generally higher than those recorded in winter.

The following ranking can be made on the directionality of pollution severity for the DDDG measurements in the summer and winter periods:

- *Summer :*

  (Highest) South → West → North → East *(Lowest)*

- *Winter:*

  (Highest) South → West → North → East (*Lowest)*

This clearly indicates that harshest pollutants were prominent in the southward direction, probably emanating from the heavy industries that lie to the south of KIPTS (refer to Figure 3-2 and Table 3-1). It therefore follows that this harsh south-dominant pollution would cause aggravated ageing conditions on the insulator surfaces due to the highly conductive electrolytes that may be formed during wetting conditions.

Table 5-10: A summary of the directional dust deposit gauge (DDDG) measurements performed at KIPTS

Date	30-day normalized conductivity , σ_{20} [µS/cm]				Severity classification			
	North	*East*	*South*	*West*	*North*	*East*	*South*	*West*
9-Feb	133	79	217	118	Medium	Medium	Heavy	Medium
16-Feb	145	198	821	646	Medium	Medium	Very heavy	Very heavy
24-Feb	397	154	2996	582	Very heavy	Medium	Very heavy	Very heavy
3-Mar	82	47	597	200	Medium	Light	Medium	Medium
11-Mar	615	135	2473	381	Very heavy	Medium	Very heavy	Very heavy
16-Mar	272	184	886	557	Heavy	Medium	Very heavy	Very heavy
25-Mar	451	218	1677	979	Very heavy	Heavy	Very heavy	Very heavy
5-Apr	331	307	851	463	Heavy	Heavy	Very heavy	Very heavy
14-Apr	305	140	932	141	Heavy	Medium	Medium	Medium
4-May	856	2537	1472	953	Very heavy	Very heavy	Very heavy	Very heavy
24-May	804	90	567	242	Very heavy	Medium	Heavy	Heavy
7-Jun	1265	314	1465	1567	Very heavy	Heavy	Very heavy	Very heavy
7-Jul	662	189	914	870	Very heavy	Medium	Very heavy	Very heavy

Table 5-11: Comparisons of DDDG values for summer and winter

Normalized conductivity , σ_{20} [µS/cm]	Summer				Winter			
	North	*East*	*South*	*West*	*North*	*East*	*South*	*West*
Maximum	614.84	306.67	2995.87	979.40	1265.22	2536.79	1471.89	1566.57
	Very heavy	Heavy	Very heavy	Very heavy	Very heavy	Very heavy	Very heavy	Very heavy
Minimum	82.24	47.01	216.89	117.80	662.07	89.85	566.54	242.18
	Medium	Light	Heavy	Medium	Very heavy	Medium	Very heavy	Heavy
Average	303.42	162.34	1272.31	451.84	896.69	782.62	1104.43	907.97
	Heavy	Medium	Very heavy	Very heavy	Very heavy	Very heavy	Very heavy	Very heavy

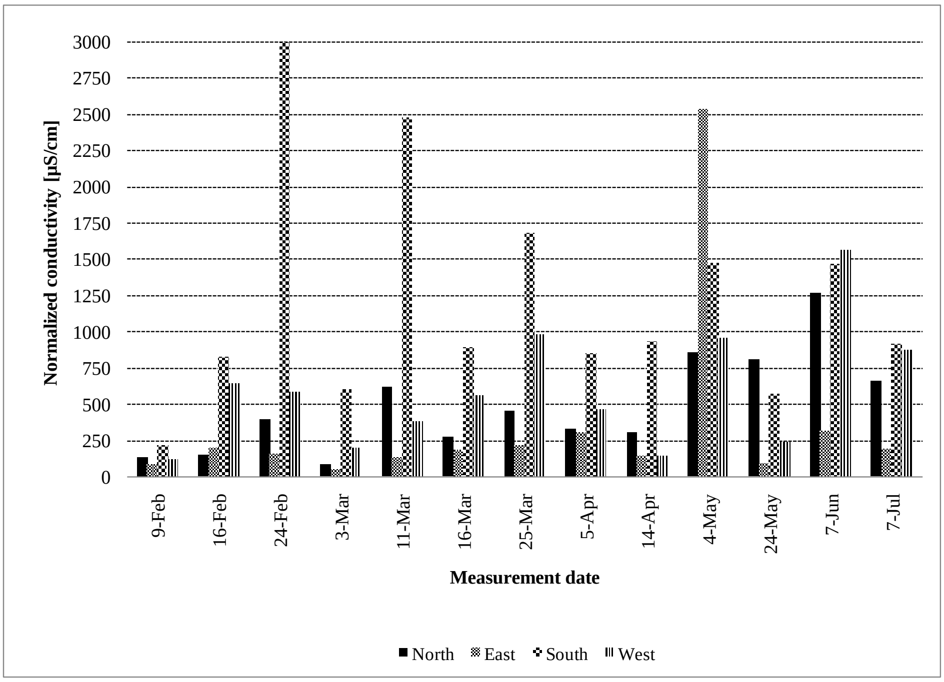

Figure 5-15: Directional dust deposit gauge (DDDG) measurements performed at KIPTS

5.3 Leakage current performance

5.3.1 Overview

Leakage current data was monitored using the OLCA device and continuously sampled at 2 kHz (40 samples/cycle on the ESKOM's 50Hz system). The sampled data was pooled into the highest peak values every 10 minutes for the entire test period (refer to section 4.3). The results reported in this section cover the first six months of the test period from February 3rd. It therefore follows that a total of 144 leakage current data points was recorded each day – giving an aggregate total of 25 632 leakage current data points for each test insulator over the six-month test period. A total of 15 high temperature vulcanized, silicone rubber (HTV-SR) and three glass disc test insulators were considered in the study. Due to this volume of data, it was vital that an appropriate presentation of data be devised that would allow for meaningful interpretation of this massive data (about 461 376 data points of leakage current in total). Consequently, a statistical approach was preferred.

The results have been presented using an approach that employs a time-of-day bin count analysis of the recorded absolute peak leakage currents. The main aim was to compare the relative leakage current performance of the test insulators, looking at both the effect of creepage length and the types of excitation voltage. Nine bin categories were defined, namely (recorded in mA): [0-2], [2-5], [5-10], [10-20], [20-50], [50-100], [100-200], [200-500] and [500-1000]. The results were thus rendered into these bin categories and a total number of counts per each category was then computed for each 10-minute instant of day. This was done in order to gain an in-depth understanding of the performance of insulators at different times of day in relation to the prevailing climatic conditions (as presented in section 5.2.1), instead of just considering average peak leakage values for the entire test period altogether. It was demonstrated in section 5.2.1 that the variations in climatic conditions are time dependent. Hence, a time-of-day approach was considered to be most appropriate to give an indication of how variations in climatic conditions would affect the performance of test insulators.

It was also necessary to assess the prominence of the occurrence of leakage current over the insulator surfaces. Accumulative coulomb-ampere was considered for this purpose. Descriptions on this parameter are given in section 4.3.4.

Sections 5.3.2 and 5.3.3 summarize the results on leakage current performance and accumulative coulomb-ampere, respectively. The results on leakage current performance are presented for each set of insulators with the same creepage length, with emphasis on the effect of excitation voltage types. For accumulative coulomb-ampere, the results are presented with the view to explore the effect of creepage length for a complete set of test insulators installed on a given excitation voltage type. All detailed results for the individual insulators are furnished in Appendix C.

5.3.2 Results for individual test insulators

5.3.2.1 Introduction

With the view that weather conditions vary greatly throughout the year at KIPTS, it was decided that each month's data be considered separately. A time-of-day bin count analysis was thus performed for each month. The time-of-day bin counts for the respective nine (9) bin categories are presented as a percentage of the total number of counts recorded at a particular 10-minute instant. For instance, if we considered the time instant 24h00, we would have a total of 30 leakage current values recorded at this time instant in a 30-day month. Thus, if for instance a total of 1 count was recorded for the [500-1000] mA category at 24h00, then we would record 3% (i.e. (1/30) x 100) for this bin category at that particular time instant for the month. The monthly time-of-day bin analyses for the respective test insulators are presented in table form in Appendices C.2 to C.7. Graphical representations of the time-of-day bin analyses are given in the same appendices for the entire test period.

Please note that the first two bin categories, i.e. [0-2] and [2-5], were considered as the noise band and they have therefore been ignored in all discussions presented in the following sections. Refer to Appendices C.2 to C.7 for full details on these two bin categories. The results pertaining to the leakage current performance of all test insulators are summarized as explained below:

- A summary of bin count analysis of the leakage current recorded for the respective insulators is presented in Table 5-12. A graphical representation of these bin counts is depicted in Figure 5-16, given per each bin category.

- The average and maximum values of the leakage current recorded for the respective insulators are presented in Table 5-13. Note that four time of day instances have been considered, namely: midnight (24h00), sunrise (06h00), midday (12h00) and sunset (18h00). The highest peak leakage current for each test insulator is also indicated in the table, quoting the time of occurrence.

- All instances of flashover events are presented in Table 5-14 for HVT-SR 29 DC+ and Glass disc 42 DC-.
- Comparisons of the highest leakage currents recorded for all test insulators over the entire test period are graphically presented in Figure 5-17.

- *Bin count analysis of leakage current*

Table 5-12: A summary of bin count analysis of the leakage current recorded for all test insulators

Bin Categories [mA]	Total Bin Counts for the Entire Test Period																	
	HTV-SR 84			HTV-SR 72			HTV-SR 56			HTV-SR 44			HTV-SR 29			Glass disc 42		
	AC	*DC+*	*DC-*	*AC*	*DC+*	**DC-*	*AC*	*DC+*	*DC-*	*AC*	*DC+*	*DC-*	*AC*	*DC+*	*DC-*	*AC*	*DC+*	*DC-*
[5-10]	1147	839	603	1423	1172	-	1602	1781	1561	1474	1748	1495	829	1092	923	142	1123	297
[10-20]	483	539	88	1222	850	-	1394	1179	1559	1228	1343	1199	845	1168	965	57	1762	392
[20-50]	252	206	0	579	267	-	749	557	159	921	825	268	1471	685	581	31	2133	487
[50-100]	1	0	0	1	2	-	24	3	0	103	49	0	687	422	72	1	891	396
[100-200]	0	0	0	0	0	-	0	0	0	4	0	0	61	64	2	0	406	202
[200-500]	0	0	0	0	0	-	0	0	0	0	0	0	2	9	0	5	5	63
[500-1000]	0	0	0	0	0	-	0	0	0	0	0	0	0	1	0	0	0	12
Total Bin Counts	1883	1584	691	3225	2291	-	3769	3520	3279	3730	3965	2962	3895	3441	2543	236	6320	1849

* Faulty sensor on HTV-SR 72 DC- (DC offsets)

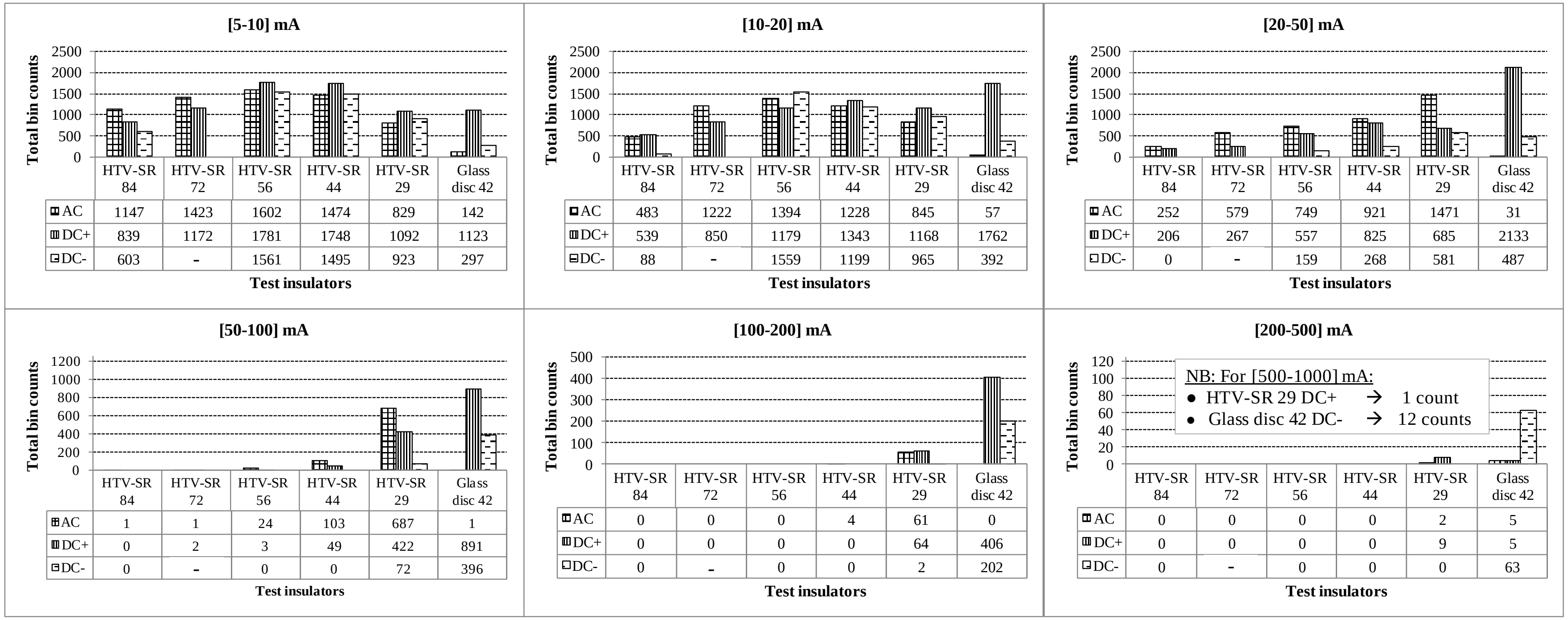

Figure 5-16: A graphical representation of bin count analysis of the leakage current recorded for all test insulators

- *Details pertaining to the actual leakage current and flashover events*

Table 5-13: The average and maximum values of the leakage current recorded for all test insulators, given per time of day

Time of day	Leakage Current [mA]	HTV-SR 84			HTV-SR 72			HTV-SR 56			HTV-SR 44			HTV-SR 29			Glass disc 42		
		AC	*DC+*	*DC-*	*AC*	*DC+*	**DC-*	*AC*	*DC+*	*DC-*	*AC*	*DC+*	*DC-*	*AC*	*FO DC+*	*DC-*	*AC*	*DC+*	*FO DC-*
Midnight (24h00)	*Average*	2.37	2.50	1.31	2.71	2.42	-	3.30	3.71	2.82	3.76	3.79	3.01	6.91	5.34	3.51	1.24	12.74	6.82
	Maximum	30.12	21.45	12.50	35.01	27.35	-	36.12	42.56	22.14	44.74	48.34	27.71	84.80	97.93	51.93	5.61	133.21	266.71
Sunrise (06h00)	*Average*	2.31	2.61	1.24	2.30	2.54	-	3.07	3.88	3.28	3.79	4.37	3.29	8.84	9.60	4.39	1.20	15.32	6.12
	Maximum	35.73	29.18	12.50	25.91	34.28	-	32.95	51.35	25.94	42.99	48.10	27.71	124.85	242.73	45.90	7.01	169.41	167.89
Midday (12h00)	*Average*	1.18	1.76	0.80	0.95	1.21	-	1.08	1.28	1.24	1.51	1.40	1.56	1.82	1.70	1.40	1.09	1.58	1.28
	Maximum	8.40	6.31	4.17	12.96	7.34	-	20.33	10.18	10.50	33.55	21.37	9.82	43.23	54.91	21.12	4.91	49.87	60.28
Sunset (18h00)	*Average*	1.83	2.12	0.92	1.99	1.65	-	2.35	2.05	1.62	2.91	2.08	1.98	3.81	2.08	2.00	1.26	5.16	1.75
	Maximum	31.52	21.80	10.17	39.92	21.39	-	49.45	22.86	22.40	52.12	35.81	20.34	104.18	31.56	47.43	19.98	116.34	61.69
Entire test period	*Maximum*	55.32	34.10	16.84	52.21	52.60	-	64.49	51.70	31.50	137.36	80.22	35.77	235.18	716.11	104.56	365.31	306.49	626.30
	Time recorded	24/6 5:40	22/3 8:30	29/3 3:30	24/6 5:40	13/3 8:40	-	24/6 5:40	13/3 6:20	13/3 8:40	24/6 5:40	18/4 3:50	13/3 9:00	24/6 5:40	12/3 6:10	26/4 4:10	28/3 12:20	22/3 8:20	18/4 22:10

* Faulty sensor on HTV-SR 72 DC- (DC offsets) *FO* Fuse operation

Table 5-14: Flashover events recorded in the entire test period

	Fuse Operation (*FO*) Events		
	Glass disc 42 DC-		HTV-SR 29 DC+
Leakage current [mA]	484.04	450.75	716.11
Time of occurrence	23/2 5:40	13/3 1:50	12/3 6:10

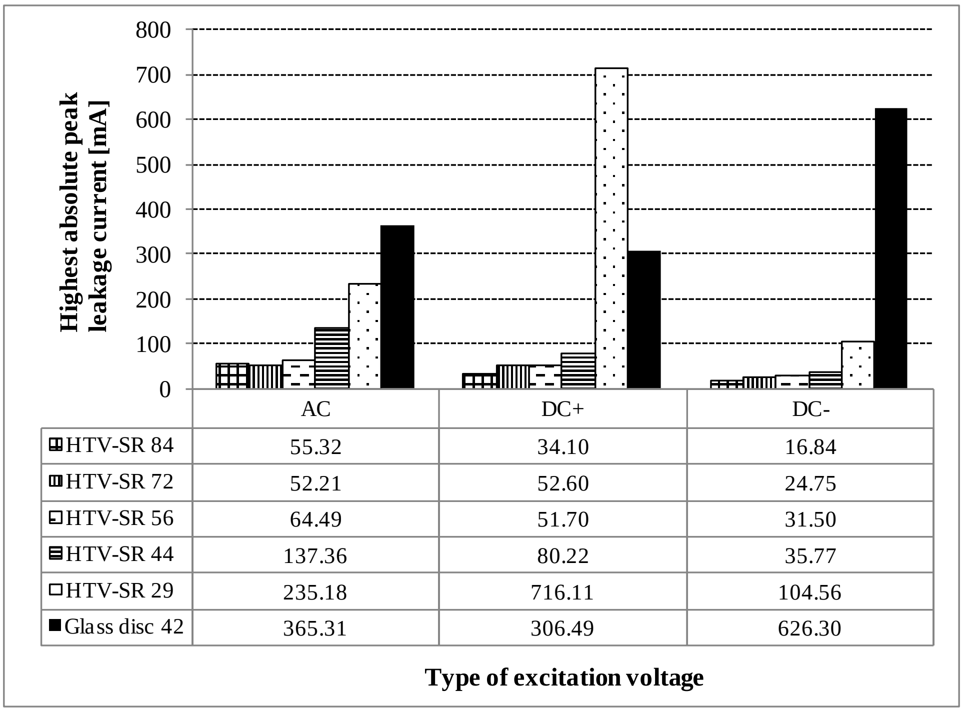

Figure 5-17: The highest absolute peak leakage currents recorded for all the test insulators

5.3.2.2 Leakage current performance for the HTV-SR 84 insulators

This section presents the results for high temperature vulcanized silicone rubber insulators with a unified specific creepage distance (USCD) of 84 mm/kV. Refer to Appendix C.2 for detailed results of the insulators with this particular USCD.

- *Bin count analysis of leakage current*

  The monthly results for the time-of-day bin count analysis are summarized in Table C-5, using the actual bin counts. It was observed that the highest counts were recorded for the lower bin categories throughout the test period for all the excitation voltage types. It should further be mentioned that higher current levels were recorded in summer when compared to those recorded in winter.

  With reference to Table 5-12 (and Table C-6), the following ranking of the total leakage current bin counts for the HTV-SR 84 insulators can be made based on the higher leakage current bin categories (> 5 mA):

  (Highest) HTV-SR 84 AC → HTV-SR 84 DC+ → HTV-SR 84 DC- *(Lowest)*

  The time-of-day bin count analyses for the entire test period are graphically presented in Figure C-8, Figure C-9 and Figure C-10. The results were split up into three bigger bin categories: [0-10], [10-100] and [100-1000]. It was observed from Figure C-8 that the lower leakage current levels were recorded throughout the day, particularly for the [0-2] category. However, with reference to Figure C-9, higher leakage current levels were mainly recorded at night and also during the early morning hours. These times coincide with the observations made with regard to variations in the climatic conditions at KIPTS; where relative humidity exceeded 75% when the difference between the ambient and dewpoint temperatures was very low (see Figure 5-5). No currents higher than 100 mA were recorded for the HTV-SR 84 insulators and this is also evident from Figure 5-17.

- *An overview of the actual leakage current profile*

An overview of the average and maximum values of the recorded peak leakage current is given in Table 5-13 (also see Table C-7), given per four time instants of day, namely: midnight (24h00), sunrise (06h00), midday (12h00) and sunset (18h00). The highest average and maximum leakage current values were recorded at sunrise (06h00) for AC, DC+ and DC- when compared to the values recorded at the other time instants presented in the table. The lowest average and maximum values were recorded at midday (12h00).

The average leakage current values were calculated from the original data for the entire test period and the following trend was established:

(Highest) HTV-SR 84 DC+ → HTV-SR 84 AC → HTV-SR 84 DC- *(Lowest)*

This trend also corresponds to the time of day profile of average leakage current presented in Figure 5-18.

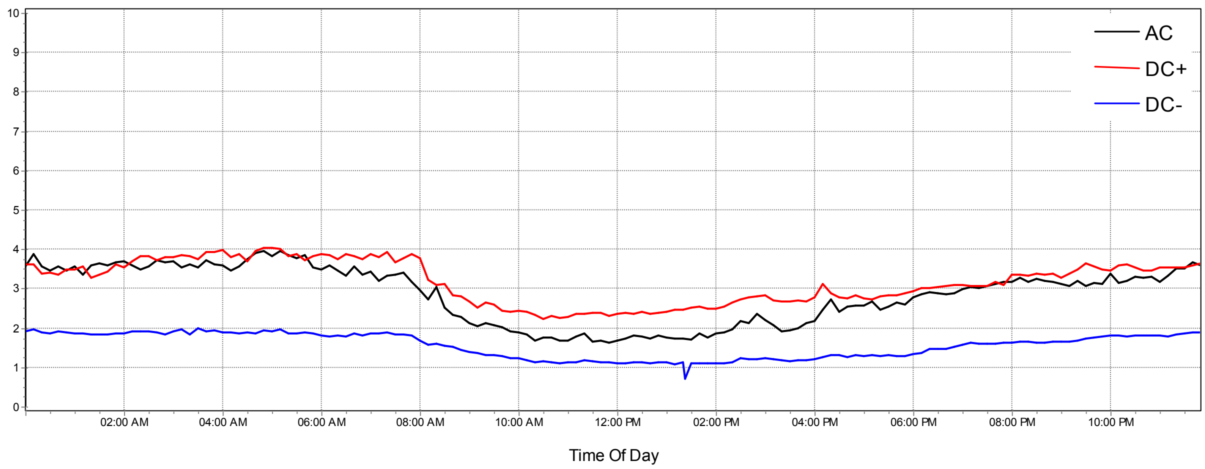

Figure 5-18: The time-of-day average absolute peak leakage current profile recorded for all the HTV-SR 84 insulators

On the basis of the information presented in Table 5-13 and Figure 5-17, the following trend can be stated with regard to the highest recorded leakage current:

(Highest) HTV-SR 84 AC → HTV-SR 84 DC+ → HTV-SR 84 DC- *(Lowest)*

The time of day profile of the maximum leakage current, as shown in Figure 5-19, confirms the above listed trend.

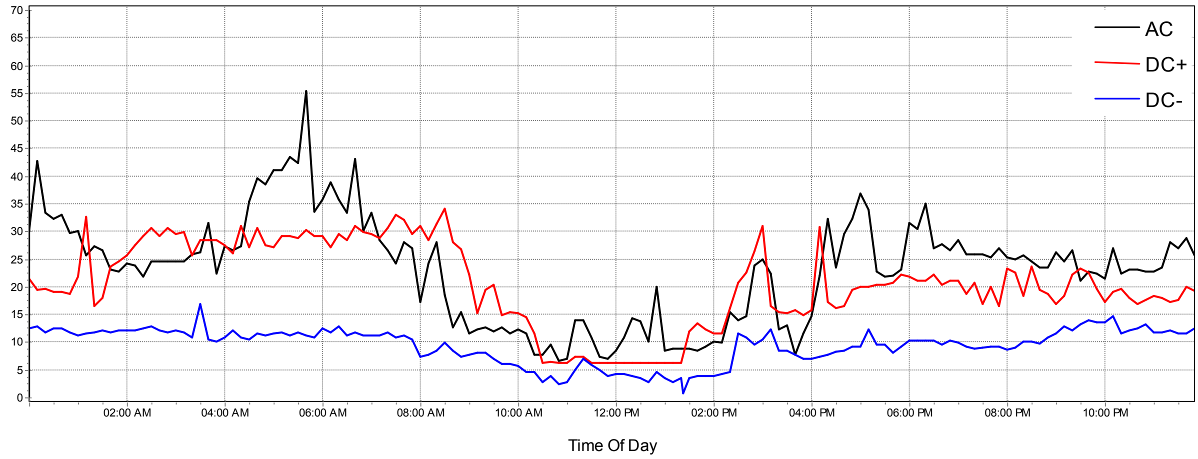

Figure 5-19: The time-of-day maximum absolute peak leakage current profile recorded for all the HTV-SR 84 insulators

5.3.2.3 Leakage current performance for the HTV-SR 72 insulators

This section presents the results for high temperature vulcanized silicone rubber insulators with a unified specific creepage distance (USCD) of 72 mm/kV. Refer to Appendix C.3 for detailed results of the insulators with this particular USCD.

- *Bin count analysis of leakage current*

  The monthly results for the time-of-day bin count analysis are summarized in Table C-8, using the actual bin counts. It was observed that the highest counts were recorded for the lower bin categories throughout the test period for all the excitation voltage types. It should further be mentioned that higher current levels were recorded in summer when compared to those recorded in winter.

  With reference to Table 5-12 (and Table C-9), the following ranking of the total leakage current bin counts for the HTV-SR 72 insulators can be made based on the higher leakage current bin categories (> 5 mA):

  (Highest) **HTV-SR 72 DC-→** HTV-SR 72 AC → HTV-SR 72 DC+ *(Lowest)*

  It must be mentioned here that persistent DC offsets were experienced on the sensor associated with HTV-SR 72 DC-. This is evident from the high count recorded for the [2-5] mA bin category which is rather too high when compared to those of HTV-SR 72 AC and HTV-SR 72 DC+ (refer to Figure C-11).This might have had an effect that the offsets would cause possible skewness in the recorded leakage current for HTV-SR 72 DC-. Thus, the HTV-SR 72 DC- data can be ignored due to the faulty sensor. The above trend therefore becomes:

  (Highest) HTV-SR 72 AC → HTV-SR 72 DC+ *(Lowest)*

  The time-of-day bin count analyses for the entire test period are graphically presented in Figure C-11, Figure C-12 and Figure C-13. The results were split up into three bigger bin categories: [0-10], [10-100] and [100-1000]. It was observed from Figure C-11 that the lower leakage current levels were recorded throughout the day, particularly for the [0-2] category. For HTV-SR 72 DC-, it was found that a considerable number of counts were recorded for the [2-5] category which serves to justify the offsets that were dominantly found to exhibit on this channel. However, with reference to Figure C-12, higher leakage current levels were mainly recorded at night and also during the early morning hours. These times coincide with the observations made with regard to variations in the climatic conditions at KIPTS; where relative humidity exceeded 75% when the difference between the ambient and dewpoint temperatures was very low (see Figure 5-5). No currents higher than 100 mA were recorded for the HTV-SR 72 insulators and this is also evident from Figure 5-17.

- *An overview of the actual leakage current profile*

An overview of the average and maximum values of the recorded peak leakage current is given in Table 5-13 (also see Table C-10), given per four time instants of day, namely: midnight (24h00), sunrise (06h00), midday (12h00) and sunset (18h00). The lowest values of the average and maximum leakage current were recorded at midday (12h00) for all the test insulators, whereas the highest were recorded at sunrise (06h00) for HTV-SR 72 DC+ and HTV-SR 72 DC- and at sunset (18h00) for HTV-SR 72 AC.

The average leakage current values were calculated from the original data for the entire test period and the following trend was established:

(Highest) HTV-SR 72 AC → HTV-SR 72 DC+ *(Lowest)*

This trend also corresponds to the time of day profile of average leakage current presented in Figure 5-20.

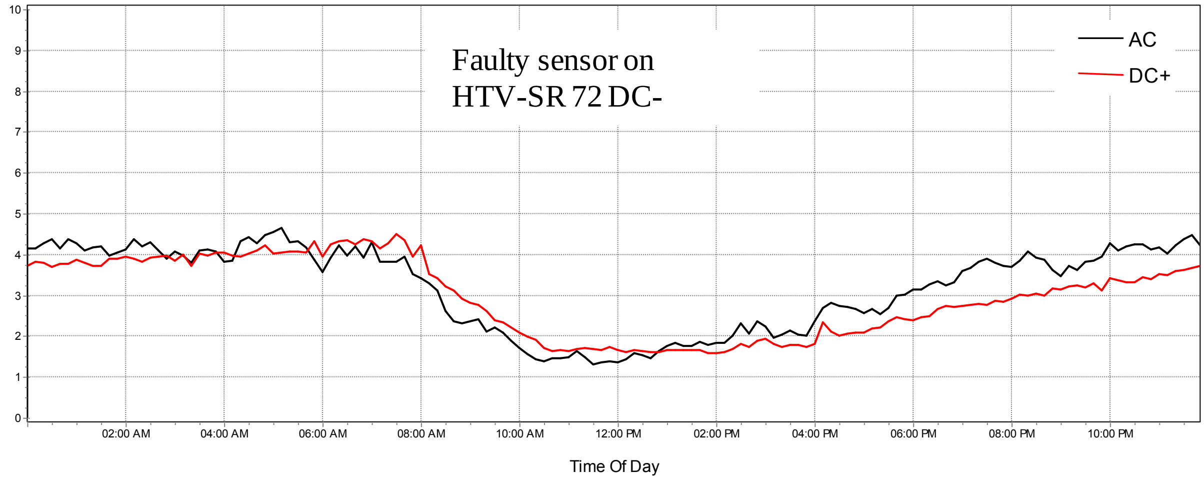

Figure 5-20: The time-of-day average absolute peak leakage current profile recorded for all the HTV-SR 72 insulators

On the basis of the information presented in Table 5-13 and Figure 5-17, the following trend can be stated with regard to the highest recorded leakage current:

(Highest) HTV-SR 72 DC+ → HTV-SR 72 AC *(Lowest)*

The time of day profile of the maximum leakage current, as shown in Figure 5-21, confirms the above listed trend.

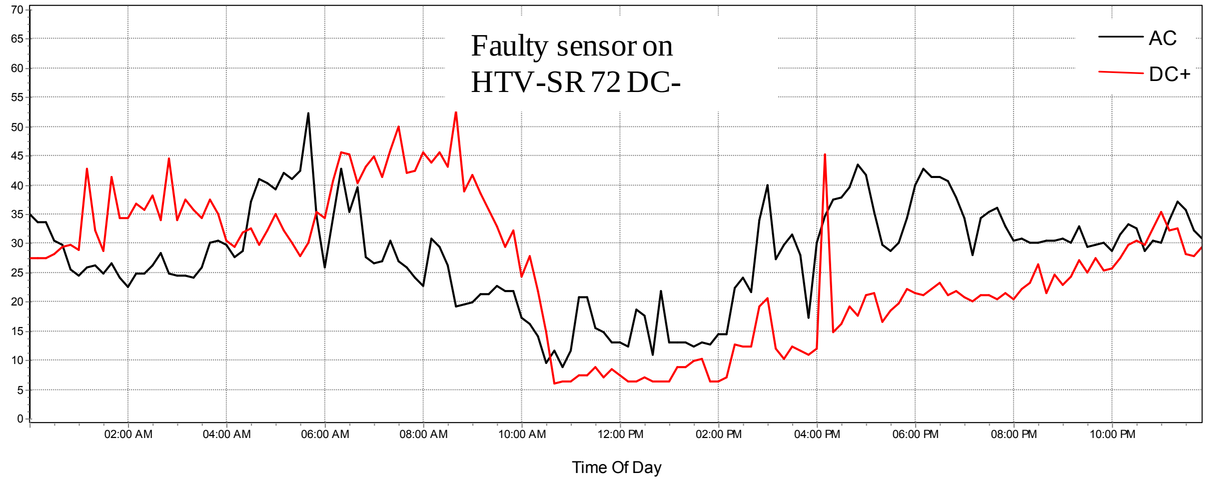

Figure 5-21: The time-of-day maximum absolute peak leakage current profile recorded for all the HTV-SR 72 insulators

It can be noted from Figure 5-21 that the maximum absolute peak leakage current values recorded for the three test insulators occurred in the morning hours: 05h40 for HTV-SR 72 AC and 08h40 for HTV-SR 72 DC+. The relative humidity was found to be 75% when the AC maximum absolute peak leakage current occurred, whereas 94% was recorded for DC+.

5.3.2.4 Leakage current performance for the HTV-SR 56 insulators

This section presents the results for high temperature vulcanized silicone rubber insulators with a unified specific creepage distance (USCD) of 56 mm/kV. Refer to Appendix C.4 for detailed results of the insulators with this particular USCD.

- *Bin count analysis of leakage current*

  The monthly results for the time-of-day bin count analysis are summarized in Table C-11, using the actual bin counts. It was observed that the highest counts were recorded for the lower bin categories throughout the test period for all the excitation voltage types. It should further be mentioned that higher current levels were recorded in summer when compared to those recorded in winter.

  With reference to Table 5-12 (and Table C-12), the following ranking of the total leakage current bin counts for the HTV-SR 56 insulators can be made based on the higher leakage current bin categories (> 5 mA):

  (Highest) HTV-SR 56 AC → HTV-SR 56 DC+ → HTV-SR 56 DC- *(Lowest)*

  The time-of-day bin count analyses for the entire test period are graphically presented in Figure C-14, Figure C-15 and Figure C-16. The results were split up into three bigger bin categories: [0-10], [10-100] and [100-1000]. It was observed from Figure C-14 that the lower leakage current levels were recorded throughout the day, particularly for the [0-2] category. However, with reference to Figure C-15, higher leakage current levels were mainly recorded at night and also during the early morning hours. These times coincide with the observations made with regard to variations in the climatic conditions at KIPTS; where relative humidity exceeded 75% when the difference between the ambient and dewpoint temperatures was very low (see Figure 5-5). No currents higher than 100 mA were recorded for the HTV-SR 56 insulators and this is also evident from Figure 5-17.

- *An overview of the actual leakage current profile*

An overview of the average and maximum values of the recorded peak leakage current is given in Table 5-13 (also see Table C-13), given per four time instants of day, namely: midnight (24h00), sunrise (06h00), midday (12h00) and sunset (18h00). The lowest values of the average and maximum leakage current were recorded at midday (12h00) for all the test insulators.

The average leakage current values were calculated from the original data for the entire test period and the following trend was established:

(Highest) HTV-SR 56 DC+ → HTV-SR 56 AC → HTV-SR 56 DC-*(Lowest)*

This trend also corresponds to the time of day profile of average leakage current presented in Figure 5-22.

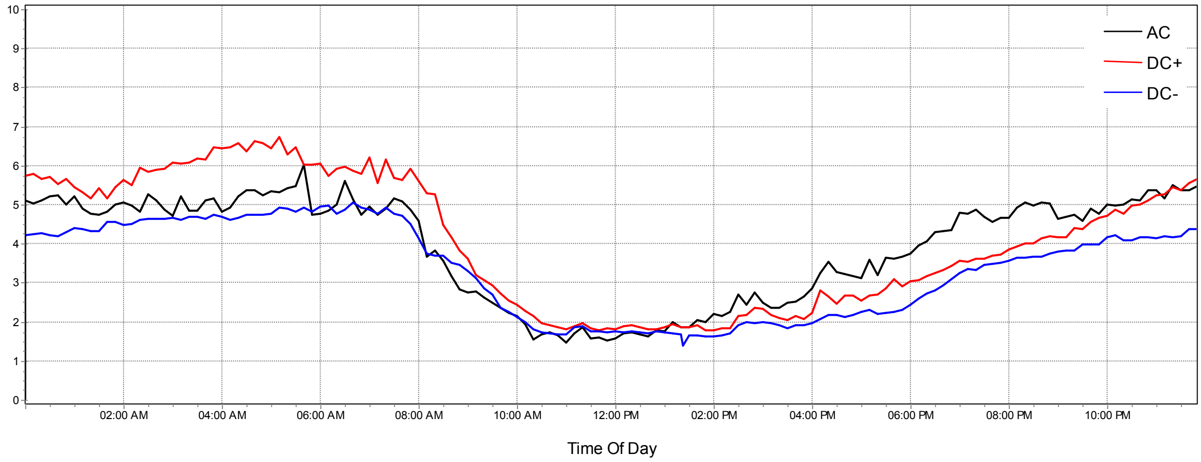

Figure 5-22: The time-of-day average absolute peak leakage current profile recorded for all the HTV-SR 56 insulators

On the basis of the information presented in Table 5-13 and Figure 5-17, the following trend can be stated with regard to the highest recorded leakage current:

(Highest) HTV-SR 56 AC → HTV-SR 56 DC+ → HTV-SR 56 DC- *(Lowest)*

The time of day profile of the maximum leakage current, as shown in Figure 5-23, confirms the above listed trend.

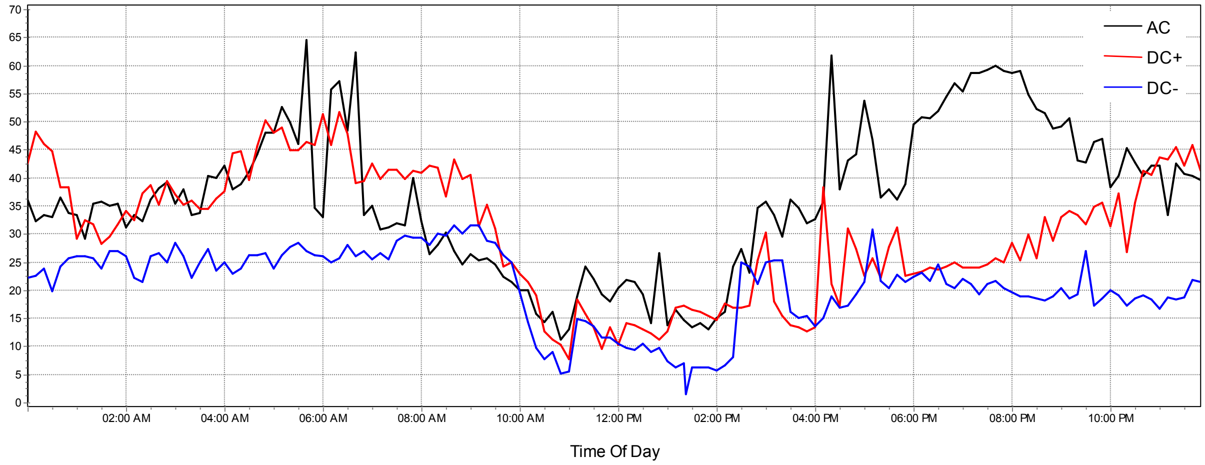

Figure 5-23: The time-of-day maximum absolute peak leakage current profile recorded for all the HTV-SR 56 insulators

Although the maximum absolute peak leakage current values recorded for the three test insulators occurred on different days (as noted in Table 5-13), it is interesting to note that they all occurred in the morning hours. The relative humidity was found to be 76% when the AC maximum absolute peak leakage current occurred, whereas 93% and 95% relative humidity levels were recorded for DC+ and DC-, respectively.

5.3.2.5 Leakage current performance for the HTV-SR 44 insulators

This section presents the results for high temperature vulcanized silicone rubber insulators with a unified specific creepage distance (USCD) of 44 mm/kV. Refer to Appendix C.5 for detailed results of the insulators with this particular USCD.

- *Bin count analysis of leakage current*

  The monthly results for the time-of-day bin count analysis are summarized in Table C-14, using the actual bin counts. It was observed that the highest counts were recorded for the lower bin categories throughout the test period for all the excitation voltage types. It should further be mentioned that higher current levels were recorded in summer when compared to those recorded in winter.

  With reference to Table 5-12 (and Table C-15), the following ranking of the total leakage current bin counts for the HTV-SR 44 insulators can be made based on the higher leakage current bin categories (> 5 mA):

  (Highest) HTV-SR 44 DC+ → HTV-SR 44 AC → HTV-SR 44 DC- *(Lowest)*

  The time-of-day bin count analyses for the entire test period are graphically presented in Figure C-17, Figure C-18 and Figure C-19. The results were split up into three bigger bin categories: [0-10], [10-100] and [100-1000]. It was observed from Figure C-17 that the lower leakage current levels were recorded throughout the day, particularly for the [0-2] category. However, with reference to Figure C-18, higher leakage current levels were mainly recorded at night and also during the early morning hours. These times coincide with the observations made with regard to variations in the climatic conditions at KIPTS; where relative humidity exceeded 75% when the difference between the ambient and dewpoint temperatures was very low (see Figure 5-5). No currents higher than 100 mA were recorded for the HTV-SR 44 DC+ and HTV-SR 44 DC- insulators and this is also evident from Figure 5-17.

- *An overview of the actual leakage current profile*

An overview of the average and maximum values of the recorded peak leakage current is given in Table 5-13 (also see Table C-16), given per four time instants of day, namely: midnight (24h00), sunrise (06h00), midday (12h00) and sunset (18h00). The lowest values of the average and maximum leakage current were recorded at midday (12h00) for all the test insulators.

The average leakage current values were calculated from the original data for the entire test period and the following trend was established:

(Highest) HTV-SR 44 AC → HTV-SR 44 DC+ → HTV-SR 44 DC- *(Lowest)*

This trend also corresponds to the time of day profile of average leakage current presented in Figure 5-24.

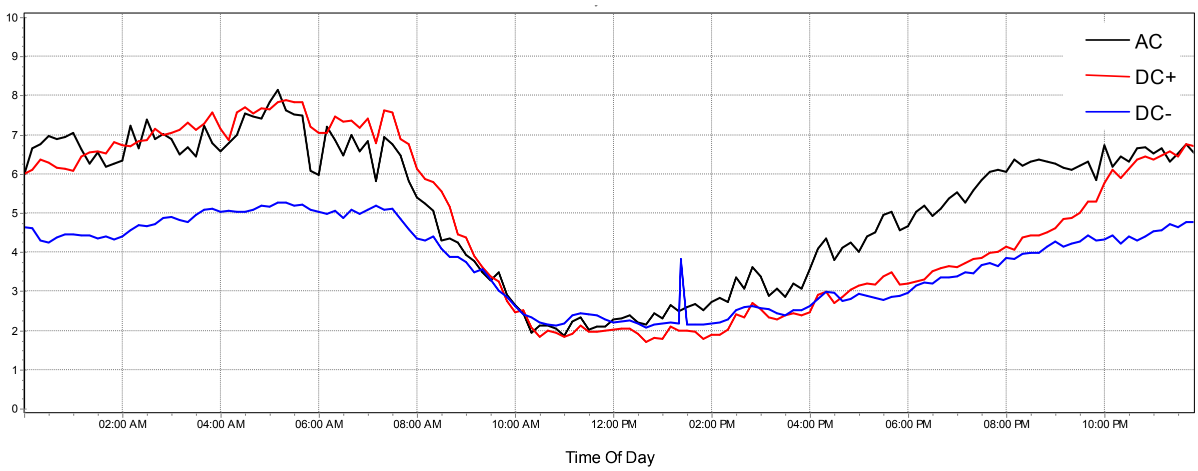

Figure 5-24: The time-of-day average absolute peak leakage current profile recorded for all the HTV-SR 44 insulators

On the basis of the information presented in Table 5-13 and Figure 5-17, the following trend can be stated with regard to the highest recorded leakage current:

(Highest) HTV-SR 44 AC → HTV-SR 44 DC+ → HTV-SR 44 DC- *(Lowest)*

The time of day profile of the maximum leakage current, as shown in Figure 5-25, confirms the above listed trend.

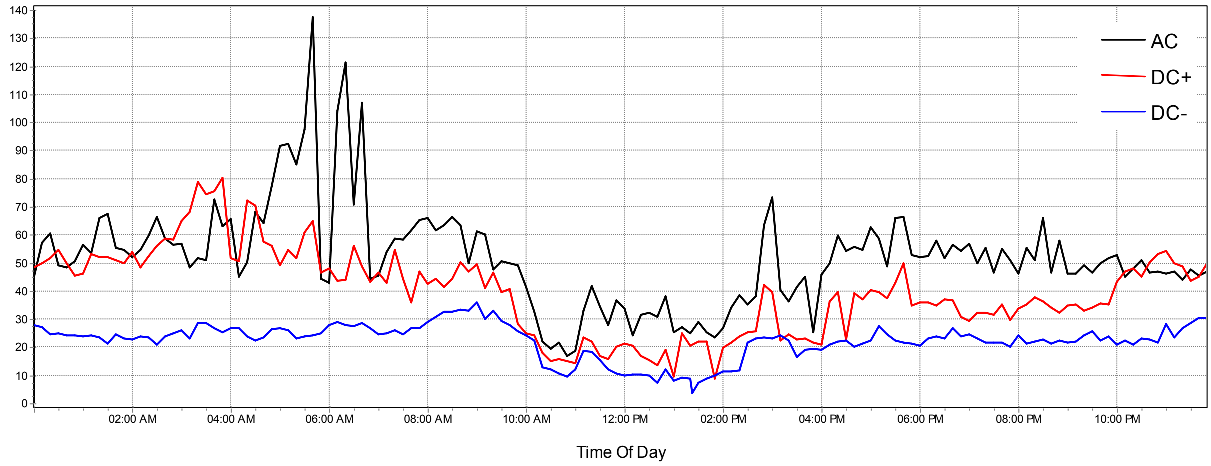

Figure 5-25: The time-of-day maximum absolute peak leakage current profile recorded for all the HTV-SR 44 insulators

Although the maximum absolute peak leakage current values recorded for the three test insulators over the entire test period occurred on different days (as noted in Table 5-13), it is interesting to note that they all occurred in the morning hours. The relative humidity was found to be 76% when the AC maximum absolute peak leakage current occurred, whereas 80% and 89% relative humidity levels were recorded for DC+ and DC-, respectively.

5.3.2.6 Leakage current performance for the HTV-SR 29 insulators

This section presents the results for high temperature vulcanized silicone rubber insulators with a unified specific creepage distance (USCD) of 29 mm/kV. Refer to Appendix C.6 for detailed results of the insulators with this particular USCD.

- *Bin count analysis of leakage current*

  The monthly results for the time-of-day bin count analysis are summarized in Table C-17, using the actual bin counts. It was observed that the highest counts were recorded for the lower bin categories throughout the test period for all the excitation voltage types. It should further be mentioned that higher current levels were recorded in summer when compared to those recorded in winter.

  With reference to Table 5-12 (and Table C-18), the following ranking of the total leakage current bin counts for the HTV-SR 29 insulators can be made based on the higher leakage current bin categories (> 5 mA):

  (Highest) HTV-SR 29 AC → HTV-SR 29 DC+ → HTV-SR 29 DC- *(Lowest)*

  The time-of-day bin count analyses for the entire test period are graphically presented in Figure C-20, Figure C-21 and Figure C-22. The results were split up into three bigger bin categories: [0-10], [10-100] and [100-1000]. It was observed from Figure C-20 that the lower leakage current levels were recorded throughout the day, particularly for the [0-2] category. However, with reference to Figure C-21 and Figure C-22, higher leakage current levels were mainly recorded at night and also during the early morning hours. These times coincide with the observations made with regard to variations in the climatic conditions at KIPTS; where relative humidity exceeded 75% when the difference between the ambient and dewpoint temperatures was very low (see Figure 5-5). No currents higher than 500 mA were recorded for the HTV-SR 29 AC and HTV-SR 29 DC- insulators and this is also evident from Figure 5-17.

- *An overview of the actual leakage current profile*

An overview of the average and maximum values of the recorded peak leakage current is given in Table 5-13 (also see Table C-19), given per four time instants of day, namely: midnight (24h00), sunrise (06h00), midday (12h00) and sunset (18h00). The lowest values of the average and maximum leakage current were recorded at midday (12h00) for all the test insulators.

The average leakage current values were calculated from the original data for the entire test period and the following trend was established:

(Highest) HTV-SR 29 AC → HTV-SR 29 DC+ → HTV-SR 29 DC- *(Lowest)*

This trend also corresponds to the time of day profile of average leakage current presented in Figure 5-26.

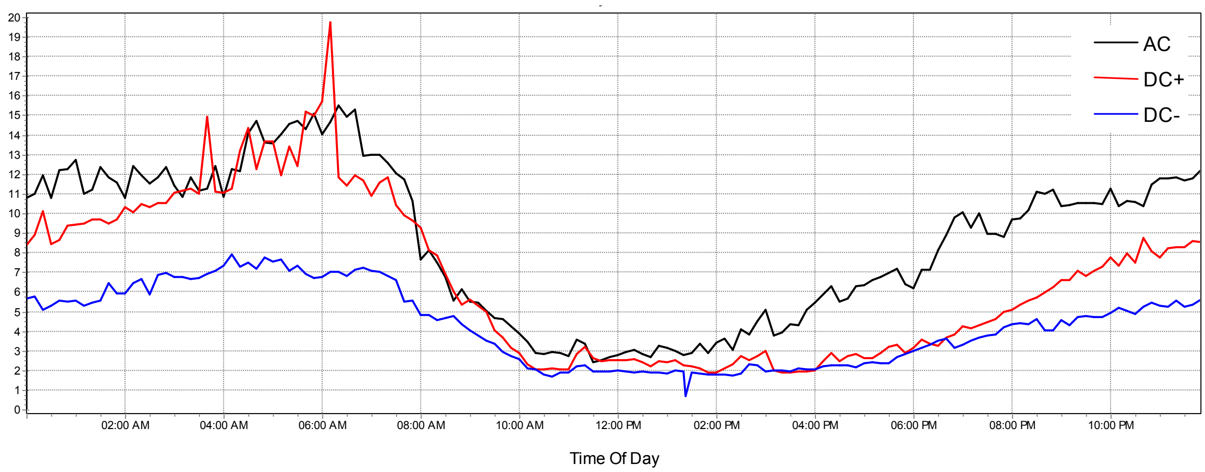

Figure 5-26: The time-of-day average absolute peak leakage current profile recorded for all the HTV-SR 29 insulators

On the basis of the information presented in Table 5-13 and Figure 5-17, the following trend can be stated with regard to the highest recorded leakage current:

(Highest) HTV-SR 29 DC+ → HTV-SR 29 AC → HTV-SR 29 DC- *(Lowest)*

The time of day profile of the maximum leakage current, as shown in Figure 5-27, confirms the above listed trend.

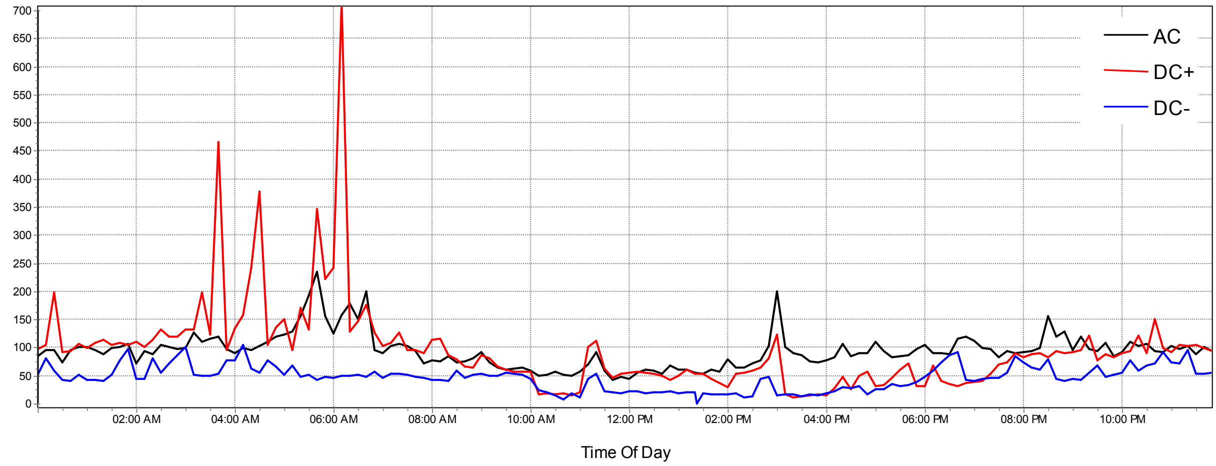

Figure 5-27: The time-of-day maximum absolute peak leakage current profile recorded for all the HTV-SR 29 insulators

A fuse operation was recorded on HTV-SR 29 DC+ and a leakage current of 716.11 mA was recorded at the time when the fuse popped. The HTV-SR 29 AC insulator had 22.50 mA, whereas HTV-SR 29 DC- had 4.56 mA at the time of the fuse operation. This information is given in Table 5-14. It would have been expected that all test insulators exhibit elevated leakage current levels given the prevailing relative humidity of 90%. However, it appears that an instantaneous pollution condition had uniquely occurred on the surface of this specific insulator (HTV-SR 29 DC+) – causing a rapid flow of high leakage currents as quoted above.

Although the maximum absolute peak leakage current values recorded for the three test insulators over the entire test period occurred on different days (as noted in Table 5-13), it is interesting to note that they all occurred in the morning hours. The relative humidity was found to be 76% when the AC maximum absolute peak leakage current occurred, whereas 90% and 83% relative humidity levels were recorded for DC+ and DC-, respectively.

5.3.2.7 Leakage current performance for the Glass disc 42 insulators

This section presents the results for glass disc insulators with a unified specific creepage distance (USCD) of 42 mm/kV. Refer to Appendix C.7 for detailed results of the insulators with this particular USCD.

- *Bin count analysis of leakage current*

  The monthly results for the time-of-day bin count analysis are summarized in Table C-20, using the actual bin counts. It was observed that the highest counts were recorded for the lower bin categories throughout the test period for all the excitation voltage types. It should further be mentioned that higher current levels were recorded in summer when compared to those recorded in winter.

  With reference to Table 5-12 (and Table C-21), the following ranking of the total leakage current bin counts for the glass disc insulators can be made based on the higher leakage current bin categories (> 5 mA):

  (Highest) Glass disc 42 DC+ → Glass disc 42 DC- → Glass disc 42 AC *(Lowest)*

  The time-of-day bin count analyses for the entire test period are graphically presented in Figure C-23, Figure C-24 and Figure C-25. The results were split up into three bigger bin categories: [0-10], [10-100] and [100-1000]. It was observed from Figure C-23 that the lower leakage current levels were recorded throughout the day, particularly for the [0-2] category. However, with reference to Figure C-24 and Figure C-25, higher leakage current levels were mainly recorded at night and also during the early morning hours. These times coincide with the observations made with regard to variations in the climatic conditions at KIPTS; where relative humidity exceeded 75% when the difference between the ambient and dewpoint temperatures was very low (see Figure 5-5). No currents higher than 500 mA were recorded for the Glass disc 42 AC and Glass disc 42 DC+ insulators and this is also evident from Figure 5-17.

- *An overview of the actual leakage current profile*

An overview of the average and maximum values of the recorded peak leakage current is given in Table 5-13 (also see Table C-22), given per four time instants of day, namely: midnight (24h00), sunrise (06h00), midday (12h00) and sunset (18h00). The lowest values of the average and maximum leakage current were recorded at midday (12h00) for all the test insulators.

The average leakage current values were calculated from the original data for the entire test period and the following trend was established:

(Highest) Glass disc 42 DC+ → Glass disc 42 DC- → Glass disc 42 AC *(Lowest)*

This trend also corresponds to the time of day profile of average leakage current presented in Figure 5-28.

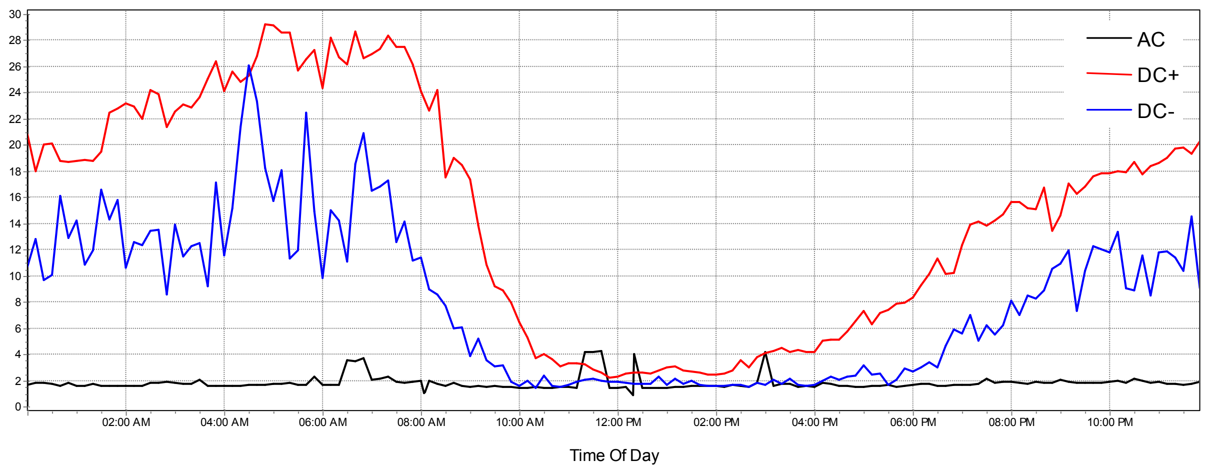

Figure 5-28: The time-of-day average absolute peak leakage current profile recorded for all the glass disc insulators

On the basis of the information presented in Table 5-13 and Figure 5-17, the following trend can be stated with regard to the highest recorded leakage current:

(Highest) Glass disc 42 DC- → Glass disc 42 AC → Glass disc 42 DC+ *(Lowest)*

The time of day profile of the maximum leakage current, as shown in Figure 5-29, confirms the above listed trend.

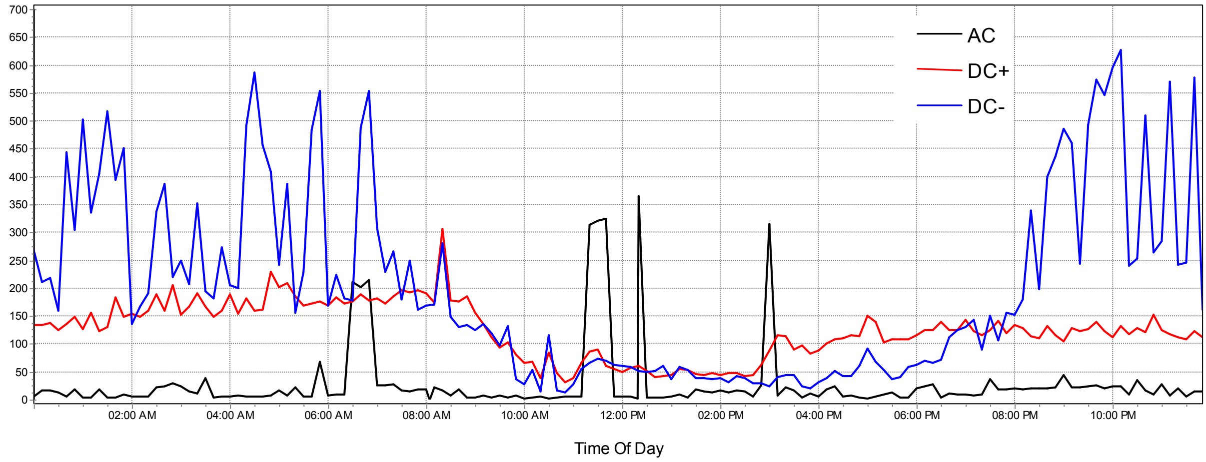

Figure 5-29: The time-of-day maximum absolute peak leakage current profile recorded for all glass disc insulators

Two instances of fuse operations were recorded for Glass disc 42 DC-, as summarized in Table 5-14. An overview of leakage current values on the glass disc insulators installed on AC and DC+ at the time of the fuse operation is also given in the table. For both instances of fuse operation, high levels of relative humidity prevailed at the time of the fuse operations as noted in Table 5-14. Although the mace fuses were designed to explode for leakage current levels above 750 mA, we can see here that the fuses popped for leakage currents in the order of about 500 mA. This might be dependent on the amount of electrical energy dissipated during the arcing events as well the duration for which such events may have persisted. Very low leakage currents (< 2 mA) were recorded for AC, whereas considerably higher leakage currents were recorded for DC+ at the time of the fuse operations on Glass disc 42 DC-.

Although the maximum absolute peak leakage current values recorded for the three test insulators over the entire test period occurred on different days (as noted in Table 5-13), it is interesting to note that they all occurred in the morning hours. The relative humidity was found to be 65% when the AC maximum absolute peak leakage current occurred, whereas 83% relative humidity level was recorded for both DC+ and DC-.

5.3.3 An overview of the results on accumulative coulomb-ampere

5.3.3.1 Introduction

The results presented in the previous section have given an overview of how a particular set of insulators with the same creepage length relate with one another under AC, DC+ and DC-. This gives information on the effect of excitation voltage types. This section compares the electrical performance of all HTV-SR insulators under the respective excitation voltage types – thereby giving information on the effect of creepage length. The accumulative coulomb-ampere was calculated for each test insulator and the results are presented in Figure 5-30, Figure 5-31 and Figure 5-32 for AC, DC+ and DC-, respectively. Notice the gaps observable in the figures, indicating that no data was logged during those periods. This accumulative coulomb-ampere parameter is representative of the incremental electrical power (or energy) dissipated over the insulator surfaces due to the flow of leakage currents. Calculations were done according to Equation(10), defined in section 4.3.4.

5.3.3.2 AC excitation voltage

Figure 5-30 depicts the relative electrical performance of HTV-SR insulators installed on the AC excitation voltage. The following ranking of electrical performance of the test insulators can be stated on the basis of the insulator with the highest accumulative coulomb-ampere at the end of the test period (consider 2011/07/15):

(Highest) HTV-SR 29→ HTV-SR 44→ HTV-SR 56→ HTV-SR 72→HTV-SR 84 *(Lowest)*

The shortest insulator had the highest dissipated energy due to high leakage currents.

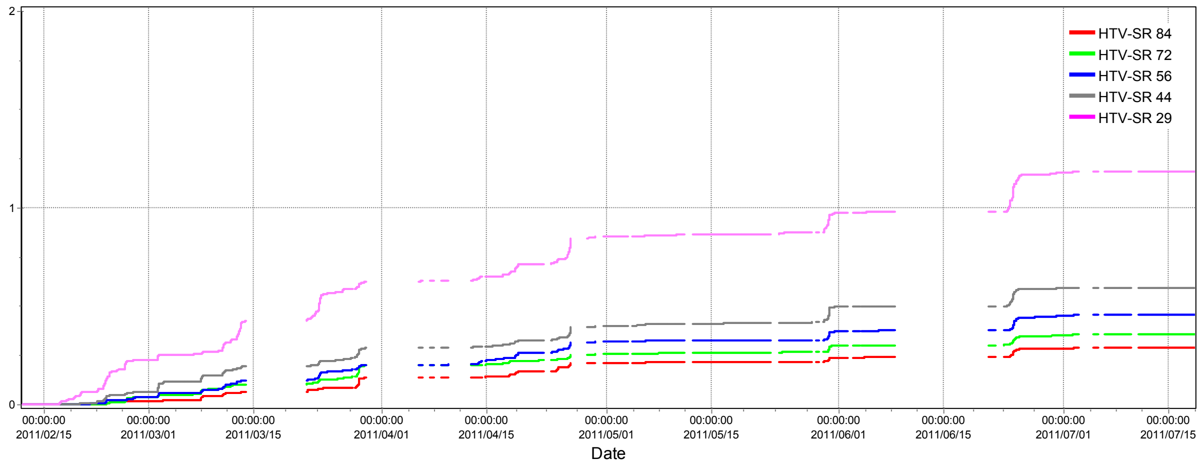

Figure 5-30: Accumulative coulomb-ampere for all the HTV-SR insulators installed on the AC excitation voltage

5.3.3.3 DC+ excitation voltage

Figure 5-31 depicts the relative electrical performance of HTV-SR insulators installed on the DC+ excitation voltage. The following ranking of electrical performance of the test insulators can be stated on the basis of the insulator with the highest accumulative coulomb-ampere at the end of the test period (consider 2011/07/15):

(Highest) HTV-SR 29→ HTV-SR 56→ HTV-SR 44→ HTV-SR 84→ HTV-SR 72 *(Lowest)*

The shortest insulator had the highest dissipated energy due to high leakage currents.

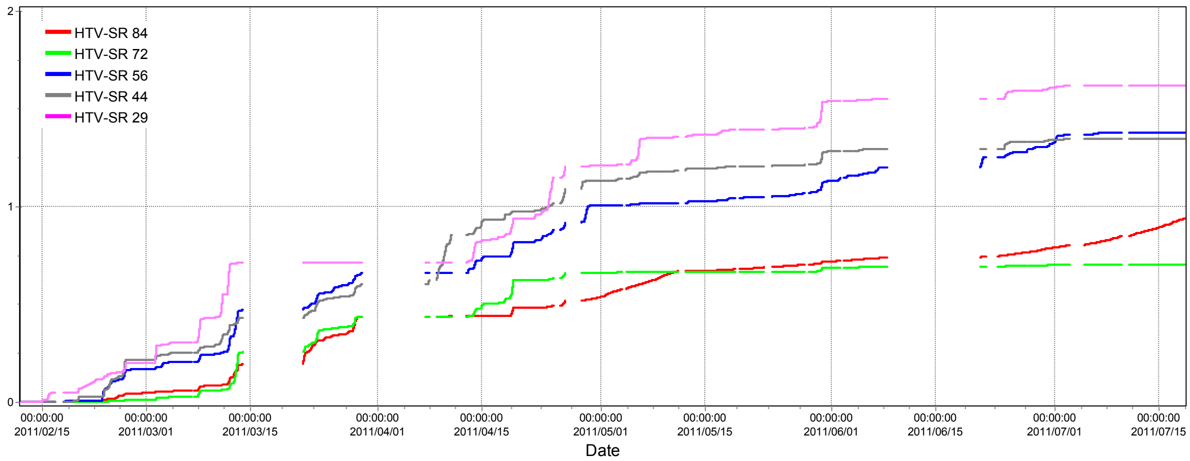

Figure 5-31: Accumulative coulomb-ampere for all the HTV-SR insulators installed on the DC+ excitation voltage

5.3.3.4 DC- excitation voltage

Figure 5-32 depicts the relative electrical performance of HTV-SR insulators installed on the DC- excitation voltage. The following ranking of electrical performance of the test insulators can be stated on the basis of the insulator with the highest accumulative coulomb-ampere at the end of the test period (consider 2011/07/15):

(Highest) HTV-SR 44→ HTV-SR 56→ HTV-SR 29→ HTV-SR 84→*(Lowest)*

Note that the data for HTV-SR 72 DC- has been ignored due to the faulty sensor associated with it.

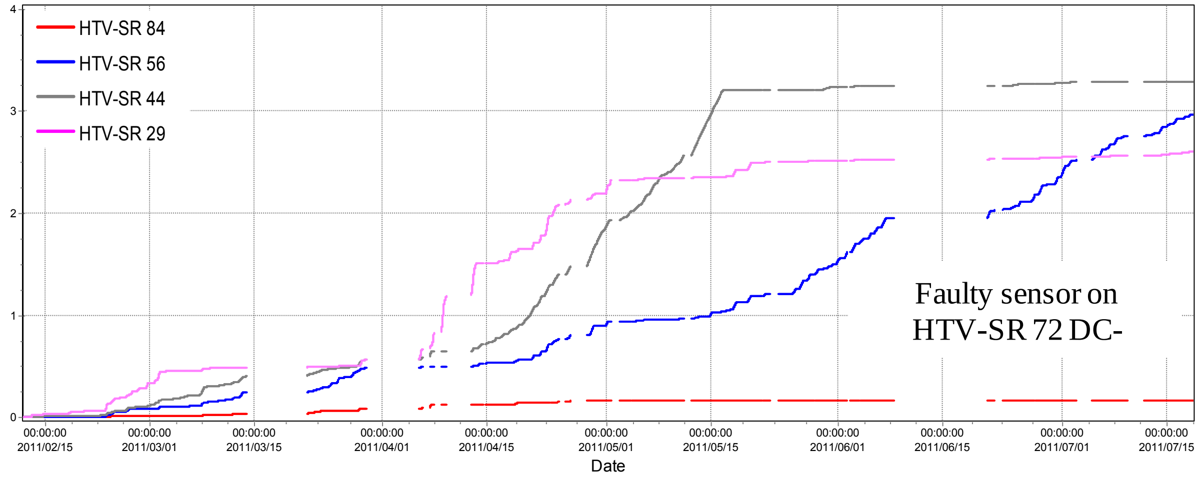

Figure 5-32: Accumulative coulomb-ampere for all the HTV-SR insulators installed on the DC- excitation voltage

5.3.4 General comments

5.3.4.1 Introductory remarks

This section presents a brief highlight of the results discussed in sections 5.3.2 and 5.3.3. The results obtained for all the test insulators have been summarized and presented in section 5.3.2.1, detailing all the aspects pertaining to the bin count analysis performed on leakage current as well as an overview of the actual leakage current profile as recorded by the OLCA device. Details of all flashover events have also been presented in Table 5-14. Notice that the results presented in section 5.3.2 are only a summary of the much more detailed results furnished in Appendix C.

With regard to the information presented in the foregoing sections, the important observations are highlighted in sections 5.3.4.2 to 5.3.4.7.

5.3.4.2 Statistical approach using time of day bin count analysis

A time-of-day leakage current bin count analysis was used for the leakage current performance of all the test insulators considered in the study. This approach was found to be useful for leakage current performance; especially as it categorizes leakage current data into bins of different magnitudes. This could be a useful approach in analyzing the ageing effects of the occurrence of leakage current with a certain magnitude. It is understood that the localized stable, low magnitude leakage currents (typically 1 to 20 mA) can cause erosion on the insulator surfaces [47, 48]. Thus, classifying leakage current into different bin categories could help with determining the range of leakage current that may be responsible for the resulting ageing conditions of the insulator materials.

In addition, the time of day analysis allows for a direct correlation of leakage current performance with the measured climatic conditions (refer to section 5.3.4.4).

5.3.4.3 Comparisons of leakage current performance for summer and winter periods

Higher leakage current levels were observed on all the three test insulators during summer when compared to those recorded in winter. This was not an unexpected observation in relation to the high pollution levels experienced in summer and the fact that negligible rainfall was recorded during summer. Given the fact that winter was found to be a rain-dominant season at KIPTS, it is obvious that a number of frequent natural washing events of insulator surfaces can be expected to have occurred in winter. It is therefore logical that low leakage current levels were recorded during winter when compared to summer. Discussions on climatic conditions recorded at KIPTS are presented in section 5.2.1.

Summer was found to be a dry season, which makes it ideal for the undisturbed build-up of pollution deposits on the insulator surfaces. These accumulated pollution deposits may therefore lead to the formation of conducting electrolytes during events of wetting conditions and hence the high levels of leakage currents in summer. In fact, only a total of 1.3 mm rain was recorded in summer and this means that there was almost no chance of natural washing of insulator surfaces. Additionally, higher ESDD levels were recorded for summer as opposed to winter (refer to section 5.2.2.2). Thus, a combination of these factors justifies the discrepancy between the leakage current levels recorded in summer and winter.

5.3.4.4 Correlation of leakage current performance with climatic conditions

It was generally observed that high leakage current levels were mainly recorded at night and also during the early morning hours. These times coincide with the observations made with regard to variations in the climatic conditions at KIPTS;: where relative humidity levels exceeded 75% and the difference between the ambient and dewpoint temperatures was very low. The inverse relationship between temperature (ambient and dewpoint) and relative humidity was established to be the main factor that determines wetting events, with an effect that high relative humidities occur when the difference between ambient and dewpoint temperature becomes very small. Refer to Figure 5-5. In support of this observation, it has been reported in reference [3] and [18] that relative humidities in excess of 75% provide enticing wetting conditions that lead to the formation of electrolytic pollution layers on polluted insulators.

The highest peak leakage currents were commonly found to have occurred in the early morning hours for all the test insulators (except for Glass disc 42 DC-), as noted in Table 5-13.

5.3.4.5 Peak leakage current and flashover events

The following was observed for HTV-SR and glass disc insulators in relation to leakage current performance:

- *HTV-SR insulators*

  High leakage current levels were generally observed on AC for HTV-SR 84, HTV-SR 72, HTV-SR 56 and HTV-SR 44, when compared to both DC+ and DC-. For these insulators, the ranking on the basis on the highest occurring leakage current was generally as follows:

  (Highest) AC → DC+ → DC- *(Lowest)*

  However, for the shortest insulator, the highest occurring leakage current was recorded on DC+. In fact, a flashover event was recorded on the shortest insulator (HTV-SR 29 DC+) installed on the DC+ excitation voltage. This seems to suggest that there is a critical range of USCD beyond which the flashover performance is compromised and it further appears that such a critical range distinctly differs for the AC, DC+ and DC- excitation voltage types.

- *Glass disc insulators*

  The highest occurring leakage current was recorded for the glass disc insulator installed on DC-. Two flashover events were recorded on this insulator.

5.3.4.6 The optimal creepage length considerations

It was mentioned in section 1.3, that one of the key questions for this research is to determine the optimal creepage length that could be considered for use on all the three excitation voltage types. An answer to this question requires thorough investigations that will take into consideration, amongst others, the following aspects:

- Leakage current levels *(flashover performance)*

- Extent of erosion *(ageing performance)*

On the basis of both leakage current and ageing performance of the insulators considered in this study, HTV-SR 44 appears to be the optimal creepage length that would yield acceptable performance (i.e. minimal flashovers and erosion). For unified specific creepage distance

(USCD) values lower tha 44 mm/kV, a flashover event was recorded for HTV-SR 29 on DC+. In addition, an increased number of instances of erosion was observed for USCD values higher than 44 mm/kV. It thus follows that 44 mm/kV is the critical USCD for the HTV-SR insulators considered in the study. Refer to Table 5-12 and Table 5-34 for evidence on this observation.

It can be added that the leakage current levels for all the HTV-SR insulators were of a similar order of magnitude for AC and DC+ and lower for DC-. Comparisons of leakage current performance for the different creepage lengths are presented below:

LEAKAGE CURRENT PERFORMANCE

	Total bin counts (> 5 mA)	**Average leakage current**	**Highest leakage current**
HTV-SR 84:	AC → DC+ → DC-	DC+ → AC → DC-	AC→ DC+ → DC-
HTV-SR 56:	AC → DC+ → DC-	DC+→ AC → DC-	AC→ DC+ → DC-
HTV-SR 44:	DC+→ AC → DC-	AC → DC+ → DC-	AC→ DC+ → DC-
HTV-SR 29:	AC → DC+ → DC-	AC → DC+ → DC-	DC+→ AC → DC-

NB: The HTV-SR 72 insulators have been ignored due to a faulty sensor on DC-.

5.3.4.7 Accumulative coulomb-ampere

No conclusive information could be obtained from this parameter in relation to the observed ageing conditions (summarized in section 5.5.3.2). It should be understood that the accumulative coulomb-ampere takes into account all the instantaneous occurrence of leakage current (including flashover events), which may not be representative of the leakage currents that can cause surface deteriorations. As mentioned earlier, it is often the localized stable, low magnitude leakage currents (typically 1 to 20 mA) that can cause erosion on the insulator surfaces.

5.4 Electrical discharge activity monitoring results

5.4.1 Overview

The electrical discharge observations were done at night between 22h00 and 02h00, as explained in the previous chapter in section 4.4. The main idea was to observe the electrical performance of all the test insulators using two types of observation cameras, namely: Corocam Mark I – a special, image-intensified, UV-sensitive camera and a night-mode suited, 0-lux Sony camcorder. The purpose of observations was not only to identify the type of electrical discharge activities that would occur on the test insulators, but also importantly to clearly identify the specific locations of the observed electrical discharge activities. This is crucial for correlation with the resulting insulator surface conditions that may be observed during surface inspections as a result of electrical discharge activities. The use of the second camera (0-lux Sony camcorder) was therefore adopted with a view to investigating whether it could be a more suitable tool in ascertaining the locations of electrical discharge activities when compared to Corocam Mark I. This became necessary due to the saturation limitations that were noted with the lens of Corocam Mark I, which made it difficult to capture a clearly focused view of the electrical discharge activities. Summaries of electrical discharge activities observed with Corocam Mark I and 0-lux Sony camcorder are given in Table 5-15 (section 5.4.3.2) and Table 5-16 (section 5.4.3.4) , respectively. Detailed results on the actual electrical discharge activity observations for each test insulator are presented in Appendix D, covering all observations made with the two aforesaid cameras.

In order to compare the relative electrical performance of the test insulators with reference to a series of the creepage lengths considered, it was necessary that the frequency of occurrence of all observed types of electrical discharge activities be noted. This was for purposes of keeping a record of the prominence of occurrence of certain electrical discharge activities on the respective test insulators. With regard to the aspect of the type of excitation voltage, each set of test insulators with a specific creepage length was monitored to ascertain the difference in the effects of AC, DC+ and DC-. Additionally, the first occurrence of all observed electrical discharge activities was noted for all the insulators. These two parameters, viz. frequency of occurrence and first occurrence of electrical discharge activities, were thus used as the basis for the evaluation of the effect of creepage length and the types of excitation voltage.

NB: References to the observed electrical discharge activities will be used as acronyms: *WDC*, *SCD*, *DBC* and *DBD*. These have been described in the previous chapter in section 4.4. A reminder is however given below:

- WDC: water drop corona
- SCD: spot corona/discharge
- DBC: dryband corona
- DBD: dryband discharge

Observations are presented per each test insulator, detailing specific electrical discharge activities in relation to the three excitation voltage types. Overall comparisons will then be given on the relative performance of all test insulators.

5.4.2 Observations specific to individual insulators

The following observations were noted for the respective test insulators and are summarized below in note form. Each type of electrical discharge activity is described separately per each set of test insulators with a specific creepage length, comparing between the three excitation voltage types.

5.4.2.1 Electrical discharge activities for the HTV-SR 84 insulators

The electrical discharge activity observations for the high temperature vulcanized, silicone rubber (HTV-SR) insulators with a unified specific creepage distance (USCD) of 84 mm/kV were categorized per each type of electrical discharge activity. Note that detailed observation results for the test insulators with this particular USCD are presented in Appendix D.2. The following is a summary that derives from the information presented in Table D-25 in section D.2.1:

- *Water drop corona*

  It was observed that WDC was commonly found to be on the shed bottoms anywhere between the live and ground end-fittings for all the three excitation voltage types.

- *Spot corona/discharge*

  SCD was observed on the shed bottoms anywhere between the live and ground end-fittings and also on the sheaths toward the live end-fitting for DC-. For AC, SCD was observed on the sheath interfacing with the live end-fitting; whereas for DC+, it was observed on the bottom of shed 5 (toward the ground end-fitting).

- *Dryband corona*

  DBC started off on the shed bottoms and the sheaths closest to the ground end-fitting for AC. However, from week 3, DBC became more prominent on the sheaths closest to the live end-fitting. For DC+, DBC was observed on the sheaths interfacing with both the live and ground end-fittings and also on the bottom of shed 4 (middle section) of the test insulator. No DBC was observed on DC-.

- *Dryband discharge*

  DBD was commonly observed toward the live end-fitting for all the three voltage types: on sheath 3 & bottom of shed 3 for AC, on sheath 1 & bottom of sheds 1, 2 & 3 for DC+ and on sheath 1 & bottom of shed 2 for DC-.

5.4.2.2 Electrical discharge activities for the HTV-SR 72 insulators

The electrical discharge activity observations for the high temperature vulcanized, silicone rubber (HTV-SR) insulators with a unified specific creepage distance (USCD) of 72 mm/kV were categorized per each type of electrical discharge activity. Note that detailed observation results for the test insulators with this particular USCD are presented in Appendix D.3. The following is a summary that derives from the information presented in Table D-29 in section D.3.1:

- *Water drop corona*

  WDC was observed on the shed rims anywhere between the live and ground end-fittings for AC, whilst observed on the shed tops and bottoms anywhere between the live and ground end-fittings for DC+. For DC-, WDC was only observed on the rim of sheds 1 & 2, toward the live end-fittings.

- *Spot corona/discharge*

  SCD was observed on the top and bottom of shed 4 (middle section of the insulator) for AC, whereas it was prominently observed on the shed bottoms toward the live end-fittings for DC+. SCD was largely observed on the shed bottoms toward the ground end-fittings for DC-.

- *Dryband corona*

  DBC was generally observed on the sheaths anywhere between the live and ground end-fittings for all the three voltage types, starting only from week 3 of the test program.

- *Dryband discharge*

  DBD was commonly observed on the sheaths and it was found to be anywhere between the live and ground end-fittings.

5.4.2.3 Electrical discharge activities for the HTV-SR 56 insulators

The electrical discharge activity observations for the high temperature vulcanized, silicone rubber (HTV-SR) insulators with a unified specific creepage distance (USCD) of 56 mm/kV were categorized per each type of electrical discharge activity. Note that detailed observation results for the test insulators with this particular USCD are presented in Appendix D.4. The following is a summary that derives from the information presented in Table D-33 in section D.4.1:

- *Water drop corona*

  WDC was largely observed on the shed rims toward the live end-fittings for AC, whereas it was also observed on the shed tops, bottoms and rims toward the live end-fittings for DC+. For DC-, WDC was only observed on the rim of shed 2 and the bottom of shed 3, toward the live end-fitting.

- *Spot corona/discharge*

  A single instance of SCD was observed on sheath 1 (interfacing with the live end-fitting) for AC, whilst observed on the rim of shed 3 and on the bottom of sheds 1, 2 & 3 toward the live end-fitting for DC-. No instance of SCD was observed for DC+.

- *Dryband corona*

  DBC was generally observed on the shed bottoms and on the sheaths toward the live end-fitting for AC, while solely on the sheath interfacing with the live end-fitting for both DC+ and DC-.

- *Dryband discharge*

  DBD was commonly observed on the shed bottoms and on the sheaths anywhere between the live and ground end-fittings for both AC and DC+. For DC-, DBD was observed on the sheaths interfacing with both the live and ground end-fittings (sheaths 1 & 5).

5.4.2.4 Electrical discharge activities for the HTV-SR 44 insulators

The electrical discharge activity observations for the high temperature vulcanized, silicone rubber (HTV-SR) insulators with a unified specific creepage distance (USCD) of 44 mm/kV were categorized per each type of electrical discharge activity. Note that detailed observation results for the test insulators with this particular USCD are presented in Appendix D.5. The following is a summary that derives from the information presented in Table D-37 in section D.5.1:

- *Water drop corona*

  WDC was observed on the shed bottoms and on the shed rims anywhere between the live and ground end-fittings for AC, whilst commonly observed on the shed tops for DC+ and on the shed bottoms for DC-, anywhere between the live and ground end-fittings.

- *Spot corona/discharge*

  No instance of SCD was observed for both AC and DC+. However, SCD was observed on the shed bottoms anywhere between the live and ground end-fittings and also on the sheath interfacing with the live end-fitting for DC-.

- *Dryband corona*

  DBC was generally observed on the shed bottoms and on the sheaths anywhere between the live and ground end-fittings for AC, whilst solely observed on the sheath interfacing with the live end-fitting for DC+. DBC was only observed on the bottom of shed 2 (toward the live end-fitting) for DC-.

- *Dryband discharge*

  DBD was commonly observed on the shed bottoms anywhere between the live and ground end-fittings and also on the sheaths interfacing with both the live and ground end-fittings (sheaths 1 & 4) for both AC and DC+. For DC-, DBD was observed on the bottom of shed 2 (toward the live end-fitting) and also on the sheaths anywhere between the live and ground end-fittings.

5.4.2.5 Electrical discharge activities for the HTV-SR 29 insulators

The electrical discharge activity observations for the high temperature vulcanized, silicone rubber (HTV-SR) insulators with a unified specific creepage distance (USCD) of 29 mm/kV were categorized per each type of electrical discharge activity. Note that detailed observation results for the test insulators with this particular USCD are presented in Appendix D.6. The following is a summary that derives from the information presented in Table D-41 in section D.6.1:

- *Water drop corona*

  WDC was observed on the shed rims and on the sheaths anywhere between the live and ground end-fittings for both AC and DC+, whilst only observed on sheath 2 for DC-, in the middle section of the insulator.

- *Spot corona/discharge*

  No instance of SCD was observed for AC. However, SCD was mainly observed on the sheaths anywhere between the live and ground end-fittings for DC+ and also on the bottom of sheds 1 & 2 for DC-.

- *Dryband corona*

  DBC was generally only observed on the sheaths interfacing with both the live and ground end-fittings for AC, whereas commonly observed on the bottom of shed 2 and on sheath 2 (middle section of insulator) for both DC+ and DC-. In addition, an instance of DBC was observed on the sheath interfacing with the ground end-fitting for DC-.

- *Dryband discharge*

  DBD was commonly observed on the shed bottoms and also on the sheaths interfacing with both the live and ground end-fittings (sheaths 1 & 3) for all the three voltage types.

5.4.2.6 Electrical discharge activities for the Glass disc 42 insulators

The electrical discharge activity observations for glass disc insulators with a unified specific creepage distance (USCD) of 42 mm/kV were categorized per each type of electrical discharge activity. Note that detailed observation results for all glass disc insulators are presented in Appendix D.7. The following is a summary that derives from the information presented in Table D-45 in section D.7.1:

- *Water drop corona*

  No WDC was observed for all the three voltage types.

- *Spot corona/discharge*

  No SCD was observed for both AC and DC-. However, one instance of SCD was observed on the bottom of the glass disc for DC+.

- *Dryband corona*

  No DBC was observed for both DC+ and DC-. Two instances of DBC were however observed for AC on the top of the glass disc around the cap and also on the bottom of the glass disc around the pin.

- *Dryband discharge*

  DBD was commonly observed on the bottom of the glass disc around the pin for all the three voltage types.

5.4.3 Overall comparisons

5.4.3.1 General discussions

With reference to the information presented in Appendix D (refer to the tables containing information on the frequency of occurrence of electrical discharge activities observed with Corocam Mark I), the following observations can be made for all the test insulators:

- It was generally found that no electrical discharge activities were observed within the first week of the test program for all the test insulators, despite the high humid conditions that were experienced during the week. This could be due to the fact that the insulators were still relatively clean and that pollution deposits on the test insulator surfaces had not accumulated that would, otherwise, have led to the formation of conductive electrolytes during wetting conditions. In addition, wind direction was found to have averaged south-easterly during the times of night observations and this might have contributed to the fact that there was little chance of instantaneous pollution events from the sea which lies to the west of the test rig. It must be noted that the first electrical discharge activities were observed on HVT-SR 29 AC and HTV-SR 44 AC towards the end of week 1, on days 6 and 7, respectively.

- Electrical discharge activities were generally found to have begun occurring on the test insulators from the second week of the test program for the HTV-SR insulators. This is a result of the now polluted test insulators getting wetted during humid conditions during the time of observation and hence the occurrence of electrical discharge activities. In contrast, no electrical discharge activities were observed on the glass disc insulators within the first three weeks. This discrepancy is an expected observation given the fact that glass disc insulators have a smooth, glassy surface which makes it difficult for pollutants to accumulate on the surfaces, whereas the HTV-SR insulators tend to have more adhesive (rubbery) surfaces that may collect pollutants relatively quicker.

- A general observation made was that both dryband corona (DBC) and dryband discharge (DBD) activities dominantly occurred on the sheaths interfacing with both the live and ground end-fittings for all the HTV-SR insulators. For glass disc insulators, the most prominent electrical activity was found to be DBD and this occurred on the bottom side of glass disc around the pin for all the three excitation voltage types (i.e. AC, DC+ and DC-). These observations are particularly interesting in connection with the findings presented in section 5.5.2 that erosion was dominantly observed on the sheaths interfacing with the live and ground end-fittings and the bottom side for HTV-SR and glass disc insulators, respectively.

5.4.3.2 Frequency of occurrence of electrical discharge activities

Having understood the prevalence of electrical discharge activities for each test insulator, it now becomes important to explore how the aspects of creepage length and the different excitation voltage types have impacted on the electrical discharge performance for the respective test insulators. For this purpose, the information presented in Table 5-15 has been summarized in a comparative manner in Figure 5-33. This figure graphically summarizes the effect of both creepage length and excitation voltage types on the electrical discharge performance of all test insulators. Note that all analyses on relative electrical discharge performance are based on the results obtained from observations made with Corocam Mark I.

Table 5-15: Summary of frequency of occurrence of electrical discharge activities observed with Corocam Mark I

	Frequency of occurrence out of total observation nights [%]: Corocam Mark I											
	AC				DC+				DC-			
	WDC	SCD	DBC	DBD	WDC	SCD	DBC	DBD	WDC	SCD	DBC	DBD
HTV-SR 84	25	4	46	4	17	4	21	17	8	8	0	21
HTV-SR 72	17	4	38	8	13	13	8	21	4	8	13	17
HTV-SR 56	13	4	42	25	13	0	4	38	8	8	4	17
HTV-SR 44	25	0	38	29	4	0	8	38	4	13	4	25
HTV-SR 29	25	0	33	29	8	13	13	29	4	8	13	29
Glass disc 42	0	0	8	4	0	4	0	25	0	0	0	13

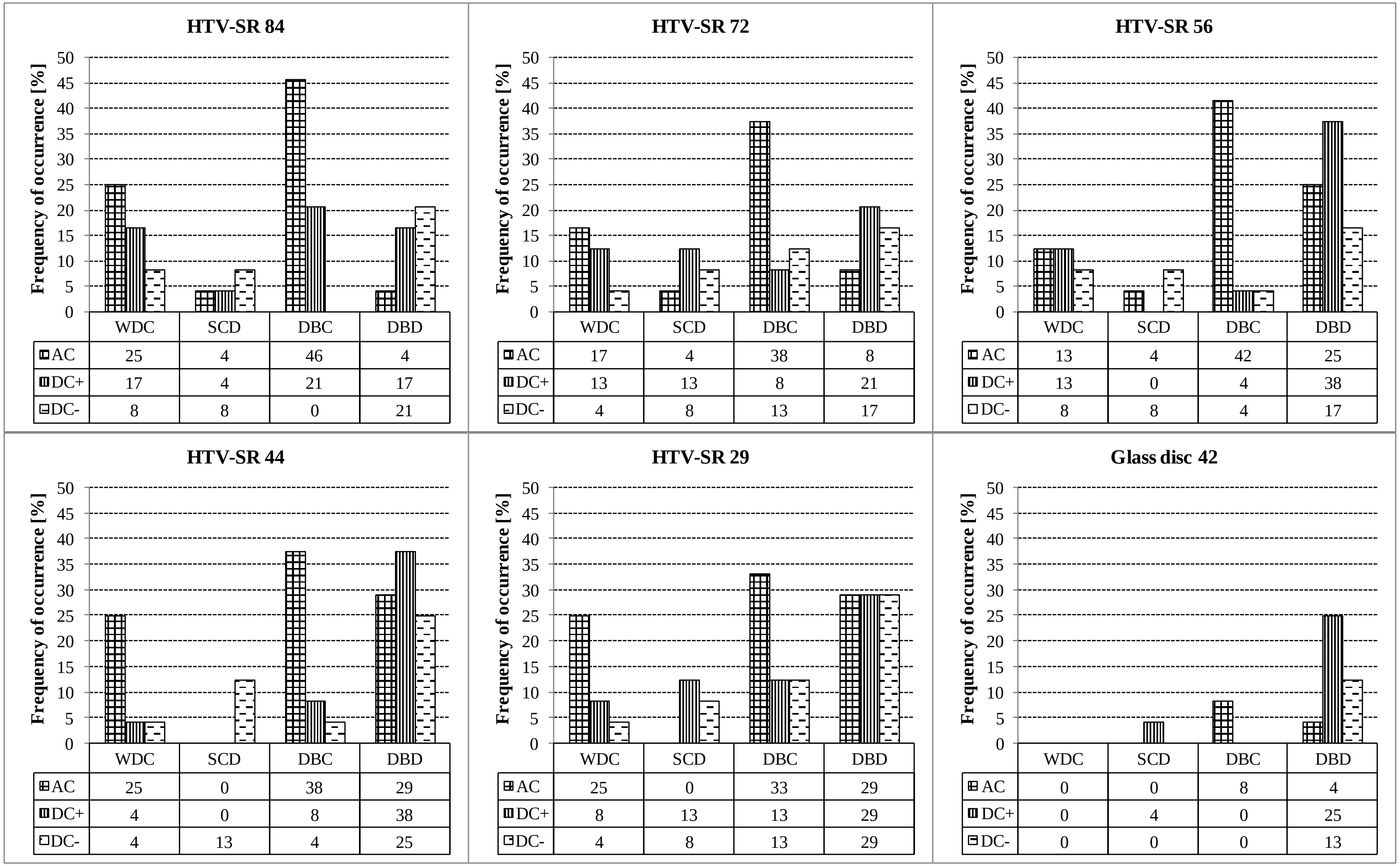

Figure 5-33: Frequency of occurrence of electrical discharge activities on the test insulators, given in terms of the number of times that they were observed out of the total observation nights

The following trends have been observed in relation to the information presented in Figure 5-33. The observed trends have been ranked in the order:

- *(Most frequent)* → *(Least frequent)*

FREQUENCY OF OCCURRENCE

	WDC	SCD	DBC	DBD
HTV-SR 84:	AC → DC+ → DC-	DC- → AC, DC+	AC → DC+ → **DC-**	DC- → DC+ → AC
HTV-SR 72:	AC → DC+ → DC-	DC+ → DC- → AC	AC → DC- → DC+	DC+ → DC- → AC
HTV-SR 56:	AC, DC+ → DC-	DC- → AC → **DC+**	AC → DC+, DC-	DC+ → AC → DC-
HTV-SR 44:	AC → DC+, DC-	DC- → **AC**, **DC+**	AC → DC+ → DC-	DC+ → AC → DC-
HTV-SR 29:	AC → DC+ → DC-	DC+ → DC- → **AC**	AC → DC+, DC-	AC, DC+, DC-
Glass disc 42:	[**None**]	DC+ → **AC**, **DC-**	AC → **DC+**, **DC-**	DC+ → DC- → AC

NB: The ranked parameters in bold indicate that a particular electrical activity was never observed.

It is interesting to note that WDC and DBC were prominently observed on the AC excitation voltage when compared to both DC+ and DC-. In fact, the highest occurrences of both WDC and DBC were recorded for AC. In contrast, the SCD and DBD activities were prominently observed on the DC excitation voltage (both polarities) in comparison to AC. The highest occurrence of DBD was actually observed on DC+.

For glass disc insulators, it can be noted that only two instances of DBC were observed on AC and no other instances of corona were observed. DBD was largely the type of electrical discharge activity that occurred on glass disc insulators, most prominently observed on DC+.

Overall, it has been observed that corona (WDC and DBC) activities were commonly observed on the AC excitation voltage, whereas discharge (SCD and DBD) activities were more prominent on the DC excitation voltage (both polarities).

5.4.3.3 First occurrence of electrical discharge activities

The foregoing sections have given an overview of the type of electrical discharge activities that occurred on the test insulators in relation to effects of both creepage and the excitation voltage types. However, it would be more interesting to explore the order in which certain electrical discharge activities began to exhibit on the test insulators. This section therefore presents the rankings of first occurrences of electrical discharge activities for all the test insulators. The rankings present the first occurrence of electrical discharge activity first, followed by the next occurring activity in order.

FIRST OCCURRENCE

	WDC	**SCD**	**DBC**	**DBD**
HTV-SR 84:	AC → DC+ → DC-	DC+ → DC- → AC	AC → DC+ → **DC-**	DC+ → DC- → AC
HTV-SR 72:	AC → DC+ → DC-	DC+ → AC → DC-	AC → DC+ → DC-	DC+ → AC → DC-
HTV-SR 56:	AC → DC+, DC-	DC- → AC → **DC+**	AC → DC+ → DC-	DC+, AC → DC-
HTV-SR 44:	AC → DC+ → DC-	DC- → **AC**, **DC+**	AC → DC- → DC+	DC-, AC → DC+
HTV-SR 29:	AC → DC+ → DC-	DC+, DC- → **AC**	AC → DC- → DC+	DC+ → AC → DC-
Glass disc 42:	[**None**]	DC+ → **AC**, **DC-**	AC → **DC+**, **DC-**	DC+, DC- → AC

NB: The ranked parameters in bold indicate that a particular electrical activity was never observed.

It can be noted here that the order of first occurrence follows a similar trend to that observed for the frequency of occurrence (refer to section 5.4.3.2). All corona activities (WDC and DBC) were first observed on the AC excitation voltage, whereas the discharge activities (SCD and DBD) were first observed on the DC excitation voltage (both polarities). In particular, DBD was solely first observed on the DC+ excitation voltage, except for the HTV-SR 44 insulator. This indicates the prominence of DBD on DC+.

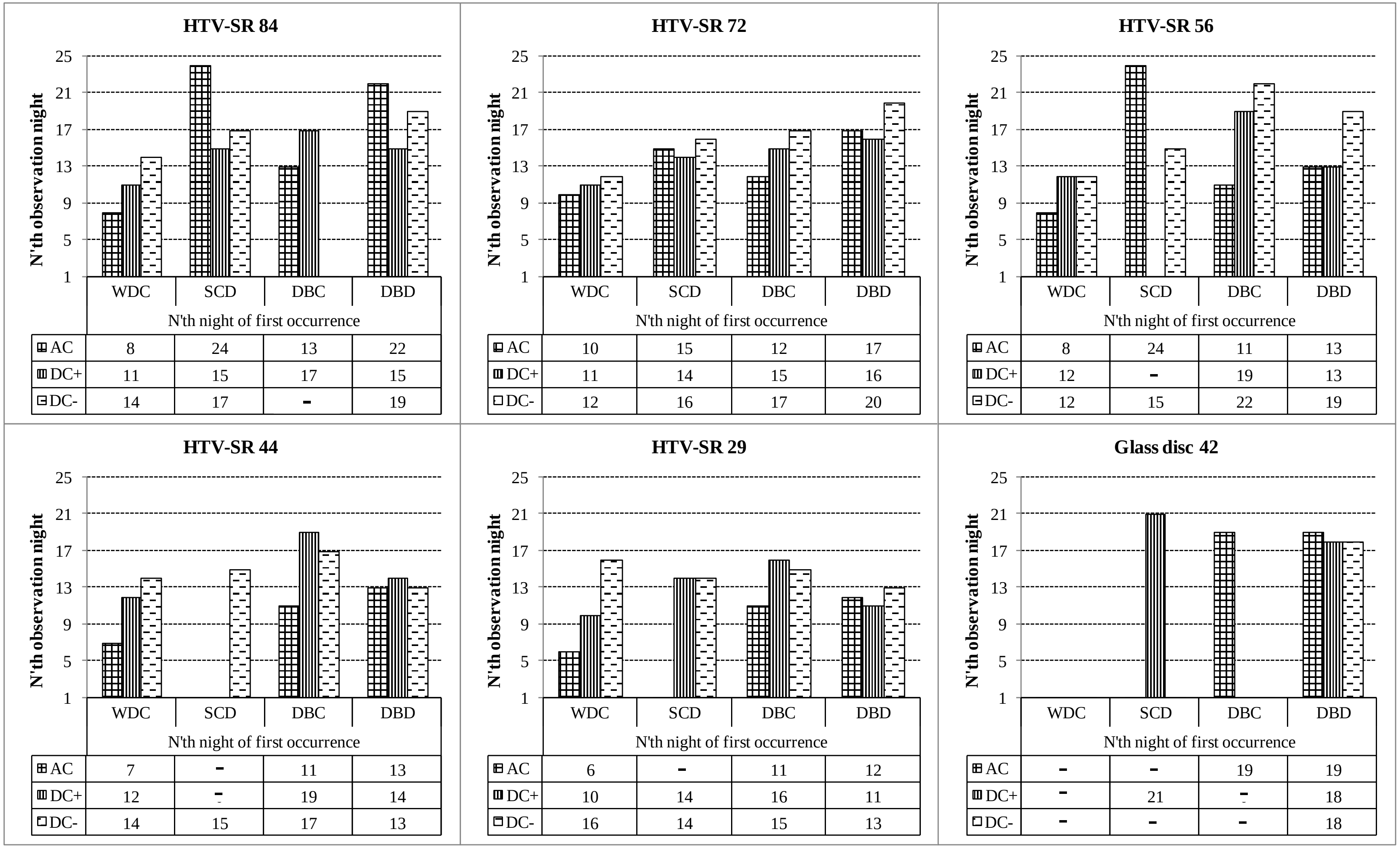

HTV-SR 84

	WDC	SCD	DBC	DBD
AC	8	24	13	22
DC+	11	15	17	15
DC-	14	17	-	19

HTV-SR 72

	WDC	SCD	DBC	DBD
AC	10	15	12	17
DC+	11	14	15	16
DC-	12	16	17	20

HTV-SR 56

	WDC	SCD	DBC	DBD
AC	8	24	11	13
DC+	12	-	19	13
DC-	12	15	22	19

HTV-SR 44

	WDC	SCD	DBC	DBD
AC	7	-	11	13
DC+	12	-	19	14
DC-	14	15	17	13

HTV-SR 29

	WDC	SCD	DBC	DBD
AC	6	-	11	12
DC+	10	14	16	11
DC-	16	14	15	13

Glass disc 42

	WDC	SCD	DBC	DBD
AC	-	-	19	19
DC+	-	21	-	18
DC-	-	-	-	18

"-" means an electrical discharge activity was never observed

Figure 5-34: First occurrence of electrical discharge activities on the test insulators, given in terms of the N'th night on which they were first observed

5.4.3.4 The relevance of a 0-lux camcorder in electrical discharge observations

Table 5-16 summarizes the results of the observations done with the 0-lux Sony camcorder. It was found that this camera could only detect dryband discharge activities, as it can be seen in Table 5-16. The less intense electrical discharge activities such as WDC and SDC could not be detected with this camera. However, it should be mentioned that this camera was most useful in ascertaining the location of these dryband discharge activities, as it allowed for clearly focused views of dryband discharge (DBD) activities to be captured.

In contrast, Corocam Mark I was more useful with the identification of discharge activities – detecting even the least intense activities such as corona. It was not easy to ascertain the exact locations of the intense electrical discharge activities such as DBD due to the saturation limitations associated with the lens, thereby causing blobs around the areas with electrical discharge activities.

It therefore follows that there is a prospect that a night suited, zero-lux Sony camera can be used alongside with Corocam Mark I for electrical discharge activities, especially for the intense electrical discharge activities such as DBC and DBD.

Table 5-16: Summary of frequency of occurrence of electrical discharge activities observed with 0-lux Sony Camcorder

	Frequency of occurrence out of total observation nights [%]: 0-lux Sony Camcorder											
	AC				DC+				DC-			
	WDC	SCD	DBC	DBD	WDC	SCD	DBC	DBD	WDC	SCD	DBC	DBD
HTV-SR 84	4	0	0	21	0	0	0	13	0	0	0	4
HTV-SR 72	4	0	0	8	0	0	0	25	0	0	0	8
HTV-SR 56	4	0	0	21	0	0	0	29	0	0	0	4
HTV-SR 44	4	0	4	29	0	0	0	25	0	0	0	8
HTV-SR 29	4	0	0	25	0	0	0	21	0	0	0	17
Glass disc 42	0	0	0	0	0	0	0	17	0	0	0	0

5.5 Surface condition inspections: Ageing performance

5.5.1 Overview

Close-up inspections were done during daytime for all test insulators, as explained in the previous chapter, section 4.5. This exercise was carried out with the aim to inspect surface deteriorations such as drybands, crazing, chalking, discolouration, erosion and tracking on the insulator surfaces. Additional details of all observed aspects were recorded and summarized in Appendix E. These include pollution conditions, salt crystals, plant threads and dead bugs.

The main purpose of insulator surface inspections was to establish the relative ageing performance of the test insulators, with particular emphasis on the impact of the three excitation voltage types (i.e. AC, DC+ and DC-). It was therefore ideal that the inspections of a given set of test insulators with the same creepage length be executed on the same day for all the three excitation voltage types. This would allow for a common benchmark for comparison purposes. However, due to the intensity of inspections, it was not practicable to complete all the 18 test insulators in one day. As an alternative, inspections were done on an ad-hoc schedule - considering test insulators on one particular excitation voltage type during each inspection session.

A three-week test cycle was chosen to allow for only one inspection session per week such that only one set of test insulators on a particular voltage type would be inspected per week. This ensures that the test rig would only be switched off once a week, in order to avoid too frequent downtimes. It should be mentioned that the consistency of the inspection period (the three-week cycle) was affected by weather conditions, in that inspections were performed outdoors on an elevated platform (scaffolding) and sometimes on a ladder. A complete test cycle may therefore, in certain instances, have extended beyond the intended three-week period due to inclement weather. In particular, misty and rainy conditions were not deemed appropriate for the inspections as this would conceal dryband conditions due to wash-offs of dryband traces and because of concerns for the safety of electronic equipment. Winds can be very stormy with gusts of sand at KIPTS. Thus, no inspections were done on windy days for the safety of both the author and the camera. Also, it was not considered practical to do a valid wettability classification on test insulators under windy conditions. The actual timelines for surface inspections are detailed in Table 5-17.

Table 5-17: Surface inspection timelines

Timelines					
Test Cycle	**Date**	**Week No.**	***AC***	***DC+***	***DC-***
1	**10-Feb**	**2**			👓
	21-Feb	**3**		👓	
	3-Mar	**5**	👓		
2	**11-Mar**	**6**			👓
	24-Mar	**8**		👓	
	5-Apr	**9**	👓		
3	**13-Apr**	**10**			👓
	19-Apr	**11**		👓	
	4-May	**13**	👓		
4	**19-May**	**16**			👓
	7-Jun	**18**		👓	
	6-Jul	**22**	👓		

👓 = Surface inspections done

With reference to the inspection approach used, it was recognized that comparisons may not easily be made between the ageing conditions of test insulators that have not been inspected on the same day. Thus, the evaluation of relative ageing performance was only based on the ageing trends observed. A summary of the observations are presented in the following section.

5.5.2 Results for individual test insulators

5.5.2.1 Surface conditions for the HTV-SR 84 insulators

The observations for the high temperature vulcanized, silicone rubber (HTV-SR) insulators with a unified specific creepage distance of 84 mm/kV were categorized per each excitation voltage type. Note that detailed observation results for each test cycle are given in Appendix E.2. This therefore gives rise to the following summary:

- *AC excitation voltage*

  Surface inspections were done on AC in weeks 5, 9, 13 and 22. The observations are presented below.

  Observations: On the first inspection, no surface deteriorations were observed on the test insulator. However, evidence of electrical activity was observed. This was in relation to the dryband areas that were recorded in week 5. It was from week 9 that the first instances of crazing and material erosion were observed. This is probably a result of the electrical stress that may have been caused by the electrical discharge activities.

The first instance of material erosion was observed on the sheath interfacing with the live end-fitting in the southward direction. It must be mentioned that there was a directionally dominant deposit of pollution that emanated from the southward direction. By the end of the test period in week 22, more signs of material erosion were observed on the sheath interfacing with the live end-fitting in the northward direction. Figure 5-35 depicts the two instances of material erosion that were observed on the sheath interfacing with the live end-fitting in week 22. Additional instances of material erosion were observed on the sheath interfacing with the ground end-fitting in week 22. A count of total instances of material erosion recorded on the sheaths and sheds is summarized in Table 5-18.

Table 5-18: A total count of instances of material erosion in week 22, HTV-SR 84 AC

Instances of Material Erosion				
Sheaths			Sheds	
Ground end-fitting	Middle section	Live end-fitting	Top	Bottom
3	0	2	0	0

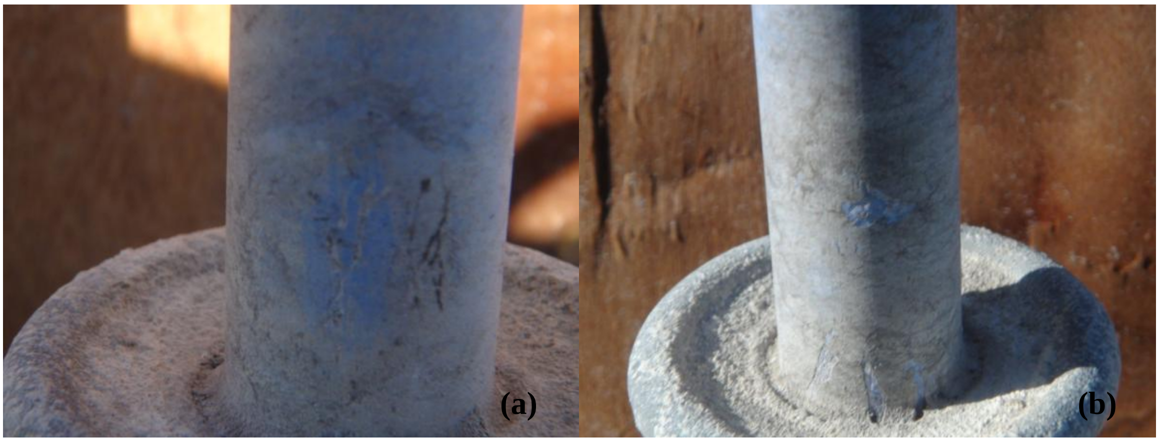

Figure 5-35: Two instances of material erosion on the sheath interfacing with the live end-fitting in the (a) southward direction and (b) northward direction, week 22

- *DC+ excitation voltage*

Surface inspections were done on DC+ in weeks 3, 8, 11 and 18. The observations are presented below.

Observations: The first instances of deterioration were observed in week 8. These included light crazing and material erosion on the sheath interfacing with the ground end-fitting. An additional instance of erosion was recorded on the bottom of a shed in the middle section of the insulator. Both of these first instances of erosion were observed in the southward direction. Traces of dryband activities were mainly observed on the shed bottoms and sheaths, with a radial pattern on the shed bottoms. A summary of all instances of material erosion is presented in Table 5-19, as noted on the fourth test cycle (week 18).

Table 5-19: A total count of instances of material erosion in week 18, HTV-SR 84 DC+

Instances of Material Erosion				
Sheaths			Sheds	
Ground end-fitting	Middle section	Live end-fitting	Top	Bottom
1	1	3	0	2

Some form of discoloration was noted on the top of shed 4 – observed as darker blue patches on the insulator surface. No evidence of dryband activities was noted around this area. It was therefore not clear as to what had led to this effect.

- *DC- excitation voltage*

Surface inspections were done on DC- in weeks 2, 6, 10 and 16. The observations are presented below.

Observations: On the second inspection cycle, traces of dryband activities were observed on the sheaths. Crazing was also first observed in week 6, mainly on the sheaths. The first sign of material of erosion was observed on a sheath in the middle section of the insulator along a heavy pollution deposit in the southward direction in week 6. An increased number erosion instances were recorded from week 10, especially on the sheaths interfacing with both the live and ground end-fittings. A summary of all instances of material erosion is presented in Table 5-20, as noted on the fourth test cycle (week 16).

Table 5-20: A total count of instances of material erosion in week 16, HTV-SR 84 DC-

Instances of Material Erosion				
Sheaths			Sheds	
Ground end-fitting	Middle section	Live end-fitting	Top	Bottom
1	1	2	0	0

Blue patches (a form of discoloration) were observed on the shed tops and no evidence of electrical activities was observed in the vicinities of the discoloured areas. This discoloration was only observed from week 16.

5.5.2.2 Surface conditions for the HTV-SR 72 insulators

The observations for the high temperature vulcanized, silicone rubber (HTV-SR) insulators with a unified specific creepage distance of 72 mm/kV were categorized per each excitation voltage type. Note that detailed observation results for each test cycle are given in Appendix E.3. This therefore gives rise to the following summary:

- *AC excitation voltage*

Surface inspections were done on AC in weeks 5, 9, 13 and 22. The observations are presented below.

Observations: Traces of dryband activities were observed from week 5, on the first inspection cycle. However, the first instances of crazing and material erosion were observed from the second inspection cycle in week 9. In addition, the first instance of material erosion was observed on sheath 5 (toward the ground end-fitting) in the southward direction in week 9. Dark burns were noted on the sheath interfacing with the live end-fitting, indicating the occurrence of electrical activity likely to have caused erosion. No erosion could however be confirmed on this sheath. An increase in the number of instances of material erosion was noted from week 13, observed on the sheaths interfacing with both the live and ground end-fittings and also on a sheath in the middle section of the insulator. Refer to Figure E-55 and Figure E-56 for the pictures of erosion noted on sheaths 3 & 5 and also on the sheaths interfacing with both the live and ground end-fittings, respectively. A summary of all instances of material erosion is presented in Table 5-21, as noted on the fourth test cycle (week 22). Erosion was most prominent on the sheaths interfacing with both the live and ground end-fittings.

Table 5-21: A total count of instances of material erosion in week 22, HTV-SR 72 AC

Instances of Material Erosion				
Sheaths			**Sheds**	
Ground end-fitting	Middle section	Live end-fitting	Top	Bottom
3	2	3	0	0

The first instances of blue patches (some form of discoloration) were observed on the top and bottom of shed 3 in the northward direction and also on top of shed 4 in the eastward direction. These were only observed from week 22.

- *DC+ excitation voltage*

Surface inspections were done on DC+ in weeks 3, 8, 11 and 18. The observations are presented below.

Observations: Traces of dryband activities were initially observed on the shed bottoms on the first inspection cycle in week 3. On the second inspection cycle (week 8), drybands were found to have a radial pattern on the shed bottoms. The first instances of crazing and erosion were observed in week 8. Light crazing was mainly observed on the shed bottoms and sheaths, whereas erosion was observed on the sheath interfacing with the ground end-fitting and also on sheath 2 (toward the live end-fitting). Both of these instances of erosion were found to have occurred in the southward direction, along the heavy pollution deposit. On the last inspection cycle (week 18), more instances of material erosion were observed on the sheaths interfacing with both the live and ground end-fittings in the northward and southward directions. The southward erosion on the sheath interfacing with the ground end-fitting is shown in Figure E-57 in section E.3.4.2 of Appendix E.3. A summary of all instances of material erosion is presented in Table 5-22, as noted on the fourth test cycle (week 18).

Table 5-22: A total count of instances of material erosion in week 18, HTV-SR 72 DC+

Instances of Material Erosion				
Sheaths			Sheds	
Ground end-fitting	Middle section	Live end-fitting	Top	Bottom
2	2	2	0	0

Blue patches (some form of discoloration) were observed on the top of shed 4 in the northward direction in week 18. No evidence of electrical activities was observed in the vicinity of the discoloured area. It could therefore not be ascertained what might have caused the discoloration.

- *DC- excitation voltage*

Surface inspections were done on DC- in weeks 2, 6, 10 and 16. The observations are presented below.

Observations: Traces of dryband activities were generally observed on the sheaths from week 6. It was only on the second inspection cycle (week 6) when both crazing and material erosion were observed. Crazing was mainly observed on the sheaths, whereas the first sign of erosion was noted on the sheath interfacing with the ground end-fitting in the southward direction, along the heavy pollution deposit. Additional erosion was observed on the sheath interfacing with the live end-fitting in the westward direction and also on sheath 5 (toward the ground end-fitting) in the eastward direction in week 16. A summary of all instances of material erosion is presented in Table 5-23, as noted on the fourth test cycle (week 16).

Table 5-23: A total count of instances of material erosion in week 16, HTV-SR 72 DC-

Instances of Material Erosion				
Sheaths			Sheds	
Ground end-fitting	Middle section	Live end-fitting	Top	Bottom
1	1	2	0	0

Some form of discolouration was noted on shed tops in the form of blue patches (spots and radial). Refer Figure E-59 in section E.3.4.3 of Appendix E.3 for the view of these blue patches.

5.5.2.3 Surface conditions for the HTV-SR 56 insulators

The observations for the high temperature vulcanized, silicone rubber (HTV-SR) insulators with a unified specific creepage distance of 56 mm/kV were categorized per each excitation voltage type. Note that detailed observation results for each test cycle are given in Appendix E.4. This therefore gives rise to the following summary:

- *AC excitation voltage*

  Surface inspections were done on AC in weeks 5, 9, 13 and 22. The observations are presented below.

  Observations: The only observation recorded on the first inspection cycle (week 5) was the evidence of dryband activities. No material erosion observed. It was only then from the second inspection cycle (week 9) that the first instances of crazing and erosion were noted. Crazing was mainly observed on the sheaths, whereas erosion was noted on the sheath interfacing with the live end-fitting and also on sheaths 3 (middle section of the insulator) & 4 (toward the ground end-fitting). Erosion was observed along the heavy pollution deposit in the southward direction. On the fourth inspection cycle (week 22), additional erosion was observed on the sheaths interfacing with both the live and ground end-fittings in the northward direction and also on the bottom of shed 3 in the southward direction. The erosion instances observed on the sheaths interfacing with both the live and ground end-fittings are depicted in Figure E-69 (refer to Appendix E.4). A summary of all instances of material erosion is presented in Table 5-24, as noted on the fourth test cycle (week 22).

Table 5-24: A total count of instances of material erosion in week 22, HTV-SR 56 AC

Instances of Material Erosion				
Sheaths			Sheds	
Ground end-fitting	Middle section	Live end-fitting	Top	Bottom
2	3	2	0	1

The first instance of blue patches (some of form of discoloration) was observed on the top of sheds 2 & 3 in the eastward direction in week 22. No evidence of electrical activity was observed in the vicinity of the discoloured area.

- *DC+ excitation voltage*

Surface inspections were done on DC+ in weeks 3, 8, 11 and 18. The observations are presented below.

Observations: Evidence of electrical activities was noted from the first inspection cycle, where drybands were observed on the shed tops and bottoms and on the sheaths. The first signs of crazing and erosion were observed from the second inspection cycle (week 8). Crazing was generally observed on the shed bottoms and sheaths, whereas the first instance of erosion was observed on the sheath interfacing with the ground end-fitting. This erosion was found to be along the heavy pollution deposit in the southward direction. An increased number of instances of erosion were noted by the fourth inspection cycle (week 18). Additional erosion was now observed on the sheath interfacing with both the live (westward direction) and end-fittings ground (westward and northward direction) and also on sheath 4 (toward the ground end-fitting) in the westward and northward directions. Some of the instances of erosion that were observed on the sheath interfacing with both the live and ground end-fitting are shown in Figure E-70 (refer to section E.4.4.2 of Appendix E.4). A summary of all instances of material erosion is presented in Table 5-25, as noted on the fourth test cycle (week 18). No discolouration was observed.

Table 5-25: A total count of instances of material erosion in week 18, HTV-SR 56 DC+

Instances of Material Erosion				
Sheaths			Sheds	
Ground end-fitting	Middle section	Live end-fitting	Top	Bottom
3	2	2	0	0

- *DC- excitation voltage*

Surface inspections were done on DC- in weeks 2, 6, 10 and 16. The observations are presented below.

Observations: Traces of dryband activities and the first signs of crazing were observed from the second inspection cycle (week 6). Crazing was generally observed on the sheaths. The first instances of material erosion were observed on the third inspection cycle (week 10) on the sheath interfacing with the live end-fitting in the northward direction and also on the sheath interfacing with the ground end-fitting in the southward direction. In week 16 (the fourth inspection cycle), more instances of erosion were noticed on the sheath interfacing with the ground end-fitting in all directions, except in the eastward direction and also on sheath 3 (all directions except south) & sheath 4 (westward direction). A peel-off was observed at the bonding interface of a sheath and shed. Refer to Figure E-71 (in section E.4.4.3 of Appendix E.4) for illustrations of the erosion that was observed on the sheath interfacing with the live end-fitting and the peel-off at the sheath-to-shed bonding interface. A summary of all instances of material erosion is presented in Table 5-26, as noted on the fourth test cycle (week 16).

Table 5-26: A total count of instances of material erosion in week 16, HTV-SR 56 DC-

Instances of Material Erosion				
Sheaths			Sheds	
Ground end-fitting	Middle section	Live end-fitting	Top	Bottom
3	4	1	0	0

The first instance of blue patches (a form of discolouration) was observed on the shed tops in the westward direction. Refer to Figure E-72 in section E.4.4.3, Appendix E.4.

5.5.2.4 Surface conditions for the HTV-SR 44 insulators

The observations for the high temperature vulcanized, silicone rubber (HTV-SR) insulators with a unified specific creepage distance of 44 mm/kV were categorized per each excitation voltage type. Note that detailed observation results for each test cycle (as explained in Table 5-17) are given in Appendix E.5. This therefore gives rise to the following summary:

- *AC excitation voltage*

  Surface inspections were done on AC in weeks 5, 9, 13 and 22. The observations are presented below.

  Observations: Traces of dryband activities were observed from the first inspection cycle (week 5). In addition, the first instance of erosion was observed in week 5. This erosion was observed on the sheath interfacing with the live end-fitting along the heavy pollution deposit in the southward direction. An additional instance of erosion was noted on sheath, also observed in the southward direction. No crazing was however observed on the first inspection cycle, it was only from week 9 that the first signs of crazing were observed on the sheaths. On the last inspection cycle (week 22), an increased number of instances of erosion were observed on the sheath interfacing with the ground end-fitting in the northward direction. A summary of all instances of material erosion is presented in Table 5-27, as noted on the fourth test cycle (week 22). No discolouration was observed.

Table 5-27: A total count of instances of material erosion in week 22, HTV-SR 44 AC

Instances of Material Erosion				
Sheaths			Sheds	
Ground end-fitting	Middle section	Live end-fitting	Top	Bottom
1	1	1	0	0

- *DC+ excitation voltage*

Surface inspections were done on DC+ in weeks 3, 8, 11 and 18. The observations are presented below.

Observations: Traces of dryband activity were observed on the first inspection cycle (week 3), mainly on the shed bottoms and sheaths. It was from the second inspection cycle (week 8) that the first instances of crazing and erosion were observed. Crazing was observed on the shed bottoms and sheaths, whereas the first instances of material erosion were observed on the sheath interfacing with the ground end-fitting in the southward direction and also on the sheath interfacing with the live end-fitting in the southward and westward directions. More instances of material erosion were noted in week 18, observed on the sheath interfacing with the ground end-fitting in the westward and northward directions and also on sheath 3 in the westward direction. A summary of all instances of material erosion is therefore presented in Table 5-28, as noted on the fourth test cycle (week 18). No discolouration was observed.

Table 5-28: A total count of instances of material erosion in week 18, HTV-SR 44 DC+

Instances of Material Erosion				
Sheaths			Sheds	
Ground end-fitting	Middle section	Live end-fitting	Top	Bottom
3	1	3	0	0

- *DC- excitation voltage*

Surface inspections were done on DC- in weeks 2, 6, 10 and 16. The observations are presented below.

Observations: Traces of dryband activities were observed on most parts of the insulator from week 6 (the second inspection cycle). In addition, light crazing was observed on the sheaths. It was only from the third inspection cycle (week 10) when the first instance of erosion was observed on the sheath interfacing with the ground end-fitting in the westward and northward directions. On the fourth inspection cycle (week 16), more erosion was then observed on the sheath interfacing with the ground end-fitting in the southward direction and also on sheath 3 in the westward, northward and eastward directions. A summary of all instances of material erosion is presented in Table 5-29, as noted on the fourth test cycle (week 16).

Table 5-29: A total count of instances of material erosion in week 16, HTV-SR 44 DC-

Instances of Material Erosion				
Sheaths			**Sheds**	
Ground end-fitting	Middle section	Live end-fitting	Top	Bottom
3	1	0	0	0

It should be mentioned that a peel-off was observed at a sheath-to-shed bonding interface in week 16. Refer to Figure E-82 in section E.5.4.3 of Appendix E.5. It was not clear what might have led to the peel-off. Drybands were observed around the peeled area.

Additionally, some form of discolouration was observed in the eastward direction in week 16. This was noted in a form of darker blue patches on the shed tops.

5.5.2.5 Surface conditions for the HTV-SR 29 insulators

The observations for the high temperature vulcanized, silicone rubber (HTV-SR) insulators with a unified specific creepage distance of 29 mm/kV were categorized per each excitation voltage type. Note that detailed observation results for each test cycle are given in Appendix E.6. This therefore gives rise to the following summary:

- *AC excitation voltage*

Surface inspections were done on AC in weeks 5, 9, 13 and 22. The observations are presented below.

Observations: Traces of dryband activities were observed on the shed bottoms and sheaths and these were noted on the first inspection cycle (week 5). It was on the following inspection cycle (week 9) when the first signs of crazing and erosion were noted. Crazing was observed on the shed bottoms and sheaths, whereas the first instance of erosion was observed on the sheath interfacing with the live end-fitting along the heavy pollution deposit in the southward direction. On the last inspection cycle (week 22), additional instances of erosion were noted just above the eroded area on the sheath interfacing with the live end-fitting. It should be mentioned that these instances of erosion were very light. This is can be seen in Figure E-88 in section E.6.4.1 of Appendix E.6. A summary of all instances of material erosion is presented in Table 5-30, as noted on the fourth test cycle (week 22). No discolouration was observed.

Table 5-30: A total count of instances of material erosion in week 22, HTV-SR 29 AC

Instances of Material Erosion				
Sheaths			Sheds	
Ground end-fitting	Middle section	Live end-fitting	Top	Bottom
0	0	2	0	0

- *DC+ excitation voltage*

Surface inspections were done on DC+ in weeks 3, 8, 11 and 18. The observations are presented below.

Observations: The first signs of dryband activities and crazing were observed on the first inspection cycle (week 3), both noted on the shed bottoms and sheaths. Crazing was mainly observed in the westward and northward directions. The first instance of material erosion was observed on the sheath interfacing with the ground end-fitting in almost all directions, except in the eastward direction. In addition, erosion was observed on the sheath interfacing with the live end-fitting in the northward direction. Another instance of erosion was also observed on a sheath in the middle section of the insulator (sheath 2) in the southward direction. All the first instances of erosion were noted on the second inspection cycle (week 8). No new instances of erosion were recorded on the last inspection cycle (week 18). A summary of all instances of material erosion is presented in Table 5-31, as noted on the fourth test cycle (week 18). No discolouration was observed.

Table 5-31: A total count of instances of material erosion in week 18, HTV-SR 29 DC+

Instances of Material Erosion				
Sheaths			**Sheds**	
Ground end-fitting	Middle section	Live end-fitting	Top	Bottom
3	1	1	0	0

- *DC- excitation voltage*

Surface inspections were done on DC- in weeks 2, 6, 10 and 16. The observations are presented below.

Observations: Traces of dryband activities were observed on the shed bottoms and sheaths on the second inspection cycle (week 6). In addition, crazing was generally observed on the sheaths. No erosion was recorded in week 6. From the third inspection cycle (week 10), the first instance of material erosion was observed on the sheath interfacing with the ground end-fitting in the southward and eastward directions. Crazing was also noted to have occurred on the shed bottoms in addition to the signs of crazing that were only observed on the sheaths in week 6. No new instances of erosion were noted on the last inspection cycle (week 16). The instance of erosion observed on the sheath interfacing with the ground end-fitting is depicted in Figure E-90 in section E.6.4.3 of Appendix E.6. A summary of all instances of material erosion is presented in Table 5-32, as noted on the fourth test cycle (week 16). No discolouration was observed.

Table 5-32: A total count of instances of material erosion in week 16, HTV-SR 29 DC-

Instances of Material Erosion				
Sheaths			Sheds	
Ground end-fitting	Middle section	Live end-fitting	Top	Bottom
2	0	0	0	0

5.5.2.1 Surface conditions for the Glass disc 42 insulators

The observations for the glass disc insulators with a unified specific creepage distance of 42 mm/kV were categorized per each excitation voltage type. Note that detailed observation results for each test cycle are given in Appendix E.7. This therefore gives rise to the following summary:

- *AC excitation voltage*

  Surface inspections were done on AC in weeks 5, 9, 13 and 22. The observations are presented below.

  Observations: No surface deteriorations were observed on the AC glass disc insulator until week 22. However, traces of dryband activities were observed on the bottom of the glass disc around the pin and also on the top of the glass disc around the cap. The traces of dryband activities were first observed on the bottom of the glass disc in week 9, whereas those on the top side of the glass disc were only observed from week 13. No sign of material erosion was observed and this shows that the glass insulator performed very well on AC when compared to both DC+ (Figure 5-37) and DC- (Figure 5-38). The bottom view of the glass disc insulator is depicted in Figure 5-36.

Figure 5-36: The bottom view of Glass disc 42 AC, week 22

- *DC+ excitation voltage*

  Surface inspections were done on DC+ in weeks 3, 8, 11 and 18. The observations are presented below.

  Observations: The first evidence of electrical activities on the insulator was observed in week 8. These included traces of dryband activities on the bottom of the glass disc around the pin and also on the top of the glass disc around the cap. Material erosion was also observed on the bottom of the glass disc around the pin in week 8. Figure 5-37 depicts material erosion as observed on DC+ in week 18. It must be mentioned that the extent of erosion on DC+ was not as severe as observed on DC-. This was evident comparing the erosion observed on DC+ to that observed on DC- (refer to Figure 5-38).

Figure 5-37: Material erosion on the bottom of Glass disc 42 DC+ around the pin, week 18

- *DC- excitation voltage*

Surface inspections were done on DC- in weeks 2, 6, 10 and 16. The observations are presented below.

Observations: Traces of dryband activities were first observed on the top of the glass disc around the cap and also on the bottom of the glass disc around the pin from week 6. In addition, the first instance of material erosion was observed on the bottom of the glass disc around pin, in week 6. The extent of erosion on the glass disc insulator energized under DC- is depicted in Figure 5-38, as observed in week 16. It should be noted that the inspections on DC- were always done earlier than those for both AC and DC+. However, the first instance of erosion was observed on DC-. This suggests that the glass disc insulator performed poorly on DC- when compared to AC and DC+. In addition, the extent of erosion on DC- was found to be more severe than the one observed on DC+ (refer to Figure 5-37).

Figure 5-38: Material erosion on the bottom of Glass disc 42 DC- around the pin, week 16

5.5.3 Overall comparisons

5.5.3.1 Introductory remarks

This section presents comparisons of the ageing performance of all test insulators as discussed in the previous section per each insulator. Table 5-33 presents a summary of all surface conditions observed on the test insulators in relation to the three excitation voltage types. It should be mentioned once again that it was considered impractical to compare the relative ageing performance for a particular set of test insulators with the same creepage length energized under the three excitation voltage types. This is due to the fact that the inspections were not done on the same day. However, comparisons of the relative ageing performance of test insulators on a given excitation voltage could be made in relation to the effect of creepage length.

5.5.3.2 Discussion on specific observations

Quantification of the extent of erosion (depth, area and mass) could not be performed, as this would otherwise have interfered with the ageing process of insulators. Therefore, in order to allow for comparisons, a total number of instances of erosion were recorded for each test insulator and this has been used as the basis of comparisons. The instances of erosion are summarized in Table 5-34.

One would have expected to observe the greatest number of instances of erosion on the shortest insulators with less electrical separation causing them to be susceptible to high electrical stresses. However, the contrary was observed. The shortest insulator with the unified specific creepage distance (USCD) of 29 mm/kV was found to have the least instances of erosion for all the excitation voltage types. It therefore appears that there is a critical range of USCD beyond which ageing performance is compromised. The middle class USCD insulators (44 mm/kV, 56 mm/kV and 72 mm/kV) were found to have a high number of instances of erosion when compared to the shortest and longest insulators. This is evident from the figures cited in Table 5-34. The observed effects of creepage length correspond with the findings presented in the IEC/TS 60815-3: 2009 document on the guidelines for the selection of insulators with respect to polluted conditions. It has been found that, for a given operating voltage and environmental stresses, the following states of performance can be obtained in relation to the increase in creepage length [44]:

- *Too short creepage length* can result in high mobility of arcs which can lead to flashover;

- *Longer creepage lengths* can result in mobility of arcs in extreme events without causing flashover and localized stable arcs that may lead to surface deteriorations;

- An *optimal creepage length* offers the best performance with little or no arcing and hence no flashover and surface deteriorations;

- *Too much creepage length* can lead to localized stable arcs that may cause surface deteriorations

- *Very high creepage lengths* (with respect to operating conditions) results in infrequent localized arcing and hence less chances of surface deteriorations.

The above statements therefore serve to explain the findings presented on the effects of creepage length with regard to the ageing performance of insulators considered in this study. The question however still remains that "*What is the optimal range of USCD for AC, DC+ and DC-?*"

Similar investigations on the dimensioning of power line insulators, especially for DC applications, have been discussed in references [45] and [46]. The latter is a very recent document by CIGRE, with particular focus on the selection and dimensioning of power line insulators for HVDC applications. However, it has been stated in the document that knowledge on the ageing performance of insulators under DC electrical stresses is still vague. This therefore highlights the need to investigate the aspect of dimensioning of insulators under DC electrical stresses in more details.

Table 5-33: A summary of surface conditions observed on all test insulators

Test Cycle	Observations	Insulator Surface Conditions																	
		HTV-SR 84			HTV-SR 72			HTV-SR 56			HTV-SR 44			HTV-SR 29			Glass disc 42		
		AC	*DC+*	*DC-*	*AC*	*DC+*	*DC-*	*AC*	*DC+*	*DC-*	*AC*	*DC+*	*DC-*	*AC*	*DC+*	*DC-*	*AC*	*DC+*	*DC-*
1	Dryband	✓	✓	-	✓	✓	-	✓	✓	-	✓	✓	-	✓	✓	-	-	-	-
	Discoloration	-	-	-	-	-	-	-	-	-	-	-	-	-	-	-	-	-	-
	Crazing	-	-	-	-	-	-	-	-	-	-	-	-	L	L	-	-	-	-
	Erosion	-	-	-	-	-	-	-	-	-	M	-	-	-	-	-	-	-	-
	Peel-off	-	-	-	-	-	-	-	-	-	-	-	-	-	-	-	-	-	-
2	Dryband	✓	✓	✓	✓	✓	✓	✓	✓	✓	✓	✓	✓	✓	✓	✓	✓	✓	✓
	Discoloration	-	-	-	-	-	-	-	-	-	-	-	-	-	-	-	-	-	-
	Crazing	L	L	L	L	L	L	L	L	L	L	L	L	L	L	L	-	-	-
	Erosion	L	L	L	M	L	L	M	L	-	M	L	-	M	M	-	-	L	L
	Peel-off	-	-	-	-	-	-	-	-	-	-	-	-	-	-	-	-	-	-
3	Dryband	✓	✓	✓	✓	✓	✓	✓	✓	✓	✓	✓	✓	✓	✓	✓	✓	✓	✓
	Discoloration	-	-	-	-	-	-	-	-	-	-	-	-	-	-	-	-	-	-
	Crazing	L	L	L	L	L	L	L	L	L	L	L	L	L	L	L	-	-	-
	Erosion	L	L	L	M	M	M	M	M	L	H	M	L	M	M	L	-	L	M
	Peel-off	-	-	-	-	-	-	-	-	-	-	-	-	-	-	-	-	-	-
4	Dryband	✓	✓	✓	✓	✓	✓	✓	✓	✓	✓	✓	✓	✓	✓	✓	✓	✓	✓
	Discoloration	-	L	L	L	L	-	L	-	L	-	-	L	-	-	-	-	-	-
	Crazing	L	L	L	L	L	L	L	L	L	L	L	L	L	L	L	-	-	-
	Erosion	M	M	M	M	M	M	M	M	L	H	M	M	M	M	M	-	M	H
	Peel-off	-	-	-	-	-	-	-	-	✓	-	-	✓	-	-	-	-	-	-

✓ = Observed L = Light M = Medium H = Heavy

Table 5-34: An overview of instances of material erosion observed on all the HTV-SR test insualtors per each excitation voltage type

	Total Instances of Material Erosion				
	HTV-SR 84	HTV-SR 72	HTV-SR 56	HTV-SR 44	HTV-SR 29
AC	5	8	8	3	2
DC+	7	6	7	7	5
DC-	4	4	8	3	2

With reference to the information presented in Table 5-33, the following observations can be made:

- The majority of the instances of erosion were generally observed to have occurred on the terminating sheaths (interfacing with both the live and ground end-fittings) and these were dominantly southward for all the HTV-SR insulators. For glass disc insulators, erosion was only observed on the bottom side around the pin. These observations derive from the discussions presented in section 5.5.2. In order to establish what could have led to the occurrences of the observed erosion, it is important to understand the electrical discharge performance presented in section 5.4 With reference to the discussions on electrical discharge activity observations, presented in section 5.4.2, it has been noted that dryband corona (DBC) and dryband discharge (DBD) activities were found to have dominantly occurred on the terminating sheaths of the HTV-SR insulators. Additionally, the same types of electrical discharge activities (i.e. DBC and DBD) were commonly observed on the bottom side of glass disc insulators. It therefore appears that these two types of electrical discharge activities could be the driving factors that may have led to the observed instances of material erosion on the terminating sheaths and on the bottom side of the HTV-SR and glass disc insulators, respectively.

- Issues relating to the material erosion of silicone rubber insulator under outdoor applications have been explored and reported in references [47] and [48]. It is stated that dryband arcing can cause erosion on non-ceramic (polymeric) insulators, especially those associated with low leakage currents of magnitudes ranging from 1 to 20 mA. This is due to the relatively stable arc-roots that may be formed at localized regions with reduced surface resistance [47, 48]. Thus, these persistent arcs can lead to the dissipation of considerably high levels of energy – thereby leading to the occurrence of surface erosion. It therefore follows that the dryband activities (DBC and DBD) observed on the terminating sheaths of the HTV-SR insulators can be contributing factors to the occurrences of erosion on insulators. This validates the observation that erosion was dominantly observed on the terminating sheaths where DBC and DBD were prominent.

- The dominant southward occurrence of erosion was a result of the severe pollution reported to have emanated from the southward direction at KIPTS, especially in the summer period. In fact, most of these instances of erosion were observed within the heavy southward pollution deposits on the HTV-SR insulators. This directionally dominant, southward pollution was recorded from pollution measurements made with the directional dust deposit gauge (DDDG) installed at the test rig. Refer to section 5.2.2.4, Figure 5-15.

The glass disc insulator on AC was generally found to have performed well in terms of erosion when compared to those energized under both DC+ and DC-. Erosion was only observed on DC+ and DC-. It must be mentioned that erosion was very severe on Glass disc 42 DC- when compared to the one observed on Glass disc 42 DC+. The common observation was that both of these instances of material deterioration occurred on the bottom side of glass disc around the pin. No cement growth or pin corrosion was observed. It therefore appears that the deterioration was an effect of electrical stress. In addition, evidence of dryband activity was observed on the eroded areas. Dryband discharge activity was also observed on the bottom side of Glass disc 42 DC+ and Glass disc 42 DC-. Two fuse operations were recorded for Glass disc 42 DC- and this agrees with the high levels of leakage currents on DC- as reported in section 5.3.2.7, Figure 5-29. Thus, on the basis of erosion, the following ranking of performance of glass disc insulators can be stated for each excitation voltage as follows:

(Worst) DC- → DC+ → AC *(Best)*

- Blue patches were mainly observed on the shed tops toward the end of the test period (week 16 – 22). These patches were in the form of darker blue dots which occurred in almost all directions. It could not be ascertained as to whether these could be a results of UV degradation or electrical stress. However, no evidence of electrical activity was noted in the vicinity of the discoloured areas. It is therefore hypothesized that these might be a result of chemical changes that might have occurred in the filler materials.

Some interesting observations were made for the DC excitation voltage types for which no logical explanations could be obtained. It was however hypothesized that these might be peculiar to the nature of electrical stress that results from the two DC polarities. Such observations are presented below:

- *DC+: Radial pattern of drybands and erosion on the shed bottoms of the HTV-SR test insulators*

  The traces of dryband activities observed on the shed bottoms were generally found to have a radial pattern for the HTV-SR insulators. Similarly, erosion with a radial pattern was also observed on the shed bottoms of HTV-SR 84 DC+ (the longest insulator on DC+). No similar observations were made on AC and DC-. This therefore indicates that there is a particular characteristic that specifically pertains to the electrical stress that results from this DC polarity.

- *DC-: Peel-off on the shed-to-sheath bonding interface of the HTV-SR test insulators*

  As noted in Table 5-33, material peel-off was observed on DC- for both HTV-SR 56 and HTV-SR 44. No similar observations were made on AC and DC+. It would therefore be interesting to investigate whether this could be a mode of deterioration that is only peculiar to DC-. In retrospect, it might be that it is only a slow process on the other voltage types. Thus, a close check should be kept on this aspect for all the excitation voltage types throughout the entire test program.

5.6 Results on wettability (hydrophobicity) classification tests

5.6.1 Overview

This section presents the results of wettability classification tests done on all the high temperature vulcanized, silicone rubber (HTV-SR) test insulators. Note that the terms "wettability" and "hydrophobicity" will be used interchangeably henceforth. No hydrophobicity tests were done on the glass disc insulators since they are already hydrophilic by nature of their smooth, glassy surfaces. The timelines adopted for the wettability classification tests are similar to those used for surface condition inspections, where a three-week test cycle approach was employed. Refer to Table 5-17 in section 5.5.1. With cognizance of the fact that the hydrophobicity tests were not done on the same day for all the excitation voltage types, comparisons of the results obtained for the respective excitation voltage types will conveniently be based on the hydrophobicity trends observed.

Details on the approach used for wettability classification tests have been described in section 4.5 and all the insulator sections that were considered are also illustrated in Figure 4-6. Please note that not all the wettability classification results are reported herein. Hydrophobicity is a localized characteristic. Hence, it was vital that a specific section of consideration be chosen for all the test insulators in order to allow for comparisons.

It should be recalled that most electrical discharge activities (especially dryband corona and dryband discharge) were observed on the terminating sheaths interfacing with the both the live and ground end-fittings of the HTV-SR insulators. Additionally, most instances of material erosion were dominantly observed on the terminating sheaths interfacing with both the live and ground end-fittings. It therefore follows that the hydrophobicity conditions on these sheaths would be representative of the worst conditions of electrical stress. Thus, for all HTV-SR insulators, the results for the sheath interfacing with the live end-fitting and the first shed from the live end-fitting have been considered in the discussions presented in the following sections. Only the results obtained from the sea side (westward direction) are reported. Additional wettability classification results are furnished in Appendix F, detailing the results obtained from both the sea and land sides.

5.6.2 Wettability classifications for individual insulators

5.6.2.1 Introduction

Sections 5.6.2.2 to 5.6.2.6 summarize wettability classification results for the individual HTV-SR test insulators. The results of wettability classifications obtained for the top and bottom of shed 1 and also for the sheath interfacing with the live end-fitting, tested from the sea side, are summarized in a comparative manner in Table 5-35 and Figure 5-39.

NB: Wettability (hydrophobicity) classifications are quoted as "HC", which signifies "hydrophobicity class".

Table 5-35: A summary of wettability classifications for all the high temeperature vulcanized, silicone rubber (HTV-SR) test insulators

		Wettability (Hydrophobicity) Classifications														
Test Cycle	Insulator section	HTV-SR 84			HTV-SR 72			HTV-SR 56			HTV-SR 44			HTV-SR 29		
		AC	*DC+*	*DC-*	*AC*	*DC+*	*DC-*	*AC*	*DC+*	*DC-*	*AC*	*DC+*	*DC-*	*AC*	*DC+*	*DC-*
1	Shed Top	7	6	-	6	6	3	6	6	4	6	6	4	6	3	6
	Shed Bottom	3	4	-	4	4	2	3	3	2	3	3	2	4	4	2
	Sheath	6	7	-	6	6	6	6	7	7	4	7	5	5	7	7
2	Shed Top	7	7	7	7	7	5	6	6	7	7	6	7	7	6	6
	Shed Bottom	4	4	5	4	5	5	4	7	5	4	6	4	4	6	5
	Sheath	7	7	7	7	6	7	7	7	7	7	5	7	7	7	7
3	Shed Top	7	7	7	7	7	7	7	7	7	7	6	7	7	6	6
	Shed Bottom	4	6	5	4	7	6	5	7	5	5	6	5	5	6	6
	Sheath	4	7	6	7	7	7	7	7	6	6	7	7	7	7	7
4	Shed Top	7	7	7	7	7	7	7	7	7	6	7	7	5	6	7
	Shed Bottom	5	5	4	5	6	6	5	6	4	6	7	6	6	6	7
	Sheath	4	6	7	4	4	7	7	6	7	5	7	7	7	6	7

Note that the graphical representation of results is done in a form of a matrix in Figure 5-39. This is done in order to compare the hydrophobicity of all test insulators for the three excitation voltage types in a single graph. This style further allows for comparisons between the hydrophobicity of insulators with different creepage lengths.

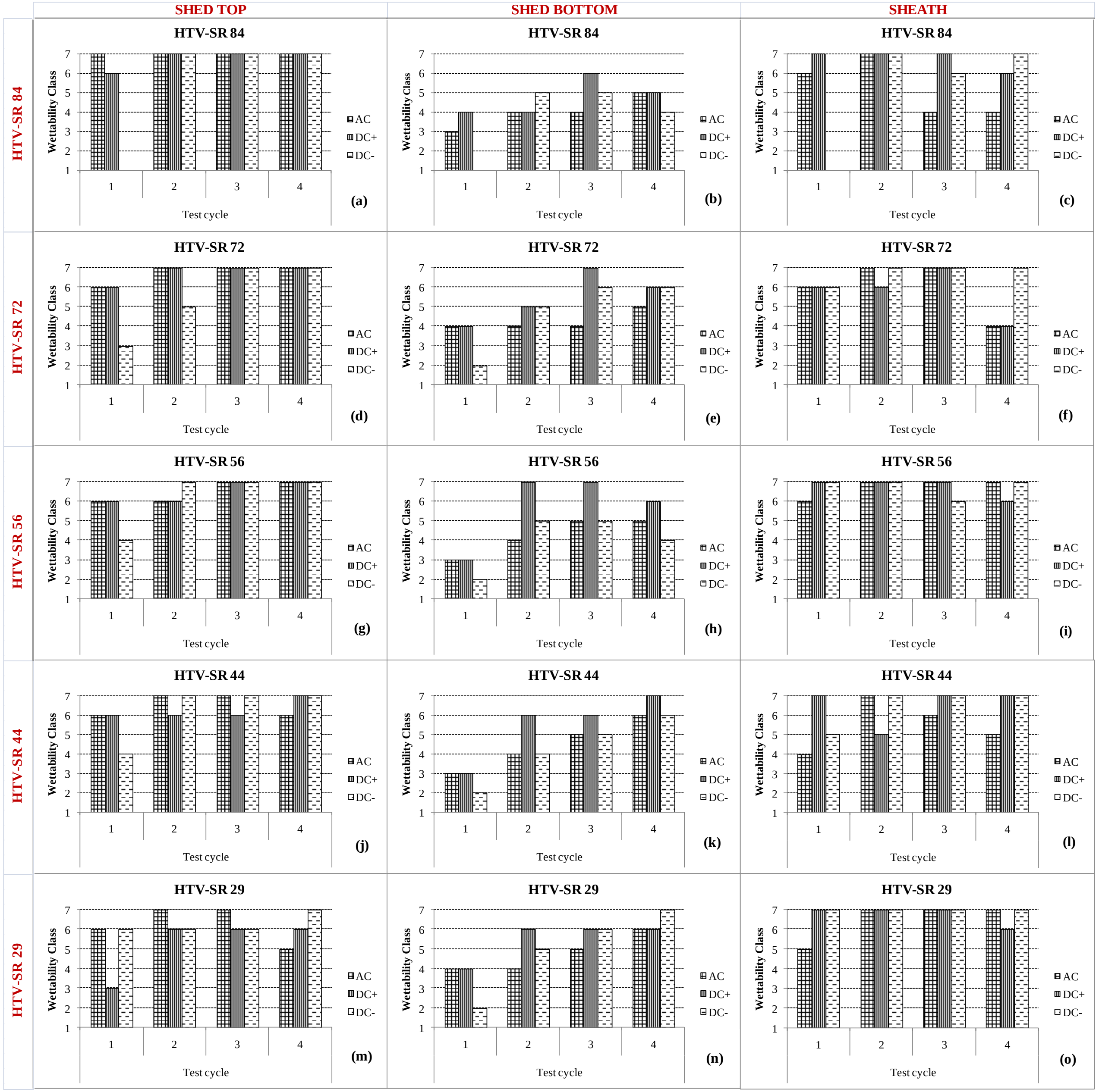

Figure 5-39: Comparisons of the wettability classifications for all the HTV-SR insulators given for the shed tops, shed bottoms and sheaths

5.6.2.2 Wettability classifications for the HTV-SR 84 insulators

This section summarizes the wettability classification results for the high temperature vulcanized silicone rubber (HTV-SR) insulators with a unified specific creepage distance (USCD) of 84 mm/kV. Detailed results on hydrophobicity classifications for all test insulators with this particular USCD are presented in Appendix F.2. This therefore gives rise to the following observations:

- *Shed top*

  Results have shown that hydrophobicity was completely lost (HC 7) from test cycle 2 (week 6) for the shed top on AC, DC+ and DC-. No recovery was observed. This can be seen in Figure 5-39 (a). It should be mentioned that no hydrophobicity tests were done for DC- in the first test cycle, but a wettability class better than HC 5 would be expected nonetheless since it was just a week after the insulators were installed.

- *Shed bottom*

  By comparing the results shown in Figure 5-39 (b) to Figure 5-39 (a), a general trend can be observed in that the shed bottom had better hydrophobicity than the shed top – with an average of HC 4 for AC and DC-, and HC 5 for DC+. It is also interesting to note that a recovery was observed for both DC+ (HC 6 to HC 5) and DC- (HC 5 to HC 4) between the 3rd and 4th test cycles, whereas none was observed for AC.

- *Sheath*

  With reference to Figure 5-39 (c), the sheaths was found to exhibit better hydrophobicity than the shed top, with an average of HC 5 for AC and HC 7 for DC+ and DC-. A recovery from HC 7 to HC 4 was observed for AC between the 2nd and 3rd test cycles, whereas an HC 7 to HC 6 recovery was observed for DC+. Hydrophobicity fluctuated between HC 6 and HC 7 for DC-.

5.6.2.3 Wettability classifications for the HTV-SR 72 insulators

This section summarizes the wettability classification results for the high temperature vulcanized silicone rubber (HTV-SR) insulators with a unified specific creepage distance (USCD) of 72 mm/kV. Detailed results on hydrophobicity classifications for all test insulators with this particular USCD are presented in Appendix F.3. This therefore gives rise to the following observations:

- *Shed top*

  The results have shown that hydrophobicity was completely lost (HC 7) on the shed top from test cycle 3 (week 10) for AC, DC+ and DC-. No recovery was observed. This is evident from Figure 5-39 (d).

- *Shed bottom*

  By comparing the results shown in Figure 5-39 (e) to those in both Figure 5-39 (d) and Figure 5-39 (f), it can be observed that the shed bottom exhibits better hydrophobicity than both the shed top and sheath – with an average of HC 4 for AC, HC 6 for DC+ and HC 5 for DC-. A general trend is observable from Figure 5-39 (e) that the hydrophobicity of test insulators deteriorated over time, as expected. It is also interesting to note that a recovery was observed for DC+ (HC 7 to HC 6) between the 3rd and 4th test cycles, whereas no recovery was observed for both AC and DC-.

- *Sheath*

  With reference to Figure 5-39 (f), the sheath was found to exhibit better hydrophobicity (albeit not particularly good) than the shed top, with an average of HC 6 for AC and DC+, and HC 7 for DC-. A recovery from HC 7 to HC 6 was observed for both AC and DC+ between the 3rd and 4th test cycles, whereas no recovery was observed for DC-.

5.6.2.4 Wettability classifications for the HTV-SR 56 insulators

This section summarizes the wettability classification results for the high temperature vulcanized silicone rubber (HTV-SR) insulators with a unified specific creepage distance (USCD) of 56 mm/kV. Detailed results on hydrophobicity classifications for all test insulators with this particular USCD are presented in Appendix F.4. This therefore gives rise to the following observations:

- *Shed top*

  The results have shown that hydrophobicity was completely lost (HC 7) on the shed top from test cycle 3 (week 10) for AC, DC+ and DC-. No recovery was observed. This is evident from Figure 5-39 (g).

- *Shed bottom*

  By comparing the results shown in Figure 5-39 (h) to those in both Figure 5-39 (g) and Figure 5-39 (i), it can be observed that the shed bottom exhibits better hydrophobicity than both the shed top and sheath – with an average of HC 4 for both AC and DC-, and HC 6 for DC+. It is interesting to note that a recovery was observed for DC+ (HC 7 to HC 6) between the 3rd and 4th test cycles and also for DC- (HC 5 to HC 4) between the 3rd and 4th test cycles. No recovery was observed for AC.

- *Sheath*

  Looking at Figure 5-39 (i), it can be seen that the hydrophobicity was found to be worse than that of both the shed top and bottom, with an average of HC 7 for AC, DC+ and DC-. A recovery from HC 7 to HC 6 was observed for DC+ between the 3rd and 4th test cycles and also for DC- (HC 7 to HC 6) between the 2nd and 3rd test cycles. No recovery was observed for AC.

5.6.2.5 Wettability classifications for the HTV-SR 44 insulators

This section summarizes the wettability classification results for the high temperature vulcanized silicone rubber (HTV-SR) insulators with a unified specific creepage distance (USCD) of 44 mm/kV. Detailed results on hydrophobicity classifications for all test insulators with this particular USCD are presented in Appendix F.5. This therefore gives rise to the following observations:

- *Shed top*

  The results have shown that hydrophobicity was completely lost (HC 7) on the shed top from test cycle 2 (week 6) for DC- and no recovery was observed. This is evident from Figure 5-39 (j). Further, the hydrophobicity for DC+ remained at HC 6 from the 1st test cycle through to the 3rd test cycle, and then a decline from HC 6 to HC 7 was observed between the 3rd and 4th test cycles. A recovery from HC 7 to HC 6 was observed for AC between the 3rd and 4th test cycles.

- *Shed bottom*

  By comparing the results shown in Figure 5-39 (k) to those in both Figure 5-39 (j) and Figure 5-39 (l), it can be observed that the shed bottom shows better hydrophobicity than both the shed top and sheath – with an average of HC 5 for AC, HC 6 for DC+ and HC 4 for DC-. It is interesting to note that the hydrophobicity continued to deteriorate almost linearly for all the excitation voltage types and no recovery was observed, as it can be seen in Figure 5-39 (k).

- *Sheath*

  Looking at Figure 5-39 (l), it can be observed that the hydrophobicity of the sheath was found to be worse than that of both the shed top and bottom, with an average of HC 6 for AC and HC 7 for both DC+ and DC-.

5.6.2.6 Wettability classifications for the HTV-SR 29 insulators

This section summarizes the wettability classification results for the high temperature vulcanized silicone rubber (HTV-SR) insulators with a unified specific creepage distance (USCD) of 29 mm/kV. Detailed results on hydrophobicity classifications for all test insulators with this particular USCD are presented in Appendix F.6. This therefore gives rise to the following observations:

- *Shed top*

  All three voltage types show an average of HC 6 on the shed top for the entire test program. Noting that the first hydrophobicity tests were done on DC- in week 2 (February 10th), it is interesting to note that a bad hydrophobicity class of HC 6 on the shed top was already recorded at such an early stage of the test program. DC+ showed relatively better hydrophobicity of HC 3 for the shed top, which was about three weeks after the installation of the test insulator. For AC, a recovery from HC 7 to HC 5 was noted between the 3rd and 4th test cycles. No recovery was observed for both DC+ and DC-. Refer to Figure 5-39 (m).

- *Shed bottom*

  Comparing the results shown in Figure 5-39 (n) to those in both Figure 5-39 (m) and Figure 5-39 (o), it can immediately be observed that the shed bottom exhibits better hydrophobicity than both the shed top and sheath – with an average of HC 5 for both AC and DC- and HC 6 for DC+. No recovery was observed for all the three excitation voltage types.

- *Sheath*

  Looking at Figure 5-39 (o), it can be observed that the hydrophobicity of the sheath was found to be worse than that of both the shed top and bottom, with an average of HC 7 for all the three excitation voltage types.

5.6.3 Overall comparisons

With reference to the foregoing discussions presented in sections 5.6.2.2 to 5.6.2.6, the following general observations can be made:

- For all the test insulators, the shed bottom was generally found to show better hydrophobicity when compared to both the shed top and sheath.

- For the shorter creepage length insulators, i.e. HTV-SR 56, HTV-SR 44 and HTV-SR 29, the sheath showed the worst hydrophobicity when compared to the longer insulators, HTV-SR 84 and HTV-SR 72. This is not an unexpected observation given that most electrical discharge activities and material erosion occurred on the sheaths, albeit with a southward-dominant prevalence. Details on electrical discharge activities and erosion are discussed in sections 5.4.3.1 and 5.5.3.2, respectively. It therefore follows that the hydrophobicity of the sheaths would, expectedly, be lower compared to other sections of the insulators where electrical discharge activities were less prominent.

- A general trend demonstrates increased recovery in hydrophobicity in both DC+ and DC- when compared to AC. One would however have expected to observe improved recoveries in the hydrophobicity of AC, since the AC voltage waveforms have the nature of zero-crossing which could help with occasional relief of electrical stress when compared to the constantly present DC electrical stress.

- *Caution*: It should be recalled that hydrophobicity is a localized property. This may therefore mean that, since the hydrophobicity tests were only done in the westward (sea side) direction, the recorded hydrophobicity results may not be generalized due to the relativity of the hydrophobicity property.

6. CHAPTER 6: Conclusions and recommendations

6.1 Overview

This section presents conclusions and recommendations based on the discussions presented in Chapter 5. Conclusions and recommendations are given in sections 6.2 and 6.3, respectively. As stated in section 1.2, under project motivation, very limited field studies have been conducted on the performance of power line insulators under HVDC applications when subjected to natural pollution environments. It therefore follows that the results presented in this thesis are expected to serve as a key basis for the analysis of relative insulator performance under the three considered excitation voltage types: AC, DC+ and DC-. The author refrains from stating firm conclusions on the obtained results. At the onset, it should be stated that this thesis has only presented the data obtained for the first six months of the test period. The test period is still in progress and final evaluations will be produced in a separate report once the entire test period is completed. Therefore, firm conclusions will only be stated then. Hence, it is envisaged that new research questions will unfold from this thesis that will lead into future studies – especially to conduct further explorations into the observations made in this study.

The discussions in the previous chapter were presented in order to address the original objectives of this thesis, as stated below:

- To design a suitable DC excitation voltage system for both DC+ and DC-.
- To perform a comparative evaluation of the performance of high temperature vulcanized, silicone rubber (HTV-SR) power line insulators under AC, DC+ and DC- when subjected to natural pollution conditions at KIPTS. All test insulators were made from the same material and sourced from the same manufacturer, but having different creepage lengths (refer to section 3.2). Note that a reference glass disc insulator was used for each excitation voltage as a control test sample.

Given the fact that all test insulators were made from the same material (HTV-SR), it was assumed that they all have the same chemical characteristics and only differ in creepage length. Additionally, it was assumed that all test insulators were subjected to the same environmental conditions and the same electrical stress. The DC excitation voltages were designed to an equivalent RMS of the AC voltage to ensure that all insulators were subjected to the same electrical stress (ageing due to electrical stress is dependent on the power dissipated over the insulator during electrical discharge activities and hence the choice of RMS equivalence). Thus, the two major aspects under investigation were: the *effect of creepage length on the performance of test insulators* and *the impact of the three excitation voltage types*.

6.2 Conclusions

6.2.1 Introductory remarks

As explained above, note that the author will refrain from stating firm conclusions on the results presented for the first six months of the test period and that firm conclusions will only be stated upon the final evaluations at the end of the test period (February 2012). This section will therefore only present a summary of the key observations made in the study for the first six months. The results are summarized in sections 6.2.1.1 to 6.2.1.5 for each of the respective aspects considered in the study. These aspects, as listed below, were investigated in order to gather data that would be useful to carry out analyses on the relative performance of the test insulators considered in the study – thereby addressing the research objectives:

- Climatic and environmental conditions at KIPTS
- Leakage current performance
- Electrical discharge activity observations
- Surface condition inspections (ageing performance)
- Wettability (hydrophobicity) classification tests

Note that the results discussed in Chapter 5 were presented in a manner such that overall conclusions were provided per each section. The following concluding remarks are therefore a compilation of the individual conclusions (as presented for the respective sections in Chapter 5) in order to tie them up into an Executive Conclusions' chapter.

6.2.1.1 Concluding remarks on the climatic and environmental conditions at KIPTS

Climatic and environmental condition monitoring were conducted in order to establish an understanding of the service conditions to which insulators were subjected. Weather sensors were thus installed at KIPTS and climatic conditions such as rainfall, relative humidity, temperature; wind conditions and UV-B radiation were continuously logged using the online-leakage current analyzer (OLCA) device. For environmental conditions, the following procedures were used: a *non-energized glass disc insulator* for equivalent salt deposit density (ESDD) and non-soluble deposit density (NSDD) measurements, and the *directional dust deposit gauges* (DDDG) for directional pollution measurements. These two procedures were used as a means of exploring the severity of pollution at KIPTS. The following findings were obtained:

- *Climatic conditions*

  The findings on climatic conditions were discussed in section 5.2.1. Summer was found to be a dry season at KIPTS, with occasional events of high relative humidity levels occurring at nights and in the early morning hours. Higher temperature, UV-B radiation and wind speed levels were recorded in summer when compared to those experienced in winter. Wind speeds were generally found to have south-easterly directions at night and in the early morning hours, whilst blowing south-westerly during the afternoons. This was true for both summer and winter. In contrast, winter was found to be a rain-dominant season. Lower levels of temperature, UV-B radiation and wind speed were experienced in winter.

  An inverse relationship between temperature and relative humidity was established. Relative humidity levels in excess of 75% were recorded when the difference between the ambient and dewpoint temperatures was smaller than 4 °C. This condition was experienced at night and in the early morning hours. This means that one would ideally expect 100% relative humidity when the difference between the ambient and dewpoint temperatures approaches zero. The greater the difference between the two temperatures, the lower the relative humidity. Thus, no critical wetting was experienced during the periods when the difference between the two temperatures exceeded 4 °C, especially during the afternoons when ambient temperatures were high.

- *Environmental conditions*

  The findings on pollution severity monitoring were discussed in section 5.2.2. For the summer period, higher ESDD levels were recorded on the top side of the glass disc insulator when compared to the bottom side. In contrast, higher ESDD levels were recorded on the bottom side when compared to the top side in winter. This suggests that rainfall appears to have played a role in the levels of the ESDD values measured on the glass disc insulator and this was not an unexpected revelation. With reference to the rain conditions presented in section 5.2.1 (refer to Figure 5-2), it is logical that there would be frequent washing of the top side of glass in winter which renders the ESDD values to be lower than the bottom side given the limited washing on the bottom side.

  The highest pollution conductivities, as high as 1272 µS/cm and 1104 µS/cm, were found to have emanated from the southward direction – recorded as average values for both summer and winter, respectively. The highest DDDG value of 2996 µS/cm was obtained from the southward direction and this was recorded in summer, as shown in Figure 5-15. With reference to the average DDDG values given in Table 5-10 for summer and winter periods, the DDDG conductivity levels recorded in summer were generally higher than those recorded in winter. This indicates that harshest pollutants were prominent in the southward direction, probably emanating from the heavy industries that lie to the south of KIPTS. It can therefore be expected that this harsh south-dominant pollution would cause aggravated conditions on the insulator surfaces due to the highly conductive electrolytes that may be formed during wetting conditions.

6.2.1.2 Concluding remarks on leakage current performance of test insulators

Discussions pertaining to the leakage current performance of all the test insulators are presented in section 5.3. This section therefore presents a brief summary of the important observations obtained with regard to the information discussed in sections 5.3.2, 5.3.3 and 5.3.4.

- A statistical approach using time of day bin count analysis was employed. This approach was found to be useful for the analysis of leakage current performance; especially in that it categorizes leakage current data into bins of different magnitudes. This could be a useful approach in analyzing the ageing effects of the occurrence of leakage current with a certain magnitude. It is understood that the localized stable, low magnitude leakage currents (typically 1 to 20 mA) can cause erosion on the insulator surfaces [47, 48]. Thus, classifying leakage current into different bin categories could help with determining the range of leakage current that may be responsible for the resulting ageing conditions of the insulator materials. In addition, the time of day analysis allows for a direct correlation of leakage current performance with the measured climatic conditions (refer to section 5.3.4.4).

- Higher leakage current levels were observed on all the three test insulators during summer when compared to those recorded in winter. This is in relation to the high pollution severity recorded in summer and the low rainfall conditions experienced in summer, resulting in limited washing events. Refer to section 6.2.1.1.

- High leakage current levels were mainly recorded at night and also during the early morning hours. These times coincide with the observations made with regard to variations in the climatic conditions at KIPTS, where relative humidity levels exceeded 75% when the difference between the ambient and dewpoint temperatures was very small.

- For the HTV-SR insulators, the shortest insulator installed on DC+ had the highest occurring leakage current. In fact, a flashover event was recorded on this particular insulator (HTV-SR 29 DC+). For glass disc insulators, in contrast, the highest occurring leakage current was recorded on DC-. Two flashover events were recorded for Glass disc 42 DC-. It was an interesting observation that HTV-SR performed worse than glass disc on DC+, whereas the converse would have been the expected observation.

- On the basis of both leakage current and ageing performance of the insulators considered in this study, the HTV-SR insulator with a unified specific creepage distance of 44 mm/kV appears to be the optimal creepage length that would yield acceptable performance (i.e. minimal flashovers and erosion). For unified specific creepage distance (USCD) values lower tha 44 mm/kV, a flashover event was recorded for HTV-SR 29 on DC+. In addition, an increased number of instances of erosion were observed for USCD values higher than 44 mm/kV. This then follows that 44 mm/kV can be considered the critical USCD for HTV-SR insulators. Refer to Table 5-12 and Table 5-34 for evidence on this observation.

- It can be added that the leakage current levels for all the HTV-SR insulators were of a similar order of magnitude for AC and DC+ and lower for DC-. Refer to section

5.3.4.6 for comparisons of leakage current performance for the HTV-SR insulators with different creepage lengths under AC, DC+ and DC-.

- Overall, no conclusive information could be obtained from accumulative coulomb-ampere in relation to the observed ageing conditions of test insulators. With the understanding that the accumulative coulomb-ampere takes into account all the instantaneous occurrence of leakage current (including high flashover events), this parameter may not be fully representative of the leakage currents that can cause surface deteriorations. As mentioned earlier, it is often the localized stable, low magnitude leakage currents (typically 1 to 20 mA) that can cause erosion on the insulator surfaces.

6.2.1.3 Concluding remarks on electrical discharge activity observations

The following observations were obtained in relation to the electrical performance of test insulators, as presented in sections 5.4.2 and 5.4.3:

- Both dryband corona (DBC) and dryband discharge (DBD) activities dominantly occurred on the terminating sheaths (interfacing with both the live and ground end-fittings) for all the HTV-SR insulators. For glass disc insulators, DBD was the most prominent electrical activity observed on the bottom side of glass disc around the pin for all the three excitation voltage types (i.e. AC, DC+ and DC-). It was particularly interesting to observe that erosion dominant on the terminating sheaths and bottom side for the HTV-SR and glass disc insulators, respectively.

- *Frequency of occurrence*: Corona (water drop corona (WDC) and DBC) activities were commonly observed on the AC excitation voltage, whereas discharge (spot corona/discharge (SCD) and DBD) activities were more prominent on the DC+ and DC- excitation voltage types.

- *First occurrence*: All corona activities (WDC and DBC) were first observed on the AC excitation voltage, whereas the discharge activities (SCD and DBD) were first observed on the DC excitation voltage (both polarities).

- The 0-lux Sony camcorder was found to be very useful in ascertaining the locations of the intense dryband discharge (DBD) activities. This camera allowed for clearly focused views of DBD activities to be captured. The less intense electrical discharge activities such as water drop corona (WDC) and spot corona discharge (SCD) could not be detected with this camera. In contrast, Corocam Mark I was more useful with the identification of electrical discharge activities – detecting even the least easily detected levels of electrical discharge activities such as corona (WDC and SCD). It was, however, not easy to ascertain the exact locations of the intense electrical discharge activities with Corocam Mark I such as DBD due to the saturation limitations associated with the lens, thereby causing blobs around the areas with electrical discharge activity. Therefore, it follows that there is a prospect that a night suited, 0-lux Sony camera could be a useful tool, alongside Corocam Mark I, especially for identifying the intense electrical discharge activities such as DBC and DBD.

6.2.1.4 Concluding remarks on surface condition inspections: ageing performance

With reference to the information presented in sections 5.5.2 and 5.5.3, the following observations can be stated:

- In general, most of the instances of erosion were observed on the terminating sheaths (interfacing with both the live and ground end-fittings) and these were dominantly southward for all the HTV-SR insulators. The southward dominant occurrence of erosion was a result of the harsh pollution severity that was reported to have emanated from the southward direction of KIPTS, especially in the summer period. It can be noted that dryband corona (DBC) and dryband discharge (DBD) activities were also found to have dominantly occurred on the terminating sheaths of the HTV-SR insulators.

- For glass disc insulators, erosion was observed on the bottom side around the pin. Additionally, the DBC and DBD activities were commonly observed on the bottom side of glass disc insulators. It therefore appears that these two types of electrical discharge activities could be the driving factors that may have led to the observed instances of material erosion on the terminating sheaths and on the bottom side of the HTV-SR and glass disc insulators, respectively.

- It would have been expected that the most significant instances of erosion be observed on the shortest insulators due to the shortest electrical separation that could be most susceptible to high electrical stresses. The findings were however contrary to this expectation. The shortest insulator with the unified specific creepage distance (USCD) of 29 mm/kV was found to have the least instances of erosion for all the excitation voltage types. The middle class USCD insulators (44 mm/kV, 56 mm/kV and 72 mm/kV) were found to have the highest number of instances of erosion when compared to the shortest and longest insulators. This suggests that there appears to be a critical range of USCD beyond which ageing performance may be compromised. For evidence on this, please refer to the figures cited in Table 5-34. These observations on the effect of creepage length correspond with the findings presented in the IEC/TS 60815-3:2009 document on the guidelines for the selection of insulators with respect to polluted conditions [44], as discussed in section 5.5.3.2.

- Some form of discoloration was observed on the HTV-SR insulators. This was in the form of blue patches, which were mainly observed as dark blue spots on the shed tops toward the end of the test period (week 16 – 22). It could not be ascertained as to whether these were a result of UV degradation or electrical stress. However, no evidence of electrical discharge activity was noted in the vicinity of the discoloured areas. It is therefore hypothesized that these might be a result of chemical changes that might have occurred in the filler materials.

The following are some of the observations made on the DC+ and DC- excitation voltage types for which no possible explanations could be established. It was however hypothesized that these might be due to the differences in the nature of electrical stress that may result from DC+ and DC-. Such observations are presented below:

- *DC+: Radial pattern of drybands and erosion on the shed bottoms of the HTV-SR test insulators*

  The traces of dryband activities observed on the shed bottoms were generally found to have a radial pattern for the HTV-SR insulators. Similarly, erosion with a radial pattern was also observed on the shed bottoms of HTV-SR 84 DC+ (the longest insulator on DC+). No similar observations were made on AC and DC-. This therefore suggests that this observation specifically pertains to the characteristic of electrical stress that results from this DC polarity.

- *DC-: Peel-off on the shed-to-sheath bonding interface of the HTV-SR test insulators*

  Material peel-off was observed on DC- for both HTV-SR 56 and HTV-SR 44. No similar observations were made on AC and DC+. It therefore appears that this could be a mode of deterioration that may be peculiar to DC-. In retrospect, it can also be possible that this type of deterioration occurs on AC and DC+ and that it might just be a slower process on these excitation voltage types. Thus, all test insulators will be continually evaluated throughout the remainder of the test period.

6.2.1.5 Concluding remarks on wettability (hydrophobicity) classification tests

Detailed discussions on the hydrophobicity conditions of the HTV-SR insulators are presented in sections 5.6.2.2 to 5.6.2.6. The following general observations can therefore be stated:

- The shed bottom generally showed better hydrophobicity when compared to both the shed top and sheath for all test insulators under AC, DC+ and DC-. .

- The sheath showed the worst hydrophobicity for the shorter creepage length insulators, i.e. HTV-SR 56, HTV-SR 44 and HTV-SR 29, when compared to the longer insulators, HTV-SR 84 and HTV-SR 72. Given the fact that most electrical discharge activities and material erosion dominantly occurred on the sheaths, albeit with a southward-dominant prevalence, this was an expected observation. Thus, it follows that the hydrophobicity on the sheaths would, expectedly, be worn out more than other sections of the insulators where electrical discharge activity was less prominent.

- Recoveries in the hydrophobicity properties were more commonly observed on both DC+ and DC- when compared to AC. One would however have expected to observe more recoveries in the hydrophobicity on AC, since the AC voltage waveforms have the nature of zero-crossing which could help with occasional relief in the electrical stress compared to the constantly present DC electrical stress.

- *Caution*: Hydrophobicity is a localized property. This would therefore mean that, since the hydrophobicity tests were only done in the westward (sea side) direction, the recorded hydrophobicity results cannot not be generalized due to the relativity of the hydrophobicity property.

6.3 Recommendations

On the basis of both the information presented in Chapter 5 and section 6.2, the following recommendations can be made:

6.3.1 The use of the energized test insulator for ESDD pollution sampling

It can be appreciated that a measure of pollution severity obtained from a non-energized sampling glass disc insulator (as used in this study) cannot give a full picture of the pollution conditions experienced on an energized insulator. This is particularly so for DC excitation voltage types, whose electrostatic fields might play a role in the attraction of pollutants. A similar concern has also been cited in reference [46]. It is therefore recommended that an energized glass disc insulator be installed on AC, DC+ and DC- in order to study the deposition processes of pollutants for these respective excitation voltage types. Additionally, it would be even better if a dedicated study be conducted with the use of silicone rubber based insulators. The author of this thesis feels that due to the difference of adhesive properties of silicone rubber and glass insulators, one would expect that the deposition processes might differ and thus further determine the type of pollutants that may be deposited. It would therefore be more logical to use a pollution sampling insulator that is as representative as possible of the test insulators under study. For example, an HTV-SR sampling insulator should be used for studies that involve HTV-SR based insulators.

6.3.2 Statistical approach to leakage current performance analysis

The statistical approach used in this thesis was found to be a powerful approach. This approach employs a time of day analysis of the occurrence of leakage current levels of categorized magnitudes. The use of this approach has the following benefits:

- The categorization of leakage current into different magnitudes may help to identify the type of current levels that may be responsible for erosion and flashover, respectively. It has been cited that currents of magnitudes 1 to 20 mA are often responsible for erosion on non-ceramic insulators.

- The time of day approach allows for a correlation to the time of day variations in weather conditions (wetting events and pollution deposition) – thereby providing information about the expected performance at a particular area.

- This approach offers a lucrative way of dealing with bulky leakage current data as obtained for this study.

6.3.3 A fundamental study on the mechanism of electrical discharge activity developments for DC excitation voltages versus AC excitation voltage

A more fundamental study is needed to explore the development processes and nature of electrical discharge activities on outdoor insulators. Additionally, associated current levels should also be recorded. This, in conjunction with ageing performance monitoring, will help to explain the types of electrical discharge activities that could be responsible for material deteriorations on AC, DC+ and DC- under natural pollution environments.

The interesting observations of star-shaped (radial) erosion on the shed bottoms observed on DC+ and the material peel-off at the shed-to-sheath bonding interface observed on DC- could not be explained due to the lack of knowledge of the fundamental processes of the development of electrical discharge activities on the respective excitation voltage types.

6.3.4 The use of corona and arcing mitigation techniques

It was observed in this study that most instances of material erosion occurred on the termination ends (both live and ground sides) of the insulators. This is due to the high concentrations of electrical stress around these areas. Therefore, for the purpose of mitigating such effects, the use of corona rings or arcing horns can be a useful consideration.

REFERENCES

1. J.P. Holtzhausen and W.L. Vosloo, *High Voltage Engineering: Practice and Theory*, Cape Town, 2009.

2. J.S.T. Looms, *Insulators for High Voltages*, Peter Peregrinnus, England, 1988.

3. W. L. Vosloo, R.E. Macey and C. de Tourreil, *The Practical Guide to: Outdoor High Voltage Insulators*, Crown Publications CC., Johannesburg, 2004.

4. B. S. Limbo, "Insulator Aging Tests with HVAC and HVDC Excitation using the Tracking Wheel Tester", *MSc Thesis*, University of Stellenbosch, March 2009.

5. G. Heger, "A Comparative Study of Insulator Materials Exposed to High Voltage AC and DC Surface Discharges", *MSc Thesis*, University of Stellenbosch, March 2009.

6. J. P. Holtzhausen, *Technical Reference on High Voltage Insulators*, [Online], June 2000.

7. W. L. Vosloo, "A Comparison of the Performance of High-Voltage Insulator Materials in a Severely Polluted Coastal Environment", *PhD Thesis*, University of Stellenbosch, March 2002.

8. J. P. Holtzhausen, "A Critical Evaluation of AC Pollution Flashover Models for HV Insulators having Hydrophilic Surfaces", *PhD Thesis*, University of Stellenbosch, South Africa, 1997.

9. O. C. T. Potgieter, "Development and Evaluation of an Insulator Pollution Monitoring Apparatus", *MSc Thesis*, University of Stellenbosch, October 1991.

10. L. Van Wyk, "Insulator Pollution monitoring: Evaluation of various methods of Severity Measurements at a Coastal Site", *MSc Thesis*, University of Stellenbosch, December 1996.

11. D. C. Jolly, "Contamination Flashover Theory and Insulator Design" *Journal of the Franklin Institute*, Vol. 294, No. 6, Pg. 483 – 490, December 1972.

12. M. Sforzini, "Testing of Polluted Insulators – The Present Situation and Problems of the Future" *Journal of the Franklin Institute*, Vol. 294, No. 6, Pg. 437 – 442, December 1972.

13. S. Wright and D. Dumora, "Design Criteria for Composite Insulators" *IEEE Colloquium on Non-Ceramic Insulators for Overhead Lines*, London, UK, April 2004.

14. D. Pathak, M. Satwani, M. Patel and C. Patel, "The Development of Silicone Rubber Composite Insulators in Power System", *International Conference on Control, Automation, Communication and Energy Conservation*, Kongu Engineering College Perundurai, Erode, India, June 2009.

15. W. L. Vosloo, R. Swinny and J. P. Holtzhausen, *Koeberg Insulator Pollution Test Station (KIPTS) –An In House Insulator Product Ageing Test Standard*, [Online], Insulator Centre, ESKOM Holdings Ltd, Cape Town, South Africa, 2001.

16. W. L. Vosloo and J. P. Holtzhausen, "Insulator Pollution and Wetting Processes at a Severe Coastal Site", *13th International Symposium on High Voltage Engineering (ISH)*, Delft, Netherlands, August 2003.

17. P. J. Pieterse, A. I. Elombo, G. N. J. Mouton, H. J. Vermeulen, J. P. Holtzhausen and W. L. Vosloo, "A Coastal Insulator Pollution Test Station for the Evaluation of the Relative Ageing Performance of Power Line Insulators under AC And DC Voltage", *17th International Symposium on High Voltage Engineering (ISH 2011)*, Hannover, Germany, August 2011.

18. *EPRI AC Transmission Line Reference Book – 200 kV and Above*, Third Edition. EPRI, Palo Alto, CA: 2005. 1011974.

19. IEC Standard 60815/3, *Selection and Dimensioning of High Voltage Insulators Intended for Use in Polluted Conditions – Part 3: Polymer Insulators for AC Systems*, Edition 1, 2008:10.

20. B. Pinnangudi, R. S. Gorur and A. J. Kroese, "Quantification of Corona Discharges on Non-ceramic Insulators", *IEEE Transactions on Dielectrics and Electrical Insulation*, Vol. 12, No. 3, pg. 513 – 523, June 2005.

21. *Technical Brochure on Corocam Mark I – Night UV Camera*, [Online], UVIRCO Technologies (Pty) Ltd, Pretoria, South Africa, April 2010.

22. *Corocam Mark I System Specifications*, Revision 7, UVIRCO Technologies (Pty) Ltd, Pretoria, South Africa, June 2003.

23. *Technical Brochure on Sony GV-HD700 Portable Recorder*, [Online], UVIRCO Technologies (Pty) Ltd, Pretoria, South Africa, April 2010.

24. STRI Guide 5, *Visual Identification of Deterioration & Damages on Suspension Composite Insulators*, STRI LAB, Ludvika, Sweden, April 2005.

25. STRI Guide 1, *Hydrophobicity Classification*, STRI LAB, Ludvika, Sweden, 1992.

26. CIGRE Work Group B2.03, *Guide for the Establishment of Naturally Polluted Insulator Testing Stations*, October 2007.

27. IEC Standard 60815/1, *Selection and Dimensioning of High Voltage Insulators Intended for Use in Polluted Conditions – Part 1: Definitions, Information and General Principles*, Edition 1, 2008:10.

28. STRI Guide 5, *Composite Insulator Status Program: Field Inspection of Composite Line Insulators*, STRI LAB, Ludvika, Sweden, April 2005.

29. A.I. Elombo, G. N. J. Mouton, H. J. Vermeulen, J. P. Holtzhausen and W. L. Vosloo, "Evaluation of the Relative Ageing Performance of Power Line Insulators Under AC And DC Voltage in a Coastal Pollution Environment: Planning And Early Results", *Southern African Universities Power Engineering Conference*, Cape Town, South Africa, July 2011.

30. N. Bashir and H. Ahmad, "Ageing of Transmission Line Insulators: The Past, Present and Future", *2nd IEEE International Conference on Power and Energy (PECon 08)*, Johor Baharu, Malaysia, December 2008.

31. N. Vasudev, P.V. Vasudevan Nambudiri ,V. Muralidhara, B. Ramachandra and K.N. Ravi, "A Detailed Study on the Quality Assessment of Insulators Subjected to DC Voltages", *Proceedings of the 9th International Conference on Properties and Applications of Dielectric Materials*, Harbin, China, July 2009.

32. Y. X. Zhou, X. Xu, Q. Nie, X. D. Liang and Z. C. Guan, "Bird Streamer Caused Flashover in EHV Transmission Line", *IEEE Transactions on Dielectrics and Electrical Insulation*, Vol. 16, No. 1, Pg. 69 – 76, February 2009.

33. X. Zhang and S. M. Rowland, "Modeling of Dry-band Discharge Events on Insulation Surfaces", *IEEE International Symposium on Electrical Insulation (ISEI)*, San Diego, CA, June 2010.

34. J. M. Seifert, W. Petrusch and H. Janssen, “A Comparison of the Pollution Performance of Long Rod and Disc Type HVDC Insulators”, *IEEE Transactions on Dielectrics and Electrical Insulation*, Vol. 14, No. 1, Pg. 125 – 129, February 2007.

35. G. Heger, H. J. Vermeulen, J. P. Holtzhausen and W. L. Vosloo, “A Comparative Study of Insulator Materials Exposed to High Voltage AC and DC Surface Discharges”, *IEEE Transactions on Dielectrics and Electrical Insulation*, Vol. 17, No. 2, Pg. 513 – 520, April 2010.

36. L. Musaba, “The Southern African Power Pool (SAPP): Overview and Interconnections”, *International conference and exhibition on energy and power,* Harare, Zimbabwe, September 2011.

37. A. Hammad, S. Boshoff, W. C. Van der Merwe, C. J. D.Van Dyk, W. S. Otto and U. H. E. Kleyenstüber, "SVC for Mitigating 50 Hz Resonance of a Long 400 kV ac Interconnection", *CIGRE Symposium,* Singapore, 1999.

38. *Caprivi Link Interconnector: A Step Further in HVDC Light Technology*, ABB Group, IEEE/PES, Calgary, July 2009

39. H. Wang and M. A. Redfern, "The Advantages and Disadvantages of using HVDC to Interconnect AC Networks", *The 45th International Universities' Power Engineering Conference (UPEC 2010),* Cardiff, Wales, August 31st - September 3rd 2010.

40. H. Wang and M. A. Redfern, "Enhancing AC Networks with HVDC Interconnections", *2010 China International Conference on Electricity Distribution (CICED),* Nanjing, September 2010.

41. T. G. Magg, H. D. Mutschler, S. Nyberg, J. Wasborg, H. Thunehed, B. Sandberg, "Caprivi Link HVDC Interconnector: Site selection, geophysical investigations, interference impacts and design of the earth electrodes", *B4-302-2010,* CIGRE 2010.

42. L. A. Koshcheev, "Environmental Characteristics of HVDC Overhead Transmission Lines", *3rd Workshop on Power Grid Interconnection in Northeast Asia,* Vladivostok, Russia, September 30th - October 3rd 2003.

43. J. P. Holtzhausen, P. J. Pieterse, H. J. Vermeulen and S. Limbo, " Insulator Aging Tests with HVAC and HVDC Excitation using the Tracking Wheel Tester", *2010 International Conference on High Voltage Engineering and Application (ICHVE),* New Orleans, USA, October 2010.

44. SANS 60815-3, *Guide for the Selection of Insulators in Respect of Polluted Conditions*, Edition 1(draft), 2009.

45. I. Gutman, L. Carlshem and T. Kiiveri, "Statistical Approach for the Dimensioning of the 500 kV HVDC Line in Scandinavia", *15th International Symposium on High Voltage Engineering (ISH)*, Ljubljana, Slovenia, August 2007.

46. CIGRE Work Group C4.303, *Polluted Insulators: Guidelines for Selection and Dimensioning*, Part 2: The D.C. Case, March 2011.

47. J. P. Reynders, I. R. Jandrell and S. M. Reynders, "Review of Aging and Recovery of Silicone Rubber Insulation for Outdoor Use", *IEEE Transactions on Dielectrics and Electrical Insulation*, Vol. 6, No. 5, Pg. 620 – 631, October 1999.

48. K. L. Chrzan and F. Moro, "Concentrated Discharges and Dry Bands on Polluted Outdoor Insulators", *IEEE Transactions on Dielectrics Power Delivery*, Vol. 22, No. 1, Pg. 466 – 471, January 2007.

APPENDICES

A. APPENDIX A: Samples of record sheets for surface condition inspections, wettability (hydrophobicity) classification tests and electrical discharge activity observations

A.1 Surface condition inspection record sheet

Table A-1: Record sheet for surface condition inspections

Surface Condition Inspection Sheet			
Date:		**Time:**	
Identity:			
A (Land, East)	**B (Sea, West)**	**C (UV, North)**	**D (South)**
P			
1S	1S	1S	1S
1T	1T	1T	1T
1B	1B	1B	1B
2S	2S	2S	2S
2T	2T	2T	2T
2B	2B	2B	2B
3S	3S	3S	3S
3T	3T	3T	3T
3B	3B	3B	3B
4S	4S	4S	4S
4T	4T	4T	4T
4B	4B	4B	4B
5S	5S	5S	5S
5T	5T	5T	5T
5B	5B	5B	5B
6S	6S	6S	6S
6T	6T	6T	6T
6B	6B	6B	6B
7S	7S	7S	7S
P - Photo file name, 1 - Live side, 7 - Ground side, S - Sheath, B - Shed Bottom, T - Shed Top			

A.2 Wettability (hydrophobicity) classification sheet

Table A-2: Record sheet for wettability classification tests

Wettability (Hydrophobicity) Classification Sheet

Date:	
Time:	
Date of Installation:	

Weather at time of measurement	
Temperature [deg C]:	
Wind speed [m/s]:	
Humidity:	

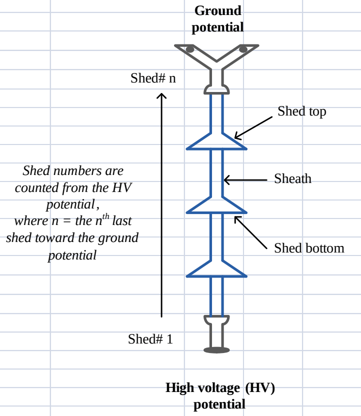

Comments

Hydrophobicity Classification (HC) Measurements						
Identity:						
Shed No	**Position**					
	Side of insulator: Sea			**Side of insulator: Land**		
	Top	**Bottom**	**Sheath**	**Top**	**Bottom**	**Sheath**
1						
2						
3						
4						
5						
6						
7						

Hydrophobicity Classification (HC) Measurements						
Identity:						
Shed No	**Position**					
	Side of insulator: Sea			**Side of insulator: Land**		
	Top	**Bottom**	**Sheath**	**Top**	**Bottom**	**Sheath**
1						
2						
3						
4						
5						
6						
7						

Hydrophobicity Classification (HC) Measurements						
Identity:						
Shed No	**Position**					
	Side of insulator: Sea			**Side of insulator: Land**		
	Top	**Bottom**	**Sheath**	**Top**	**Bottom**	**Sheath**
1						
2						
3						
4						
5						
6						
7						

Hydrophobicity Classification (HC) Measurements						
Identity:						
Shed No	**Position**					
	Side of insulator: Sea			**Side of insulator: Land**		
	Top	**Bottom**	**Sheath**	**Top**	**Bottom**	**Sheath**
1						
2						
3						
4						
5						
6						
7						

Hydrophobicity Classification (HC) Measurements						
Identity:						
Shed No	**Position**					
	Side of insulator: Sea			**Side of insulator: Land**		
	Top	**Bottom**	**Sheath**	**Top**	**Bottom**	**Sheath**
1						
2						
3						
4						
5						
6						
7						

A.3 Electrical discharge observation record sheets

A.3.1 Corocam Mark I

Table A-3: Record sheet for electrical discharge activity observations: Corocam Mark I

Video Tape #	COROCAM MARK I VIDEO TAPE RECORDING														
	Excitation Voltage Type *(tick the applicable)*:			AC	DC+	DC-	Observation Point		Tape Position		Starting Time	Date	Comments	Day	Week
	HTV-SR 84	*HTV-SR 72*	*HTV-SR 56*	*HTV-SR 44*	*HTV-SR 29*	*Glass disc 42*	*Land Side*	*Sea Side*	*From*	*To*					

A.3.2 0-lux Sony Camcorder

Table A-4: Record sheet for electrical discharge activity observations: 0-lux Sony Camcorder

0-LUX SONY CAMCORDER VIDEO RECORDING													
Excitation Voltage Type *(tick the applicable)*:			AC	DC+	DC-	Observation Point		Video File Name	Starting Time	Date	Comments	Day	Week
HTV-SR 84	*HTV-SR 72*	*HTV-SR 56*	*HTV-SR 44*	*HTV-SR 29*	*Glass disc 42*	*Land Side*	*Sea Side*						

B. APPENDIX B: The monthly climatic conditions that were recorded at KIPTS during the entire test period

B.1 Overview

This appendix gives an overview of the monthly meteorological data as recorded at KIPTS. This data was obtained from the continuous measurements performed with the use of weather sensors as explained in Chapter 3, section 3.5 . The online leakage current analyzer was used for data logging purposes.

Weather data is presented for the respective months of the entire test period, considering the time-of-day profiles of the measured parameters. The considered weather parameters include rainfall, relative humidity, ambient and dewpoint temperatures, wind speed and direction as well as UV-B radiation. The average values of these parameters were therefore used to draw the time-of-day weather profiles.

Please refer to section 5.2.1 in Chapter 5 for detailed discussions on weather conditions at KIPTS.

B.2 Rainfall profile for the first six months of the test period

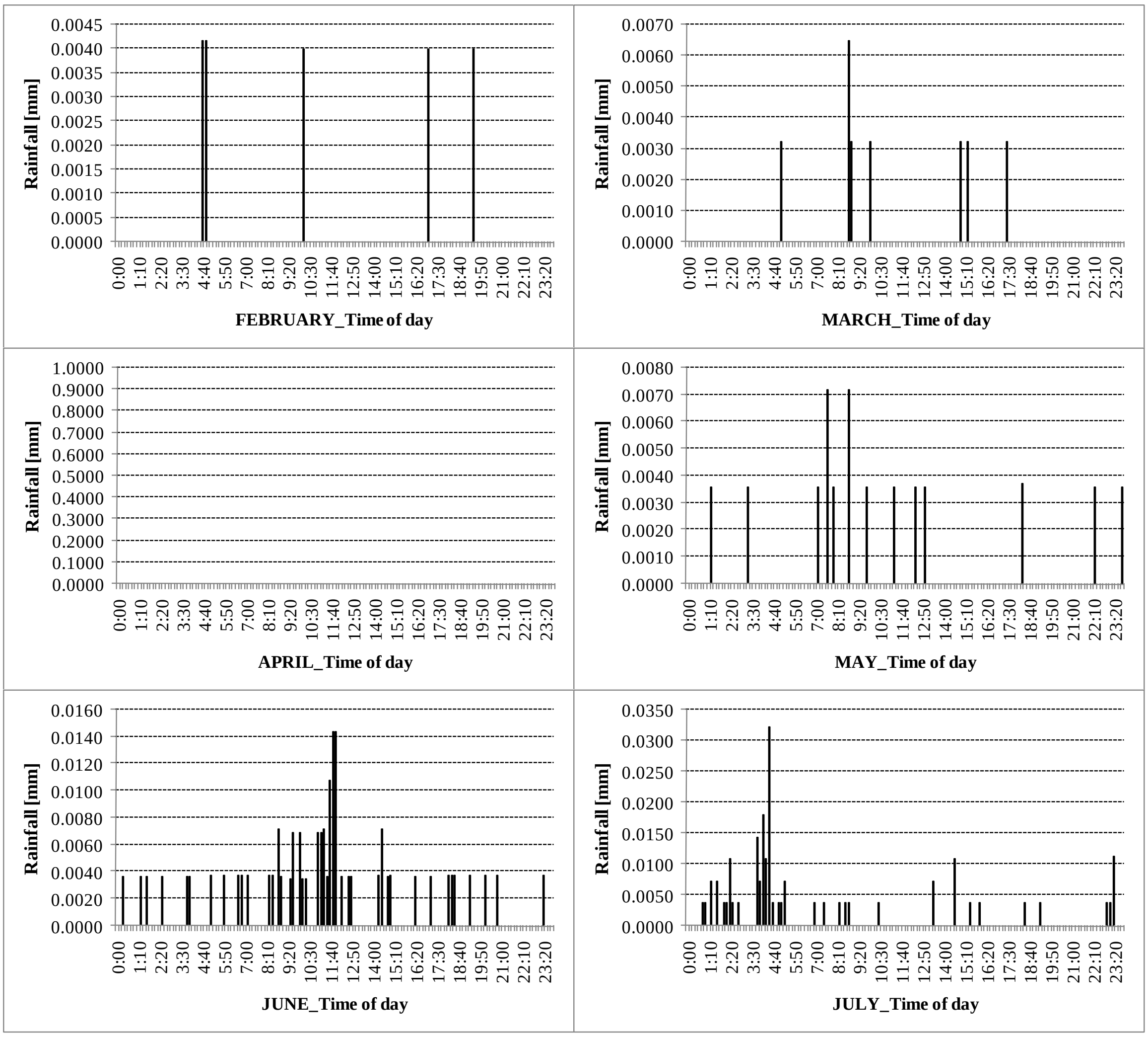

Figure B-1: Profile of the time-of-day average rainfall for the entire test period, given for the respective months

B.3 Relative humidity profile for the first six months of the test period

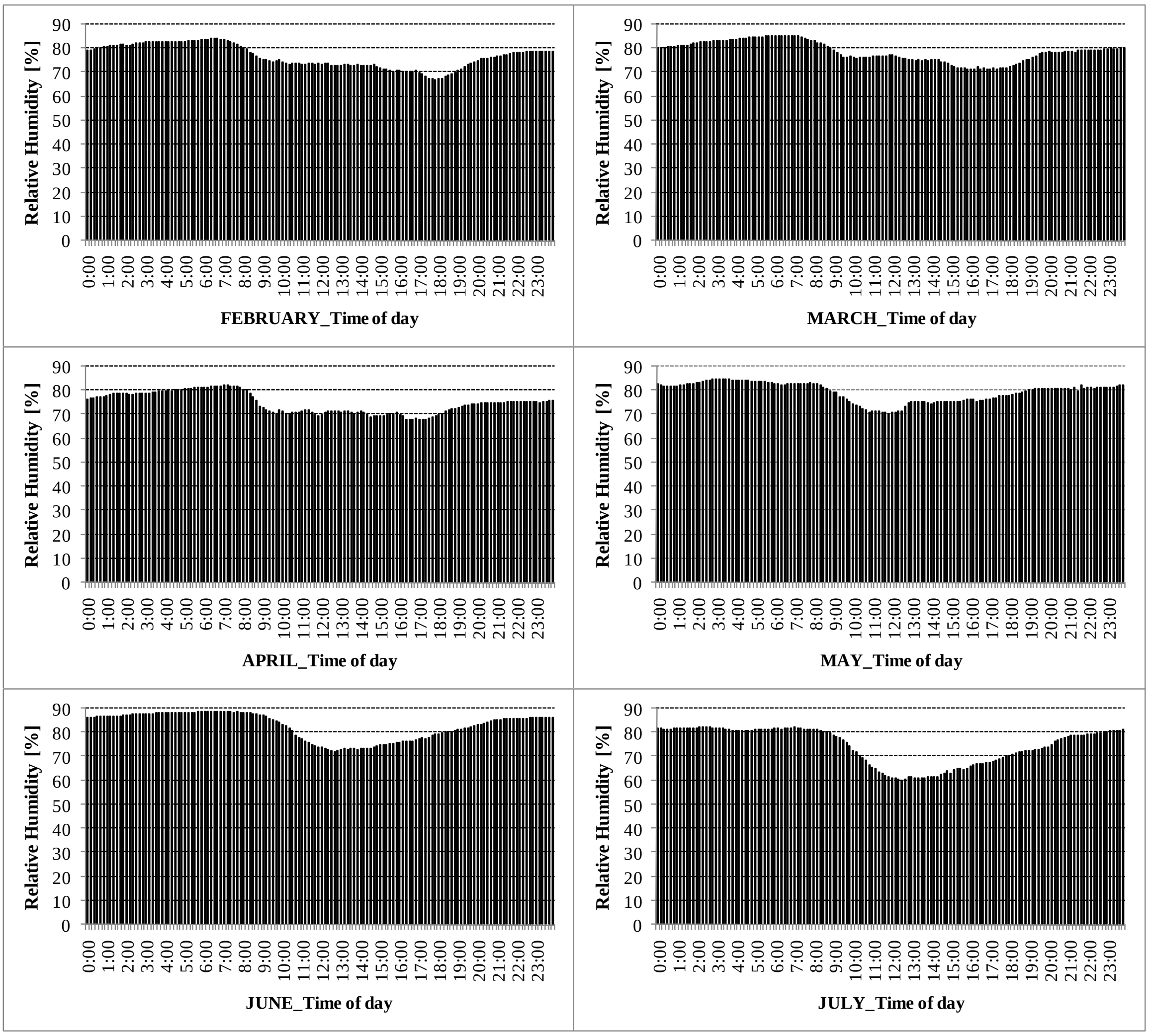

Figure B-2: Profile of the time-of-day average relative humidity for the entire test period, given for the respective months

B.4 Ambient temperature profile for the first six months of the test period

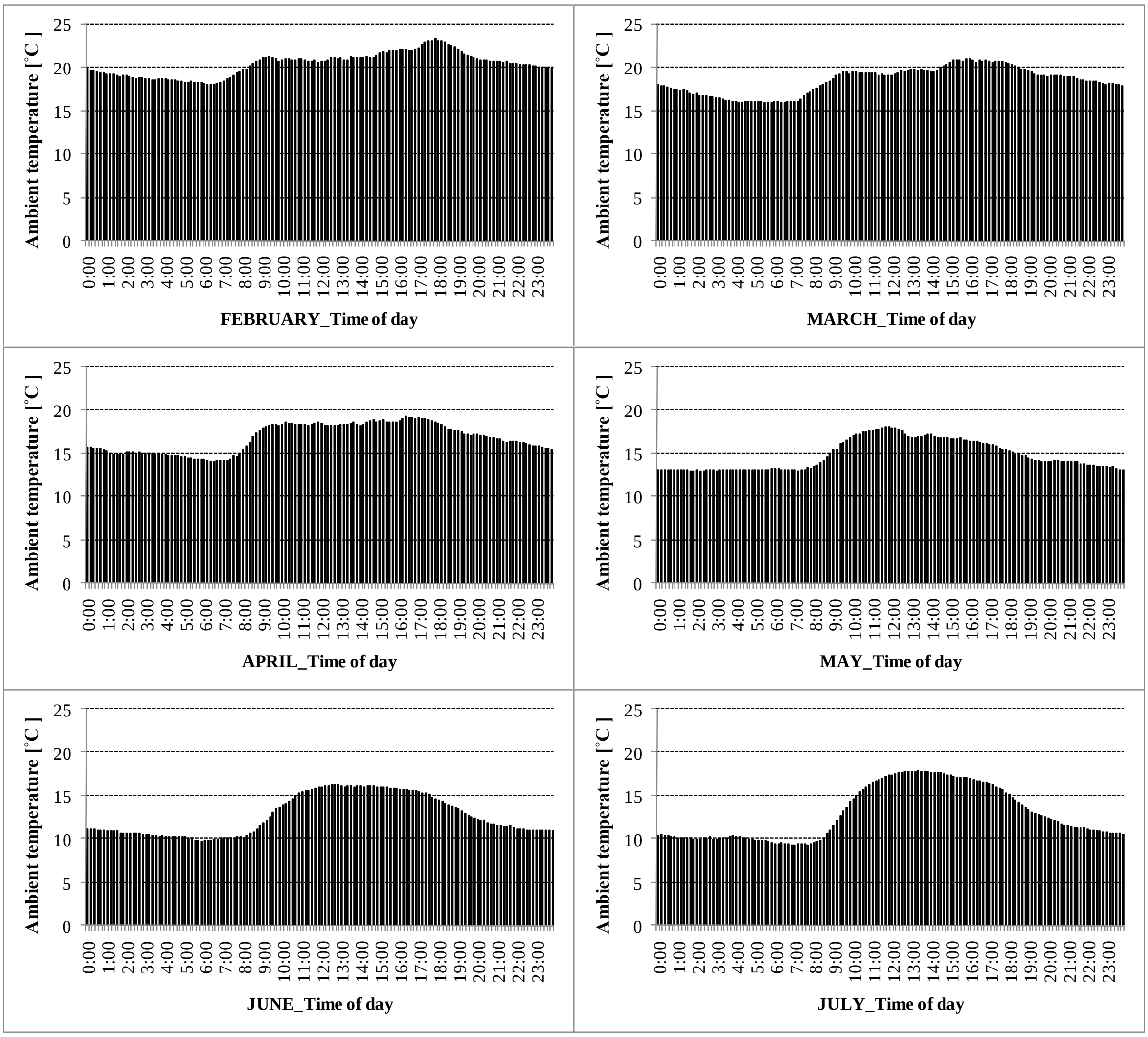

Figure B-3: Profile of the time-of-day average ambient temperature for the entire test period, given for the respective months

B.5 Wind speed and direction profiles for the first six months of the test period

B.5.1 Wind speed profile

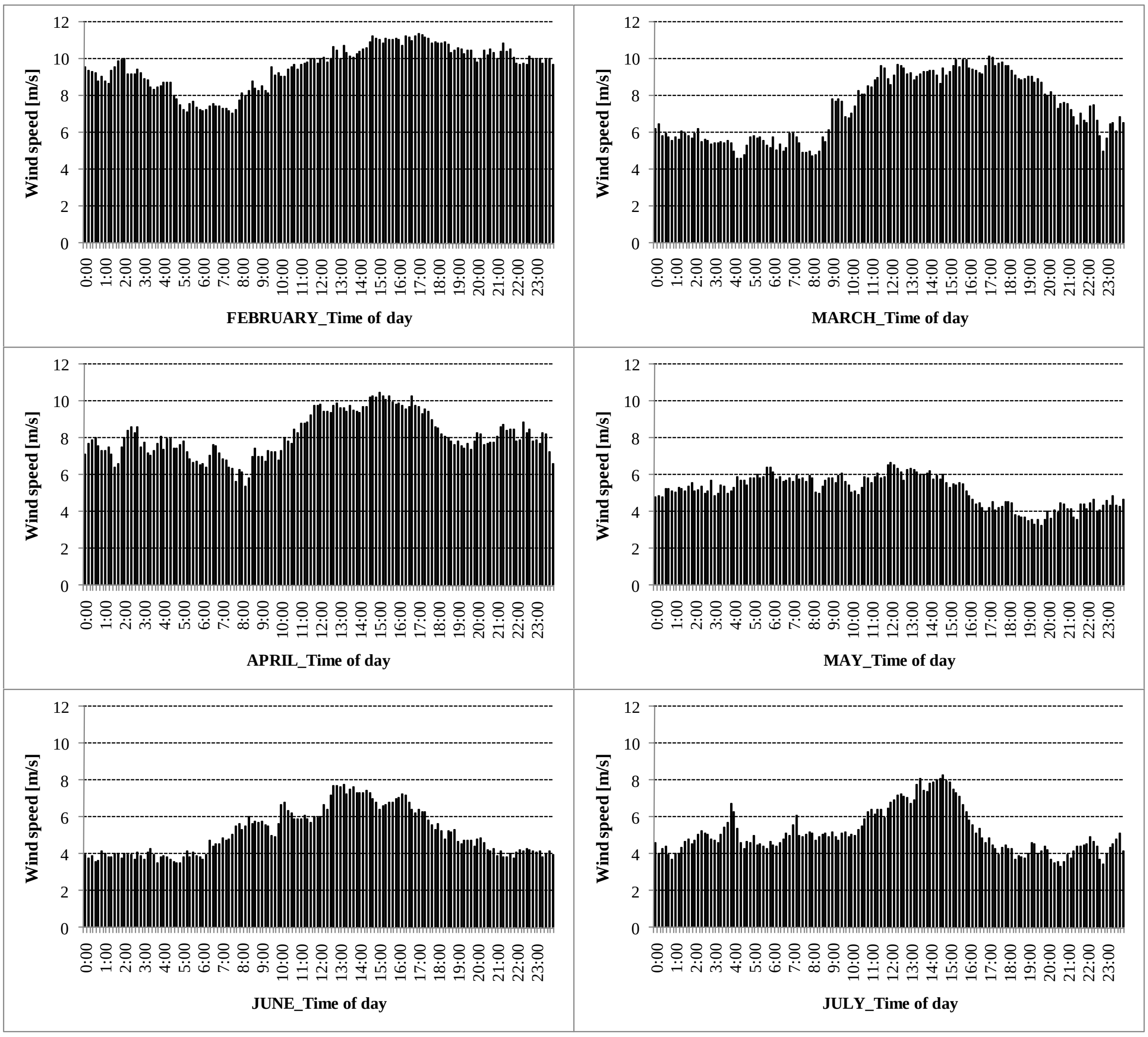

Figure B-4: Profile of the time-of-day average wind speed for the entire test period, given for the respective months

B.5.2 Wind direction profile

B.5.2.1 *Introduction*

Please note that the wind direction profile, as shown in Figure B-6, has been given in terms of degrees. It is therefore advised to refer to Figure B-5 in order to interpret the quoted degrees into the conventional compass directions.

B.5.2.2 *Conventional compass directions*

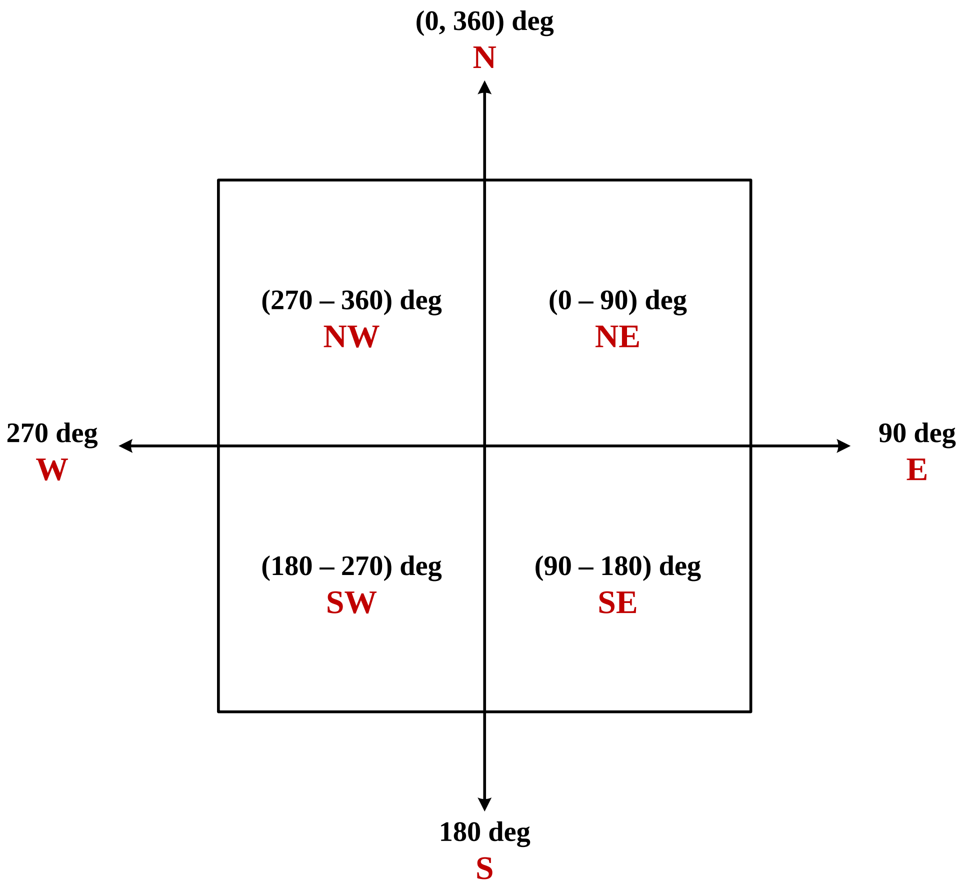

Figure B-5: Compass directions in degrees

B.5.2.3 *The actual wind direction profile in degrees*

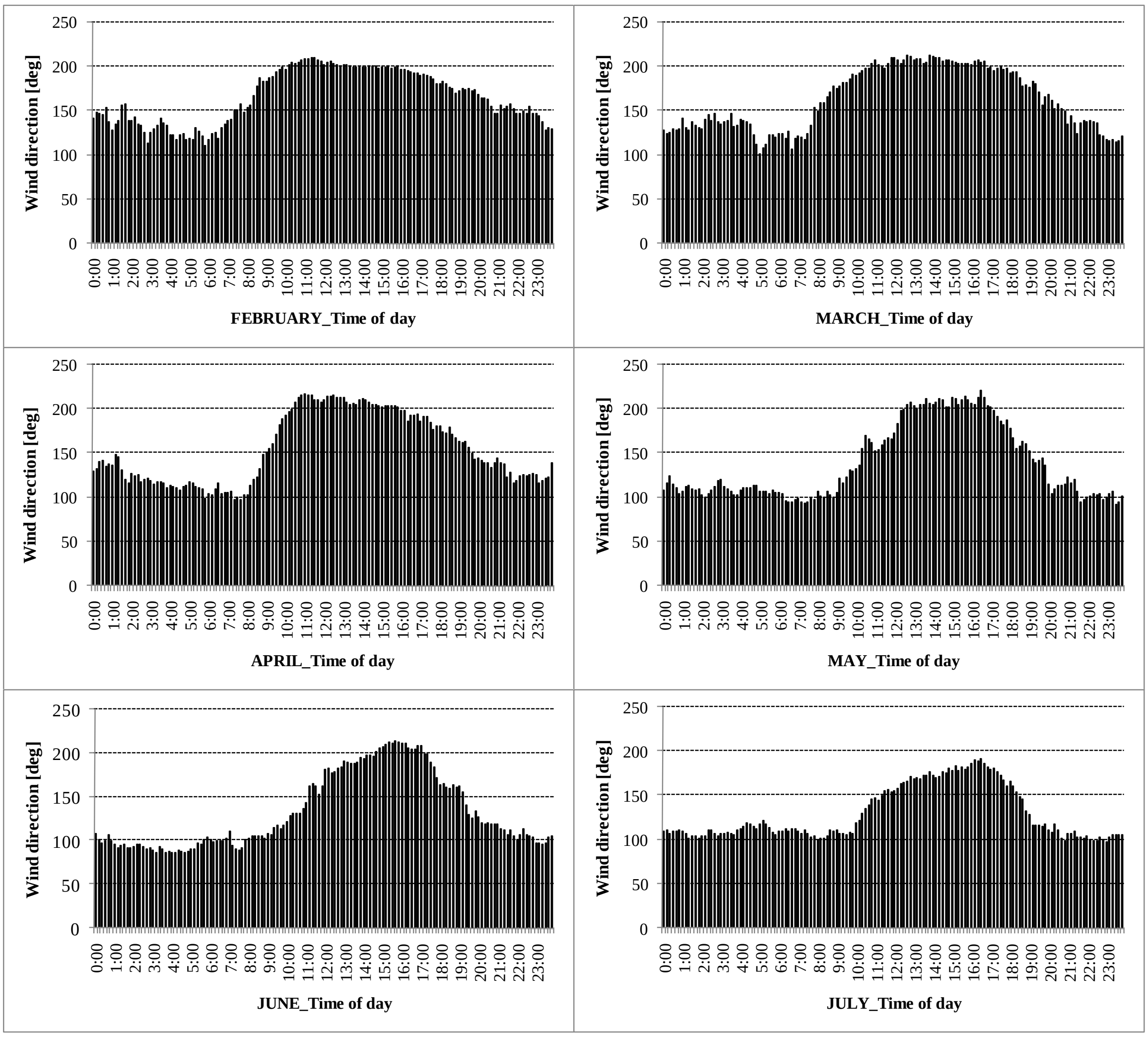

Figure B-6: Profile of the time-of-day average wind direction for the entire test period, given for the respective months *(please refer to Figure B-5 for corresponding compass directions)*

B.6 UV-B radiation profile for the first six months of the test period

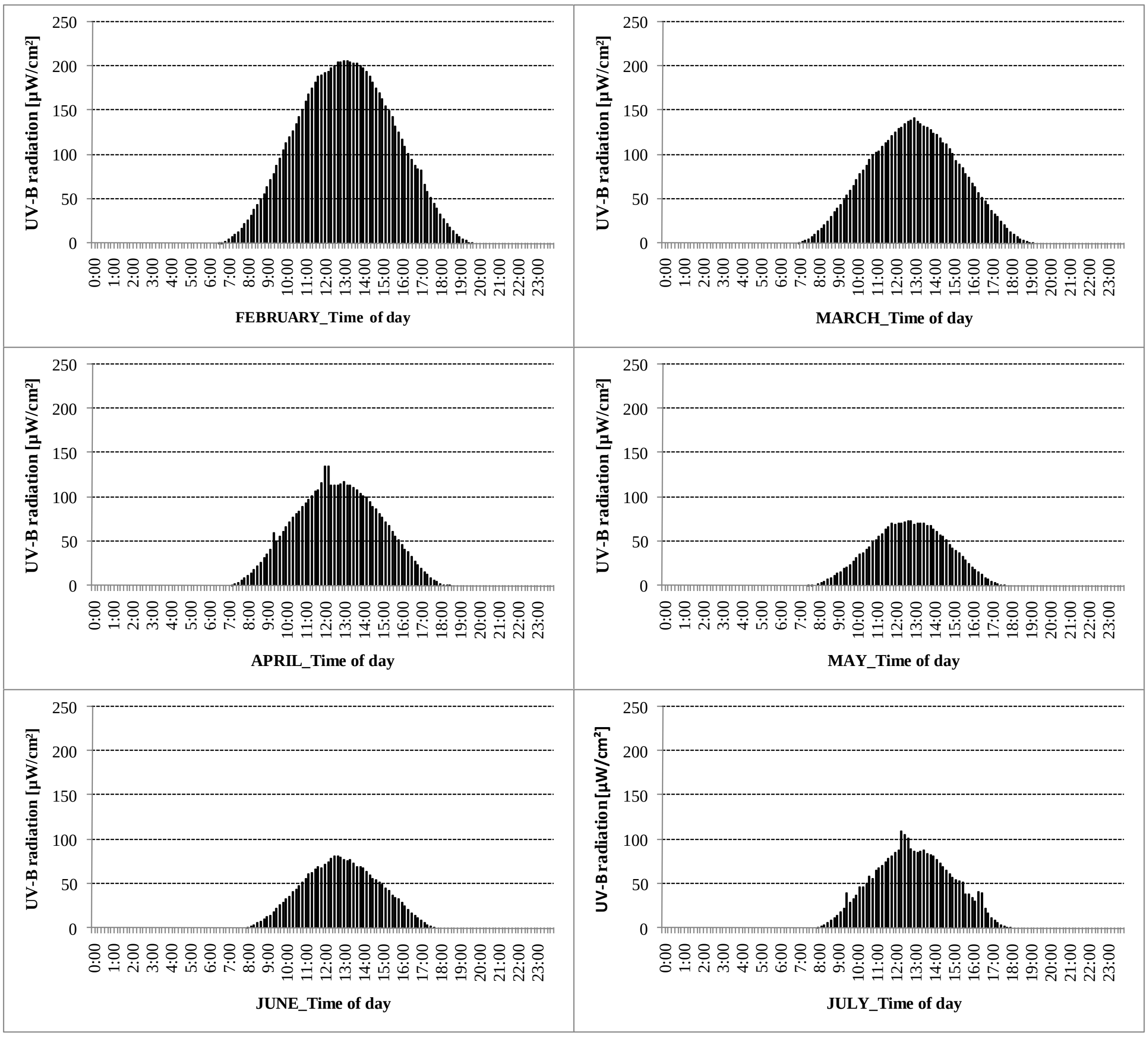

Figure B-7: Profile of the time-of-day average UV-B radiation for the entire test period, given for the respective months

C. APPENDIX C: Leakage current performance for individual test insulators

C.1 Overview

This appendix presents a summary of the results obtained for the leakage current performance of all test insulators. A statistical approach was used, which renders the recorded leakage current values into selected nine bin categories. The categories that were considered are as follows (recorded in mA): [0-2], [2-5], [5-10], [10-20], [20-50], [50-100], [100-200], [200-500] and [500-1000]. The first two categories were considered as the noise band and they are highlighted in gray on the tables presented in sections C.2 to C.7. Notice that the results are presented per time of day, given at ten minute intervals.

An overview of the average and maximum values of the leakage current that were recorded over the entire test period is also presented, considering only four snapshots in a day. Thus, the average and maximum values are presented for midnight (24h00), sunrise (06h00), midday (12h00) and sunset (18h00). Detailed time-of-day average and maximum values of the recorded leakage current are presented graphically in sections 5.3.2.2 to 5.3.2.7. Please refer to section 5.3 for all discussions on leakage current performance of the test insulators.

C.2 Leakage current performance for high temperature vulcanized, silicone rubber insulators with a unified specific creepage length of 84 mm/kV – HTV-SR 84

This section summarizes all leakage current results for the HTV-SR 84 insulators installed on AC, DC+ and DC-. Note that all results are presented in a comparative manner between the three excitation voltage types. Refer to section 5.3.2.2 for a detailed discussion on these results.

C.2.1 Leakage current bin count analysis

C.2.1.1 *Monthly leakage current bin counts*

Table C-5: Monthly bin counts of absolute peak leakage currents for the HTV-SR 84 insulators

		Monthly leakage current bin counts: HTV-SR 84																										
		**[0 - 2] mA			**[2 - 5] mA			[5 - 10] mA			[10 - 20] mA			[20 - 50] mA			[50 - 100] mA			[100 - 200] mA			[200 - 500] mA			[500 - 1000] mA		
		AC	*DC+*	*DC-*	*AC*	*DC+*	*DC-*	*AC*	*DC+*	*DC-*	*AC*	*DC+*	*DC-*	*AC*	*DC+*	*DC-*	*AC*	*DC+*	*DC-*	*AC*	*DC+*	*DC-*	*AC*	*DC+*	*DC-*	*AC*	*DC+*	*DC-*
SUMMER	February	3131	1784	3463	358	1352	103	83	395	30	26	29	0	0	38	0	0	0	0	0	0	0	0	0	0	0	0	0
	March	3152	2173	3344	462	1347	688	476	376	414	225	434	15	148	132	0	0	0	0	0	0	0	0	0	0	0	0	0
	April	3409	3064	3709	378	1088	385	374	54	151	86	76	73	72	36	0	0	0	0	0	0	0	0	0	0	0	0	0
	TOTAL	9692	7021	10516	1198	3787	1176	933	825	595	337	539	88	220	206	0	0	0	0	0	0	0	0	0	0	0	0	0
WINTER	May	4012	1677	4391	344	2772	68	88	14	4	20	0	0	0	0	0	0	0	0	0	0	0	0	0	0	0	0	0
	June	3793	2585	4200	250	1735	116	118	0	4	126	0	0	32	0	0	1	0	0	0	0	0	0	0	0	0	0	0
	July	4403	431	4459	52	4032	4	8	0	0	0	0	0	0	0	0	0	0	0	0	0	0	0	0	0	0	0	0
	TOTAL	12208	4693	13050	646	8539	188	214	14	8	146	0	0	32	0	0	1	0	0	0	0	0	0	0	0	0	0	0
Entire test period total counts		**21900**	**11714**	**23566**	**1844**	**12326**	**1364**	**1147**	**839**	**603**	**483**	**539**	**88**	**252**	**206**	**0**	**1**	**0**	**0**	**0**	**0**	**0**	**0**	**0**	**0**	**0**	**0**	**0**

** Noise band categories

C.2.1.2 *Total bin counts for the entire test period*

Table C-6: Comparisons between the three excitation voltages, HTV-SR 84

	Entire Test Period Bin Counts		
Bin Categories [mA]	*HTV-SR 84 AC*	*HTV-SR 84 DC+*	*HTV-SR 84 DC-*
****[0 - 2]**	21900	11714	23566
****[2 - 5]**	1844	12326	1364
[5 - 10]	1147	839	603
[10 - 20]	483	539	88
[20 - 50]	252	206	0
[50 - 100]	1	0	0
[100 - 200]	0	0	0
[200 - 500]	0	0	0
[500 - 1000]	0	0	0

** Noise band categories

NB: Graphical representation of the time of day leakage current profile, per bin category, is depicted in Figure C-8, Figure C-9 and Figure C-10.

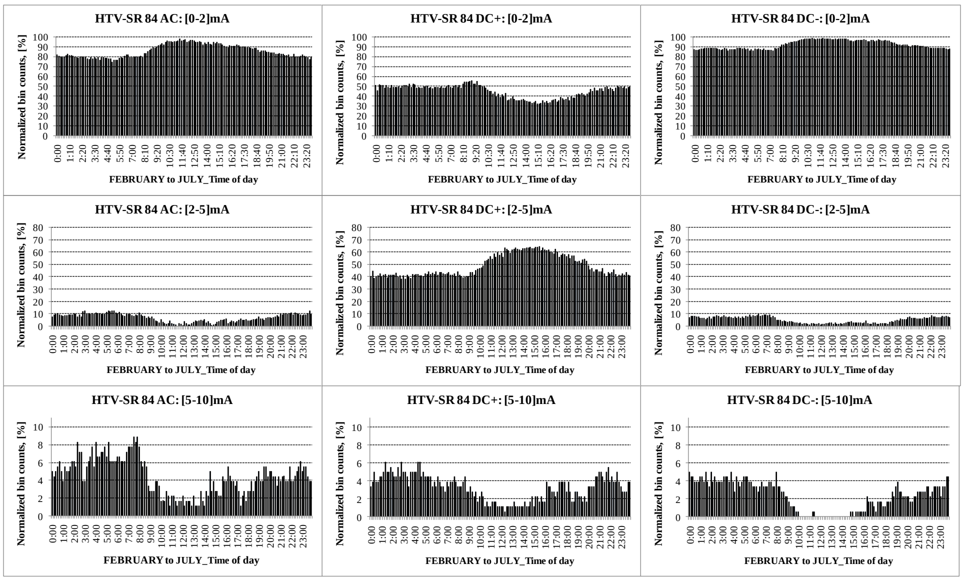

Figure C-8: Time of day leakage current bin counts for [0-10] mA, HTV-SR 84

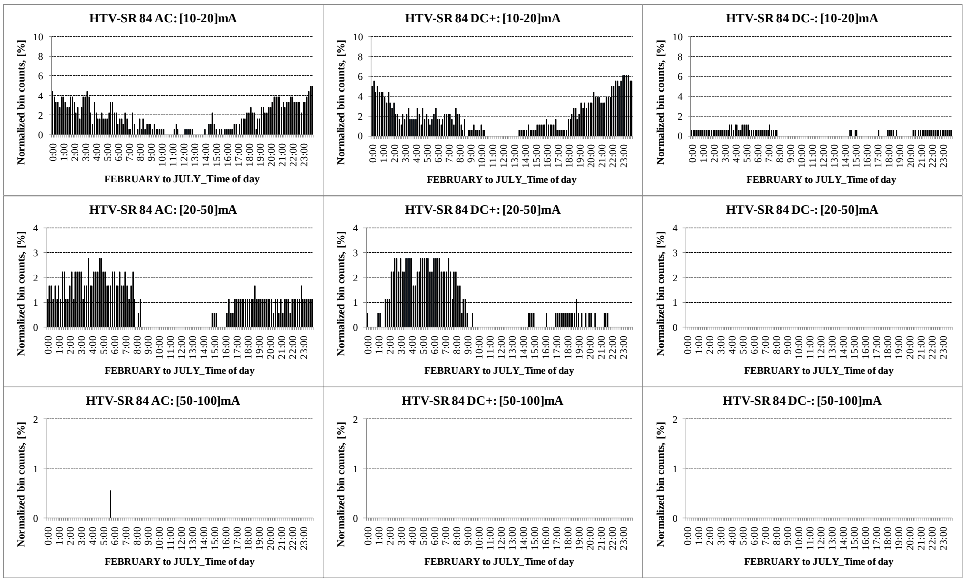

Figure C-9: Time of day leakage current bin counts for [10-100] mA, HTV-SR 84

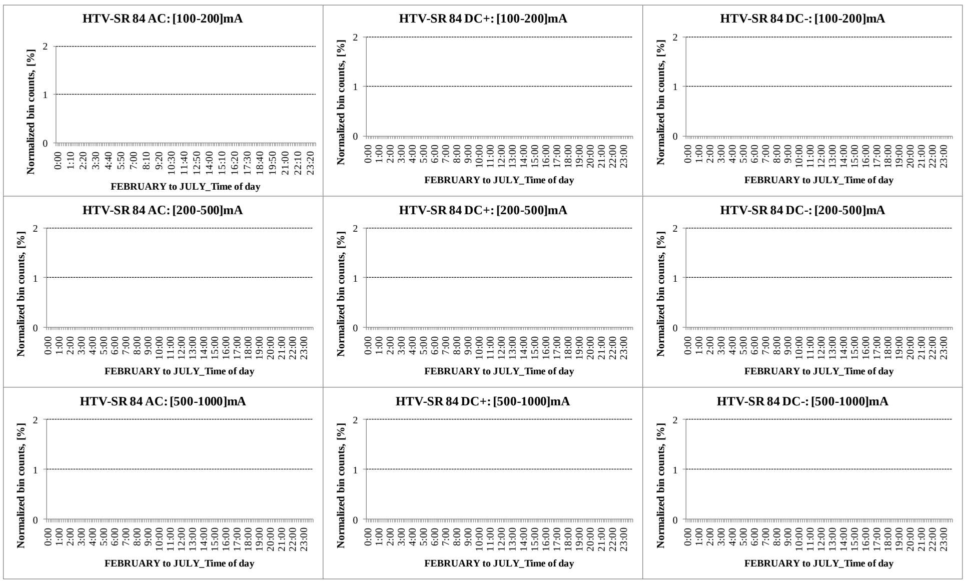

Figure C-10: Time of day leakage current bin counts for [100-1000] mA, HTV-SR 84

C.2.2 Average and maximum values of the recorded leakage current

Table C-7 gives a snapshot of the time of day average and maximum values of the actual leakage current. Elaborate graphs of the time of day average and maximum values of leakage current are presented and discussed in section 5.3.2.2.

Table C-7: The time-of-day average and maximum absolute peak leakage currents

		Absolute Peak Leakage Current [mA]		
		HTV-SR 84 AC	*HTV-SR 84 DC+*	*HTV-SR 84 DC-*
Midnight (24h00)	*Average*	2.37	2.50	1.31
	Maximum	30.12	21.45	12.50
Sunrise (06h00)	*Average*	2.31	2.61	1.24
	Maximum	35.73	29.18	12.50
Midday (12h00)	*Average*	1.18	1.76	0.80
	Maximum	8.40	6.31	4.17
Sunset (18h00)	*Average*	1.83	2.12	0.92
	Maximum	31.52	21.80	10.17
Entire test period	*Maximum*	55.32	34.10	16.84
	Time recorded	24/6 5:40	22/3 8:30	29/3 3:30

C.3 Leakage current performance for high temperature vulcanized, silicone rubber insulators with a unified specific creepage length of 72 mm/kV – HTV-SR 72

This section summarizes all leakage current results for the HTV-SR 72 insulators installed on AC, DC+ and DC-. Note that all results are presented in a comparative manner between the three excitation voltage types. Refer to section 5.3.2.3 for a detailed discussion on these results. It should be mentioned that the sensor associated with HTV-SR 72 DC- was found to be faulty and this has been specifically indicated on the results below.

C.3.1 Leakage current bin count analysis

C.3.1.1 *Monthly leakage current bin counts*

Table C-8: Monthly bin counts of absolute peak leakage currents for the HTV-SR 72 insulators

		Monthly leakage current bin counts: HTV-SR 72																										
		**[0 - 2] mA			**[2 - 5] mA			[5 - 10] mA			[10 - 20] mA			[20 - 50] mA			[50 - 100] mA			[100 - 200] mA			[200 - 500] mA			[500 - 1000] mA		
		AC	*DC+*	**DC-*	*AC*	*DC+*	**DC-*	*AC*	*DC+*	**DC-*	*AC*	*DC+*	**DC-*	*AC*	*DC+*	**DC-*	*AC*	*DC+*	**DC-*	*AC*	*DC+*	**DC-*	*AC*	*DC+*	**DC-*	*AC*	*DC+*	**DC-*
SUMMER	**February**	3022	3027	-	395	238	-	92	332	-	82	0	-	7	0	-	0	0	-	0	0	-	0	0	-	0	0	-
	March	2279	2316	-	550	881	-	563	585	-	660	508	-	411	171	-	0	1	-	0	0	-	0	0	-	0	0	-
	April	2883	2947	-	613	847	-	453	124	-	279	305	-	91	94	-	0	1	-	0	0	-	0	0	-	0	0	-
	TOTAL	8184	8290	-	1558	1966	-	1108	1041	-	1021	813	-	509	265	-	0	2	-	0	0	-	0	0	-	0	0	-
WINTER	**May**	3514	4016	-	678	345	-	185	66	-	74	34	-	13	2	-	0	0	-	0	0	-	0	0	-	0	0	-
	June	3826	3897	-	187	355	-	122	65	-	127	3	-	57	0	-	1	0	-	0	0	-	0	0	-	0	0	-
	July	4423	4403	-	32	60	-	8	0	-	0	0	-	0	0	-	0	0	-	0	0	-	0	0	-	0	0	-
	TOTAL	11763	12316	-	897	760	-	315	131	-	201	37	-	70	2	-	1	0	-	0	0	-	0	0	-	0	0	-
Entire test period total counts		**19947**	**20606**	**-**	**2455**	**2726**	**-**	**1423**	**1172**	**-**	**1222**	**850**	**-**	**579**	**267**	**-**	**1**	**2**	**-**	**0**	**0**	**-**	**0**	**0**	**-**	**0**	**0**	**-**

* Faulty sensor on HTV-SR 72 DC- (DC offsets)
** Noise band categories

C.3.1.2 *Total bin counts for the entire test period*

Table C-9: Comparisons between the three excitation voltages, HTV-SR 72

	Entire Test Period Bin Counts		
Bin Categories [mA]	*HTV-SR 72 AC*	*HTV-SR 72 DC+*	**HTV-SR 72 DC-*
****[0 - 2]**	19947	20606	-
****[2 - 5]**	2455	2726	-
[5 - 10]	1423	1172	-
[10 - 20]	1222	850	-
[20 - 50]	579	267	-
[50 - 100]	1	2	-
[100 - 200]	0	0	-
[200 - 500]	0	0	-
[500 - 1000]	0	0	-

* Faulty sensor on HTV-SR 72 DC- (DC offsets)
** Noise band categories

NB: Graphical representation of the time of day leakage current profile, per bin category, is depicted in Figure C-11, Figure C-12 and Figure C-13.

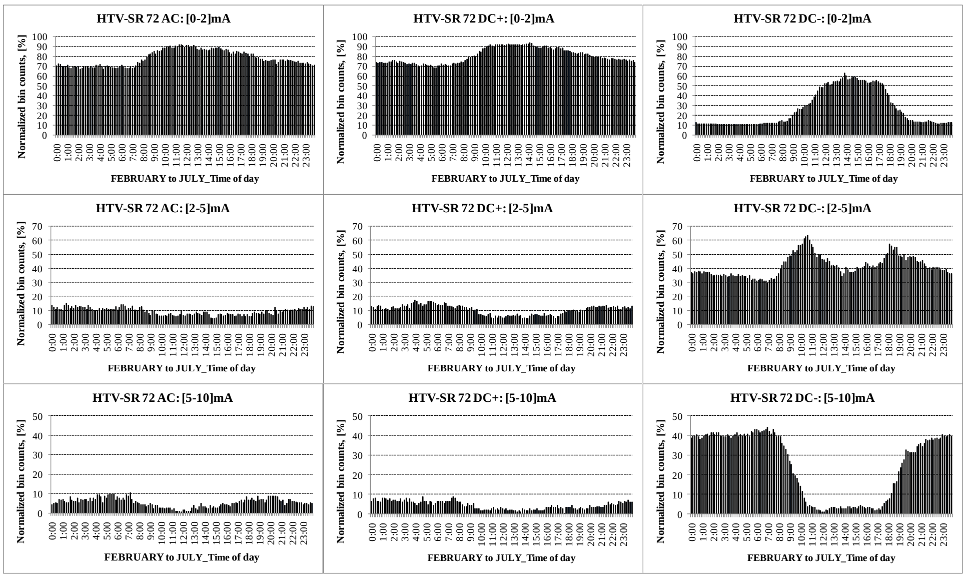

Figure C-11: Time of day leakage current bin counts for [0-10] mA, HTV-SR 72

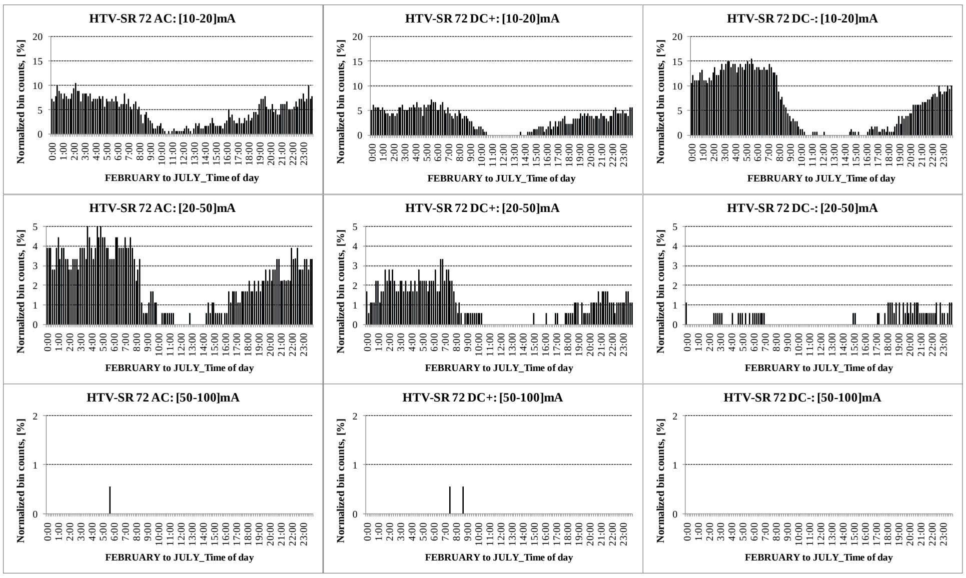

Figure C-12: Time of day leakage current bin counts for [10-100] mA, HTV-SR 72

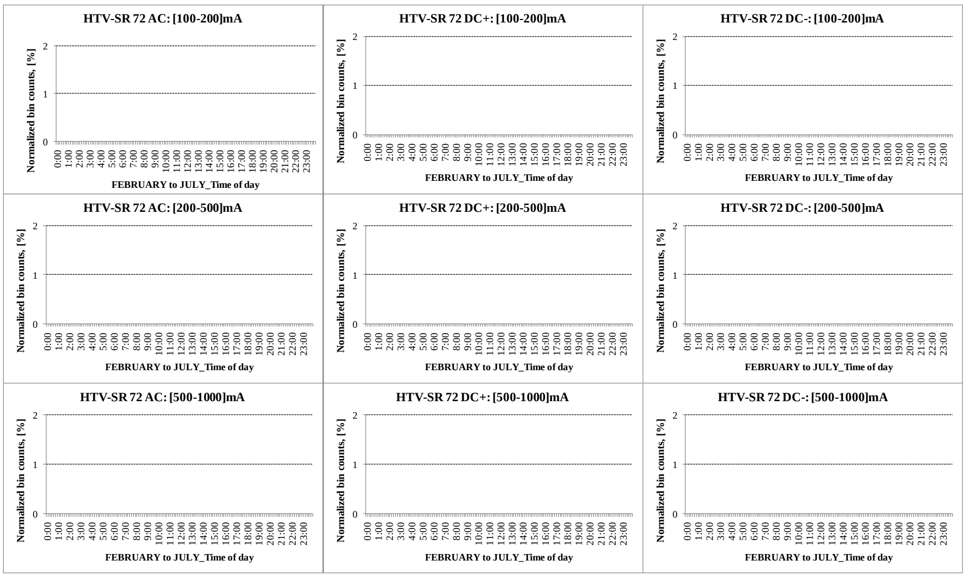

Figure C-13: Time of day leakage current bin counts for [100-1000] mA, HTV-SR 72

C.3.2 Average and maximum values of the recorded leakage current

Table C-10 gives a snapshot of the time of day average and maximum values of the actual leakage current. Elaborate graphs of the time of day average and maximum values of leakage current are presented and discussed in section 5.3.2.3.

Table C-10: The time-of-day average and maximum absolute peak leakage currents

		Absolute Peak Leakage Current [mA]		
		HTV-SR 72 AC	*HTV-SR 72 DC+*	*HTV-SR 72 DC-*
Midnight (24h00)	*Average*	2.71	2.42	4.68
	Maximum	35.01	27.35	21.97
Sunrise (06h00)	*Average*	2.30	2.54	4.94
	Maximum	25.91	34.28	20.22
Midday (12h00)	*Average*	0.95	1.21	1.70
	Maximum	12.96	7.34	9.66
Sunset (18h00)	*Average*	1.99	1.65	2.22
	Maximum	39.92	21.39	19.18
Entire test period	*Maximum*	52.21	52.60	24.75
	Time recorded	24/6 5:40	13/3 8:40	28/3 23:50

C.4 Leakage current performance for high temperature vulcanized, silicone rubber insulators with a unified specific creepage length of 56 mm/kV – HTV-SR 56

This section summarizes all leakage current results for the HTV-SR 56 insulators installed on AC, DC+ and DC-. Note that all results are presented in a comparative manner between the three excitation voltage types. Refer to section 5.3.2.4 for a detailed discussion on these results.

C.4.1 Leakage current bin count analysis

C.4.1.1 *Monthly leakage current bin counts*

Table C-11: Monthly bin counts of absolute peak leakage currents for the HTV-SR 56 insulators

		Monthly leakage current bin counts: HTV-SR 56																										
		**[0 - 2] mA			**[2 - 5] mA			[5 - 10] mA			[10 - 20] mA			[20 - 50] mA			[50 - 100] mA			[100 - 200] mA			[200 - 500] mA			[500 - 1000] mA		
		AC	*DC+*	*DC-*	*AC*	*DC+*	*DC-*	*AC*	*DC+*	*DC-*	*AC*	*DC+*	*DC-*	*AC*	*DC+*	*DC-*	*AC*	*DC+*	*DC-*	*AC*	*DC+*	*DC-*	*AC*	*DC+*	*DC-*	*AC*	*DC+*	*DC-*
SUMMER	February	2858	2738	3246	449	170	76	211	429	149	56	129	125	24	131	0	0	0	0	0	0	0	0	0	0	0	0	0
	March	2176	2418	2108	636	538	650	521	564	738	722	676	892	390	264	73	18	2	0	0	0	0	0	0	0	0	0	0
	April	2761	2829	2448	497	578	780	434	456	473	413	302	531	214	152	86	0	1	0	0	0	0	0	0	0	0	0	0
	TOTAL	7795	7985	7802	1582	1286	1506	1166	1449	1360	1191	1107	1548	628	547	159	18	3	0	0	0	0	0	0	0	0	0	0
WINTER	May	3704	3175	2519	503	1081	1800	176	139	137	65	59	7	16	9	0	0	0	0	0	0	0	0	0	0	0	0	0
	June	3453	2839	1783	375	1291	2472	246	176	61	135	13	4	105	1	0	6	0	0	0	0	0	0	0	0	0	0	0
	July	4326	4292	2631	120	154	1829	14	17	3	3	0	0	0	0	0	0	0	0	0	0	0	0	0	0	0	0	0
	TOTAL	11483	10306	6933	998	2526	6101	436	332	201	203	72	11	121	10	0	6	0	0	0	0	0	0	0	0	0	0	0
Entire test period total counts		**19278**	**18291**	**14735**	**2580**	**3812**	**7607**	**1602**	**1781**	**1561**	**1394**	**1179**	**1559**	**749**	**557**	**159**	**24**	**3**	**0**	**0**	**0**	**0**	**0**	**0**	**0**	**0**	**0**	**0**

** Noise band categories

C.4.1.2 *Total bin counts for the entire test period*

Table C-12: Comparisons between the three excitation voltages, HTV-SR 56

	Entire Test Period Bin Counts		
Bin Categories [mA]	*HTV-SR 56 AC*	*HTV-SR 56 DC+*	*HTV-SR 56 DC-*
****[0 - 2]**	19278	18291	14735
****[2 - 5]**	2580	3812	7607
[5 - 10]	1602	1781	1561
[10 - 20]	1394	1179	1559
[20 - 50]	749	557	159
[50 - 100]	24	3	0
[100 - 200]	0	0	0
[200 - 500]	0	0	0
[500 - 1000]	0	0	0

** Noise band categories

NB: Graphical representation of the time of day leakage current profile, per bin category, is depicted in Figure C-14, Figure C-15 and Figure C-16.

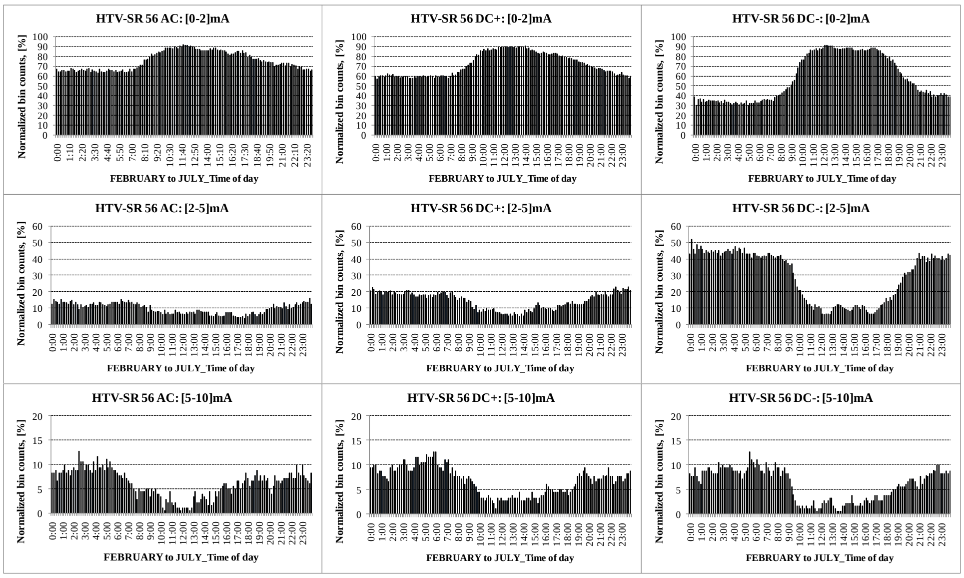

Figure C-14: Time of day leakage current bin counts for [0-10] mA, HTV-SR 56

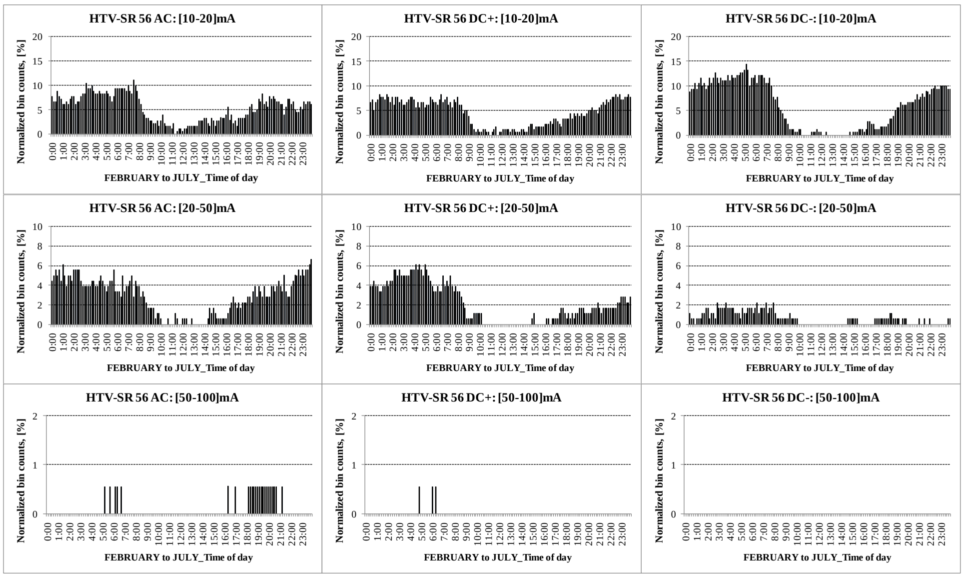

Figure C-15: Time of day leakage current bin counts for [10-100] mA, HTV-SR 56

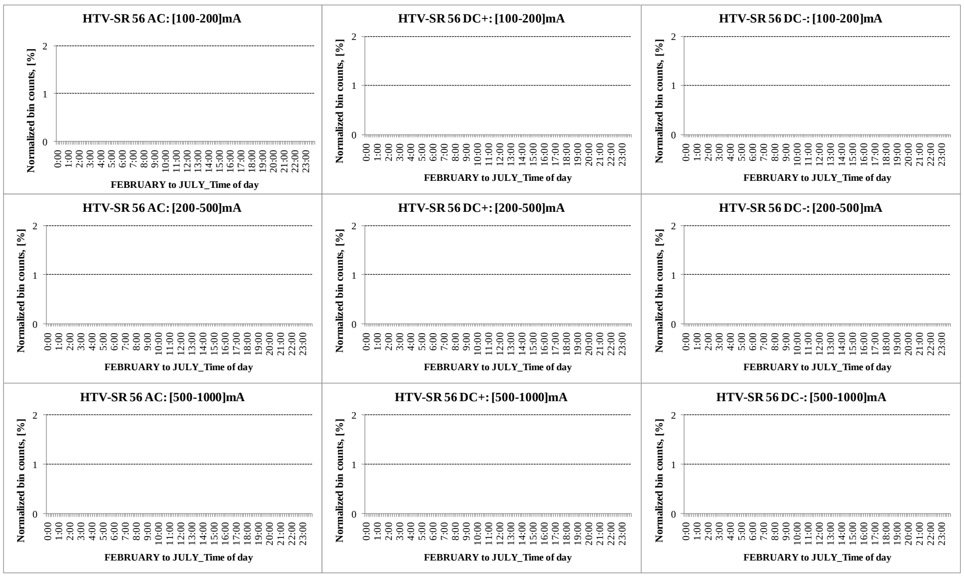

Figure C-16: Time of day leakage current bin counts for [100-1000] mA, HTV-SR 56

C.4.1.3 *Average and maximum values of the recorded leakage current*

Table C-13 gives a snapshot of the time of day average and maximum values of the actual leakage current. Elaborate graphs of the time of day average and maximum values of leakage current are presented and discussed in section 5.3.2.4.

Table C-13: The time-of-day average and maximum absolute peak leakage currents

		Absolute Peak Leakage Current [mA]		
		HTV-SR 56 AC	*HTV-SR 56 DC+*	*HTV-SR 56 DC-*
Midnight (24h00)	*Average*	3.30	3.71	2.82
	Maximum	36.12	42.56	22.14
Sunrise (06h00)	*Average*	3.07	3.88	3.28
	Maximum	32.95	51.35	25.94
Midday (12h00)	*Average*	1.08	1.28	1.24
	Maximum	20.33	10.18	10.50
Sunset (18h00)	*Average*	2.35	2.05	1.62
	Maximum	49.45	22.86	22.40
Entire test period	*Maximum*	64.49	51.70	31.50
	Time recorded	24/6 5:40	13/3 6:20	13/3 8:40

C.5 Leakage current performance for high temperature vulcanized, silicone rubber insulators with a unified specific creepage length of 44 mm/kV – HTV-SR 44

This section summarizes all leakage current results for the HTV-SR 44 insulators installed on AC, DC+ and DC-. Note that all results are presented in a comparative manner between the three excitation voltage types. Refer to section 5.3.2.5 for a detailed discussion on these results.

C.5.1 Leakage current bin count analysis

C.5.1.1 *Monthly leakage current bin counts*

Table C-14: Monthly bin counts of absolute peak leakage currents for the HTV-SR 44 insulators

		Monthly leakage current bin counts: HTV-SR 44																										
		**[0 - 2] mA			**[2 - 5] mA			[5 - 10] mA			[10 - 20] mA			[20 - 50] mA			[50 - 100] mA			[100 - 200] mA			[200 - 500] mA			[500 - 1000] mA		
		AC	*DC+*	*DC-*	*AC*	*DC+*	*DC-*	*AC*	*DC+*	*DC-*	*AC*	*DC+*	*DC-*	*AC*	*DC+*	*DC-*	*AC*	*DC+*	*DC-*	*AC*	*DC+*	*DC-*	*AC*	*DC+*	*DC-*	*AC*	*DC+*	*DC-*
SUMMER	**February**	2704	2827	2811	332	84	445	327	358	156	162	147	178	64	172	6	9	9	0	0	0	0	0	0	0	0	0	0
	March	2939	2808	2338	266	224	647	217	330	580	500	781	695	500	311	201	41	8	0	0	0	0	0	0	0	0	0	0
	April	3306	3226	2128	176	294	1602	331	291	293	230	196	235	246	285	60	30	26	0	0	0	0	0	0	0	0	0	0
	TOTAL	8949	8861	7277	774	602	2694	875	979	1029	892	1124	1108	810	768	267	80	43	0	0	0	0	0	0	0	0	0	0
WINTER	**May**	3459	3293	2126	331	527	2035	433	458	238	198	138	64	39	45	0	4	2	0	0	0	0	0	0	0	0	0	0
	June	3587	3496	3496	334	444	581	166	285	215	138	79	27	72	12	1	19	4	0	4	0	0	0	0	0	0	0	0
	July	4353	4342	4300	110	93	150	0	26	13	0	2	0	0	0	0	0	0	0	0	0	0	0	0	0	0	0	0
	TOTAL	11399	11131	9922	775	1064	2766	599	769	466	336	219	91	111	57	1	23	6	0	4	0	0	0	0	0	0	0	0
Entire test period total counts		**20348**	**19992**	**17199**	**1549**	**1666**	**5460**	**1474**	**1748**	**1495**	**1228**	**1343**	**1199**	**921**	**825**	**268**	**103**	**49**	**0**	**4**	**0**	**0**	**0**	**0**	**0**	**0**	**0**	**0**

** Noise band categories

C.5.1.2 *Total bin counts for the entire test period*

Table C-15: Comparisons between the three excitation voltages, HTV-SR 44

	Entire Test Period Bin Counts		
Bin Categories [mA]	*HTV-SR 44 AC*	*HTV-SR 44 DC+*	*HTV-SR 44 DC-*
****[0 - 2]**	20348	19992	17199
****[2 - 5]**	1549	1666	5460
[5 - 10]	1474	1748	1495
[10 - 20]	1228	1343	1199
[20 - 50]	921	825	268
[50 - 100]	103	49	0
[100 - 200]	4	0	0
[200 - 500]	0	0	0
[500 - 1000]	0	0	0

** Noise band categories

NB: Graphical representation of the time of day leakage current profile, per bin category, is depicted in Figure C-17, Figure C-18 and Figure C-19.

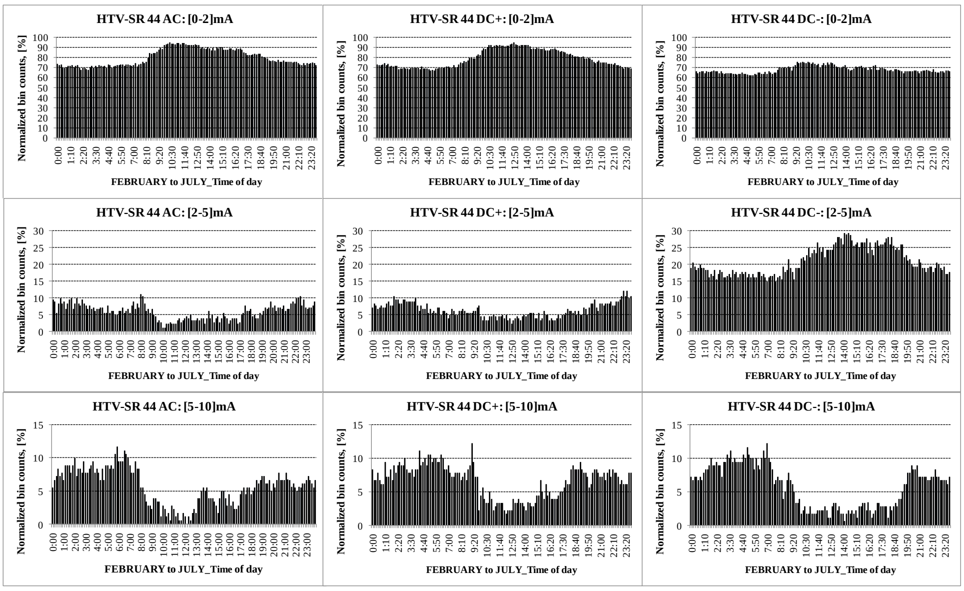

Figure C-17: Time of day leakage current bin counts for [0-10] mA, HTV-SR 44

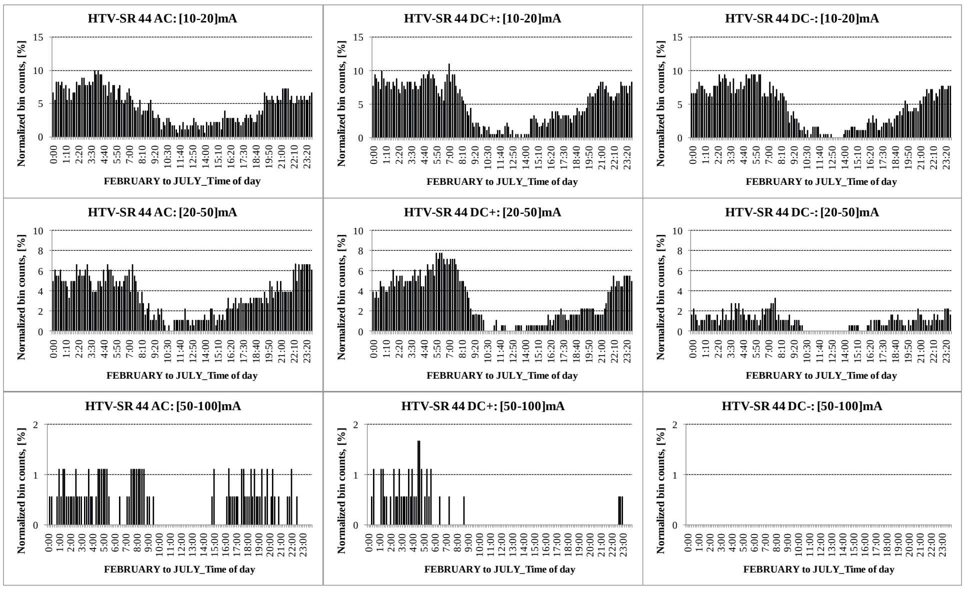

Figure C-18: Time of day leakage current bin counts for [10-100] mA, HTV-SR 44

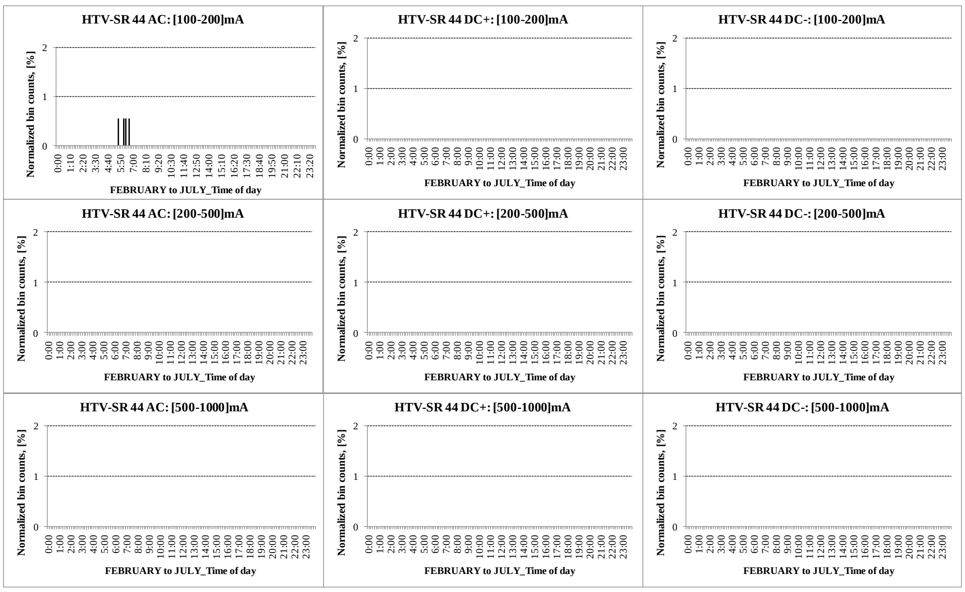

Figure C-19: Time of day leakage current bin counts for [100-1000] mA, HTV-SR 44

C.5.2 Average and maximum values of the recorded leakage current

Table C-16 gives a snapshot of the time of day average and maximum values of the actual leakage current. Elaborate graphs of the time of day average and maximum values of leakage current are presented and discussed in section 5.3.2.5.

Table C-16: The time-of-day average and maximum absolute peak leakage currents

		Absolute Peak Leakage Current [mA]		
		HTV-SR 44 AC	*HTV-SR 44 DC+*	*HTV-SR 44 DC-*
Midnight (24h00)	*Average*	3.76	3.79	3.01
	Maximum	44.74	48.34	27.71
Sunrise (06h00)	*Average*	3.79	4.37	3.29
	Maximum	42.99	48.10	27.71
Midday (12h00)	*Average*	1.51	1.40	1.56
	Maximum	33.55	21.37	9.82
Sunset (18h00)	*Average*	2.91	2.08	1.98
	Maximum	52.12	35.81	20.34
Entire test period	*Maximum*	137.36	80.22	35.77
	Time recorded	24/6 5:40	18/4 3:50	13/3 9:00

C.6 Leakage current performance for high temperature vulcanized, silicone rubber insulators with a unified specific creepage length of 29 mm/kV – HTV-SR 29

This section summarizes all leakage current results for the HTV-SR 29 insulators installed on AC, DC+ and DC-. Note that all results are presented in a comparative manner between the three excitation voltage types. Refer to section 5.3.2.6 for a detailed discussion on these results.

C.6.1 Leakage current bin count analysis

C.6.1.1 *Monthly leakage current bin counts*

Table C-17: Monthly bin counts of absolute peak leakage currents for the HTV-SR 29 insulators

		Monthly leakage current bin counts: HTV-SR 29																										
		**[0 - 2] mA			**[2 - 5] mA			[5 - 10] mA			[10 - 20] mA			[20 - 50] mA			[50 - 100] mA			[100 - 200] mA			[200 - 500] mA			[500 - 1000] mA		
		AC	*DC+*	*DC-*	*AC*	*DC+*	*DC-*	*AC*	*DC+*	*DC-*	*AC*	*DC+*	*DC-*	*AC*	*DC+*	*DC-*	*AC*	*DC+*	*DC-*	*AC*	*DC+*	*DC-*	*AC*	*DC+*	*DC-*	*AC*	*DC+*	*DC-*
SUMMER	February	2555	2684	2594	281	63	485	149	119	56	117	475	237	366	188	211	129	62	13	1	6	0	0	0	0	0	0	0
	March	2944	3673	2787	206	258	589	215	124	510	224	151	461	563	110	109	301	111	5	10	30	0	0	4	0	0	1	0
	April	3426	3298	2938	130	232	632	107	114	250	181	209	186	266	217	256	181	216	54	28	27	2	0	5	0	0	0	0
	TOTAL	8925	9655	8319	617	553	1706	471	357	816	522	835	884	1195	515	576	611	389	72	39	63	2	0	9	0	0	1	0
WINTER	May	3573	2919	2736	365	692	1543	207	415	98	199	269	81	102	138	5	16	29	0	2	1	0	0	0	0	0	0	0
	June	3603	3539	3281	239	428	1030	116	255	9	108	62	0	172	32	0	60	4	0	20	0	0	2	0	0	0	0	0
	July	4288	4310	2661	122	86	1802	35	65	0	16	2	0	2	0	0	0	0	0	0	0	0	0	0	0	0	0	0
	TOTAL	11464	10768	8678	726	1206	4375	358	735	107	323	333	81	276	170	5	76	33	0	22	1	0	2	0	0	0	0	0
Entire test period total counts		**20389**	**20423**	**16997**	**1343**	**1759**	**6081**	**829**	**1092**	**923**	**845**	**1168**	**965**	**1471**	**685**	**581**	**687**	**422**	**72**	**61**	**64**	**2**	**2**	**9**	**0**	**0**	**1**	**0**

** Noise band categories

C.6.1.2 *Total bin counts for the entire test period*

Table C-18: Comparisons between the three excitation voltages, HTV-SR 29

	Entire Test Period Bin Counts		
Bin Categories [mA]	*HTV-SR 29 AC*	*HTV-SR 29 DC+*	*HTV-SR 29 DC-*
****[0 - 2]**	20389	20423	16997
****[2 - 5]**	1343	1759	6081
[5 - 10]	829	1092	923
[10 - 20]	845	1168	965
[20 - 50]	1471	685	581
[50 - 100]	687	422	72
[100 - 200]	61	64	2
[200 - 500]	2	9	0
[500 - 1000]	0	1	0

** Noise band categories

NB: Graphical representation of the time of day leakage current profile, per bin categories, is depicted in Figure C-20, Figure C-21 and Figure C-22.

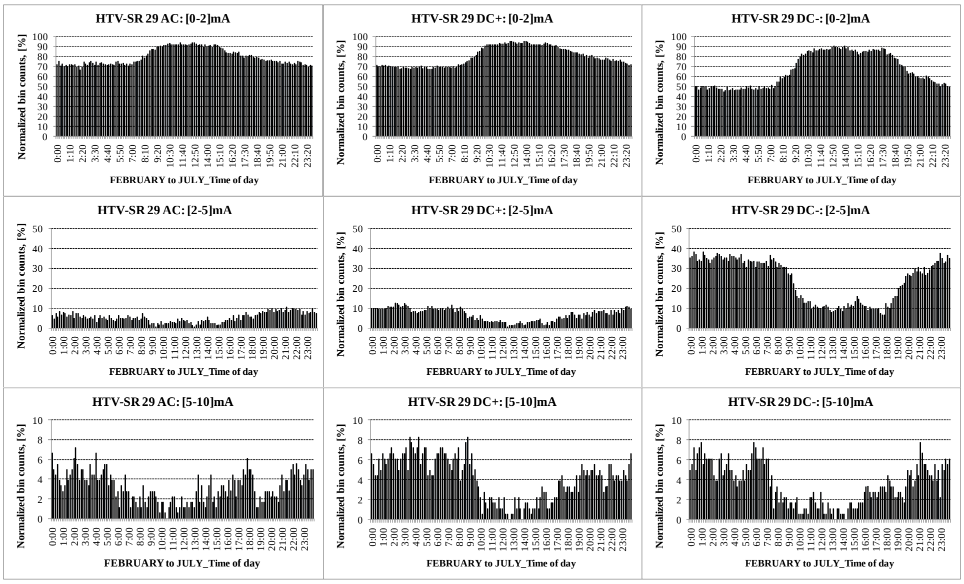

Figure C-20: Time of day leakage current bin counts for [0-10] mA, HTV-SR 29

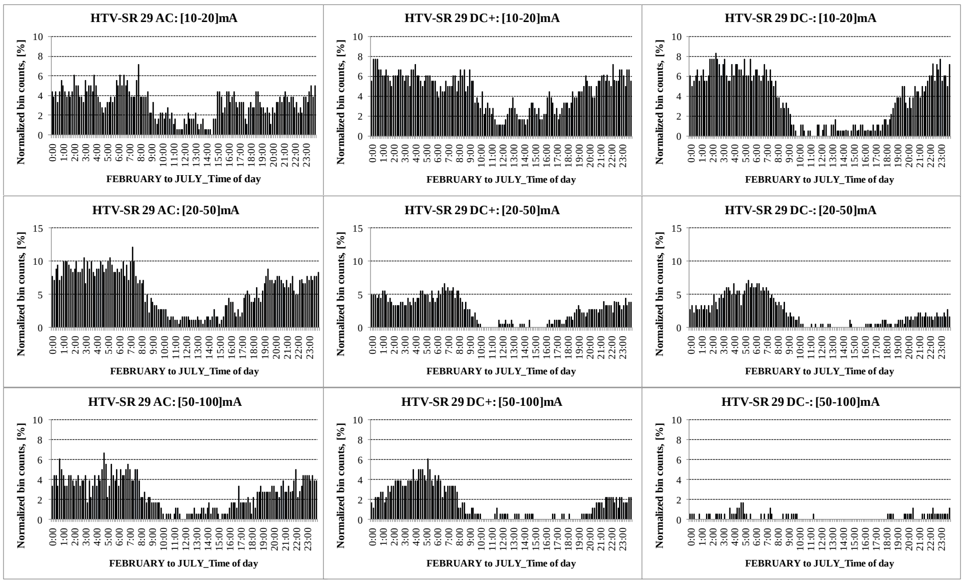

Figure C-21: Time of day leakage current bin counts for [10-100] mA, HTV-SR 29

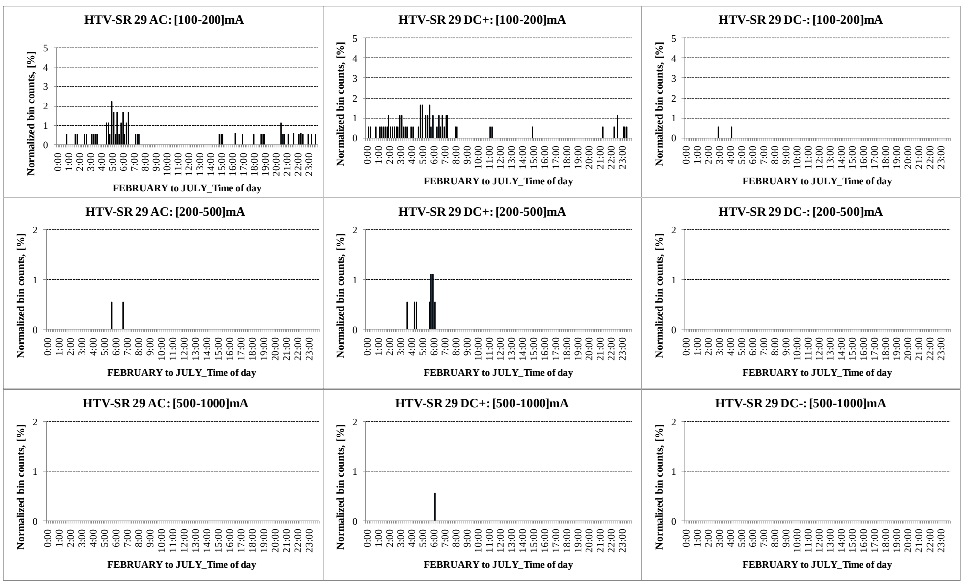

Figure C-22: Time of day leakage current bin counts for [100-1000] mA, HTV-SR 29

C.6.2 Average and maximum values of the recorded leakage current

Table C-19 gives a snapshot of the time of day average and maximum values of the actual leakage current. Elaborate graphs of the time of day average and maximum values of leakage current are presented and discussed in section 5.3.2.6.

Note that a flashover event was recorded on HTV-SR 29 DC+, which was signified by the fuse operation recorded on this insulator. Refer to Figure 3-5 (Chapter 3, section 3.3) for the mace fuse used in this study. A leakage current of 716 mA was recorded during the flashover event on March 12th just around sunrise (06h10). No flashover events were recorded for the other test insulators (i.e. HTV-SR 29 AC and HTV-SR 29 DC-).

Table C-19: The time-of-day average and maximum absolute peak leakage currents

		Absolute Peak Leakage Current [mA]		
		HTV-SR 29 AC	*FO HTV-SR 29 DC+*	*HTV-SR 29 DC-*
Midnight (24h00)	*Average*	6.91	5.34	3.51
	Maximum	84.80	97.93	51.93
Sunrise (06h00)	*Average*	8.84	9.60	4.39
	Maximum	124.85	242.73	45.90
Midday (12h00)	*Average*	1.82	1.70	1.40
	Maximum	43.23	54.91	21.12
Sunset (18h00)	*Average*	3.81	2.08	2.00
	Maximum	104.18	31.56	47.43
Entire test period	*Maximum*	235.18	716.11	104.56
	Time recorded	24/6 5:40	12/3 6:10	26/4 4:10

FO Fuse operation

C.7 Leakage current performance for glass disc insulators with a unified specific creepage length of 42 mm/kV – Glass disc 42

This section summarizes all leakage current results for the Glass disc 42 insulators installed on AC, DC+ and DC-. Note that all results are presented in a comparative manner between the three excitation voltage types. Refer to section 5.3.2.7 for a detailed discussion on these results.

C.7.1 Leakage current bin count analysis

C.7.1.1 *Monthly leakage current bin counts*

Table C-20: Monthly bin counts of absolute peak leakage currents for the Glass disc 42 insulators

		Monthly leakage current bin counts: Glass disc 42																										
		[0 - 2] mA			**[2 - 5] mA**			**[5 - 10] mA**			**[10 - 20] mA**			**[20 - 50] mA**			**[50 - 100] mA**			**[100 - 200] mA**			**[200 - 500] mA**			**[500 - 1000] mA**		
		AC	*DC+*	*DC-*	*AC*	*DC+*	*DC-*	*AC*	*DC+*	*DC-*	*AC*	*DC+*	*DC-*	*AC*	*DC+*	*DC-*	*AC*	*DC+*	*DC-*	*AC*	*DC+*	*DC-*	*AC*	*DC+*	*DC-*	*AC*	*DC+*	*DC-*
SUMMER	**February**	3477	3095	3462	94	29	55	24	116	3	4	90	34	1	113	27	0	119	3	0	35	5	0	0	7	0	0	0
	March	4002	2875	3645	307	89	206	98	99	74	38	151	124	15	520	158	0	409	132	0	314	102	4	5	19	0	0	1
	April	4257	2825	3865	34	535	57	5	72	26	11	277	42	13	379	76	0	179	118	0	51	86	0	0	37	0	0	11
	TOTAL	11736	8795	10972	435	653	318	127	287	103	53	518	200	29	1012	261	0	707	253	0	400	193	4	5	63	0	0	12
WINTER	**May**	4258	2258	3956	191	477	164	10	471	131	2	491	68	2	607	62	0	159	82	0	0	0	1	0	0	0	0	0
	June	4267	2879	3946	49	260	78	1	230	24	2	545	103	0	375	112	1	25	48	0	6	9	0	0	0	0	0	0
	July	4439	2370	4304	20	1611	34	4	135	39	0	208	21	0	139	52	0	0	13	0	0	0	0	0	0	0	0	0
	TOTAL	12964	7507	12206	260	2348	276	15	836	194	4	1244	192	2	1121	226	1	184	143	0	6	9	1	0	0	0	0	0
Entire test period total counts		**24700**	**16302**	**23178**	**695**	**3001**	**594**	**142**	**1123**	**297**	**57**	**1762**	**392**	**31**	**2133**	**487**	**1**	**891**	**396**	**0**	**406**	**202**	**5**	**5**	**63**	**0**	**0**	**12**

** Noise band categories

C.7.1.2 *Total bin counts for the entire test period*

Table C-21: Comparisons between the three excitation voltages, Glass disc 42

	Entire Test Period Bin Counts		
Bin Categories [mA]	*Glass disc 42 AC*	*Glass disc 42 DC+*	*Glass disc 42 DC-*
****[0 - 2]**	24700	16302	23178
****[2 - 5]**	695	3001	594
[5 - 10]	142	1123	297
[10 - 20]	57	1762	392
[20 - 50]	31	2133	487
[50 - 100]	1	891	396
[100 - 200]	0	406	202
[200 - 500]	5	5	63
[500 - 1000]	0	0	12

** Noise band categories

NB: Graphical representation of the time of day leakage current profile, per bin category, is depicted in Figure C-23, Figure C-24 and Figure C-25.

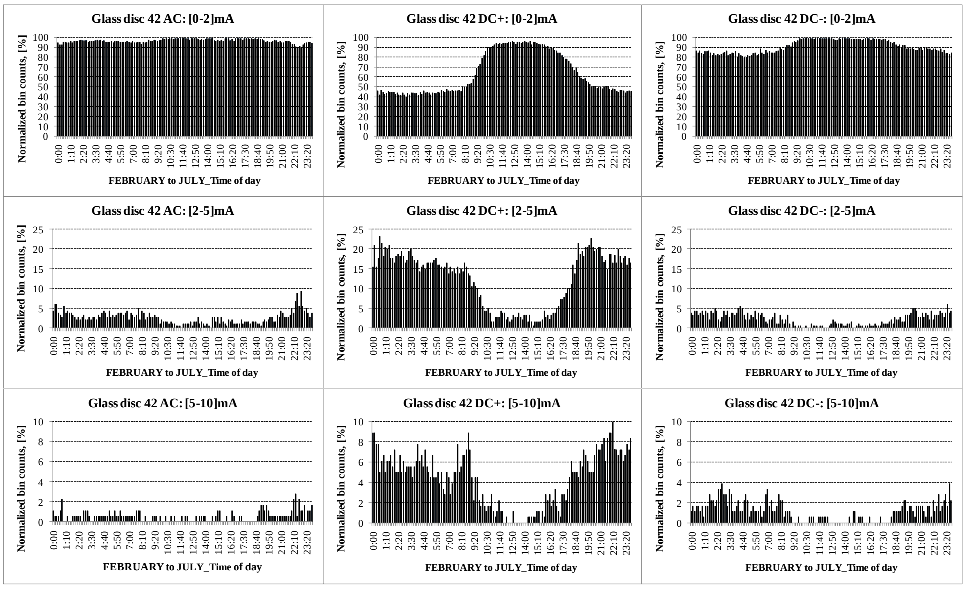

Figure C-23: Time of day leakage current bin counts for [0-10] mA, Glass disc 42

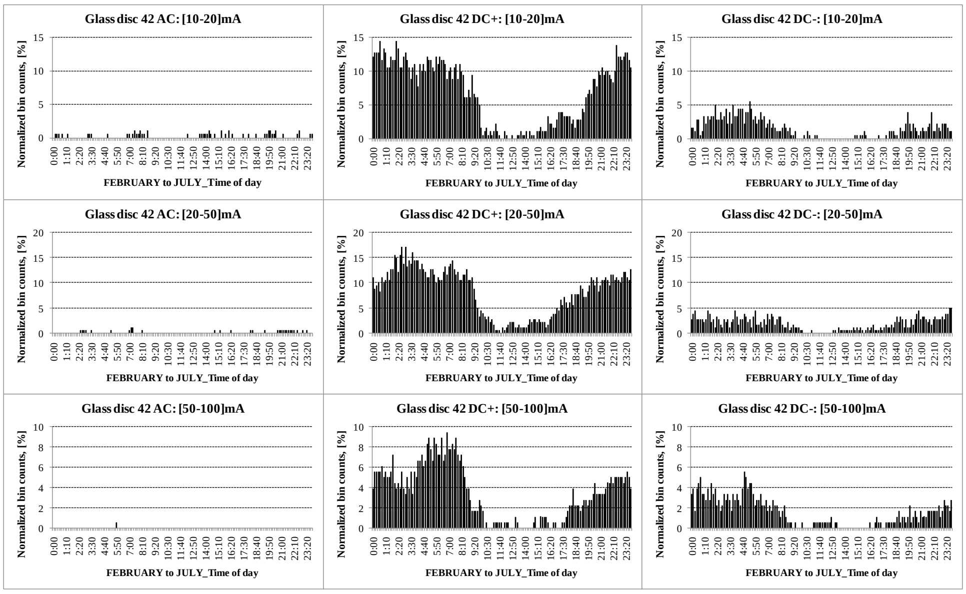

Figure C-24: Time of day leakage current bin counts foor [10-100] mA, Glass disc 42

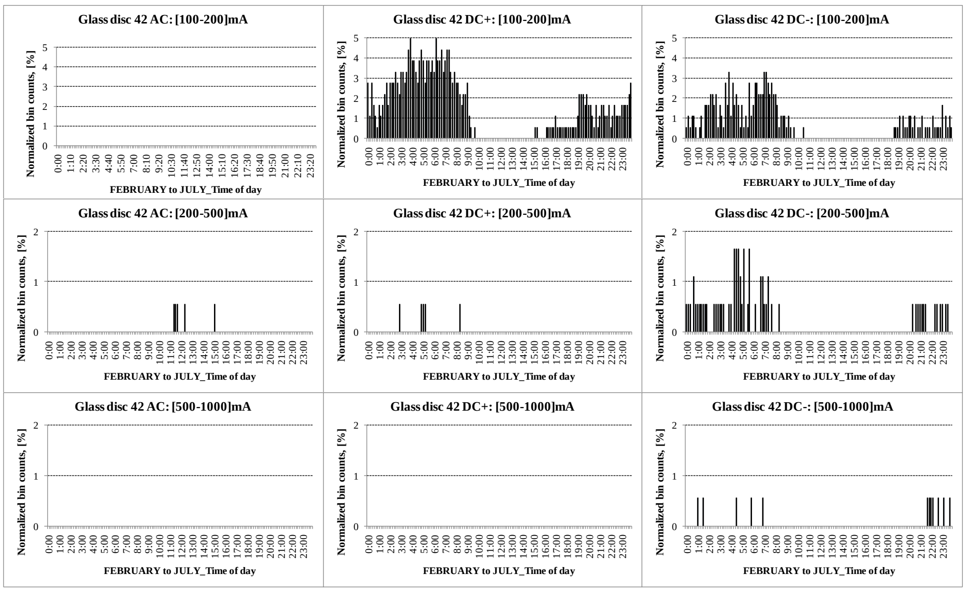

Figure C-25: Time of day leakage current bin counts for [100-1000] mA, Glass disc 42

C.7.2 Average and maximum values of the recorded leakage current

Table C-22 gives a snapshot of the time of day average and maximum values of the actual leakage current. Elaborate graphs of the time of day average and maximum values of leakage current are presented and discussed in section 5.3.2.7.

Table C-22: The time-of-day average and maximum absolute peak leakage currents

		Absolute Peak Leakage Current [mA]		
		Glass disc 42 AC	*Glass disc 42 DC+*	*FO Glass disc 42 DC-*
Midnight (24h00)	*Average*	1.24	12.74	6.82
	Maximum	5.61	133.21	266.71
Sunrise (06h00)	*Average*	1.20	15.32	6.12
	Maximum	7.01	169.41	167.89
Midday (12h00)	*Average*	1.09	1.58	1.28
	Maximum	4.91	49.87	60.28
Sunset (18h00)	*Average*	1.26	5.16	1.75
	Maximum	19.98	116.34	61.69
Entire test period	*Maximum*	365.31	306.49	626.30
	Time recorded	28/3 12:20	22/3 8:20	18/4 22:10

FO Fuse operation

Note that two instances of flashover events were recorded on Glass disc 42 DC-, which was signified by the fuse operations recorded on this insulator. Refer to Figure 3-5 (Chapter 3, section 3.3) for the mace fuse used in this study. The two instances of flashover events are summarized in Table C-23. The prevailing relative humidity conditions are also indicated in the table. Additionally, the leakage currents that flew on Glass disc 42 AC and Glass disc 42 DC- have been recorded and highlighted in Table C-23. Notice the low leakage currents on AC when compared to those on DC+ during the two flashover events on DC-.

Table C-23: Flashover events recorded on the glass disc insulator installed on DC-

	Fuse operations for Glass disc 42 DC-			Other test insulators	
	Time recorded	*Recorded leakage current [mA]*	*Relative humidity [%]*	*Glass disc 42 AC*	*Glass disc 42 DC+*
1st	23/2 5:40	484.04	93.62	1.40	132.51
2nd	13/3 1:50	450.75	89.98	1.75	148.32

D. APPENDIX D: Detailed observations of electrical discharge activities for individual test insulators

D.1 Overview

This appendix summarizes all observations made with Corocam Mark I and 0-lux Sony Camcorder for each set of test insulators with the same creepage length. The observations are tabulated in the form that a comparison is given between AC, DC+ and DC-. These tables provide information on the frequency of occurrence of each type of electrical discharge activity as a percentage of total observation nights. Details on the actual location of all observed electrical discharge activity also provided. Observations were done over a total period of 24 nights.

D.2 Electrical discharge activity observations for high temperature vulcanized, silicone rubber insulators with a unified specific creepage length of 84 mm/kV – HTV-SR 84

D.2.1 Corocam Mark I

D.2.1.1 *Frequency of occurrence*

Table D-24: Frequency of occurrence of electrical discharge activity observed with Corocam Mark I, HTV-SR 84

Electrical discharge activities for HTV-SR 84: COROCAM MARK I																				
Week No.	**Day**	**Date**	**AC**				**DC+**				**DC-**				**Prevailing weather conditions**					
			WDC	**SCD**	**DBC**	**DBD**	**WDC**	**SCD**	**DBC**	**DBD**	**WDC**	**SCD**	**DBC**	**DBD**	**Relative humdity [%]**	**Ambient temperature [°C]**	**Dewpoint temperature [°C]**	**Wind speed [m/s]**	**Wind direction**	**Rainfall [mm]**
1	1	3-Feb																		
	2	4-Feb																		
	3	5-Feb																		
	4	6-Feb																		
	5	7-Feb													82	20	16	2	SE	0.10
	6	8-Feb													75	21	16	5	SE	0.00
	7	9-Feb													57	26	17	3	SE	0.00
2	2	11-Feb	✓												75	19	15	2	SE	0.00
	3	12-Feb	✓												78	20	16	3	SE	0.00
	4	13-Feb	✓												70	21	16	4	SE	0.00
	5	14-Feb					✓								87	18	16	2	SW	0.00
	6	15-Feb	✓				✓								80	21	18	6	SE	0.00
3	1	17-Feb	✓		✓		✓								78	20	16	6	SE	0.00
	2	18-Feb			✓						✓				75	21	17	4	SE	0.00
	3	19-Feb			✓			✓		✓					77	19	15	5	SE	0.00
	4	20-Feb			✓					✓					71	20	15	4	SE	0.00
	6	22-Feb			✓		✓		✓			✓			79	21	17	3	SE	0.00
4	1	24-Feb			✓										87	22	19	8	SE	0.00
5	6	8-Mar			✓				✓			✓		✓	78	19	15	0	SE	0.00
6	5	14-Mar			✓				✓					✓	79	17	13	3	SW	0.00
8	6	29-Mar	✓		✓					✓	✓			✓	94	14	13	0	NE	0.00
11	1	14-Apr			✓	✓			✓					✓	80	19	15	5	SE	0.00
13	1	28-Apr			✓				✓	✓				✓	90	7	6	1	SE	0.10
23	7	13-Jul		✓											88	10	9	0	SE	0.00
Frequency of occurrence out of total observation nights [%]			**25**	**4**	**46**	**4**	**17**	**4**	**21**	**17**	**8**	**8**	**0**	**21**	*NB: All first occurrences are highlighted in GRAY.*					

D.2.1.2 *Locations of electrical discharge activities*

Table D-25: Location of electrical discharge activity observed with Corocam Mark I, HTV-SR 84

Electrical discharge activities for HTV-SR 84: COROCAM MARK I														
Week No.	**Day**	**Date**	**AC**				**DC+**				**DC-**			
			WDC	**SCD**	**DBC**	**DBD**	**WDC**	**SCD**	**DBC**	**DBD**	**WDC**	**SCD**	**DBC**	**DBD**
1	1	3-Feb												
	2	4-Feb												
	3	5-Feb												
	4	6-Feb												
	5	7-Feb												
	6	8-Feb												
	7	9-Feb												
2	2	11-Feb	Bottom shed 6, SE dir											
	3	12-Feb	Bottom shed 6, S dir											
	4	13-Feb	Rim shed 1, NE dir											
	5	14-Feb					Top sheds 1, 4 & 5							
	6	15-Feb	Rim shed 4, N dir + Bottom shed 6, E dir				All sheds, NW dir							
3	1	17-Feb	Bottom shed 3, E dir		Bottom shed 4, E dir		Bottom sheds 2 & 5, N & S dir							
	2	18-Feb			Sheath 7, E dir						Rim shed 6, NE dir			
	3	19-Feb			Bottom shed 6, all dir			Bottom shed 5, S dir		Bottom shed 1, all dir				
	4	20-Feb			Sheath 7, all dir					Sheath 2 + Bottom shed 3, all dir				
	6	22-Feb			Sheaths 1 & 2, E-dir		Bottom shed 4, E dir		Bottom shed 4, N dir			All bottom sheds, N dir		
4	1	24-Feb			Sheath 2, all dir									
5	6	8-Mar			Sheaths 1 & 2, E dir				Sheath 1, all dir			Sheath 1, N dir		Sheath 1, N dir
6	5	14-Mar			Sheath 1, all dir				Sheath 7, all dir					Sheath 1, all dir
8	6	29-Mar	Bottom all sheds, E dir		Shed 3, all dir					Bottom sheds 1 & 6, all dir	Shed 2, W dir			Bottom shed 2
11	1	14-Apr			Sheath 3, E dir	Bottom shed 3, W dir + Sheath 3, E-dir			Sheath 7, W dir					Sheath 1, S dir
13	1	28-Apr			Sheath 1, all dir				Sheath 1, all dir	Sheath 1, W dir				Sheath 1, N dir
23	7	13-Jul		Sheath 1, S dir										

D.2.2 0-lux Sony Camcorder

D.2.2.1 *Frequency of occurrence*

Table D-26: Frequency of occurrence of electrical discharge activity observed with 0-lux Sony Camcorder, HTV-SR 84

Electrical discharge activities for HTV-SR 84: 0-LUX SONY CAMERA																				
Week No.	Day	Date	AC				DC+				DC-				Prevailing weather conditions					
			WDC	SCD	DBC	DBD	WDC	SCD	DBC	DBD	WDC	SCD	DBC	DBD	Relative humdity [%]	Ambient temperature [°C]	Dewpoint temperature [°C]	Wind speed [m/s]	Wind direction	Rainfall [mm]
1	1	3-Feb																		
	2	4-Feb																		
	3	5-Feb																		
	4	6-Feb																		
	5	7-Feb													82	20	16	2	SE	0.10
	6	8-Feb													75	21	16	5	SE	0.00
	7	9-Feb													57	26	17	3	SE	0.00
2	2	11-Feb													75	19	15	2	SE	0.00
	3	12-Feb													78	20	16	3	SE	0.00
	4	13-Feb													70	21	16	4	SE	0.00
	5	14-Feb													87	18	16	2	SW	0.00
	6	15-Feb													80	21	18	6	SE	0.00
3	1	17-Feb													78	20	16	6	SE	0.00
	2	18-Feb													75	21	17	4	SE	0.00
	3	19-Feb				✓				✓					77	19	15	5	SE	0.00
	4	20-Feb				✓									71	20	15	4	SE	0.00
	6	22-Feb				✓									79	21	17	3	SE	0.00
4	1	24-Feb													87	22	19	8	SE	0.00
5	6	8-Mar													78	19	15	0	SE	0.00
6	5	14-Mar								✓					79	17	13	3	SW	0.00
8	6	29-Mar	✓			✓				✓				✓	94	14	13	0	NE	0.00
11	1	14-Apr				✓									80	19	15	5	SE	0.00
13	1	28-Apr													90	7	6	1	SE	0.10
23	7	13-Jul													88	10	9	0	SE	0.00
Frequency of occurrence out of total observation nights [%]			4	0	0	21	0	0	0	13	0	0	0	4	*NB: All first occurrences are highlighted in GRAY.*					

D.2.2.2 *Location of electrical discharge activity*

Table D-27: Location of electrical discharge activity observed with 0-lux Sony Camcorder, HTV-SR 84

Electrical discharge activities for HTV-SR 84: 0-LUX SONY CAMERA														
Week No.	Day	Date	AC				DC+				DC-			
			WDC	SCD	DBC	DBD	WDC	SCD	DBC	DBD	WDC	SCD	DBC	DBD
1	1	3-Feb												
	2	4-Feb												
	3	5-Feb												
	4	6-Feb												
	5	7-Feb												
	6	8-Feb												
	7	9-Feb												
2	2	11-Feb												
	3	12-Feb												
	4	13-Feb												
	5	14-Feb												
	6	15-Feb												
3	1	17-Feb												
	2	18-Feb												
	3	19-Feb				Bottom shed 6, N dir				Bottom shed 1, all dir				
	4	20-Feb				Sheath 7, SE dir								
	6	22-Feb				Top and bottom shed 1, S dir								
4	1	24-Feb												
5	6	8-Mar												
6	5	14-Mar								Sheath 7, W dir				
8	6	29-Mar	Bottom shed 5, S dir			Bottom shed 3, S dir				Sheds 1 & 6, all dir				Bottom shed 2, E dir
11	1	14-Apr				Sheath 3, S dir								
13	1	28-Apr												
23	7	13-Jul												

D.3 Electrical discharge activity observations for high temperature vulcanized, silicone rubber insulators with a unified specific creepage length of 72 mm/kV – HTV-SR 72

D.3.1 Corocam Mark I

D.3.1.1 *Frequency of occurrence*

Table D-28: Frequency of occurrence of electrical discharge activity observed with Corocam Mark I, HTV-SR 72

Electrical discharge activities for HTV-SR 72: COROCAM MARK I																					
Week No.	Day	Date	AC				DC+				DC-				Prevailing weather conditions					
			WDC	SCD	DBC	DBD	WDC	SCD	DBC	DBD	WDC	SCD	DBC	DBD	Relative humdity [%]	Ambient temperature [°C]	Dewpoint temperature [°C]	Wind speed [m/s]	Wind direction	Rainfall [mm]
1	1	3-Feb																		
	2	4-Feb																		
	3	5-Feb																		
	4	6-Feb																		
	5	7-Feb													82	20	16	2	SE	0.10
	6	8-Feb													75	21	16	5	SE	0.00
	7	9-Feb													57	26	17	3	SE	0.00
2	2	11-Feb													75	19	15	2	SE	0.00
	3	12-Feb													78	20	16	3	SE	0.00
	4	13-Feb	✓												70	21	16	4	SE	0.00
	5	14-Feb					✓								87	18	16	2	SW	0.00
	6	15-Feb	✓		✓		✓				✓				80	21	18	6	SE	0.00
3	1	17-Feb			✓		✓								78	20	16	6	SE	0.00
	2	18-Feb	✓		✓			✓							75	21	17	4	SE	0.00
	3	19-Feb		✓				✓	✓						77	19	15	5	SE	0.00
	4	20-Feb			✓					✓		✓			71	20	15	4	SE	0.00
	6	22-Feb				✓		✓				✓	✓		79	21	17	3	SE	0.00
4	1	24-Feb			✓										87	22	19	8	SE	0.00
5	6	8-Mar			✓					✓			✓		78	19	15	0	SE	0.00
6	5	14-Mar			✓					✓				✓	79	17	13	3	SW	0.00
8	6	29-Mar	✓		✓					✓				✓	94	14	13	0	NE	0.00
11	1	14-Apr				✓				✓			✓	✓	80	19	15	5	SE	0.00
13	1	28-Apr			✓				✓					✓	90	7	6	1	SE	0.10
23	7	13-Jul													88	10	9	0	SE	0.00
Frequency of occurrence out of total observation nights [%]			17	4	38	8	13	13	8	21	4	8	13	17	*NB: All first occurrences are highlighted in GRAY.*					

D.3.1.2 *Location of electrical discharge activity*

Table D-29: Location of electrical discharge activity observed with Corocam Mark I, HTV-SR 72

Electrical discharge activities for HTV-SR 72: COROCAM MARK I														
Week No.	Day	Date	AC				DC+				DC-			
			WDC	SCD	DBC	DBD	WDC	SCD	DBC	DBD	WDC	SCD	DBC	DBD
1	1	3-Feb												
	2	4-Feb												
	3	5-Feb												
	4	6-Feb												
	5	7-Feb												
	6	8-Feb												
	7	9-Feb												
2	2	11-Feb												
	3	12-Feb												
	4	13-Feb	Rim shed 2, NE dir											
	5	14-Feb					Bottom shed 5							
	6	15-Feb	Rim shed 5, N dir		Bottom shed 4, E dir		Top sheds 2, 3 & 4, NW dir				Rim sheds 1 & 2, N dir			
3	1	17-Feb			Bottom shed 2, E dir		Bottom shed 2, N dir							
	2	18-Feb	Bottom shed 5, E dir		Sheath 6, E dir			Bottom shed 4, SW dir						
	3	19-Feb		Bottom and top shed 4, all dir				Bottom shed 2, N & W dir	Bottom shed 3, N dir					
	4	20-Feb			Sheaths 5 & 6, all dir					Bottom shed 4 + sheath 5, all dir		Bottom sheds 2 & 4, N dir		
	6	22-Feb				Sheaths 1 & 2, E dir		Bottom shed 1, N dir				Bottom shed 4, N dir	Bottom shed 4, N dir	
4	1	24-Feb			Sheath 2, all dir									
5	6	8-Mar			Sheath 1, E dir					Sheath 6, all dir			Sheath 1, N dir	
6	5	14-Mar			Sheath 1, all dir					Sheath 6, all dir				Sheath 6, W dir
8	6	29-Mar	Rim sheds 1 & 3, E dir		Sheath 6, all dir					Bottom shed 1, all dir				Bottom shed 3, all dir
11	1	14-Apr				Sheath 6, W dir				Sheath 6, W dir			Sheath 3, E dir	Bottom shed 3, N dir
13	1	28-Apr			Sheath 1, all dir				Sheath 6, all dir					Sheath 1, NE & SE dir
23	7	13-Jul												

D.3.2 0-lux Sony Camcorder

D.3.2.1 *Frequency of occurrence*

Table D-30: Frequency of occurrence of electrical discharge activity observed with 0-lux Sony Camcorder, HTV-SR 72

Electrical discharge activities for HTV-SR 72: 0-LUX SONY CAMERA																				
Week No.	Day	Date	AC				DC+				DC-				Prevailing weather conditions					
			WDC	SCD	DBC	DBD	WDC	SCD	DBC	DBD	WDC	SCD	DBC	DBD	Relative humdity [%]	Ambient temperature [°C]	Dewpoint temperature [°C]	Wind speed [m/s]	Wind direction	Rainfall [mm]
1	1	3-Feb																		
	2	4-Feb																		
	3	5-Feb																		
	4	6-Feb																		
	5	7-Feb													82	20	16	2	SE	0.10
	6	8-Feb													75	21	16	5	SE	0.00
	7	9-Feb													57	26	17	3	SE	0.00
2	2	11-Feb													75	19	15	2	SE	0.00
	3	12-Feb													78	20	16	3	SE	0.00
	4	13-Feb													70	21	16	4	SE	0.00
	5	14-Feb													87	18	16	2	SW	0.00
	6	15-Feb													80	21	18	6	SE	0.00
3	1	17-Feb													78	20	16	6	SE	0.00
	2	18-Feb													75	21	17	4	SE	0.00
	3	19-Feb								✓					77	19	15	5	SE	0.00
	4	20-Feb								✓					71	20	15	4	SE	0.00
	6	22-Feb				✓									79	21	17	3	SE	0.00
4	1	24-Feb													87	22	19	8	SE	0.00
5	6	8-Mar													78	19	15	0	SE	0.00
6	5	14-Mar								✓					79	17	13	3	SW	0.00
8	6	29-Mar	✓							✓				✓	94	14	13	0	NE	0.00
11	1	14-Apr				✓				✓				✓	80	19	15	5	SE	0.00
13	1	28-Apr								✓					90	7	6	1	SE	0.10
23	7	13-Jul													88	10	9	0	SE	0.00
Frequency of occurrence out of total observation nights [%]			4	0	0	8	0	0	0	25	0	0	0	8	*NB: All first occurrences are highlighted in GRAY.*					

D.3.2.2 *Location of electrical discharge activity*

Table D-31: Location of electrical discharge activity observed with 0-lux Sony Camcorder, HTV-SR 72

Electrical discharge activities for HTV-SR 72: 0-LUX SONY CAMERA														
Week No.	Day	Date	AC				DC+				DC-			
			WDC	SCD	DBC	DBD	WDC	SCD	DBC	DBD	WDC	SCD	DBC	DBD
1	1	3-Feb												
	2	4-Feb												
	3	5-Feb												
	4	6-Feb												
	5	7-Feb												
	6	8-Feb												
	7	9-Feb												
2	2	11-Feb												
	3	12-Feb												
	4	13-Feb												
	5	14-Feb												
	6	15-Feb												
3	1	17-Feb												
	2	18-Feb												
	3	19-Feb								Bottom shed 2, all dir				
	4	20-Feb								Bottom sheds 4 & 5, SW dir				
	6	22-Feb				Sheath 1 + bottom shed 1, S dir								
4	1	24-Feb												
5	6	8-Mar												
6	5	14-Mar								Sheath 6, W dir				
8	6	29-Mar	Rim sheds 1 & 3, E dir							Sheath 1, E dir				Bottom shed 3, all dir
11	1	14-Apr				Sheath 6, S dir				Sheath 6, SW dir				Bottom shed 3, S dir
13	1	28-Apr								Sheath 6, S & W dir				
23	7	13-Jul												

D.4 Electrical discharge activity observations for high temperature vulcanized, silicone rubber insulators with a unified specific creepage length of 56 mm/kV – HTV-SR 56

D.4.1 Corocam Mark I

D.4.1.1 *Frequency of occurrence*

Table D-32: Frequency of occurrence of electrical discharge activity observed with Corocam Mark I, HTV-SR 56

Electrical discharge activities for HTV-SR 56: COROCAM MARK I																					
Week No.	**Day**	**Date**	**AC**				**DC+**				**DC-**				**Prevailing weather conditions**					
			WDC	**SCD**	**DBC**	**DBD**	**WDC**	**SCD**	**DBC**	**DBD**	**WDC**	**SCD**	**DBC**	**DBD**	**Relative humdity [%]**	**Ambient temperature [°C]**	**Dewpoint temperature [°C]**	**Wind speed [m/s]**	**Wind direction**	**Rainfall [mm]**
1	1	3-Feb																		
	2	4-Feb																		
	3	5-Feb																		
	4	6-Feb																		
	5	7-Feb													82	20	16	2	SE	0.10
	6	8-Feb													75	21	16	5	SE	0.00
	7	9-Feb													57	26	17	3	SE	0.00
2	2	11-Feb	✓												75	19	15	2	SE	0.00
	3	12-Feb	✓												78	20	16	3	SE	0.00
	4	13-Feb	✓												70	21	16	4	SE	0.00
	5	14-Feb			✓										87	18	16	2	SW	0.00
	6	15-Feb			✓		✓				✓				80	21	18	6	SE	0.00
3	1	17-Feb			✓	✓				✓					78	20	16	6	SE	0.00
	2	18-Feb			✓					✓	✓				75	21	17	4	SE	0.00
	3	19-Feb				✓	✓			✓		✓			77	19	15	5	SE	0.00
	4	20-Feb				✓				✓					71	20	15	4	SE	0.00
	6	22-Feb				✓				✓		✓			79	21	17	3	SE	0.00
4	1	24-Feb			✓										87	22	19	8	SE	0.00
5	6	8-Mar			✓				✓	✓				✓	78	19	15	0	SE	0.00
6	5	14-Mar			✓	✓	✓			✓				✓	79	17	13	3	SW	0.00
8	6	29-Mar			✓					✓				✓	94	14	13	0	NE	0.00
11	1	14-Apr			✓	✓				✓			✓		80	19	15	5	SE	0.00
13	1	28-Apr			✓									✓	90	7	6	1	SE	0.10
23	7	13-Jul		✓											88	10	9	0	SE	0.00
Frequency of occurrence out of total observation nights [%]			**13**	**4**	**42**	**25**	**13**	**0**	**4**	**38**	**8**	**8**	**4**	**17**	*NB: All first occurrences are highlighted in GRAY.*					

D.4.1.2 *Location of electrical discharge activity*

Table D-33: Location of electrical discharge activity observed with Corocam Mark I, HTV-SR 56

Electrical discharge activities for HTV-SR 56: COROCAM MARK I														
Week No.	Day	Date	AC				DC+				DC-			
			WDC	SCD	DBC	DBD	WDC	SCD	DBC	DBD	WDC	SCD	DBC	DBD
1	1	3-Feb												
	2	4-Feb												
	3	5-Feb												
	4	6-Feb												
	5	7-Feb												
	6	8-Feb												
	7	9-Feb												
2	2	11-Feb	Rim shed 1, N dir											
	3	12-Feb	Rim shed 1, NE dir											
	4	13-Feb	Bottom shed 1,E dir + Rim sheds 2 & 4, NE dir											
	5	14-Feb			Rim sheds 2 & 4, N dir									
	6	15-Feb			Bottom shed 2, E dir		Top sheds 1 & 3, NW dir				Rim shed 2, N dir			
3	1	17-Feb			Sheath 1 & bottom shed 1, E dir	Rim shed 3, NE dir				Bottom shed 2, N dir				
	2	18-Feb			Bottom shed 3, E dir					Bottom shed 3, all dir	Bottom shed 3, N dir			
	3	19-Feb				Sheath 5, E dir + Bottom shed 3, all dir	Bottom shed 2, W & S dir			Bottom shed 2, W & S dir		Rim shed 3, N dir		
	4	20-Feb				Bottom shed 4, all dir				Sheath 4, all dir				
	6	22-Feb				Sheath 3, E dir				Bottom shed 2, N & S dir		Bottom sheds 1, 2 & 3, N dir		
4	1	24-Feb			Sheath 5, all dir									
5	6	8-Mar			Sheath 5, E dir				Sheath 1, W dir	Sheath 1, W dir				Sheath 1, E dir
6	5	14-Mar			Sheath 1, all dir	Bottom shed 1, W dir	Rim shed 3, NW dir			Sheath 5, W dir				Sheath 5, SW dir
8	6	29-Mar			Sheath 1, all dir					Bottom shed 2, all dir				Sheath 5, all dir
11	1	14-Apr			Sheath 1, E dir	Bottom shed 1, W dir				Sheath 5, W dir			Sheath 1, N dir	
13	1	28-Apr			Sheath 1, all dir									Sheath 1, N dir
23	7	13-Jul		Sheath 1, N dir										

D.4.2 0-lux Sony Camcorder

D.4.2.1 *Frequency of occurrence*

Table D-34: Frequency of occurrence of electrical discharge activity observed with 0-lux Sony Camcorder, HTV-SR 56

Electrical discharge activities for HTV-SR 56: 0-LUX SONY CAMERA																				
Week No.	**Day**	**Date**	**AC**				**DC+**				**DC-**				**Prevailing weather conditions**					
			WDC	**SCD**	**DBC**	**DBD**	**WDC**	**SCD**	**DBC**	**DBD**	**WDC**	**SCD**	**DBC**	**DBD**	**Relative humdity [%]**	**Ambient temperature [°C]**	**Dewpoint temperature [°C]**	**Wind speed [m/s]**	**Wind direction**	**Rainfall [mm]**
	1	3-Feb																		
	2	4-Feb																		
	3	5-Feb																		
1	4	6-Feb																		
	5	7-Feb													82	20	16	2	SE	0.10
	6	8-Feb													75	21	16	5	SE	0.00
	7	9-Feb													57	26	17	3	SE	0.00
	2	11-Feb													75	19	15	2	SE	0.00
	3	12-Feb													78	20	16	3	SE	0.00
2	4	13-Feb													70	21	16	4	SE	0.00
	5	14-Feb													87	18	16	2	SW	0.00
	6	15-Feb													80	21	18	6	SE	0.00
	1	17-Feb								✓					78	20	16	6	SE	0.00
	2	18-Feb								✓					75	21	17	4	SE	0.00
3	3	19-Feb				✓				✓					77	19	15	5	SE	0.00
	4	20-Feb				✓				✓					71	20	15	4	SE	0.00
	6	22-Feb				✓									79	21	17	3	SE	0.00
4	1	24-Feb													87	22	19	8	SE	0.00
5	6	8-Mar													78	19	15	0	SE	0.00
6	5	14-Mar				✓				✓					79	17	13	3	SW	0.00
8	6	29-Mar	✓							✓				✓	94	14	13	0	NE	0.00
11	1	14-Apr				✓				✓					80	19	15	5	SE	0.00
13	1	28-Apr													90	7	6	1	SE	0.10
23	7	13-Jul													88	10	9	0	SE	0.00
Frequency of occurrence out of total observation nights [%]			**4**	**0**	**0**	**21**	**0**	**0**	**0**	**29**	**0**	**0**	**0**	**4**	*NB: All first occurrences are highlighted in GRAY.*					

D.4.2.2 *Location of electrical discharge activity*

Table D-35: Location of electrical discharge activity observed with 0-lux Sony Camcorder, HTV-SR 56

Electrical discharge activities for HTV-SR 56: 0-LUX SONY CAMERA														
Week No.	Day	Date	AC				DC+				DC-			
			WDC	SCD	DBC	DBD	WDC	SCD	DBC	DBD	WDC	SCD	DBC	DBD
	1	3-Feb												
	2	4-Feb												
	3	5-Feb												
1	4	6-Feb												
	5	7-Feb												
	6	8-Feb												
	7	9-Feb												
	2	11-Feb												
	3	12-Feb												
2	4	13-Feb												
	5	14-Feb												
	6	15-Feb												
	1	17-Feb								Bottom shed 2, N dir + Shed 4, E dir				
	2	18-Feb								Bottom shed 3, all dir				
3	3	19-Feb				Bottom shed 3, N dir + Sheath 5, SE dir				Bottom shed 2, NW dir				
	4	20-Feb				Sheath 4, SE dir				Sheath 5, SW dir				
	6	22-Feb				Bottom shed 3 + sheath 3, S dir								
4	1	24-Feb												
5	6	8-Mar												
6	5	14-Mar				Sheath 1, W dir				Sheath 5, all dir				
8	6	29-Mar	Rim sheds 1, 2 & 4, all dir							Bottom shed 2, all dir				Sheath 5, all dir
11	1	14-Apr				Sheath 1, S dir				Sheath 5, SW dir + Sheath 1, E dir				
13	1	28-Apr												
23	7	13-Jul												

D.5 Electrical discharge activity observations for high temperature vulcanized, silicone rubber insulators with a unified specific creepage length of 44 mm/kV – HTV-SR 44

D.5.1 Corocam Mark I

D.5.1.1 *Frequency of occurrence*

Table D-36: Frequency of occurrence of electrical discharge activity observed with Corocam Mark I, HTV-SR 44

Electrical discharge activities for HTV-SR 44: COROCAM MARK I																					
			AC				DC+				DC-				Prevailing weather conditions						
Week No.	Day	Date	WDC	SCD	DBC	DBD	WDC	SCD	DBC	DBD	WDC	SCD	DBC	DBD	Relative humdity [%]	Ambient temperature [°C]	Dewpoint temperature [°C]	Wind speed [m/s]	Wind direction	Rainfall [mm]
1	1	3-Feb																		
	2	4-Feb																		
	3	5-Feb																		
	4	6-Feb																		
	5	7-Feb													82	20	16	2	SE	0.10
	6	8-Feb													75	21	16	5	SE	0.00
	7	9-Feb	✓												57	26	17	3	SE	0.00
2	2	11-Feb	✓												75	19	15	2	SE	0.00
	3	12-Feb	✓												78	20	16	3	SE	0.00
	4	13-Feb	✓												70	21	16	4	SE	0.00
	5	14-Feb	✓		✓										87	18	16	2	SW	0.00
	6	15-Feb			✓		✓								80	21	18	6	SE	0.00
3	1	17-Feb				✓								✓	78	20	16	6	SE	0.00
	2	18-Feb			✓					✓	✓				75	21	17	4	SE	0.00
	3	19-Feb				✓				✓		✓			77	19	15	5	SE	0.00
	4	20-Feb				✓				✓					71	20	15	4	SE	0.00
	6	22-Feb				✓				✓		✓	✓		79	21	17	3	SE	0.00
4	1	24-Feb			✓										87	22	19	8	SE	0.00
5	6	8-Mar			✓				✓					✓	78	19	15	0	SE	0.00
6	5	14-Mar			✓	✓				✓				✓	79	17	13	3	SW	0.00
8	6	29-Mar	✓		✓					✓				✓	94	14	13	0	NE	0.00
11	1	14-Apr			✓	✓				✓				✓	80	19	15	5	SE	0.00
13	1	28-Apr				✓			✓	✓				✓	90	7	6	1	SE	0.10
23	7	13-Jul			✓					✓		✓			88	10	9	0	SE	0.00
Frequency of occurrence out of total observation nights [%]			25	0	38	29	4	0	8	38	4	13	4	25	*NB: All first occurrences are highlighted in GRAY.*					

D.5.1.2 *Locations of electrical discharge activities*

Table D-37: Location of electrical discharge activity observed with Corocam Mark I, HTV-SR 44

Electrical discharge activities for HTV-SR 44: COROCAM MARK I														
Week No.	Day	Date	AC				DC+				DC-			
			WDC	SCD	DBC	DBD	WDC	SCD	DBC	DBD	WDC	SCD	DBC	DBD
	1	3-Feb												
	2	4-Feb												
	3	5-Feb												
1	4	6-Feb												
	5	7-Feb												
	6	8-Feb												
	7	9-Feb	Sheds 2 &3, S dir											
	2	11-Feb	Sheath 4, W dir + Rim sheds 2 & 3, NE dir											
	3	12-Feb	Rim sheds 1 & 3, NE dir											
2	4	13-Feb	Sheath 4 + Bottom shed 1, E dir											
	5	14-Feb	Bottom shed 1, E dir		Rim shed 2, E dir									
	6	15-Feb			Bottom shed 3, E dir		Top sheds 1 & 2, NW dir							
	1	17-Feb				Sheath 1, E dir								Bottom shed 2 & sheath 3, N dir
	2	18-Feb			Bottom shed 2, E dir					Bottom shed 1, all dir	Bottom shed 2, E & W dir			
3	3	19-Feb				Bottom shed 3, SE dir				Sheath 4 & Bottom shed 3, all dir		Bottom shed 2, N dir		
	4	20-Feb				Sheath 4, all dir + Bottom shed 2, SE dir				Bottom shed 1, all dir				
	6	22-Feb				Sheath 4 & Bottom shed 2				Bottom shed 3, N & S dir		Bottom osheds 2 & 3, N dir	Bottom shed 2, N dir	
4	1	24-Feb			Sheath 3, all dir									
5	6	8-Mar			Sheath 4, E dir				Sheath 1, W dir					Sheath 1, all dir
6	5	14-Mar			Sheath 1, all dir	Bottom shed 1, W dir				Sheath 4, all dir				Sheath 1, S dir
8	6	29-Mar	Rim sheds 1 & 3, N & S dir		Bottom shed 1, all dir					Bottom shed 1, all dir				Sheath 4, NE dir
11	1	14-Apr			Sheath 2, E dir	Bottom shed 2, W dir				Sheath 4, SW dir				Bottom shed 2, N dir
13	1	28-Apr				Sheath 1, all dir			Sheath 1, SW dir	Sheath 1, all dir				Sheath 1, N dir
23	7	13-Jul			Sheath 1, S dir					Sheath 1, SW dir		Sheath 1, W dir		

D.5.2 0-lux Sony Camcorder

D.5.2.1 *Frequency of occurrence*

Table D-38: Frequency of occurrence of electrical discharge activity observed with 0-lux Sony Camcorder, HTV-SR 44

Electrical discharge activities for HTV-SR 44: 0-LUX SONY CAMERA																				
Week No.	Day	Date	AC				DC+				DC-				Prevailing weather conditions					
			WDC	SCD	DBC	DBD	WDC	SCD	DBC	DBD	WDC	SCD	DBC	DBD	Relative humdity [%]	Ambient temperature [°C]	Dewpoint temperature [°C]	Wind speed [m/s]	Wind direction	Rainfall [mm]
1	1	3-Feb																		
	2	4-Feb																		
	3	5-Feb																		
	4	6-Feb																		
	5	7-Feb													82	20	16	2	SE	0.10
	6	8-Feb													75	21	16	5	SE	0.00
	7	9-Feb													57	26	17	3	SE	0.00
2	2	11-Feb													75	19	15	2	SE	0.00
	3	12-Feb													78	20	16	3	SE	0.00
	4	13-Feb													70	21	16	4	SE	0.00
	5	14-Feb													87	18	16	2	SW	0.00
	6	15-Feb			✓										80	21	18	6	SE	0.00
3	1	17-Feb				✓									78	20	16	6	SE	0.00
	2	18-Feb				✓									75	21	17	4	SE	0.00
	3	19-Feb				✓				✓					77	19	15	5	SE	0.00
	4	20-Feb				✓									71	20	15	4	SE	0.00
	6	22-Feb				✓									79	21	17	3	SE	0.00
4	1	24-Feb													87	22	19	8	SE	0.00
5	6	8-Mar								✓					78	19	15	0	SE	0.00
6	5	14-Mar				✓				✓					79	17	13	3	SW	0.00
8	6	29-Mar	✓							✓				✓	94	14	13	0	NE	0.00
11	1	14-Apr				✓				✓				✓	80	19	15	5	SE	0.00
13	1	28-Apr								✓					90	7	6	1	SE	0.10
23	7	13-Jul													88	10	9	0	SE	0.00
Frequency of occurrence out of total observation nights [%]			4	0	4	29	0	0	0	25	0	0	0	8	*NB: All first occurrences are highlighted in GRAY.*					

D.5.2.2 *Location of electrical discharge activity*

Table D-39: Location of electrical discharge activity observed with 0-lux Sony Camcorder, HTV-SR 44

Electrical discharge activities for HTV-SR 44: 0-LUX SONY CAMERA														
Week No.	Day	Date	AC				DC+				DC-			
			WDC	SCD	DBC	DBD	WDC	SCD	DBC	DBD	WDC	SCD	DBC	DBD
1	1	3-Feb												
	2	4-Feb												
	3	5-Feb												
	4	6-Feb												
	5	7-Feb												
	6	8-Feb												
	7	9-Feb												
2	2	11-Feb												
	3	12-Feb												
	4	13-Feb												
	5	14-Feb												
	6	15-Feb			Bottom shed 3, N dir									
3	1	17-Feb				Bottom shed 1, S dir								
	2	18-Feb				Bottom shed 2, E dir								
	3	19-Feb				Bottom shed 3, SE dir				Bottom shed 3 & Sheath 4, all dir				
	4	20-Feb				Sheath 4, SE dir + Bottom shed 2, E dir								
	6	22-Feb				Bottom shed 2, all dir + Sheath 4, S dir								
4	1	24-Feb												
5	6	8-Mar								Sheath 1, W dir				
6	5	14-Mar				Sheath 1, SW dir				Sheath 4, all dir				
8	6	29-Mar	Rim shed 1 & 3, all dir							Sheath 1, E dir				Sheath 4, NE dir
11	1	14-Apr				Sheath 2, S dir				Sheath 4, SW dir				Bottom shed 2, N dir
13	1	28-Apr								Sheath 1, NW & E dir				
23	7	13-Jul												

D.6 Electrical discharge activity observations for high temperature vulcanized, silicone rubber insulators with a unified specific creepage length of 29 mm/kV – HTV-SR 29

D.6.1 Corocam Mark I

D.6.1.1 *Frequency of occurrence*

Table D-40: Frequency of occurrence of electrical discharge activity observed with Corocam Mark I, HTV-SR 29

Electrical discharge activities for HTV-SR 29: COROCAM MARK I																					
Week No.	Day	Date	AC				DC+				DC-				Prevailing weather conditions					
			WDC	SCD	DBC	DBD	WDC	SCD	DBC	DBD	WDC	SCD	DBC	DBD	Relative humdity [%]	Ambient temperature [°C]	Dewpoint temperature [°C]	Wind speed [m/s]	Wind direction	Rainfall [mm]
1	1	3-Feb																		
	2	4-Feb																		
	3	5-Feb																		
	4	6-Feb																		
	5	7-Feb													82	20	16	2	SE	0.10
	6	8-Feb	✓												75	21	16	5	SE	0.00
	7	9-Feb	✓												57	26	17	3	SE	0.00
2	2	11-Feb	✓												75	19	15	2	SE	0.00
	3	12-Feb	✓												78	20	16	3	SE	0.00
	4	13-Feb	✓				✓								70	21	16	4	SE	0.00
	5	14-Feb			✓					✓					87	18	16	2	SW	0.00
	6	15-Feb	✓			✓	✓			✓					80	21	18	6	SE	0.00
3	1	17-Feb				✓								✓	78	20	16	6	SE	0.00
	2	18-Feb				✓		✓				✓			75	21	17	4	SE	0.00
	3	19-Feb				✓				✓			✓	✓	77	19	15	5	SE	0.00
	4	20-Feb				✓			✓		✓				71	20	15	4	SE	0.00
	6	22-Feb				✓		✓					✓		79	21	17	3	SE	0.00
4	1	24-Feb			✓										87	22	19	8	SE	0.00
5	6	8-Mar			✓					✓		✓		✓	78	19	15	0	SE	0.00
6	5	14-Mar			✓	✓				✓				✓	79	17	13	3	SW	0.00
8	6	29-Mar			✓				✓	✓			✓		94	14	13	0	NE	0.00
11	1	14-Apr			✓			✓						✓	80	19	15	5	SE	0.00
13	1	28-Apr			✓				✓	✓				✓	90	7	6	1	SE	0.10
23	7	13-Jul			✓									✓	88	10	9	0	SE	0.00
Frequency of occurrence out of total observation nights [%]			25	0	33	29	8	13	13	29	4	8	13	29	*NB: All first occurrences are highlighted in GRAY.*					

D.6.1.2 *Location of electrical discharge activity*

Table D-41: Location of electrical discharge activity observed with Corocam Mark I, HTV-SR 29

Electrical discharge activities for HTV-SR 29: COROCAM MARK I														
Week No.	Day	Date	AC				DC+				DC-			
			WDC	SCD	DBC	DBD	WDC	SCD	DBC	DBD	WDC	SCD	DBC	DBD
1	1	3-Feb												
	2	4-Feb												
	3	5-Feb												
	4	6-Feb												
	5	7-Feb												
	6	8-Feb	Rim sheds 1 & 2 + Bottom shed 1											
	7	9-Feb	Sheath 3, N & S dir											
2	2	11-Feb	Sheath 3, all dir + shed 1, N dir											
	3	12-Feb	Rim shed 1, E dir + shed 2, N dir											
	4	13-Feb	Sheath 3, SE & N dir				Sheath 3, NW dir + Rim shed 1, SW dir							
	5	14-Feb			Sheath 3, E & N dir					Sheath 3, SW dir				
	6	15-Feb	Bottom shed 1, NE dir			Bottom shed 2, E dir	Sheath 3, SW dir			Sheath 1 & 3, SW dir				
3	1	17-Feb				Sheath 3, E dir + Bottom shed 1								Bottom shed 2, E & W dir
	2	18-Feb				Sheath 1, E dir		Bottom shed 2, all dir				Bottom shed 2, N dir		
	3	19-Feb				Sheath 3 & Bottom shed 1, all dir				Bottom shed 2, all dir			Bottom shed 2, NW dir	Bottom shed 2, N dir
	4	20-Feb				Sheath 3, all dir			Bottom shed 2, all dir		Sheath 2, all dir			
	6	22-Feb				Sheath 3 + bottom shed 2		Sheath 1, N & S dir					Bottom shed 2, N dir	
4	1	24-Feb			Sheath 1, all dir									
5	6	8-Mar			Sheath 1, E dir					Sheath 3, NW dir		Bottom shed 1, SW dir		Sheath 5, E dir
6	5	14-Mar			Sheath 1, all dir	Bottom shed 2, W dir				Sheath 1 & 3, all dir				Sheath 3, SW dir
8	6	29-Mar			Sheath 3, all dir				Sheath 2, W dir	Sheath 2, E dir			Sheath 2, NE dir	
11	1	14-Apr			Sheath 1, E-dir			Sheath 2, SW dir						Sheath 2, W dir
13	1	28-Apr			Sheath 1, E dir				Sheath 3, SW dir	Sheath 3, all dir				Sheath 1, N & S dir
23	7	13-Jul			Sheath 3, S dir									Sheath 1, W dir

D.6.2 0-lux Sony Camcorder

D.6.2.1 *Frequency of occurrence*

Table D-42: Frequency of occurrence of electrical discharge activity observed with 0-lux Sony Camcorder, HTV-SR 29

Electrical discharge activities for HTV-SR 29: 0-LUX SONY CAMERA

Week No.	Day	Date	AC				DC+				DC-				Prevailing weather conditions					
			WDC	SCD	DBC	DBD	WDC	SCD	DBC	DBD	WDC	SCD	DBC	DBD	Relative humdity [%]	Ambient temperature [°C]	Dewpoint temperature [°C]	Wind speed [m/s]	Wind direction	Rainfall [mm]
1	1	3-Feb																		
	2	4-Feb																		
	3	5-Feb																		
	4	6-Feb																		
	5	7-Feb													82	20	16	2	SE	0.10
	6	8-Feb													75	21	16	5	SE	0.00
	7	9-Feb													57	26	17	3	SE	0.00
2	2	11-Feb													75	19	15	2	SE	0.00
	3	12-Feb													78	20	16	3	SE	0.00
	4	13-Feb													70	21	16	4	SE	0.00
	5	14-Feb								✓					87	18	16	2	SW	0.00
	6	15-Feb				✓				✓					80	21	18	6	SE	0.00
3	1	17-Feb				✓									78	20	16	6	SE	0.00
	2	18-Feb				✓									75	21	17	4	SE	0.00
	3	19-Feb				✓				✓				✓	77	19	15	5	SE	0.00
	4	20-Feb				✓									71	20	15	4	SE	0.00
	6	22-Feb				✓									79	21	17	3	SE	0.00
4	1	24-Feb													87	22	19	8	SE	0.00
5	6	8-Mar													78	19	15	0	SE	0.00
6	5	14-Mar								✓				✓	79	17	13	3	SW	0.00
8	6	29-Mar	✓							✓				✓	94	14	13	0	NE	0.00
11	1	14-Apr													80	19	15	5	SE	0.00
13	1	28-Apr												✓	90	7	6	1	SE	0.10
23	7	13-Jul													88	10	9	0	SE	0.00
Frequency of occurrence out of total observation nights [%]			4	0	0	25	0	0	0	21	0	0	0	17	*NB: All first occurrences are highlighted in GRAY.*					

D.6.2.2 *Location of electrical discharge activity*

Table D-43: Location of electrical discharge activity observed with 0-lux Sony Camcorder, HTV-SR 29

Electrical discharge activities for HTV-SR 29: 0-LUX SONY CAMERA														
Week No.	Day	Date	AC				DC+				DC-			
			WDC	SCD	DBC	DBD	WDC	SCD	DBC	DBD	WDC	SCD	DBC	DBD
1	1	3-Feb												
	2	4-Feb												
	3	5-Feb												
	4	6-Feb												
	5	7-Feb												
	6	8-Feb												
	7	9-Feb												
2	2	11-Feb												
	3	12-Feb												
	4	13-Feb												
	5	14-Feb								Sheath 3, SW dir				
	6	15-Feb				Bottom shed 2, E dir				Sheaths 1, 2 & 3, W dir				
3	1	17-Feb				Sheath 3, S dir + Bottom shed 1, N dir								
	2	18-Feb				Sheath 1, E dir								
	3	19-Feb				Sheath 3 + bottom shed 1, all dir				Bottom shed 2, W dir				Bottom shed 2, E dir
	4	20-Feb				Sheath 3, all dir								
	6	22-Feb				Sheaths 2 & 3, E-dir								
4	1	24-Feb												
5	6	8-Mar												
6	5	14-Mar								Sheaths 1 & 3, all dir				Sheath 3, S dir
8	6	29-Mar	Bottom sheds 1 & 2, E dir							Sheath 2, E dir				Sheath 2, NE dir
11	1	14-Apr												
13	1	28-Apr												Sheath 1, NW dir
23	7	13-Jul												

D.7 Electrical discharge activity observations for glass disc insulators with a unified specific creepage length of 42 mm/kV – Glass disc 42

D.7.1 Corocam Mark I

D.7.1.1 *Frequency of occurrence*

Table D-44: Frequency of occurrence of electrical discharge activity observed with Corocam Mark I, Glass disc 42

Electrical discharge activities for Glass disc 42: COROCAM MARK I																					
Week No.	Day	Date	AC				DC+				DC-				Prevailing weather conditions						
			WDC	SCD	DBC	DBD	WDC	SCD	DBC	DBD	WDC	SCD	DBC	DBD	Relative humdity [%]	Ambient temperature [°C]	Dewpoint temperature [°C]	Wind speed [m/s]	Wind direction	Rainfall [mm]
	1	3-Feb																		
	2	4-Feb																		
	3	5-Feb																		
1	4	6-Feb																		
	5	7-Feb													82	20	16	2	SE	0.10
	6	8-Feb													75	21	16	5	SE	0.00
	7	9-Feb													57	26	17	3	SE	0.00
	2	11-Feb													75	19	15	2	SE	0.00
	3	12-Feb													78	20	16	3	SE	0.00
2	4	13-Feb													70	21	16	4	SE	0.00
	5	14-Feb													87	18	16	2	SW	0.00
	6	15-Feb													80	21	18	6	SE	0.00
	1	17-Feb													78	20	16	6	SE	0.00
	2	18-Feb													75	21	17	4	SE	0.00
3	3	19-Feb													77	19	15	5	SE	0.00
	4	20-Feb													71	20	15	4	SE	0.00
	6	22-Feb													79	21	17	3	SE	0.00
4	1	24-Feb								✓				✓	87	22	19	8	SE	0.00
5	6	8-Mar			✓	✓				✓					78	19	15	0	SE	0.00
6	5	14-Mar			✓					✓					79	17	13	3	SW	0.00
8	6	29-Mar						✓						✓	94	14	13	0	NE	0.00
11	1	14-Apr								✓				✓	80	19	15	5	SE	0.00
13	1	28-Apr								✓					90	7	6	1	SE	0.10
23	7	13-Jul								✓					88	10	9	0	SE	0.00
Frequency of occurrence out of total observation nights [%]			**0**	**0**	**8**	**4**	**0**	**4**	**0**	**25**	**0**	**0**	**0**	**13**	*NB: All first occurrences are highlighted in GRAY.*					

D.7.1.2 *Location of electrical discharge activity*

Table D-45: Location of electrical discharge activity observed with Corocam Mark I, Glass disc 42

Electrical discharge activities for Glass disc 42: COROCAM MARK I														
Week No.	Day	Date	AC				DC+				DC-			
			WDC	SCD	DBC	DBD	WDC	SCD	DBC	DBD	WDC	SCD	DBC	DBD
1	1	3-Feb												
	2	4-Feb												
	3	5-Feb												
	4	6-Feb												
	5	7-Feb												
	6	8-Feb												
	7	9-Feb												
2	2	11-Feb												
	3	12-Feb												
	4	13-Feb												
	5	14-Feb												
	6	15-Feb												
3	1	17-Feb												
	2	18-Feb												
	3	19-Feb												
	4	20-Feb												
	6	22-Feb												
4	1	24-Feb								Bottom glass, all dir				Bottom glass, all dir
5	6	8-Mar			Top glass, all dir	Bottom glass, all dir				Bottom glass, all dir				
6	5	14-Mar			Bottom glass, SW dir					Bottom glass, all dir				
8	6	29-Mar						Bottom glass, NW dir						Bottom glass, E dir
11	1	14-Apr								Bottom glass, all dir				Bottom glass, all dir
13	1	28-Apr								Bottom glass, N dir				
23	7	13-Jul								Bottom glass, all dir				

D.7.2 0-lux Sony Camcorder

D.7.2.1 *Frequency of occurrence*

Table D-46: Frequency of occurrence of electrical discharge activity observed with 0-lux Sony Camcorder, Glass disc 42

Electrical discharge activities for Glass disc 42: 0-LUX SONY CAMERA																				
Week No.	Day	Date	AC				DC+				DC-				Prevailing weather conditions					
			WDC	SCD	DBC	DBD	WDC	SCD	DBC	DBD	WDC	SCD	DBC	DBD	Relative humdity [%]	Ambient temperature [°C]	Dewpoint temperature [°C]	Wind speed [m/s]	Wind direction	Rainfall [mm]
1	1	3-Feb																		
	2	4-Feb																		
	3	5-Feb																		
	4	6-Feb																		
	5	7-Feb													82	20	16	2	SE	0.10
	6	8-Feb													75	21	16	5	SE	0.00
	7	9-Feb													57	26	17	3	SE	0.00
2	2	11-Feb													75	19	15	2	SE	0.00
	3	12-Feb													78	20	16	3	SE	0.00
	4	13-Feb													70	21	16	4	SE	0.00
	5	14-Feb													87	18	16	2	SW	0.00
	6	15-Feb													80	21	18	6	SE	0.00
3	1	17-Feb													78	20	16	6	SE	0.00
	2	18-Feb													75	21	17	4	SE	0.00
	3	19-Feb													77	19	15	5	SE	0.00
	4	20-Feb													71	20	15	4	SE	0.00
	6	22-Feb													79	21	17	3	SE	0.00
4	1	24-Feb								✓					87	22	19	8	SE	0.00
5	6	8-Mar													78	19	15	0	SE	0.00
6	5	14-Mar													79	17	13	3	SW	0.00
8	6	29-Mar								✓					94	14	13	0	NE	0.00
11	1	14-Apr								✓					80	19	15	5	SE	0.00
13	1	28-Apr													90	7	6	1	SE	0.10
23	7	13-Jul								✓					88	10	9	0	SE	0.00
Frequency of occurrence out of total observation nights [%]			0	0	0	0	0	0	0	17	0	0	0	0	*NB: All first occurrences are highlighted in GRAY.*					

D.7.2.2 *Location of electrical discharge activity*

Table D-47: Location of electrical discharge activity observed with 0-lux Sony Camcorder, Glass disc 42

Electrical discharge activities for Glass disc 42: 0-LUX SONY CAMERA														
Week No.	Day	Date	AC				DC+				DC-			
			WDC	SCD	DBC	DBD	WDC	SCD	DBC	DBD	WDC	SCD	DBC	DBD
	1	3-Feb												
	2	4-Feb												
	3	5-Feb												
1	4	6-Feb												
	5	7-Feb												
	6	8-Feb												
	7	9-Feb												
	2	11-Feb												
	3	12-Feb												
2	4	13-Feb												
	5	14-Feb												
	6	15-Feb												
	1	17-Feb												
	2	18-Feb												
3	3	19-Feb												
	4	20-Feb												
	6	22-Feb												
4	1	24-Feb								Bottom glass, all dir				
5	6	8-Mar												
6	5	14-Mar												
8	6	29-Mar								Bottom glass, all dir				
11	1	14-Apr								Bottom glass, all dir				
13	1	28-Apr												
23	7	13-Jul								Bottom glass, all dir				

E. APPENDIX E: A summary of detailed observations of insulator surface conditions per test cycle

E.1 Overview

This appendix presents a summary of the detailed observations that emanated from surface inspections conducted for all test insulators. The observations are given per test cycle for each set of test insulators with the same creepage length energized under AC, DC+ and DC-. Four test cycles were considered and are explained in Table E-48. All observations are given in note form, detailing all aspects that pertain to material deteriorations such as erosion. Additional details such pollution conditions and all other miscellaneous aspects such as salt crystals, plant threads and dead insects are also provided. It was envisaged that these conditions might have a role to play in the process that leads to insulator surface deteriorations. Thus, all observed conditions were noted and presented in the following sections.

Table E-48: Timelines for surface inspection test cycles

Timelines					
Test Cycle	**Date**	**Week No.**	***AC***	***DC+***	***DC-***
1	**10-Feb**	**2**			👓
	21-Feb	**3**		👓	
	3-Mar	**5**	👓		
2	**11-Mar**	**6**			👓
	24-Mar	**8**		👓	
	5-Apr	**9**	👓		
3	**13-Apr**	**10**			👓
	19-Apr	**11**		👓	
	4-May	**13**	👓		
4	**19-May**	**16**			👓
	7-Jun	**18**		👓	
	6-Jul	**22**	👓		
👓 = Surface inspections done					

E.2 Surface conditions for high temperature vulcanized, silicone rubber insulators with a unified specific creepage length of 84 mm/kV – HTV-SR 84

E.2.1 Test cycle 1

E.2.1.1 *HTV-SR 84 AC (Week 5)*

- *Deterioration*: Although not necessarily a form of deterioration, it is noteworthy that traces of dryband activities were generally observed on the shed bottoms and sheaths in all directions. No other signs of deterioration were observed.

- *Other observations:* Light pollution build-up was observed over the entire insulator, with medium to heavy pollution mainly on the shed tops and sheaths in the southward direction. Figure E-26 shows heavy pollution deposit (mainly sand) on the sheath of the test insulator in the southward direction. Salt crystals were observed in all directions, except in the southward direction.

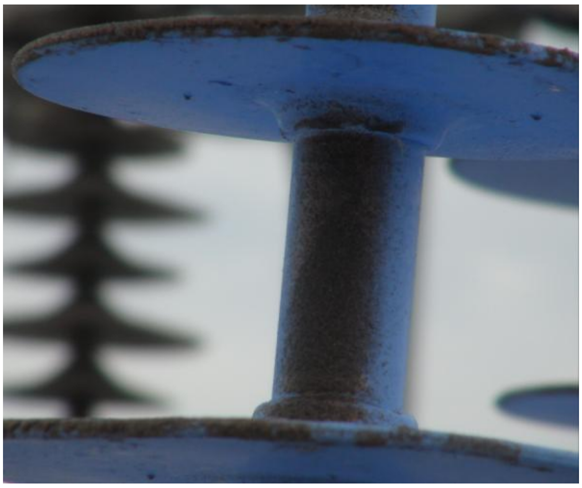

Figure E-26: Heavy pollution on the sheath of HTV-SR 84 AC (Week 5)

E.2.1.2 *HTV-SR 84 DC+ (Week 3)*

- *Deterioration*: Traces of dryband activity was prominently observed on the shed bottoms in all directions. This is evident from Figure E-27, depicting the drybands that were generally observed on the test insulator. No other signs of deterioration were observed.

Figure E-27: Traces of dryband activity visible on the shed bottom of HTV-SR 84 DC+ (Week 3)

- *Other observations:* Similar to the AC test insulator, light pollution build-up was observed over the entire insulator, with medium to heavy pollution (see Figure E-28(a)) on the shed tops and sheaths in the southward direction. Salt crystals were observed dominantly on the shed tops in all directions. Figure E-28(b) shows a sample of the salt crystals that were observed on the test insulator.

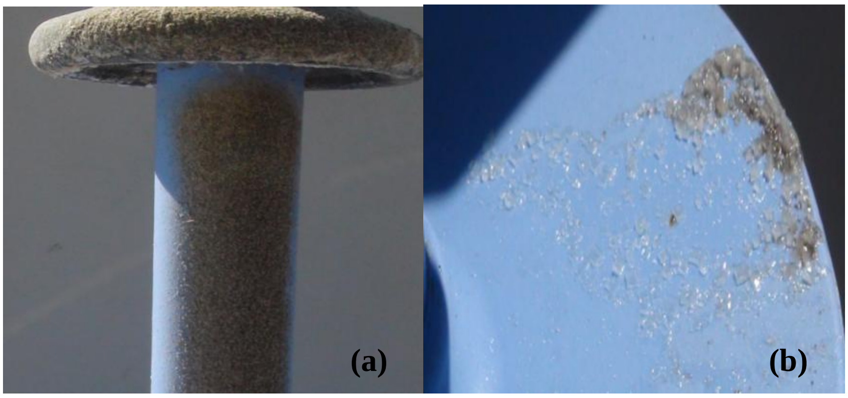

Figure E-28: (a) Heavy pollution deposits on the sheath and (b) salt crystals on the shed top of HTV-SR 84 DC+ (Week 3)

E.2.1.3 *HTV-SR 84 DC- (Week 2)*

- *Deterioration*: No signs of deterioration were observed in the second week of the test program.

- *Other observations:* The test insulator was still relatively clean with only light pollution build-up observed, mainly dominant on the shed tops and sheaths in the southward direction. Salt crystals were observed on the shed tops in all directions. The general pollution conditions and a close-up view of the salt crystals observed are depicted in Figure E-29 (a) & (b), respectively.

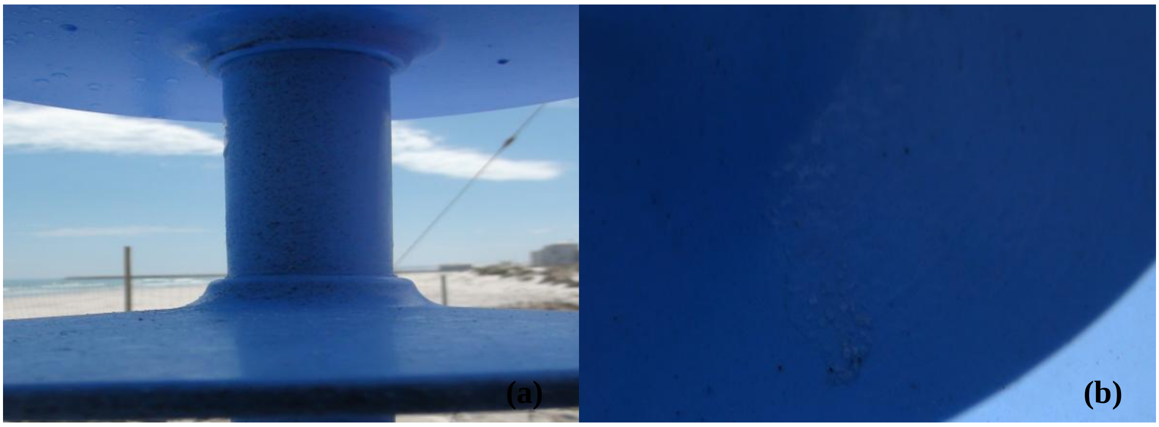

Figure E-29: (a) Light pollution build-up and (b) a close-up view of the salt crystals on HTV-SR 84 DC- (Week 2)

E.2.2 Test cycle 2

E.2.2.1 *HTV-SR 84 AC (Week 9)*

- *Deterioration*: Traces of dryband activities were observed on the shed bottoms and sheaths in all directions. Light crazing was observed on the sheaths in all directions. The first sign of material erosion was spotted on the sheath interfacing with the live end-fitting in the southward direction. It was particularly noted that evidence of dryband activity was visible around the crazed and eroded areas. This can be seen in Figure E-30.

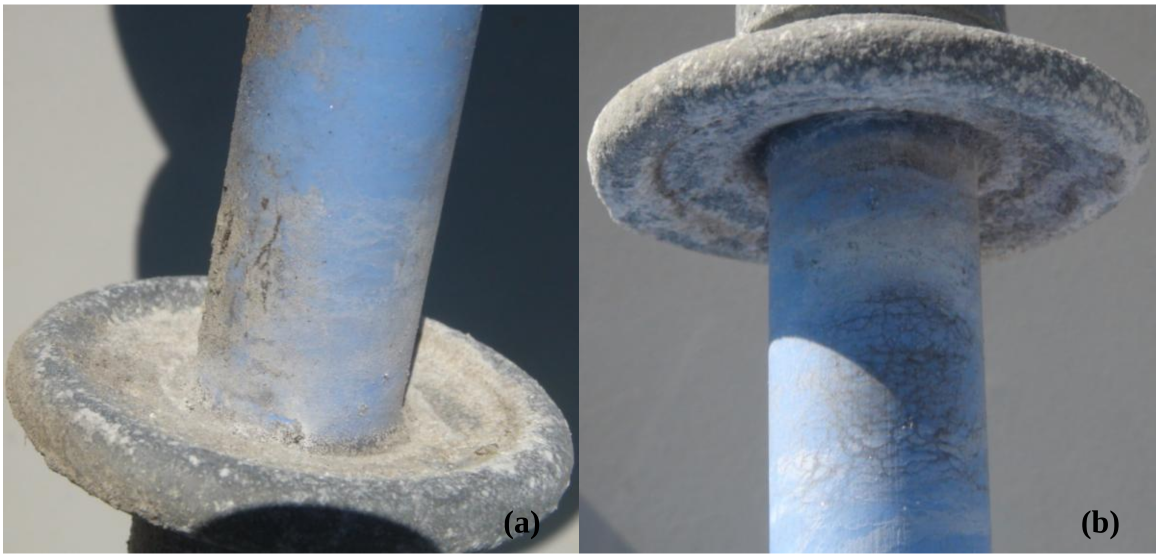

Figure E-30: Material erosion on the sheath interfacing with the live end-fitting and (b) light crazing on the sheath interfacing with the ground end-fitting (Week 9)

- *Other observations:* Light to medium pollution build-up was generally observed over the entire insulator, with medium to heavy pollution in the southward direction on the sheaths and shed tops. Salt crystals were observed in the eastward and northward directions. Plant threads were observed in all directions.

E.2.2.2 *HTV-SR 84 DC+ (Week 8)*

- *Deterioration*: Traces of dryband activities were observed in all directions, with a radial pattern on the shed bottoms, as it can be seen in Figure E-31 (b). Light crazing was observed on the shed bottoms and sheaths in all directions. The first sign of material erosion was observed on the sheath interfacing with the ground end-fitting and also on the bottom of the shed (shed 3) in the middle section of the insulator in the southward direction. Evidence of dark burns was visible on pollution layer around the dryband and eroded areas. See Figure E-31 (a).

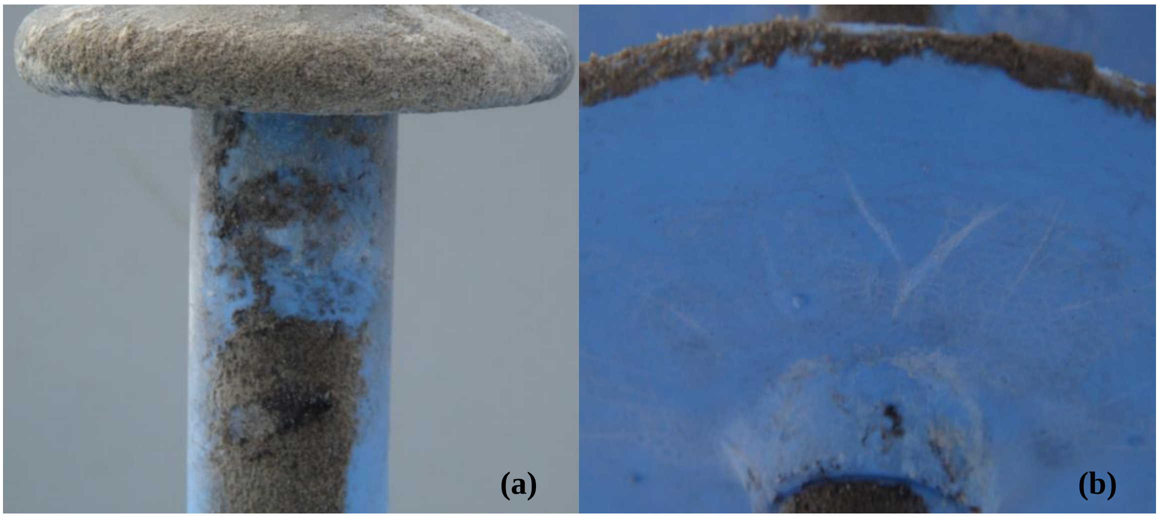

Figure E-31: (a) Dark burns on pollution layer on the sheath interfacing with the ground end-fitting and (b) drybands on the shed bottom of HTV-SR 84 DC+ (Week 8)

- *Other observations:* Light pollution build-up was generally observed over the entire insulator, with medium to heavy pollution in the southward direction on the shed tops and sheaths. Salt crystals were observed in all directions. Figure E-32 shows the one type of plant threads that were observed on the test insulator in all directions, except in the westward direction. A heavy pollution deposit is also clearly visible in Figure E-32.

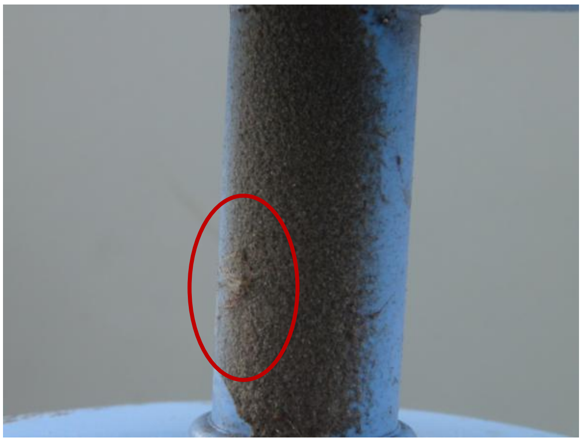

Figure E-32: A sample of the plant threads that were observed on HTV-SR 84 DC+(Week 8)

E.2.2.3 *HTV-SR 84 DC- (Week 6)*

- *Deterioration*: On the second inspection cycle, traces of dryband activities could now be observed, mainly on the sheaths. Light crazing was also generally observed on the sheaths in all directions. The first sign of material erosion was observed on the middle section sheath (sheath 4) along the heavy pollution deposit in the southward direction. See Figure E-33. Evidence of dryband activities was also observed around the eroded area.

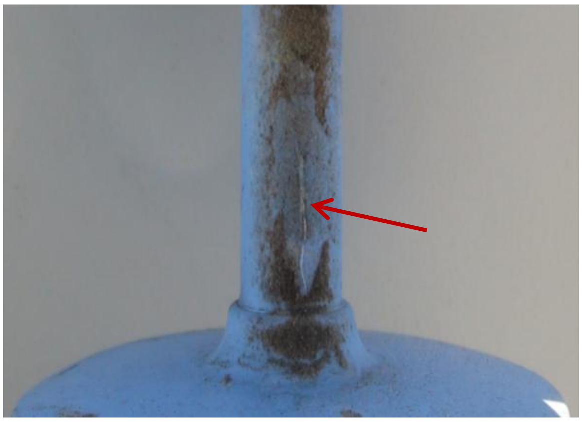

Figure E-33: Material erosion along the heavy pollution deposit on sheath 4 of HTV-SR 84 DC- (Week 6)

- *Other observations:* Light pollution was generally observed over the entire insulator, with medium to heavy pollution on the sheaths in the southward direction.

E.2.3 Test cycle 3

E.2.3.1 *HTV-SR 84 AC (Week 13)*

- *Deterioration*: Traces of dryband activities were observed on the shed bottoms and sheaths in all directions. Light crazing was generally observed on the sheaths in all directions. The same material erosion, as was first observed in week 9 (see Figure E-30), was still observable on the sheath interfacing with the live end-fitting in the southward direction. This is depicted in Figure E-34. No new instance of material erosion was observed.

Figure E-34: Material erosion on the sheath interfacing with the live end-fitting of HTV-SR 84 AC (Week 13)

- *Other observations:* Light to medium pollution build-up was observed over the entire insulator, with medium to heavy pollution on the shed tops and sheaths in the southward direction. Salt crystals were observed in the eastward direction. Plant threads were observed in the eastward and southward directions. A dead insect was observed on the sheath interfacing with the live end-fitting in the northward direction.

E.2.3.2 *HTV-SR 84 DC+ (Week 11)*

- *Deterioration*: Dryband traces, with a radial pattern on the shed bottoms, were observed in all directions. Light crazing was observed in all directions. More instances of material erosion were observed on sheath 5 closest to the ground end-fitting in the southward direction and also on the bottom of shed 3 in the westward direction. These were in addition to the first signs of material erosion previously reported on the sheath interfacing with the ground end-fitting and also on the bottom of the shed 3 in the southward direction in section E.2.2.2. Figure E-35 shows the light erosion and the signs of light crazing and drybands that were observed on the bottom of shed 3. Dark burns on pollution were observed around dryband and eroded areas.

Figure E-35: Light material erosion, light crazing and drybands on the bottom of shed 3 of HTV-SR 84 DC+ (Week 11)

- *Other observations:* Light pollution build-up was observed over the entire insulator, with medium to heavy pollution on the shed tops and sheaths in the southward direction. Salt crystals were observed in all directions. Plant threads were observed in all directions, except in the northward direction. Dead insects (flies) were observed in the northward and southward directions. Samples of the plant threads and the dead insects that were observed are shown in Figure E-36.

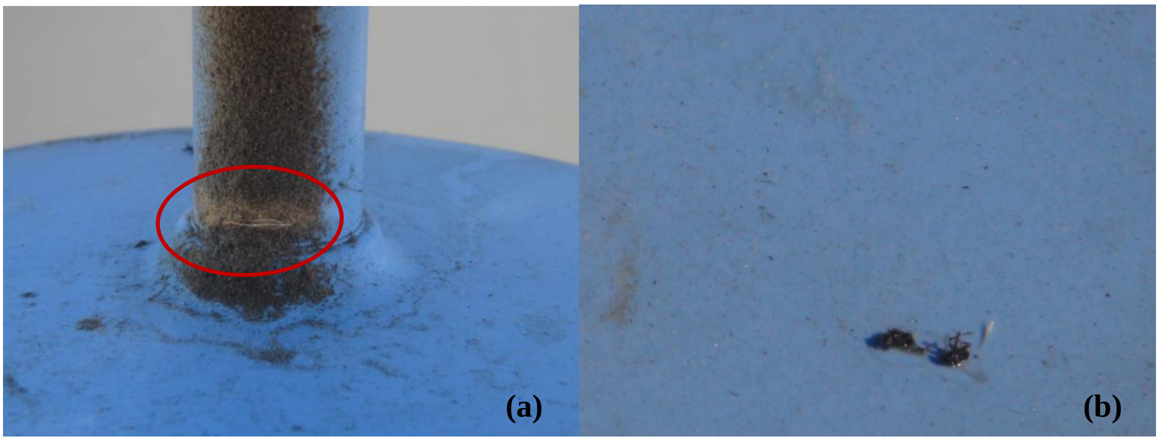

Figure E-36: Samples of (a) the plant threads and (b) the dead insects that were observed on HTV-SR 84 DC+ (Week 11)

E.2.3.3 *HTV-SR 84 DC- (Week 10)*

- *Deterioration*: Traces of dryband activities (with visible dark burns on the pollution layer) were observed dominantly on the shed bottoms and sheaths in all directions. Light crazing was prominently observed on the sheaths in all directions. In addition to material erosion noted on sheath 4 in the southward direction (see Figure E-33) in week 6, more material erosion was now observed on the sheaths interfacing with both the ground and live end-fittings in the southward direction. The light erosion observed on the sheath interfacing with the ground end-fitting is shown in Figure E-37.

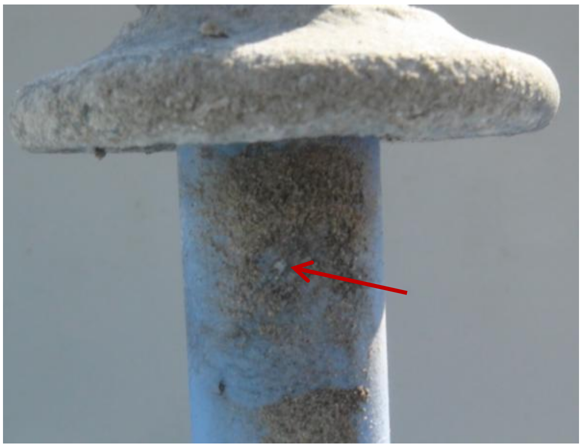

Figure E-37: Material erosion on the sheath interfacing with the ground end-fitting along the heavy pollution deposit on HTV-SR 84 DC- (Week 10)

- *Other observations:* Light pollution was generally observed over the entire insulator, with medium to heavy pollution in the southward direction. Salt crystals and plant threads were also observed in all directions.

E.2.4 Test cycle 4

E.2.4.1 *HTV-SR 84 AC (Week 22)*

- *Deterioration*: Traces of dryband activities were generally observed in all directions. Light crazing was still observed on the shed bottoms and sheaths in all directions. More signs of material erosion were observed on the sheath interfacing with the live end-fitting in the northward direction, in addition to the erosion that was noted on the same sheath in weeks 9 and 13 in the southward direction. Additional instances of material erosion were observed on the sheath interfacing with the ground end-fitting in all directions, except in the eastward direction. Dark burns were observed around dryband and eroded areas. Figure E-38 and Figure E-39 depict material erosion on the sheath interfacing with the live and ground end-fittings, respectively.

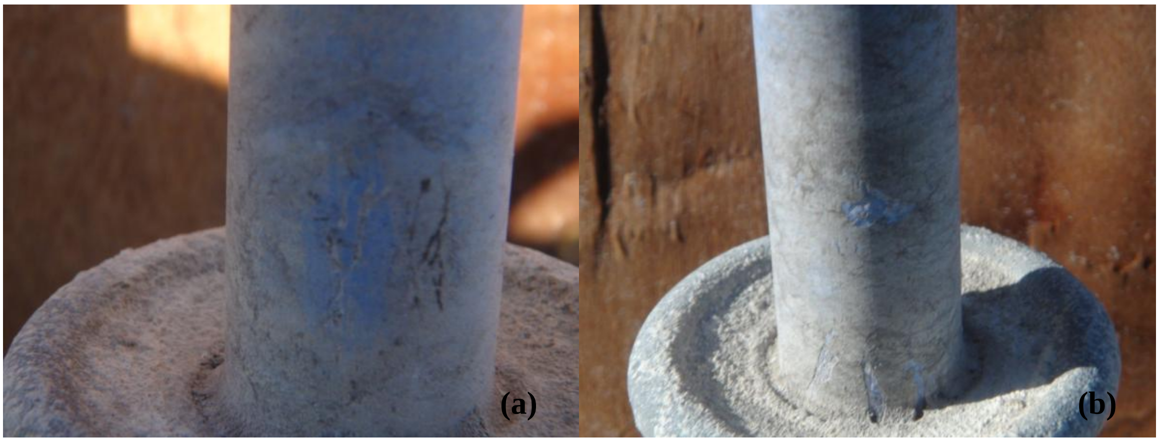

Figure E-38: Material erosion on the sheath interfacing with the live end-fitting in the (a) southward direction and (b) northward direction (Week 22)

Figure E-39: Material erosion on the sheath interfacing with the ground end-fitting (Week 22)

- *Other observations:* Light to medium pollution build-up was observed over the entire insulator in all directions. Salt crystals were observed in the eastward direction. Plant threads were observed in all directions, except in the northward direction. The first instances of rust patches were observed on sheath 4 (in the middle section of insulator) in the eastward direction and also on the top of shed 4 in the northward direction.

E.2.4.2 *HTV-SR 84 DC+ (Week 18)*

- *Deterioration*: Dryband traces were observed in all directions. Light crazing was observed on the shed bottoms and sheaths in all directions. All instances of material erosion, as previously reported for week 11, were observed in week 18. Additional erosion was now observed on the sheath interfacing with the live end-fitting in all directions, except in the eastward direction. The erosion in the southward direction is shown in Figure E-40. Blue patches (some forms of discoloration) were observed on the top of shed 4 in the eastward direction, the area around which some rust patches were also observed.

Figure E-40: Material erosion on the sheath interfacing with the live end-fitting in the southward direction (Week 18)

- *Other observations:* Light pollution build-up was observed over the entire insulator in all directions. No salt crystals were observed. Plant threads were observed in all directions, except in the northward direction. Rust patches were observed on the sheaths and shed tops in all directions.

E.2.4.3 *HTV-SR 84 DC- (Week 16)*

- *Deterioration*: Traces of dryband activities were observed on most parts of the insulator. Light crazing was observed on the sheaths, especially dominant around dryband areas. The instances of material erosion on the sheaths interfacing with both the ground and live end-fittings and also on sheath 4 in the southward direction were observed, as previously reported for week 10. Additional erosion was however observed on the sheath interfacing with the live end-fitting in the westward direction, as shown in Figure E-41. Blue patches (some forms of discoloration) were observed on the shed tops in all directions, except in the westward direction. It should be mentioned here that no evidence of electrical discharge activities was observed in the vicinities of the discoloured areas. See Figure E-42 below.

Figure E-41: Material erosion on the sheath interfacing the the live end-fitting in the westward direction (Week 16)

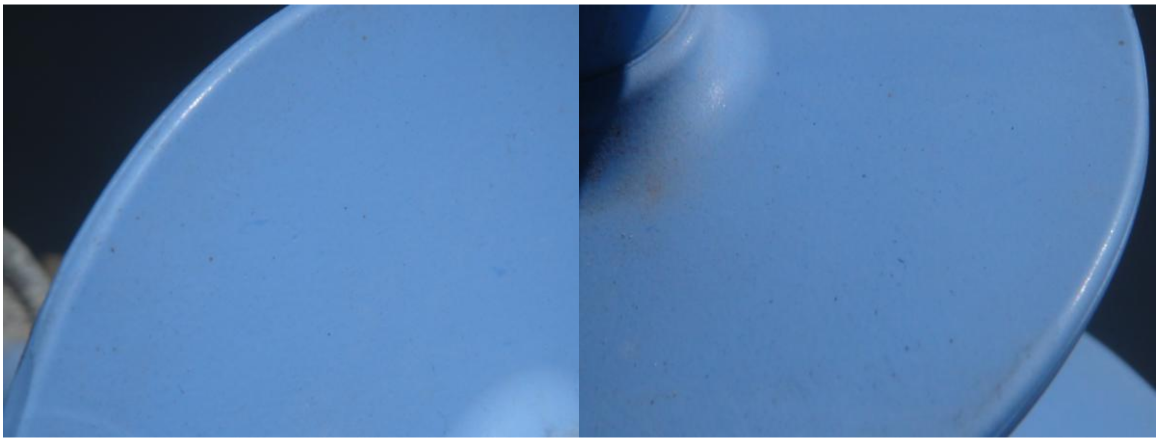

Figure E-42: Blue patches on the shed tops (a form of discoloration) of HTV-SR 84 DC- (Week 16) (*please zoom in*)

- *Other observations:* Light pollution was observed over the entire insulator, with medium pollution on the sheaths in the southward direction. Salt crystals and plant threads were also observed.

E.3 Surface conditions for high temperature vulcanized, silicone rubber insulators with a unified specific creepage length of 72 mm/kV – HTV-SR 72

E.3.1 Test cycle 1

E.3.1.1 *HTV-SR 72 AC (Week 5)*

- *Deterioration*: Traces of dryband activity was observed in all directions. Dark burns were evident on the pollution layer on the sheaths interfacing with both the ground and live end-fittings in the southward direction, as shown in Figure E-43. No other signs of deterioration were observed.

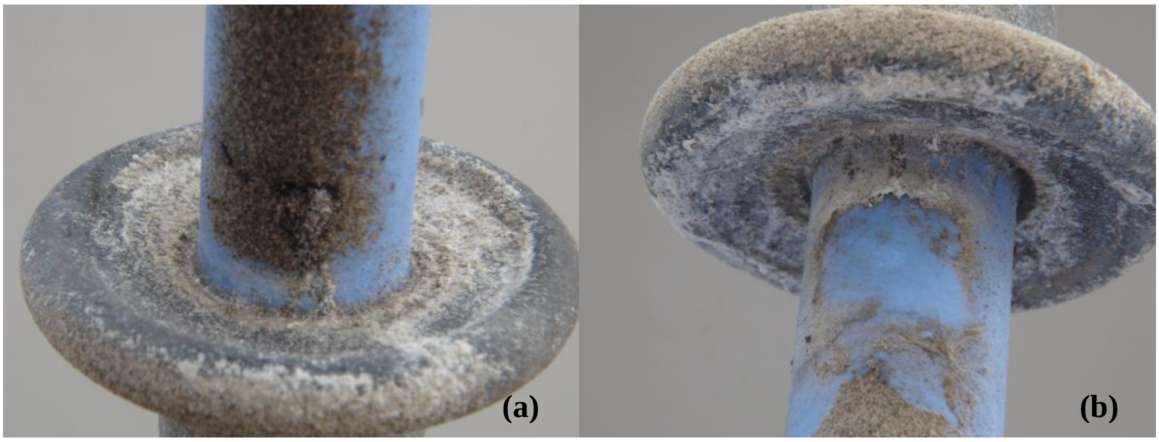

Figure E-43: Evidence of dryband activity on the sheaths interfacing with the (a) live and (b) ground end-fittings in the southward direction (Week 5)

- *Other observations:* Light to medium pollution build-up was observed over the entire insulator, with medium to heavy pollution on the shed tops and sheaths in the southward direction. Salt crystals were observed in all directions.

E.3.1.2 *HTV-SR 72 DC+ (Week 3)*

- *Deterioration*: Traces of dryband activities were prominently observed on the shed bottoms in all directions. Figure E-44 shows the traces of dryband activities on the shed bottom. No other signs of deterioration were observed.

- *Other observations:* Light pollution build-up was observed over the entire insulator, with medium to heavy pollution (see Figure E-44) on the shed tops and sheaths in the southward direction. Salt crystals were observed in all directions.

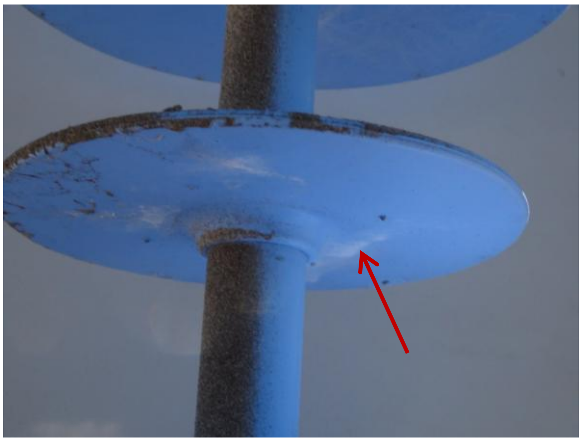

Figure E-44: Traces of dryband activities on the shed bottom and heavy pollution on the sheaths of HTV-SR 72 DC+ (Week 3)

E.3.1.3 *HTV-SR 72 DC- (Week 2)*

- *Deterioration*: No signs of deterioration were observed in the second week of the test program.

- *Other observations:* As would be expected, just about a week after the installation of the test insulator, light pollution build-up was observed over the entire insulator - mainly dominant on the shed tops and sheaths in the southward direction. Salt crystals were observed on the shed tops in all directions.

E.3.2 Test cycle 2

E.3.2.1 *HTV-SR 72 AC (Week 9)*

- *Deterioration*: Traces of dryband activities were observed in all directions. The first instance of light crazing was observed on the sheaths in all directions. Dark burns were observed on the pollution layer on the sheath interfacing with the live end-fitting in the southward direction. It is evident from Figure E-45 (a) that intense dryband arcing occurred on the sheath – likely to have caused erosion although it could not be confirmed. The first sign of material erosion was spotted on sheath 5 (toward the ground end-fitting) in the southward direction. Figure E-45 (b) depicts the erosion that was spotted on sheath 5, along the heavy pollution deposit in the southward direction.

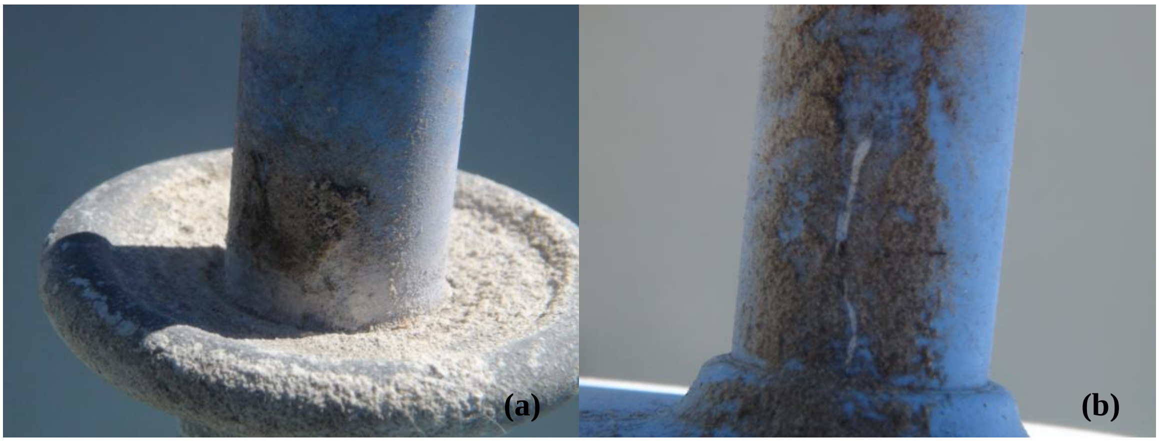

Figure E-45: (a) Dark burns on the sheath interfacing with the live end end-fitting and (b) material erosion on sheath 5 in the southward direction (Week 9)

- *Other observations:* Light to medium pollution build-up was observed over the entire insulator, with medium to heavy pollution in the southward direction on the shed tops and sheaths. Salt crystals were observed in all directions. Plant threads were observed in all directions. A dead insect was observed on sheath 3 in the eastward direction, as shown in Figure E-45.

Figure E-46: Dead insect (fly) spotted on sheath 3 of HTV-SR 72 AC in the eastward direction (Week 9)

E.3.2.2 *HTV-SR 72 DC+ (Week 8)*

- *Deterioration*: Traces of dryband activities were observed in all directions, with a radial pattern on the shed bottoms. See Figure E-47. Light crazing was observed on the shed bottoms and sheaths in all directions. The first sign of material erosion was observed on the sheath interfacing with the ground end-fitting in the southward direction and also on sheath 2 (toward the live end-fitting) in the southward direction.

Figure E-47: Traces of dryband activities on the shed bottom of HTV-SR 72 DC+ (Week 8)

- *Other observations:* Light pollution build-up was observed over the entire insulator, with medium to heavy pollution on the shed tops and sheaths in the southward direction. Salt crystals were observed in all directions, except in the southward direction. Plant threads were observed in all directions. A sample of the plant threads that were observed on the test insulator is depicted in Figure E-48.

Figure E-48: A sample of plant threads observed on HTV-SR 72 DC+ (Week 8)

E.3.2.3 *HTV-SR 72 DC- (Week 6)*

- *Deterioration*: Traces of dryband activities were dominantly observed on the sheaths in all directions. The first instance of light crazing was observed on the sheaths in all directions. The first sign of material erosion was observed on the sheath interfacing with the ground end-fitting, along the heavy pollution layer in the southward direction. This is shown below in Figure E-49.

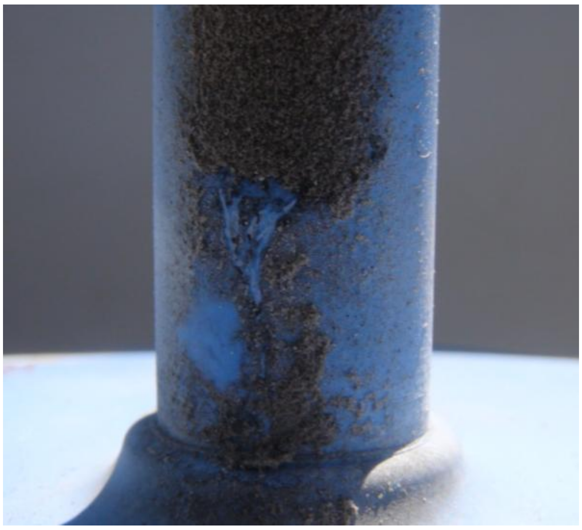

Figure E-49: Material erosion on the sheath interfacing with the ground end-fitting in the southward direction (Week 6)

- *Other observations:* Light pollution was generally observed over the entire insulator, with medium to heavy pollution on the sheaths in the southward direction.

E.3.3 Test cycle 3

E.3.3.1 *HTV-SR 72 AC (Week 13)*

- *Deterioration*: Traces of dryband activity were observed in all directions. Light crazing was observed in all directions. In addition to the first sign of material erosion that was observed on sheath 5 in the southward direction in week 9, more instances of erosion were now observed on the sheath interfacing with the live end-fitting in the northward and southward directions, on the sheath interfacing with the ground end-fitting and also on sheath 3 in the southward direction. Dark burns on pollution were observed on sheath 3 in the southward direction. The instances of material erosion on sheaths 3 & 5 and on the sheath interfacing with the live end-fitting are shown in Figure E-50 and Figure E-51, respectively.

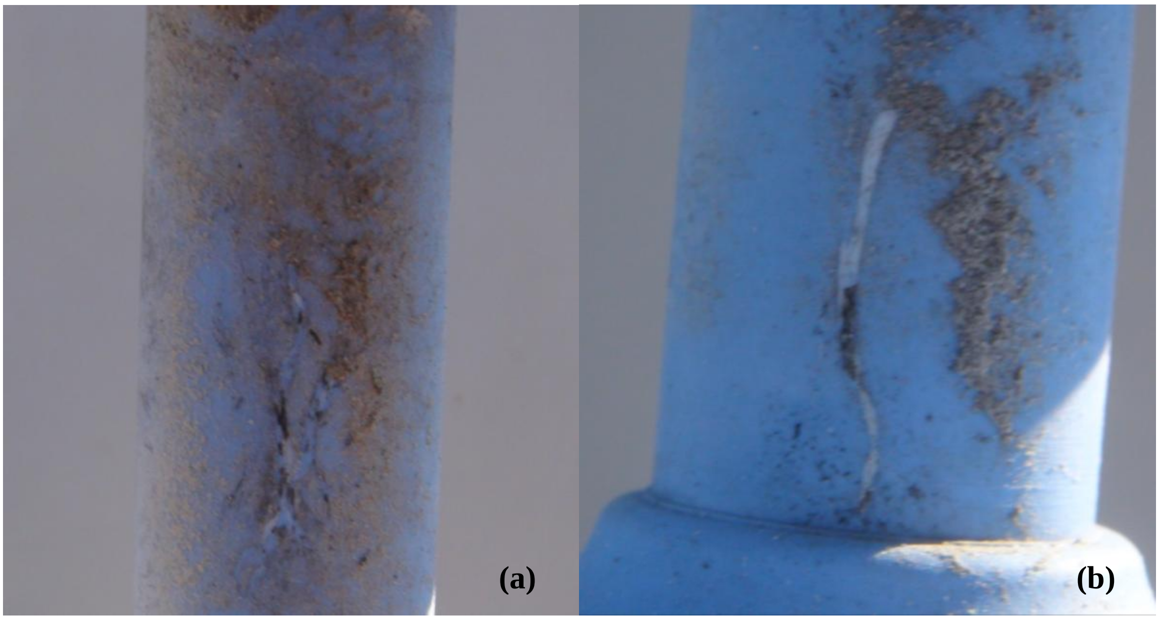

Figure E-50: Material erosion on (a) sheath 3 and (b) sheath 5 in the southward direction (Week 13)

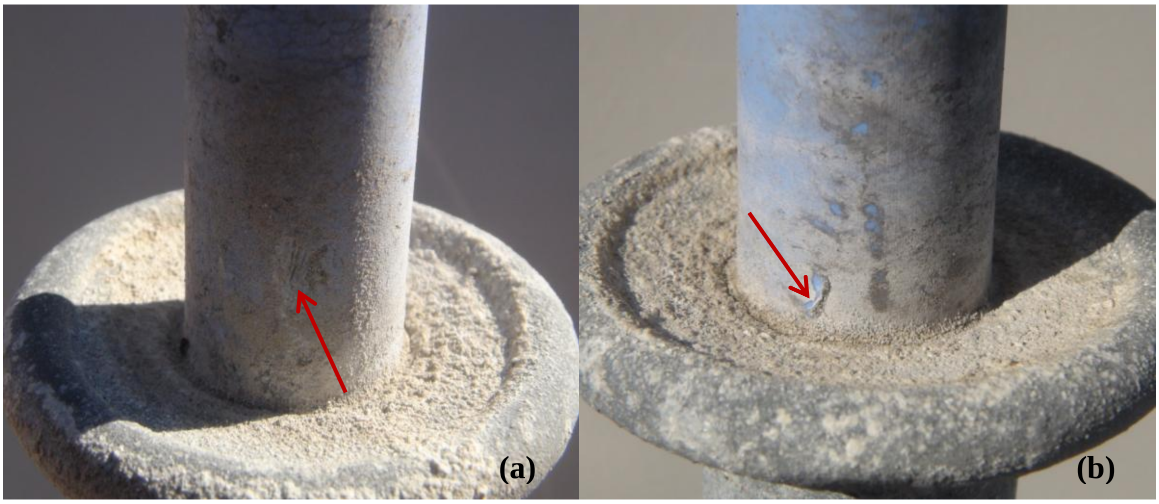

Figure E-51: Material erosion on the sheath interfacing with the live end-fitting in the (a) southward and (b) northward directions (Week 13)

- *Other observations:* Light to medium pollution build-up was observed over the entire insulator, with medium to heavy pollution on the shed tops and sheaths in the southward direction. Salt crystals were observed in the northward direction. Plant threads were observed in all directions.

E.3.3.2 *HTV-SR 72 DC+ (Week 11)*

- *Deterioration*: Traces of dryband activities were observed in all directions. See Figure E-52 (a). Light crazing was generally observed on the shed bottoms and sheaths in all directions. The instances of material erosion, as previously reported for week 8, were still observable on the sheath interfacing with the ground end-fitting in the southward direction and also on sheath 2 in the southward direction. Additional material erosion was noted on the sheath interfacing with the ground end-fitting in the northward direction; on the sheath interfacing with the live end-fitting and on the bottom of shed 3 in the southward direction. Figure E-52 shows the erosion that was observed on the bottom of shed 3 and on the sheath interfacing with the ground end-fitting.

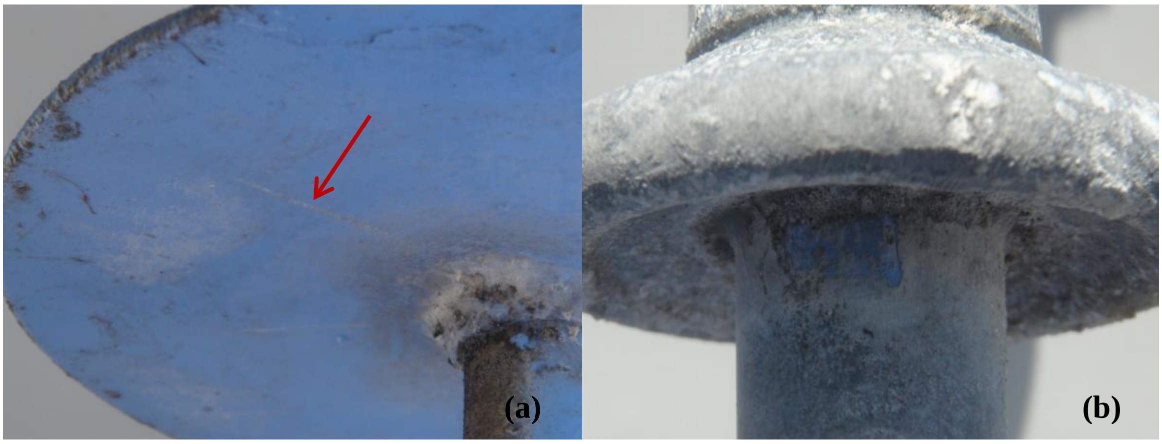

Figure E-52: Material erosion (a) on the bottom of shed 3 in the southward direction and (b) on the sheath interfacing with the ground end-fitting in the northward direction (week 11)

- *Other observations:* Light pollution build-up was observed over the entire insulator, with medium to heavy pollution on the shed tops and sheaths in the southward direction. Salt crystals were observed in all directions. Plant threads were observed in all directions, except in the westward direction. Dead insects were observed in the westward and southward directions.

E.3.3.3 *HTV-SR 72 DC- (Week 10)*

- *Deterioration*: Traces of dryband activity were dominantly observed on the shed bottoms and sheaths. Light crazing was commonly observed on the sheaths in all directions. Material erosion was now observed on the sheath interfacing with the live end-fitting in the southward direction, additional to the first sign of erosion in the southward direction noted on the sheath interfacing with the ground end-fitting in week 6. The new instance of material erosion is shown in Figure E-53.

Figure E-53: Material erosion on the sheath interfacing with the live end-fitting (Week 10)

- *Other observations:* Light pollution was observed over the entire insulator, with medium to heavy pollution on the shed tops and sheaths in the southward direction. Salt crystals and plant threads were also observed. Dead insects were observed on the shed tops in the westward and southward directions. The dead insect that was observed in the southward direction is shown in Figure E-54.

Figure E-54: Dead insect on the shed top in the southward direction (Week 10)

E.3.4 Test cycle 4

E.3.4.1 *HTV-SR 72 AC (Week 22)*

- *Deterioration*: Traces of dryband activities were observed in all directions. Light crazing was observed on the shed bottoms and sheaths in all directions. The instances of material erosion were noted to have increased - now observed on the sheaths interfacing with both the live and ground end-fitting in all directions, except in the eastward direction. Figure E-56 depicts some instances of material erosion observed on the sheaths interfacing with both the live and ground end-fittings. The erosion on sheaths 3 & 5 was still observed in the southward direction, without any more deterioration since week 13 as shown in Figure E-55. The first instances of blue patches (some form of discoloration) were observed on the top and bottom of shed 3 in the northward direction and also on top of shed 4 in the eastward direction.

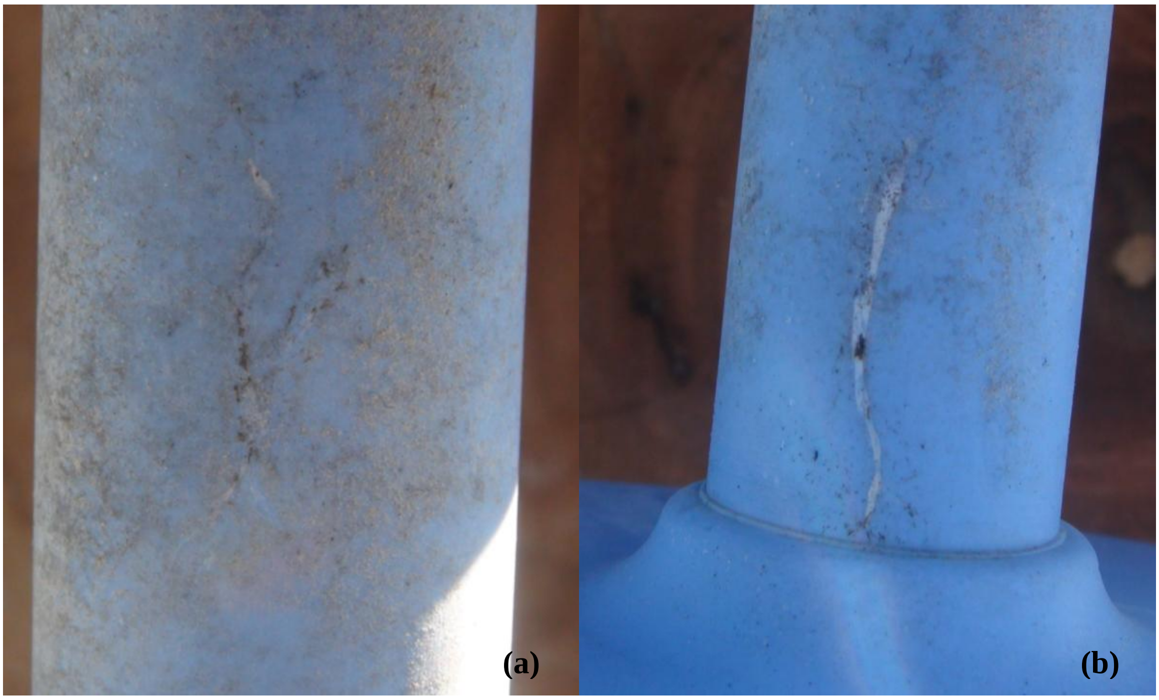

Figure E-55: Material erosion on (a) sheath 3 and (b) sheath 5 in the southward direction (Week 22)

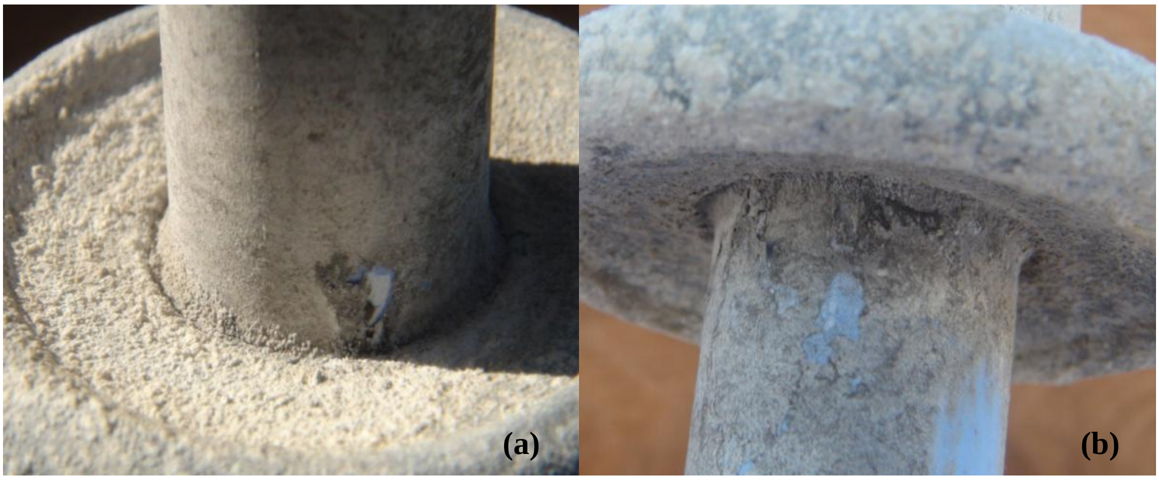

Figure E-56: Material erosion on the sheaths interfacing with the (a) live end-fitting and (b) ground end-fitting (Week 22)

- *Other observations:* Light to medium pollution build-up was observed over the entire insulator in all directions. Salt crystals were observed in all directions, except in the southward direction. Plant threads were observed in all directions. Rust patches were observed on the top of shed 1 in the westward direction and also on the top of shed 3 in the eastward direction.

E.3.4.2 *HTV-SR 72 DC+ (Week 18)*

- *Deterioration*: Traces of dryband activities were observed in all directions. Light crazing was observed on the shed bottoms and sheaths in all directions. More instances of material erosion were observed on the sheaths interfacing with both the live and ground end-fittings – now observed in the northward and southward directions. Figure E-57 shows the erosion noted on the sheath interfacing with the ground end-fitting in the southward direction. The erosions on sheath 2 and bottom of shed 3 were still observed in the southward direction. Blue patches (some form of discoloration) were observed on the top of shed 4 in the northward direction.

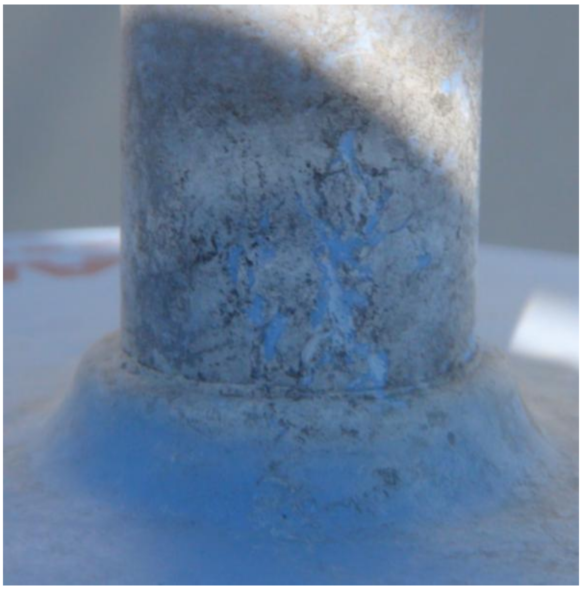

Figure E-57: Material erosion on the sheath interfacing with the ground end-fitting (Week 18)

- *Other observations:* Light pollution build-up was observed over the entire insulator in all directions. No salt crystals were observed. Plant threads were observed in all directions, except in the westward direction. Rust patches were observed on the sheath interfacing with the live end-fitting in the northward direction, as shown in Figure E-58.

Figure E-58: Rust pacthes on the sheath interfacing with the live end-fitting (Week 18)

E.3.4.3 *HTV-SR 72 DC- (Week 16)*

- *Deterioration*: Traces of dryband activities were observed on most parts of the insulator. Light crazing was observed on the sheaths, especially around the dryband areas. The instances of material erosion, as reported for week 10, were observed on the sheaths interfacing with both the live and ground end-fittings in the southward direction. Additional erosion was noted on the sheath interfacing with the live end-fitting in the westward direction and also on sheath 5 (toward the ground end-fitting) in the eastward direction. Blue patches (spots and radial) were observed on shed tops in all directions, except in the westward direction. See Figure E-59.

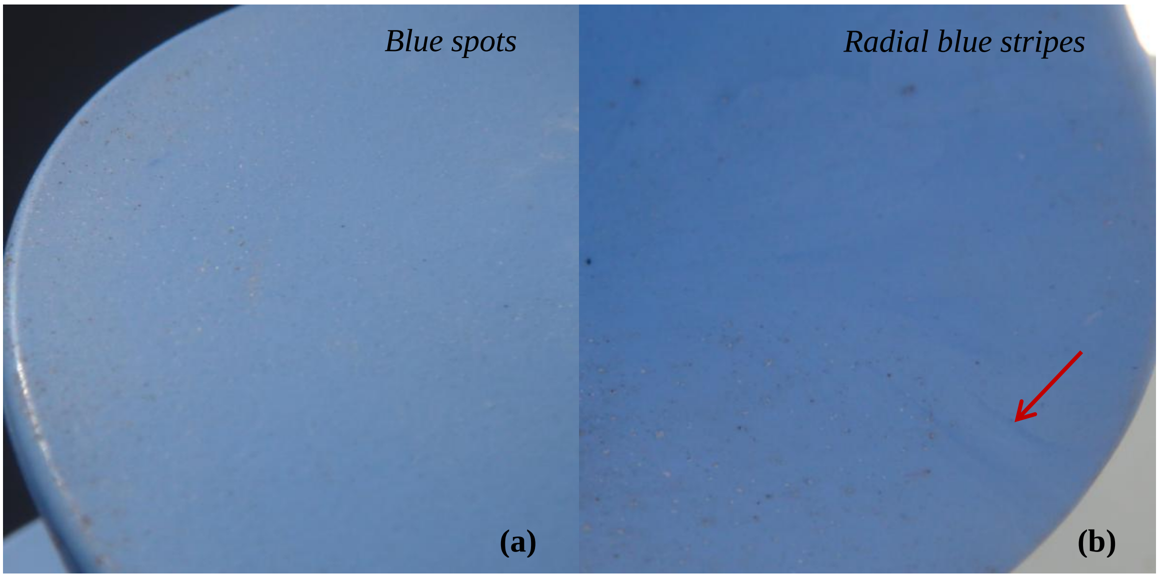

Figure E-59: Some form of discoloration on the shed top in patterns of darker blue (a) spot and (b) radial patches (Week 16) ***(please zoom in)***

- *Other observations:* Light pollution was observed over the entire insulator, with medium pollution on the sheaths in the southward direction. A dead insect and plant thread were observed in all directions. Rust spots were observed on top of shed 1 (toward the live end-fitting) in the northward direction.

E.4 Surface conditions for high temperature vulcanized, silicone rubber insulators with a unified specific creepage length of 56 mm/kV – HTV-SR 56

E.4.1 Test cycle 1

E.4.1.1 *HTV-SR 56 AC (Week 5)*

- *Deterioration*: Traces of dryband activities were observed in all directions. Dark burns were observed on pollution layer on the sheaths interfacing with the ground end-fitting and also on sheath 3 (middle section of insulator) in the southward direction. It was suspected that an intense dryband activity had occurred. This was in relation to the dark burns observed, as shown in Figure E-60. No other signs of deterioration were observed.

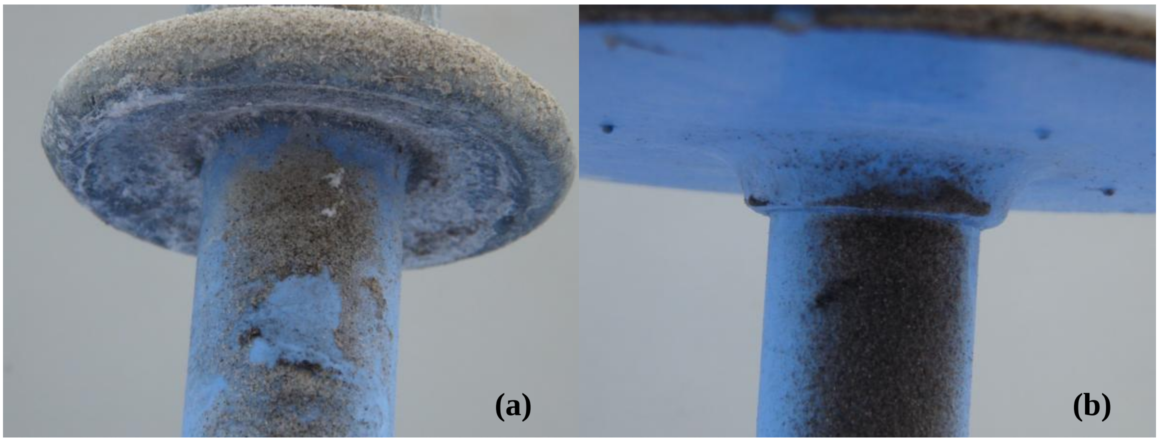

Figure E-60: Traces of dark burns on pollution layer (a) on the sheath interfacing with the ground end-fitting and (b) on sheath 3 in the southward direction (Week 5)

- *Other observations:* Light pollution build-up was observed over the entire insulator, with medium to heavy pollution on the shed tops and sheaths in the southward direction. Salt crystals were observed in all directions.

E.4.1.2 *HTV-SR 56 DC+ (Week 3)*

- *Deterioration*: Traces of dryband activities were generally observed on the shed bottoms, shed tops and sheaths in all directions. Figure E-61 shows traces of dryband activities observed on the shed tops. No other signs of deterioration were observed.

Figure E-61: Traces of dryband activities on the shed top of HTV-SR 56 DC+ (Week 3)

- *Other observations:* Light pollution build-up was observed over the entire insulator, with medium to heavy pollution on the shed tops and sheaths in the southward direction. Salt crystals were observed in all directions.

E.4.1.3 *HTV-SR 56 DC- (Week 2)*

- *Deterioration*: No signs of deterioration were observed in week 2.

- *Other observations:* Pollution build-up was generally observed in the southward direction, with light pollution on the shed tops and bottoms and medium pollution on the sheaths. Salt crystals were largely observed in the westward and northward directions.

E.4.2 Test cycle 2

E.4.2.1 *HTV-SR 56 AC (Week 9)*

- *Deterioration*: Dryband traces were observed in all directions. Light crazing was observed on the sheaths in all directions. The first signs of material erosion were observed on the sheath interfacing with the live end-fitting and also on sheaths 3 (middle section of insulator) & 4 (toward the ground end-fitting) in the southward direction. All instances of erosion were noticed along the heavy pollution deposits, as it can be seen in Figure E-62 and Figure E-63.

Figure E-62: Material erosion on the sheath interfacing with the live end-fitting in the southward direction (Week 9)

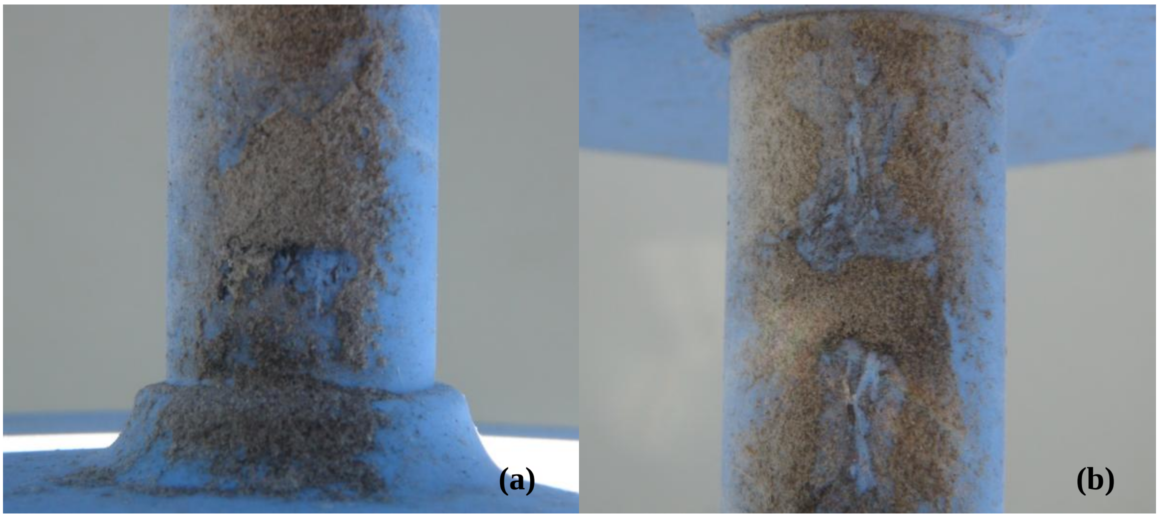

Figure E-63: Material erosion on (a) sheath 3 and (b) sheath 4 in the southward direction (Week 9)

- *Other observations:* Light pollution build-up was observed over the entire insulator, with medium to heavy pollution on the shed tops and sheaths in the southward direction. Salt crystals were observed in all directions, except in the southward direction. Plant threads were observed in all directions, except in the northward direction.

E.4.2.2 *HTV-SR 56 DC+ (Week 8)*

- *Deterioration*: Traces of dryband activities were observed in all directions. Light crazing was observed on the shed bottoms and sheaths in all directions. The first instance of material erosion was observed on the sheath interfacing with the ground end-fitting in the southward direction, as shown in Figure E-64.

Figure E-64: Material erosion observed on the sheath interfacing with the ground end-fitting in the southward direction (Week 8)

- *Other observations:* Light pollution build-up was observed over the entire insulator, with medium to heavy pollution on the shed tops and sheaths in the southward direction. Salt crystals were observed in the northward direction. No plant threads were observed.

E.4.2.3 *HTV-SR 56 DC- (Week 6)*

- *Deterioration*: Traces of dryband activities were observed in all directions. Light crazing was generally observed on the sheaths in all directions. No other signs of deterioration were observed.

- *Other observations:* Light pollution was observed over the entire insulator, with medium to heavy pollution on the sheaths in the southward direction.

E.4.3 Test cycle 3

E.4.3.1 *HTV-SR 56 AC (Week 13)*

- *Deterioration*: Traces of dryband activities were observed in all directions. Light crazing was observed on the shed bottoms and sheaths in all directions. The first signs of material erosion on the sheath interfacing with the live end-fitting and also on sheaths 3 (middle section of insulator) & 4 (toward the ground end-fitting) in the southward direction were still observable, as reported in week 9. Additional instances of erosion were now observed on the sheath interfacing with the ground end-fitting and sheath 2 in the southward direction. Dark burns were observed on pollution around the eroded area on sheath 2. Figure E-65 shows the instances of erosion as observed on sheath 3 and on the sheath interfacing with the live end-fitting.

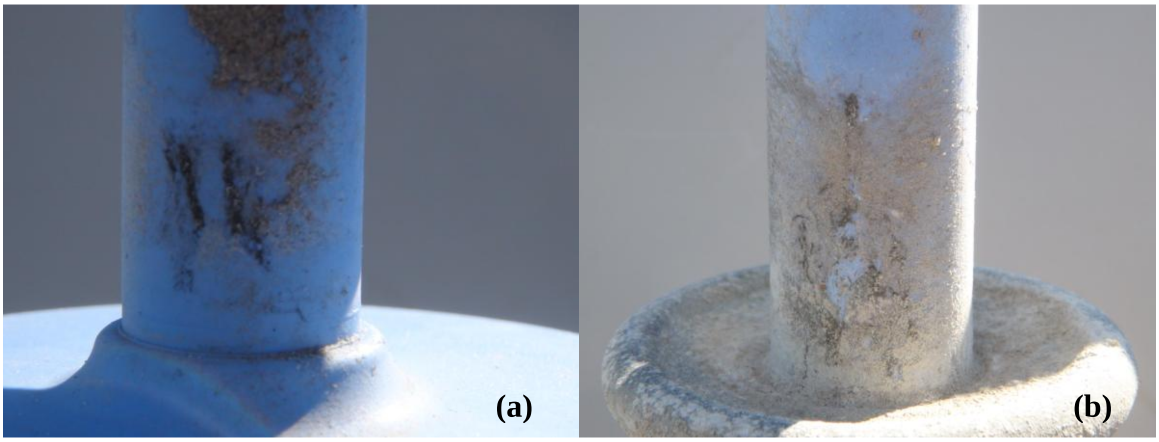

Figure E-65: Instances of material erosion (a) on sheath 3 and (b) on the sheath interfacing with the live end-fitting in the shouthward direction (Week 13)

- *Other observations:* Light to medium pollution build-up was observed over the entire insulator, with medium to heavy pollution on the shed tops and sheaths in the southward direction. Salt crystals were observed in the northward direction. Plant threads were observed in all directions, except in the northward direction.

E.4.3.2 *HTV-SR 56 DC+ (Week 11)*

- *Deterioration*: Dryband traces were observed on the shed bottoms and sheaths in all directions. Light crazing was observed on the shed bottoms and sheaths in all directions. As was reported for week 8, material erosion was still observed on the sheath interfacing with the ground end-fitting in the southward direction. It should be stated that no further erosion was observed on this sheath and as it can be seen on Figure E-66 (a), the eroded area is now stuffed with pollution deposits. Additional erosion was now observed on the sheath interfacing with the live end-fitting in the southward direction (see Figure E-66 (b)).

- *Other observations:* Light pollution build-up was observed, with medium to heavy pollution in the southward direction on the sheaths and shed tops. Salt crystals were observed in all directions. Plant threads were observed in all directions. A dead bug was observed top of shed 4 in the westward direction.

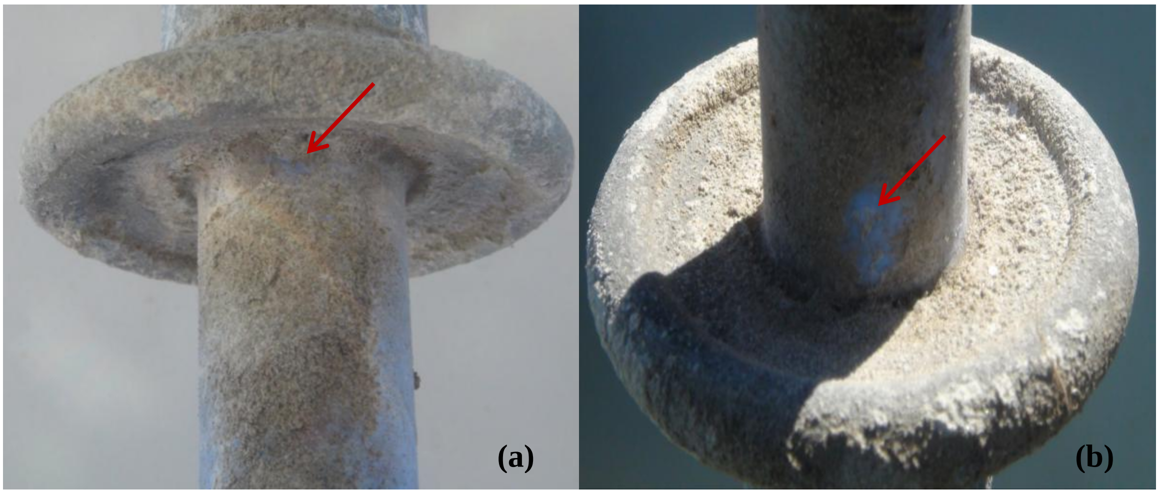

Figure E-66: Instances of material erosion observed on the sheaths interfacing with both the (a) ground and (b) live end-fittings (Week 11)

E.4.3.3 *HTV-SR 56 DC- (Week 10)*

- *Deterioration*: Traces of dryband activities were observed commonly on the shed bottoms and sheaths in all directions. Light crazing was observed, mainly prominent in dryband areas. The first instances of material erosion were observed on the sheath interfacing with the live end-fitting in the northward direction and also on the sheath interfacing with the ground end-fitting in the southward direction. The erosion on the sheath interfacing with the live end-fitting is depicted in Figure E-67. It can be seen from the figure that there seems to be some form of tracking around the eroded area.

Figure E-67: Material erosion observed on the sheath interfacing with the live end-fitting (Week 10)

- *Other observations:* Light pollution was generally observed over the entire insulator, with medium to heavy pollution on the shed tops and sheaths in the southward direction. Salt crystals were observed in the westward and northward directions. Dead insects were observed on the shed tops in the westward and northward directions. A sample of the dead insects observed on the shed tops is shown in Figure E-68. Plant threads were also observed.

Figure E-68: A dead insect observed on the shed top of HTV-SR 56 DC- (Week 10)

E.4.4 Test cycle 4

E.4.4.1 *HTV-SR 56 AC (Week 22)*

- *Deterioration*: Traces of dryband activities were observed in all directions. Light crazing was observed on the shed bottoms and sheaths in all directions. The following instances of material erosion were observed in the southward direction, as reported in week 13: on the sheaths interfacing with both the live and ground end-fittings, on sheaths 3 (middle section of insulator) & 4 (toward the ground end-fitting and sheath 2. Additional erosion was observed on the sheaths interfacing with both the live and ground end-fittings in the northward direction and also on the bottom of shed 3 in the southward direction. Figure E-69 shows a sample of erosion instances observed on the sheaths interfacing with both the live and ground end-fittings. The first instance of blue patches (some of form of discoloration) was observed on the top of sheds 2 & 3 in the eastward direction.

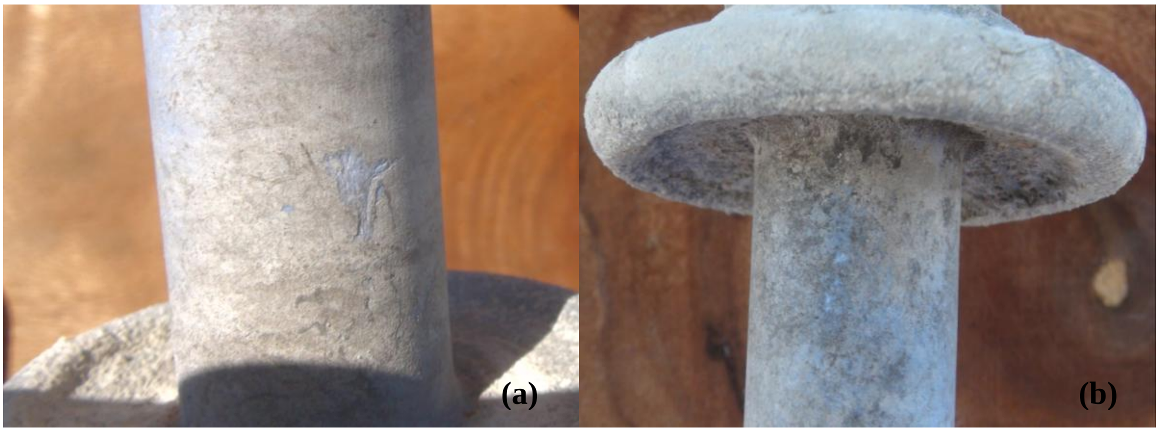

Figure E-69: Instances of material erosion on the sheaths interfacing with both the (a) live and (b) ground end-fittings (Week 22)

- *Other observations:* Light to medium pollution build-up was observed over the entire insulator. Salt crystals were observed in the westward direction. Plant threads were observed in the eastward and southward directions. Rust patches were observed on the top of sheds 2 & 4 in the southward direction.

E.4.4.2 *HTV-SR 56 DC+ (Week 18)*

- *Deterioration*: Traces of dryband activities were observed in all directions. Light crazing was observed on the shed bottoms and sheaths in all directions. Instances of material erosion were observed on the sheaths interfacing with both the live and ground end-fittings in the southward direction, as was reported for week 11. Additional erosion was now observed on the sheath interfacing with both the live (westward direction) and ground (westward and northward direction) end-fittings and also on sheath 4 (toward the ground end-fitting) in the westward and northward directions. Figure E-70 shows some of the instances of erosion that were observed on the sheath interfacing with both the live and ground end-fittings.

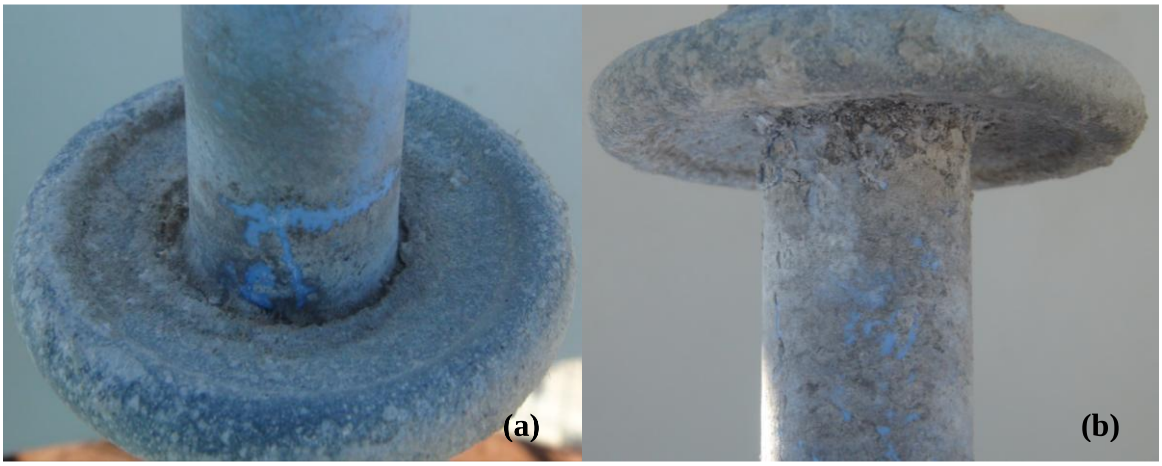

Figure E-70: Material erosion observed on the sheaths interfacing with both the (a) live and (b) ground end-fittings (Week 18)

- *Other observations:* Light pollution build-up was observed over the entire insulator in all directions. No salt crystals were observed. Plant threads were observed in all directions.

E.4.4.3 *HTV-SR 56 DC- (Week 16)*

- *Deterioration*: Traces of dryband activities were observed on most parts of the insulator. Light crazing was observed on the sheaths, especially around the dryband areas. The first instances of material erosion were still observable on the sheath interfacing with the live end-fitting in the northward direction and also on the sheath interfacing with the ground end-fitting in the southward direction, as reported for week 10. However, more instances of erosion were noticed on the sheath interfacing with the ground end-fitting in all directions, except in the eastward direction and also on sheath 3 (all directions except south) & sheath 4 (westward direction). A peel-off was observed at the bonding interface of a sheath and shed, and evidence of dryband activities was also visible. Figure E-71 illustrates the erosion that was observed on the sheath interfacing with the live end-fitting and the peel-off at the sheath-to-shed bonding interface. From Figure E-71 (a), it can be seen that no tracking was present around the eroded area as suspected during week 10. The first instance of blue patches (a form of discoloration) was observed in the westward direction. See Figure E-72.

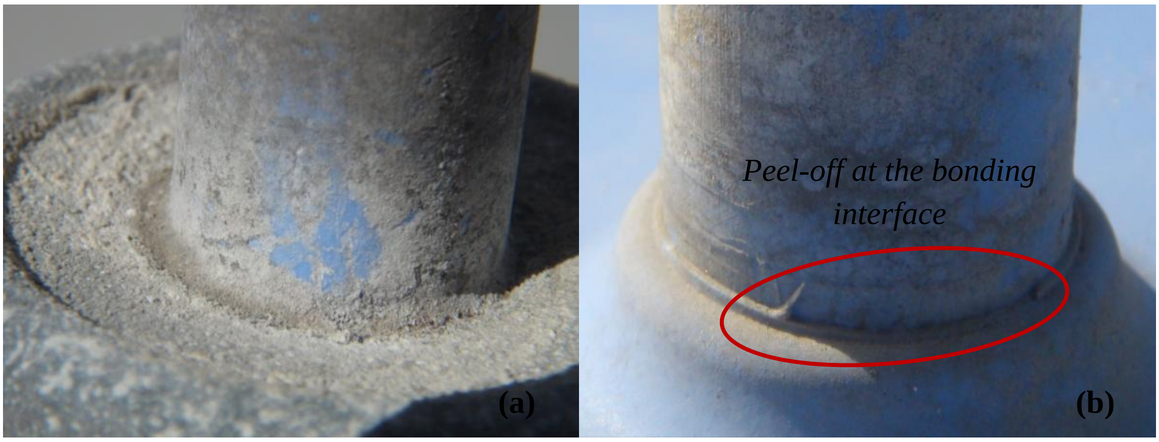

Figure E-71: (a) Material erosion on the sheath interfacing with the live end-fitting in the northward direction and (b) material peel-off at the sheath-to-shed bonding interface (Week 16)

Figure E-72: Blue patches (a form of discoloration) spotted on the shed top of HTV-SR 56 DC- (Week 16) *(please zoom in)*

- *Other observations:* Light pollution was observed over the entire insulator. Salt crystals were observed in the northward direction. Plant threads were observed in all directions. Dead bug was observed in the southward direction. See Figure E-73. Rust spots were observed on the sheath interfacing with the ground end-fitting in the northward direction.

Figure E-73: A dead insect on the shed top of HTV-SR 56 DC- (Week 16)

E.5 Surface conditions for high temperature vulcanized, silicone rubber insulators with a unified specific creepage length of 44 mm/kV – HTV-SR 44

E.5.1 Test cycle 1

E.5.1.1 *HTV-SR 44 AC (Week 5)*

- *Deterioration*: Traces of dryband activities were observed in all directions. The first instance of material erosion was observed on the sheath interfacing with the live end-fitting in the southward direction. This erosion is shown in Figure E-74. Dark burns were observed on pollution layer on the sheath interfacing with the ground end-fitting in the southward direction.

Figure E-74: The first sign of material erosion on the sheath interfacing with the live end-fitting in the southward direction (Week 5)

- *Other observations:* Light pollution build-up was observed over the entire insulator, with medium to heavy pollution on the shed tops and sheaths in the southward direction. Salt crystals were observed in all directions.

E.5.1.2 *HTV-SR 44 DC+ (Week 3)*

- *Deterioration*: Traces of dryband activities were observed on the shed bottoms and sheaths. No other signs of deterioration were observed.

- *Other observations:* Light pollution build-up was observed over the entire insulator, with medium to heavy pollution on the shed tops and sheaths in the southward direction. Salt crystals were observed in all directions.

E.5.1.3 *HTV-SR 44 DC- (Week 2)*

- *Deterioration*: No signs of deterioration were observed in week 2.

- *Other observations:* Pollution build-up was dominantly observed in the southward direction, with light pollution on the shed tops and bottoms and medium pollution on the sheaths. Salt crystals were generally observed in all directions, but most prominent in the westward direction.

E.5.2 Test cycle 2

E.5.2.1 *HTV-SR 44 AC (Week 9)*

- *Deterioration*: Traces of dryband activities were observed in all directions. Light crazing was generally observed on the sheaths in all directions. The first instance of material erosion was still observed on the sheath interfacing with the live end-fitting in the southward direction, as reported in week 2. Refer to Figure E-75.

Figure E-75: Erosion on the sheath interfacing with the live end-fitting in the southward direction (Week 9)

- *Other observations:* Light pollution build-up was observed over the entire insulator, with medium to heavy pollution on the shed tops and sheaths in the southward direction. Salt crystals were observed in all directions. Plant threads were observed in the eastward and southward directions.

E.5.2.2 *HTV-SR 44 DC+ (Week 8)*

- *Deterioration*: Traces of dryband activities were observed in all directions. Light crazing was observed on the shed bottoms and sheaths in all directions. The first signs of material erosion were observed on the sheath interfacing with the ground end-fitting in the southward direction and also on the sheath interfacing with the live end-fitting in the westward and southward directions.

- *Other observations:* Light pollution build-up was observed over the entire insulator, with medium to heavy pollution on the shed tops and sheaths in the southward direction. Salt crystals were observed in the northward and southward directions. No plant threads were observed.

E.5.2.3 *HTV-SR 44 DC- (Week 6)*

- *Deterioration*: Traces of dryband activities were observed. Light crazing was observed on the sheaths. No other signs of deterioration were observed.

- *Other observations:* The insulator was lightly polluted, with medium to heavy pollution on the shed tops and sheaths in the southward direction. Salt crystals were observed in the westward, northward and eastward directions, a sample of which is shown in Figure E-76.

Figure E-76: Salt crystals on the shed top of HTV-SR 44 DC- (Week 6)

E.5.3 Test cycle 3

E.5.3.1 *HTV-SR 44 AC (Week 13)*

- *Deterioration*: Traces of dryband activity were observed in all directions. Light crazing was observed in all directions. In addition to the first instance of material erosion that was observed on the sheath interfacing with the live end-fitting in the southward direction, an additional instance of erosion was now observed on sheath 2 in the southward direction. Both of these instances of erosion are shown in Figure E-77. It can been seen that the erosion on the sheath interfacing with the live end-fitting is now clearly visible compared to the inspections for week 9 (refer to Figure E-75) and it appears that the eroded area has increased in comparison to the first observations made in week 5 (refer to Figure E-74).

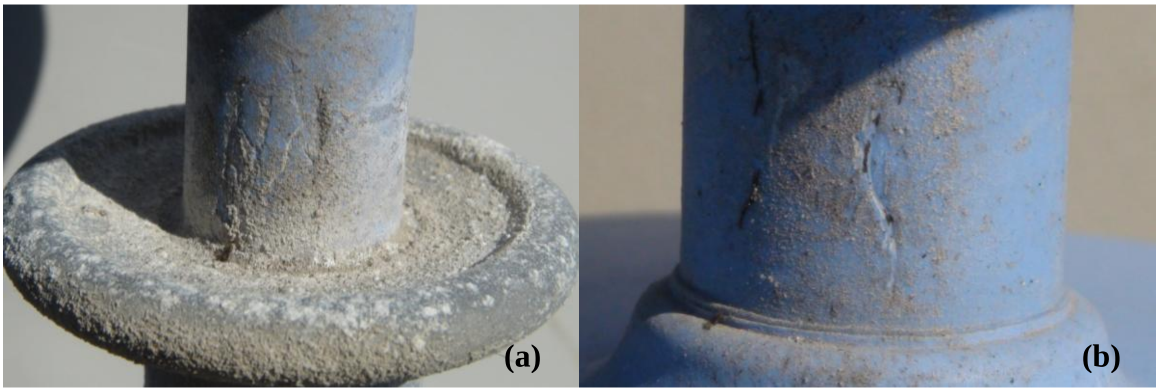

Figure E-77: Instances of material erosion (a) on the sheath interfacing with the live end-fitting and (b) on sheath 2 (Week 13)

- *Other observations:* Light to medium pollution build-up was observed over the entire insulator, with medium to heavy pollution on the shed tops and sheaths in the southward direction. Salt crystals were observed in the eastward and northward directions. Plant threads were observed in the westward and southward directions.

Dead insects were observed on the bottom of shed 1 and on sheath 1 in the northward direction.

E.5.3.2 *HTV-SR 44 DC+ (Week 11)*

- *Deterioration*: Traces of dryband activities were observed in all directions. Light crazing was observed on the shed bottoms and sheaths in all directions. Material erosion was observed on the sheath interfacing with the ground end-fitting in the southward direction and also on the sheath interfacing with the live end-fitting in the westward and southward directions, as previously reported for week 8. More instances of material erosion were now observed on the sheath interfacing with the live end-fitting in the northward direction (see Figure E-78).

Figure E-78: Material erosion on the sheath interfacing with the live end-fitting (Week 11)

- *Other observations:* Light pollution build-up was observed over the entire insulator, with medium to heavy pollution on the shed tops and sheaths in the southward direction. Salt crystals were observed in all directions. Plant threads were observed in all directions. A dead insect was observed on the top of shed 1 in the westward direction.

E.5.3.3 *HTV-SR 44 DC- (Week 10)*

- *Deterioration*: Traces of dryband activity were observed. Light crazing was generally observed on the sheaths. The first instances of material erosion were observed on the sheath interfacing with the ground end-fitting in the westward and northward directions. See Figure E-79.

Figure E-79: The first instance of material erosion on the sheath interfacing with the ground end-fitting (Week 10)

- *Other observations:* Light pollution was generally observed over the entire insulator, with medium to heavy pollution on the sheaths in the southward direction. Salt crystals were observed in all directions, except in the southward direction. Plant threads were observed in the eastward and southward directions.

E.5.4 Test cycle 4

E.5.4.1 *HTV-SR 44 AC (Week 22)*

- *Deterioration*: Traces of dryband activity were observed in all directions. Light crazing was observed on the sheaths in all directions. As previously reported for week 13, material erosion was still observed on the sheath interfacing with the live end-fitting and on sheath 2 in the southward direction. More erosion was now observed on the sheath interfacing with the ground end-fitting in the northward direction. All the instances of material erosion that were observed are shown below in Figure E-80. It can be seen in Figure E-80 (a) that there is now additional erosion just above the eroded area that was first observed in week 5.

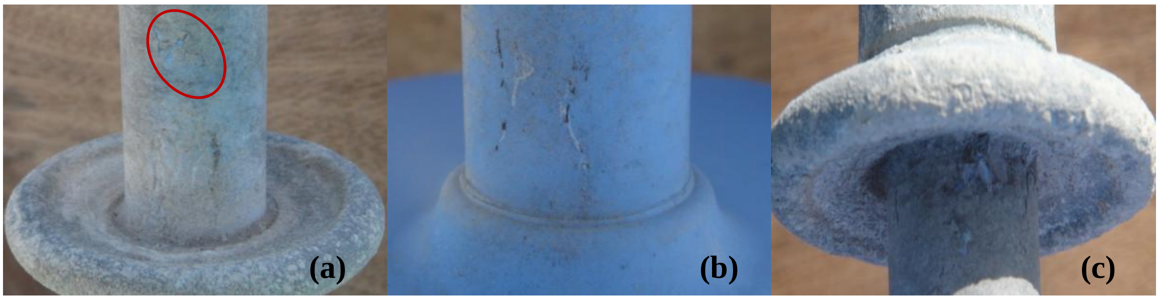

Figure E-80: Instances of material erosion observed (a) on the sheath interfacing with the live end-fitting, (b) on sheath 2 and (c) on the sheath interfacing with the ground end-fitting

- *Other observations:* Light to medium pollution build-up was observed over the entire insulator in all directions. Salt crystals were observed in the southward direction. Plant threads were observed in the westward and southward directions. Rust patches were observed on the top of shed 1 in the westward direction.

E.5.4.2 *HTV-SR 44 DC+ (Week 18)*

- *Deterioration*: Traces of dryband activities were observed in all directions. Light crazing was observed on the shed bottoms and sheaths in all directions. Material erosion was observed on the sheath interfacing with the ground end-fitting in the southward direction and also on the sheath interfacing with the live end-fitting in the westward, northward and southward directions, as previously reported for week 11. More instances of material erosion were now observed on the sheath interfacing with the ground end-fitting in the westward and northward directions and also on sheath 3 in the westward direction. The erosion on the sheaths interfacing with both the live and ground end-fittings is shown in Figure E-81. On a close look at Figure E-81 (a), it would appear as if there are some sign of tracking along the eroded area on the sheath interfacing with the live end-fitting, whereas in Figure E-81 (b) it appears as if tracking occurs at the bonding interface of the sheath and the end-fitting.

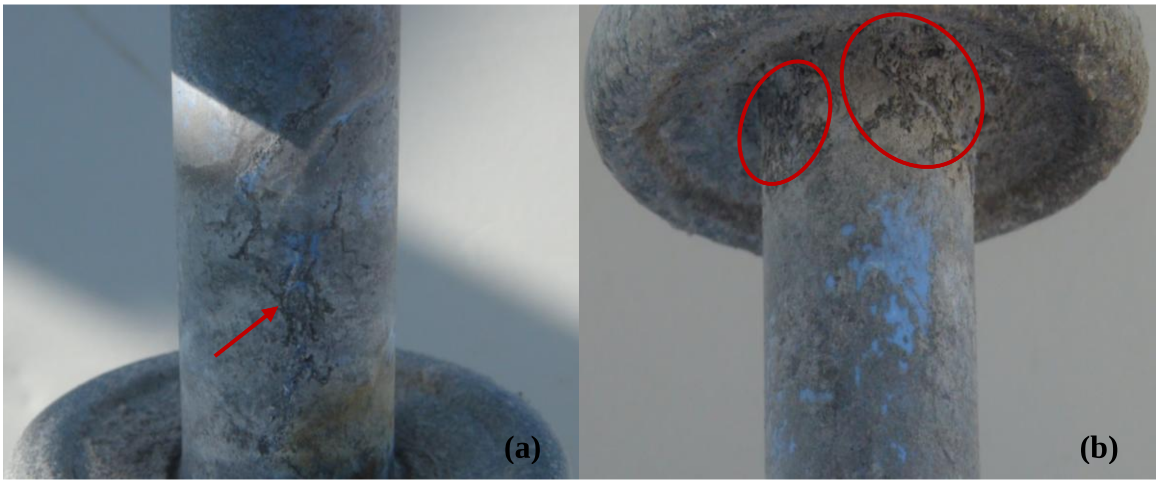

Figure E-81: Material erosion on the sheaths interfacing with both the (a) live and (b) ground end-fitting (Week 18)

- *Other observations:* Light pollution build-up was observed over the entire insulator in all directions. No salt crystals were observed. Plant threads were observed in all directions, except in the westward direction. Rust patches were observed on the sheath interfacing with the live end-fitting in the westward direction.

E.5.4.3 *HTV-SR 44 DC- (Week 16)*

- *Deterioration*: Traces of dryband activities were observed on most parts of the insulator. Light crazing was observed on the sheaths and especially on the dryband areas. Material erosion was observed on the sheath interfacing with the ground end-fitting in the westward and northward directions, as reported in week 10. More erosion was observed on the sheath interfacing with the ground end-fitting in the southward direction and also on sheath 3 in the westward, northward and eastward directions. The first instance of blue patches (a form of discoloration) was observed in the eastward direction. A peel-off was observed at the sheath-to-shed bonding interface of a sheath and shed and evidence of dryband activities was also visible, as it can be seen in Figure E-82.

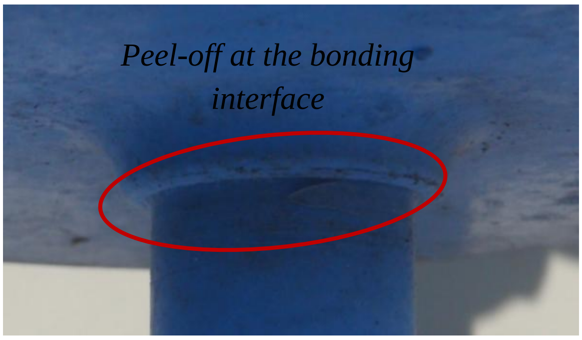

Figure E-82: Material peel-off at the sheath-to-shed bonding interface (week 16)

- *Other observations:* Light pollution was observed over the entire insulator. Salt crystals were observed in the northward direction. Plant threads were observed in all directions, except in the northward direction. A dead bug was observed in the eastward direction. Rust spots were observed on the top of shed 3 in the northward direction.

E.6 Surface conditions for high temperature vulcanized, silicone rubber insulators with a unified specific creepage length of 29 mm/kV – HTV-SR 29

E.6.1 Test cycle 1

E.6.1.1 *HTV-SR 29 AC (Week 5)*

- *Deterioration*: Traces of dryband activity were observed on the shed bottoms and sheaths. It was suspected that an intense dryband activity had occurred. This was due to the dark burns that were observed, as shown in Figure E-83. It was however not possible to confirm whether material erosion was present. Light crazing was observed on the shed bottoms and sheaths in all directions.

Figure E-83: Dark burns on pollution on the sheath interfacing with the live end-fitting (Week 5)

- *Other observations:* Light pollution build-up was observed over the entire insulator, with medium pollution on the shed tops and sheaths in the southward direction. Salt crystals were observed in all directions, except in the southward direction.

E.6.1.2 *HTV-SR 29 DC+ (Week 3)*

- *Deterioration*: Traces of dryband activities were observed on the shed bottoms and sheaths. Light crazing was observed in the westward and northward directions. No other signs of deterioration were observed.

- *Other observations:* Light pollution build-up was observed over the entire insulator, with medium to heavy pollution on the shed tops and sheaths in the southward direction. Salt crystals were observed in all directions.

E.6.1.3 *HTV-SR 29 DC- (Week 2)*

- *Deterioration*: No signs of deterioration were observed in week 2.

- *Other observations:* Light pollution build-up was observed in all directions, with medium pollution on the sheaths in the southward direction. Salt crystals were only observed in the westward direction.

E.6.2 Test cycle 2

E.6.2.1 *HTV-SR 29 AC (Week 9)*

- *Deterioration*: Traces of dryband activities were observed in all directions. Light crazing was observed on the shed bottoms and sheaths in all directions. The first instance of material erosion, as shown in Figure E-84, was observed on the sheath interfacing with the live end-fitting in the southward direction and this erosion occurred at exactly the same spot where dark burns were observed in week 5 (refer to Figure E-83).

Figure E-84: The first sign of material erosion on the sheath interfacing with the live end-fitting in the southward direction (Week 9)

- *Other observations:* Light pollution build-up was observed over the entire insulator, with medium to heavy pollution on the shed tops and sheaths in the southward direction. Salt crystals were observed in all directions. Plant threads were observed in all directions, except in the northward direction.

E.6.2.2 *HTV-SR 29 DC+ (Week 8)*

- *Deterioration*: Traces of dryband activities were observed in all directions. Light crazing was observed on the shed bottoms and sheaths in all directions. The first signs of material erosion were observed on the sheath interfacing with the ground end-fitting in all directions, except in the eastward direction and also on the sheath interfacing with the live end-fitting in the northward direction. Additionally, a sign of material erosion was observed on sheath 2 (middle section of the insulator) in the southward direction. The figure below shows the signs of erosion that were observed on the sheaths interfacing with both the live and ground end-fittings, Figure E-85 (a) and Figure E-85 (b) respectively.

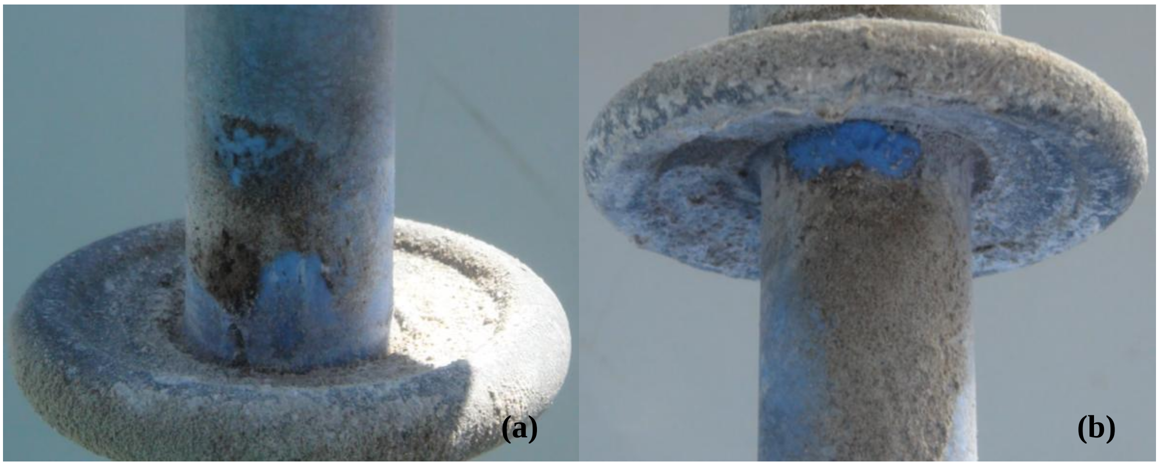

Figure E-85: The first signs of erosion on the sheaths interfacing with both the (a) live and (b) ground end-fittings in the southward direction (week 8)

- *Other observations:* Light pollution build-up was observed over the entire insulator, with medium to heavy pollution on the shed tops and sheaths in the southward direction. Salt crystals were observed in the westward and northward directions. No plant threads were observed.

E.6.2.3 *HTV-SR 29 DC- (Week 6)*

- *Deterioration*: Traces of dryband activities were mainly observed on the shed bottoms and sheaths. Light crazing was observed on sheaths. No other signs of deterioration were observed.

- *Other observations:* Light pollution was generally observed over the entire insulator, with medium pollution on the shed tops and sheaths in the southward direction. Salt crystals were observed around dryband areas, commonly on the shed bottoms.

E.6.3 Test cycle 3

E.6.3.1 *HTV-SR 29 AC (Week 13)*

- *Deterioration*: Traces of dryband activities were observed in all directions. Light crazing was observed on the shed bottoms and sheaths in all directions. As reported for week 9, material erosion was still observed on the sheath interfacing with the live end-fitting in the southward direction. See Figure E-86 below.

Figure E-86: Material erosion on the sheath interfacing with the live end-fitting (week 13)

- *Other observations:* Light to medium pollution build-up was observed over the entire insulator. Salt crystals were observed in the northward direction. Plant threads were observed in all directions.

E.6.3.2 *HTV-SR 29 DC+ (Week 11)*

- *Deterioration*: Traces of dryband activities were observed in all directions. Light crazing was observed on the shed bottoms and sheaths in all directions. As reported for week 8, the following signs of material erosion were still observed: on the sheath interfacing with the ground end-fitting in all directions, except in the eastward direction; on the sheath interfacing with the live end-fitting in the northward direction; on sheath 2 (middle section of the insulator) in the southward direction.

- *Other observations:* Light pollution build-up was observed over the entire insulator, with medium pollution on the shed tops and sheaths in the southward direction. Salt crystals were observed in all directions. Plant threads were observed in all directions, except in the southward direction. A dead insect was observed on the bottom of shed 2 in the westward direction. Rust deposits were observed on the sheath interfacing with the live end-fitting in the westward direction, as shown in Figure E-87.

Figure E-87: Rust deposit on the sheath interfacing with the live end-fitting in the westward direction (Week 11)

E.6.3.3 *HTV-SR 29 DC- (Week 10)*

- *Deterioration*: Traces of dryband activities were observed. Light crazing was observed on the sheaths and also the shed bottoms (closer to the ground side) in the southward direction. The first signs of material erosion were observed on the sheath interfacing with the ground end-fitting in the eastward and southward directions.

- *Other observations:* Light pollution was observed over the entire insulator, with medium to heavy pollution in the southward direction. Salt crystals were observed in all directions, except in the southward direction. Plant threads were observed in the eastward and southward directions. Rust patches were observed on the top of shed 2, possibly a wash off from the ground end-fitting.

E.6.4 Test cycle 4

E.6.4.1 *HTV-SR 29 AC (Week 22)*

- *Deterioration*: Traces of dryband activity were observed in all directions. Light crazing was observed in all directions. As reported for week 13, material erosion was still observed on the sheath interfacing with the live end-fitting in the southward direction. Additional erosion was however observed just above the eroded area that was previously recorded in week 13, as it can been seen in Figure E-88.

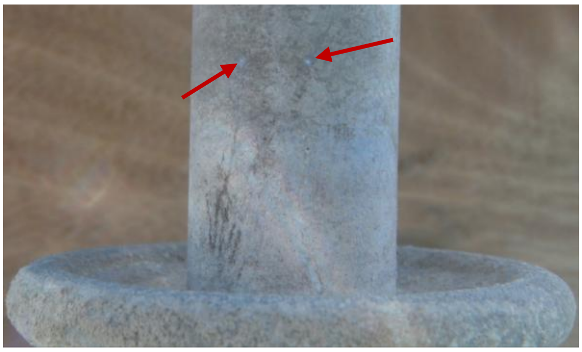

Figure E-88: Material erosion on the sheath interfacing with the live end-fitting (Week 22)

- *Other observations:* Light pollution build-up was observed over the entire insulator in all directions. Salt crystals were observed in the eastward direction. Plant threads were observed in all directions except north. Rust patches were observed on the top of shed 2 in the westward and southward directions.

E.6.4.2 *HTV-SR 29 DC+ (Week 18)*

- *Deterioration*: Traces of dryband activities were observed in all directions. Light crazing was observed in all directions, but none on the top of shed 1. As reported for week 11, the following signs of material erosion were still observed: on the sheath interfacing with the ground end-fitting in all directions, except in the eastward direction; on the sheath interfacing with the live end-fitting in the northward direction; on sheath 2 (middle section of the insulator) in the southward direction. No new signs of erosion were observed.

- *Other observations:* Light pollution build-up was observed over the entire insulator. No salt crystals were observed. No plant threads were observed. Rust patches were observed on the sheath interfacing with the live end-fitting in the westward direction, as previously reported for week 11. See Figure E-89.

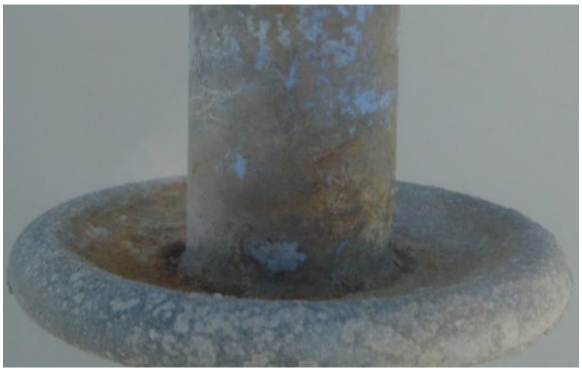

Figure E-89: Rust deposit on the sheath interfacing with the live end-fitting in the westward direction (Week 18)

E.6.4.3 *HTV-SR 29 DC- (Week 16)*

- *Deterioration*: Traces of dryband activities were observed on most parts of the insulator. Light crazing was observed on the sheaths, especially around the dryband areas. Light crazing was also observed on the bottom of shed 2 in the northward and southward directions. Signs of material erosion were still observed on the sheath interfacing with the ground end-fitting in the eastward and southward directions, as reported for week 10. This is depicted in Figure E-90.

Figure E-90: Material erosion on the sheath interfacing with the ground end-fitting (Week 16)

- *Other observations:* Light pollution was observed over the entire insulator. Rust spots were observed on the sheath interfacing with the ground end-fitting in the westward direction, as well as on top of the shed 2 in the northward direction.

E.7 Surface conditions for glass disc insulators with a unified specific creepage length of 42 mm/kV – Glass disc 42

E.7.1 Test cycle 1

E.7.1.1 *Glass disc 42 AC (Week 5)*

- *Deterioration*: No signs of deterioration were observed.

- *Other observations:* Light pollution was generally observed over the entire insulator, with medium pollution on the top and bottom of glass disc in the southward direction. Figure E-91 shows pollution conditions for both the top and bottom of glass disc. Salt crystals were observed on the bottom side of glass disc in the eastward and westward directions.

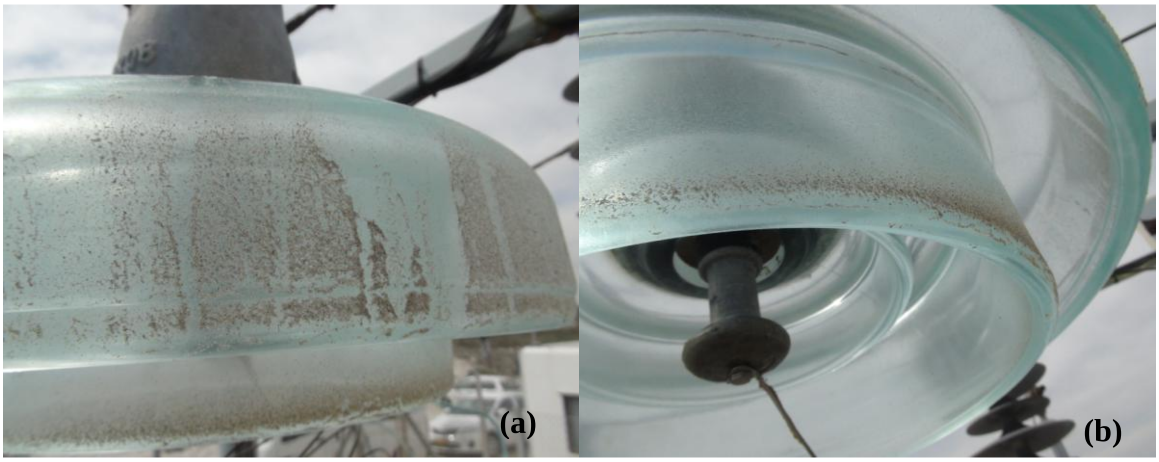

Figure E-91: Pollution conditions on the (a) top and (b) bottom of glass disc (Week 5)

E.7.1.2 *Glass disc 42 DC+ (Week 3)*

- *Deterioration*: No signs of deterioration were observed.

- *Other observations:* Light pollution was generally observed over the entire insulator, with medium pollution on the top of glass disc in the southward direction. See Figure E-92. Salt crystals were observed on the top of glass disc in all directions, except in the northward direction.

Figure E-92: Pollution conditions on the top of glass disc (Week 3)

E.7.1.3 *Glass disc 42 DC- (Week 2)*

- *Deterioration*: No signs of deterioration were observed.

- *Other observations:* Light pollution build-up was observed in all directions, with medium pollution on the sheaths in the southward direction. Salt crystals were only observed in the westward direction.

E.7.2 Test cycle 2

E.7.2.1 *Glass 42 AC (Week 9)*

- *Deterioration*: The first traces of dryband activities were observed on the bottom of glass disc in the southward direction. Figure E-93 shows the traces of dryband activity that were spotted on the bottom of glass disc. No other signs of deterioration were observed.

- *Other observations:* Light pollution was generally observed over the entire insulator, with medium pollution on the bottom of glass disc in the southward direction. Salt crystals were observed on the bottom of glass disc in all directions, except in the westward direction. A plant thread was observed on the bottom of glass disc in the southward direction.

Figure E-93: Traces of dryband activity on the bottom of glass disc (Week 9)

E.7.2.2 *Glass disc 42 DC+ (Week 8)*

- *Deterioration*: The first traces of dryband activities were observed on both bottom and top of glass disc in all directions. The first instance of material erosion was observed on the bottom of glass disc around the pin. See Figure E-94.

Figure E-94: Light material erosion on the bottom of glass disc around the pin (Week 8)

- *Other observations:* Light pollution was generally observed over the entire insulator, with medium pollution on the bottom of glass disc in the westward, northward and southward directions; whereas heavy pollution was observed on the top of glass disc in the southward direction. Salt crystals were observed on the top of glass disc in the westward direction. A plant thread was observed on the top of glass disc in the westward direction. Grease stain was observed on the top of glass disc in the southward direction.

E.7.2.3 *Glass disc 42 DC- (Week 6)*

- *Deterioration*: The first traces of dryband activities were observed on the bottom of glass disc, prominent around the pin. Material erosion was first observed on the bottom of glass disc around the pin, as can be seen in Figure E-95.

Figure E-95: The first instance of material erosion on the bottom of glass disc around the pin (Week 6)

- *Other observations:* The insulator was lightly polluted, with medium pollution observed on the top of glass disc in the southward direction. Salt crystals were observed on the innermost rim in the southward direction.

E.7.3 Test cycle 3

E.7.3.1 *Glass disc 42 AC (Week 13)*

- *Deterioration*: Traces of dryband activity were seen on the bottom side of glass disc around the pin (refer to Figure E-96) and also on the top of glass disc around the cap. No other signs of deterioration were observed. No material erosion was observed, as can be seen below in Figure E-96.

Figure E-96: Traces of dryband activity on the bottom of glass disc around the pin (Week 13)

- *Other observations:* Light pollution was observed over the entire insulator, with medium pollution on the bottom of glass disc in the southward direction. Salt crystals were observed on the bottom of glass disc in the northward and southward directions. Plant threads were observed on the bottom of glass in all directions, except in the southward. A dead insect was observed on the top of glass in the eastward direction.

E.7.3.2 *Glass disc 42 DC+ (Week 11)*

- *Deterioration*: Traces of dryband activity were observed on the bottom of glass disc around the pin. As reported for week 8, light material erosion was still observed on the bottom of glass disc around the pin. See Figure E-97.

Figure E-97: Material erosion on the bottom of glass disc around the pin (Week 11)

- *Other observations:* Light pollution was observed over the entire insulator, with heavy pollution on the bottom of glass disc in the northward and southward directions. No salt crystals were observed. Plant threads were observed on the bottom and top of glass disc in the northward direction and also on the top of glass disc in the westward direction. A dead insect was seen on the top of glass disc in the westward direction. Grease stains were observed on the top of glass disc in the westward direction.

E.7.3.3 *Glass disc 42 DC- (Week 10)*

- *Deterioration*: Traces of dryband activity were observed on the bottom of glass disc around the pin. Material erosion was still observed on the bottom of glass disc around the pin, as it can be seen in Figure E-98.

Figure E-98: Material erosion on the bottom of glass disc around the pin (Week 10)

- *Other observations:* Light pollution was observed over the entire insulator, with medium pollution in the southward direction. Salt crystals were observed on the bottom of glass disc (outermost rim) in the southward direction. Plant threads were observed on the bottom of glass disc in the westward and northward directions. Depicted in Figure E-99, a dead insect was observed on the top of glass disc in the northward direction.

Figure E-99: A dead insect on the top of glass disc (Week 10)

E.7.4 Test cycle 4

E.7.4.1 *Glass disc 42 AC (Week 22)*

- *Deterioration*: Traces of dryband activity were seen on the bottom of glass disc around the pin and also on the top of glass disc around the cap in all directions. No other signs of deterioration were observed. It is also evident from Figure E-100 that no sign of material erosion was observed on AC when compared to both DC+ (Figure E-101(b)) and DC- (Figure E-102 (b)).

Figure E-100: The bottom view of glass disc (Week 22)

- *Other observations:* Light pollution was observed over the entire glass disc, whereas medium pollution was observed on the bottom of glass disc in the southward direction. Salt crystals were observed on the top in the westward direction. Plant threads were observed on the bottom of glass disc in the southward direction. Some dark stains were observed on the inner rim of glass disc in the northward direction.

E.7.4.2 *Glass disc 42 DC+ (Week 18)*

- *Deterioration*: Traces of dryband activity were observed on the bottom of glass disc around the pin and also on the top of glass disc around cap in all directions. Material erosion was observed on the bottom of glass disc around the pin, as reported for week 11. The traces of dryband activities and material erosion are shown in Figure E-101.

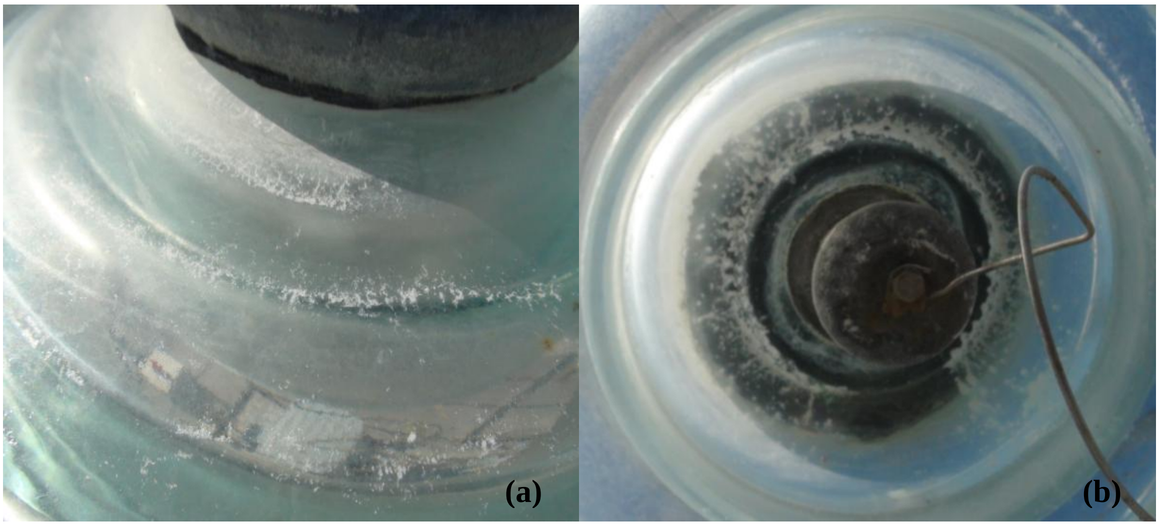

Figure E-101: (a) Traces of dryband activity on the top of glass disc around the cap and (b) the signs of dryband activity and material erosion on the bottom side around the pin (Week 18)

- *Other observations:* Light pollution was observed on the top of glass disc, whereas medium pollution was observed on the bottom of glass disc. Salt crystals were observed on the top of glass disc in the westward direction and also on the bottom of glass disc in southward direction. Plant threads were observed on the bottom and top of glass disc in all directions, except in the eastward direction.

E.7.4.3 *Glass disc 42 DC- (Week 16)*

- *Deterioration*: Traces of dryband activity were observed on the top of glass disc around the cap in all directions and also on the bottom of glass disc around pin in all directions. Material erosion was still observed on the bottom of glass disc around pin, as reported for week 10. The traces of dryband activity and material erosion are shown in Figure E-102. It should be mentioned that the erosion has worsened compared to the observations reported for week 10 (refer to Figure E-98).

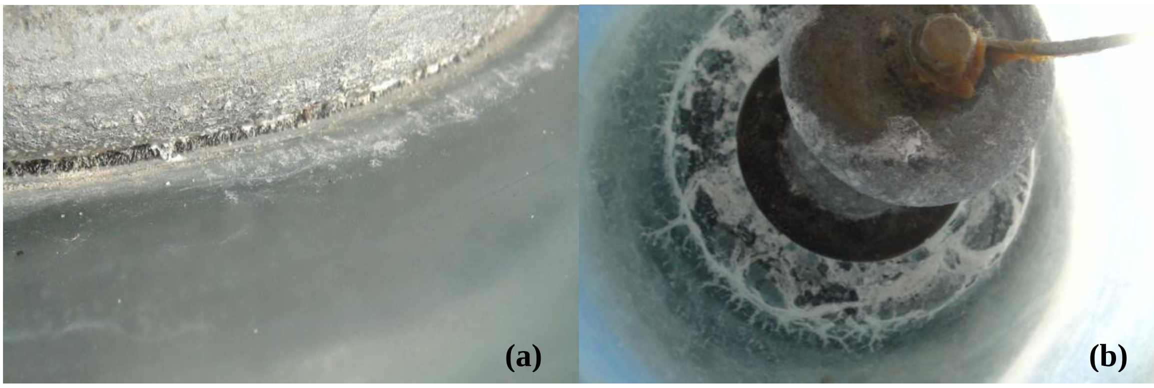

Figure E-102: (a) Traces of dryband activity on the top of glass disc around the cap and (b) the signs of dryband activity and material erosion on the bottom side around the pin (Week 16)

- *Other observations:* Light pollution was generally observed over the entire insulator, with medium pollution on the bottom of glass disc in the northward and southward directions. A plant thread was observed on the innermost rib in the northward direction.

F. APPENDIX F: Wettability (hydrophobicity) classifications for the respective high temperature vulcanized, silicone rubber (HTV-SR) insulators

F.1 Overview

This appendix presents the wettability classifications for all the HTV-SR insulators. These results were obtained from the wettability tests performed on the same timelines as those used for surface condition inspections (refer to Table E-48 in Appendix E.1). Details on the classification tests have been described in section 4.5 and the entire insulator sections that were considered are also illustrated in Figure 4-6 (see page 75). Please note that the results presented here do not include the classifications for the middle section of test insulators. Only the terminating sheaths and the sheds interfacing with the terminating sheaths are considered, detailing the results obtained from the sea and land sides.

F.2 Wettability classifications for high temperature vulcanized, silicone rubber insulators with a unified specific creepage length of 84 mm/kV – HTV-SR 84

F.2.1 Live-end insulator section

Table F-49: A summary of wettability classifications for HTV-SR 84, live-end section

Wettability (hydrophobicity) classification for HTV-SR 84: Live-end Section																			
		SEA SIDE									LAND SIDE								
		AC			DC+			DC-			AC			DC+			DC-		
Test cycle	Date	Shed top	Shed bottom	Sheath	Shed top	Shed bottom	Sheath	Shed top	Shed bottom	Sheath	Shed top	Shed bottom	Sheath	Shed top	Shed bottom	Sheath	Shed top	Shed bottom	Sheath
1	10-Feb							-	-	-							-	-	-
	21-Feb				6	4	7							6	4	3			
	3-Mar	7	3	6							5	3	3						
2	11-Mar							7	5	7							6	6	6
	24-Mar				7	4	7							7	7	7			
	5-Apr	7	4	7							7	5	5						
3	13-Apr							7	5	6							7	6	5
	19-Apr				7	6	7							7	7	6			
	4-May	7	4	4							7	5	4						
4	19-May							7	4	7							7	5	5
	7-Jun				7	5	6							7	6	5			
	6-Jul	7	5	4							7	6	4						

F.2.2 Ground-end insulator section

Table F-50: A summary of wettability classifications for HTV-SR 84, ground-end section

Wettability (hydrophobicity) classification for HTV-SR 84: Ground-end Section																			
		SEA SIDE									LAND SIDE								
		AC			DC+			DC-			AC			DC+			DC-		
Test cycle	Date	Shed top	Shed bottom	Sheath	Shed top	Shed bottom	Sheath	Shed top	Shed bottom	Sheath	Shed top	Shed bottom	Sheath	Shed top	Shed bottom	Sheath	Shed top	Shed bottom	Sheath
1	10-Feb							-	-	-							-	-	-
	21-Feb				7	4	6							7	4	3			
	3-Mar	5	4	5							6	4	3						
2	11-Mar							7	4	7							7	5	5
	24-Mar				6	5	7							6	7	4			
	5-Apr	7	3	7							7	5	3						
3	13-Apr							7	4	7							7	5	4
	19-Apr				7	5	7							7	6	6			
	4-May	7	4	7							7	7	7						
4	19-May							7	4	7							7	6	3
	7-Jun				7	5	7							7	6	6			
	6-Jul	7	6	7							7	7	4						

F.3 Wettability classifications for high temperature vulcanized, silicone rubber insulators with a unified specific creepage length of 72 mm/kV –HTV-SR 72

F.3.1 Live-end insulator section

Table F-51: A summary of wettability classifications for HTV-SR 72, live-end section

Wettability (hydrophobicity) classification for HTV-SR 72: Live-end Section																			
Test cycle	Date	SEA SIDE									LAND SIDE								
		AC			DC+			DC-			AC			DC+			DC-		
		Shed top	Shed bottom	Sheath	Shed top	Shed bottom	Sheath	Shed top	Shed bottom	Sheath	Shed top	Shed bottom	Sheath	Shed top	Shed bottom	Sheath	Shed top	Shed bottom	Sheath
1	10-Feb							3	2	6							4	2	3
	21-Feb				6	4	6							6	4	3			
	3-Mar	6	4	6							6	3	3						
2	11-Mar							5	5	7							6	6	6
	24-Mar				7	5	6							7	6	5			
	5-Apr	7	4	7							7	4	4						
3	13-Apr							7	6	7							7	6	6
	19-Apr				7	7	7							7	7	7			
	4-May	7	4	7							7	6	4						
4	19-May							7	6	7							7	6	5
	7-Jun				7	6	4							7	6	5			
	6-Jul	7	5	4							7	7	4						

F.3.2 Ground-end insulator section

Table F-52: A summary of wettability classifications for HTV-SR 72, ground-end section

Wettability (hydrophobicity) classification for HTV-SR 72: Ground-end Section																			
Test cycle	Date	SEA SIDE									LAND SIDE								
		AC			DC+			DC-			AC			DC+			DC-		
		Shed top	Shed bottom	Sheath	Shed top	Shed bottom	Sheath	Shed top	Shed bottom	Sheath	Shed top	Shed bottom	Sheath	Shed top	Shed bottom	Sheath	Shed top	Shed bottom	Sheath
1	10-Feb							3	2	4							3	2	2
	21-Feb				6	4	5							6	6	3			
	3-Mar	6	3	5							6	3	3						
2	11-Mar							6	5	5							6	6	5
	24-Mar				7	6	7							7	5	5			
	5-Apr	6	4	7							7	5	3						
3	13-Apr							7	4	7							7	5	6
	19-Apr				7	5	7							7	6	5			
	4-May	7	4	6							7	6	5						
4	19-May							7	4	7							7	7	4
	7-Jun				7	6	7							7	6	7			
	6-Jul	7	6	4							7	7	4						

F.4 Wettability classifications for high temperature vulcanized, silicone rubber insulators with a unified specific creepage length of 56 mm/kV –HTV-SR 56

F.4.1 Live-end insulator section

Table F-53: A summary of wettability classifications for HTV-SR 56, live-end section

Hydrophobicity classification for HTV-SR 56: Live-end Section																			
Test cycle	Date	SEA SIDE									LAND SIDE								
		AC			DC+			DC-			AC			DC+			DC-		
		Shed top	Shed bottom	Sheath	Shed top	Shed bottom	Sheath	Shed top	Shed bottom	Sheath	Shed top	Shed bottom	Sheath	Shed top	Shed bottom	Sheath	Shed top	Shed bottom	Sheath
1	10-Feb							4	2	7							4	2	2
	21-Feb				6	3	7							5	5	4			
	3-Mar	6	3	6							6	2	2						
2	11-Mar							7	5	7							7	5	5
	24-Mar				6	7	7							6	7	7			
	5-Apr	6	4	7							7	4	4						
3	13-Apr							7	5	6							7	6	7
	19-Apr				7	7	7							7	6	7			
	4-May	7	5	7							7	5	4						
4	19-May							7	4	7							7	5	7
	7-Jun				7	6	6							7	7	6			
	6-Jul	7	5	7							7	6	4						

F.4.2 Ground-end insulator section

Table F-54: A summary of wettability classifications for HTV-SR 56, ground-end section

Hydrophobicity classification for HTV-SR 56: Ground-end Section																			
Test cycle	Date	SEA SIDE									LAND SIDE								
		AC			DC+			DC-			AC			DC+			DC-		
		Shed top	Shed bottom	Sheath	Shed top	Shed bottom	Sheath	Shed top	Shed bottom	Sheath	Shed top	Shed bottom	Sheath	Shed top	Shed bottom	Sheath	Shed top	Shed bottom	Sheath
1	10-Feb							4	7	2							4	2	2
	21-Feb				6	3	6							5	4	3			
	3-Mar	6	3	5							7	3	4						
2	11-Mar							7	4	4							7	5	4
	24-Mar				7	7	7							7	6	6			
	5-Apr	7	4	7							5	5	3						
3	13-Apr							7	4	7							7	6	7
	19-Apr				7	6	6							7	6	6			
	4-May	7	3	7							7	6	4						
4	19-May							7	4	7							7	5	6
	7-Jun				7	6	7							7	6	7			
	6-Jul	7	6	6							7	6	4						

F.5 Wettability classifications for high temperature vulcanized, silicone rubber insulators with a unified specific creepage length of 44 mm/kV –HTV-SR 44

F.5.1 Live-end insulator section

Table F-55: A summary of wettability classifications for HTV-SR 44, live-end section

Hydrophobicity classification for HTV-SR 44: Live-end Section																			
Test cycle	Date	SEA SIDE									LAND SIDE								
		AC			DC+			DC-			AC			DC+			DC-		
		Shed top	Shed bottom	Sheath	Shed top	Shed bottom	Sheath	Shed top	Shed bottom	Sheath	Shed top	Shed bottom	Sheath	Shed top	Shed bottom	Sheath	Shed top	Shed bottom	Sheath
1	10-Feb							4	2	5							4	3	3
	21-Feb				6	3	7							6	4	3			
	3-Mar	6	3	4							6	4	3						
2	11-Mar							7	4	7							7	5	6
	24-Mar				6	6	5							7	6	5			
	5-Apr	7	4	7							7	5	4						
3	13-Apr							7	5	7							7	5	6
	19-Apr				6	6	7							7	7	6			
	4-May	7	5	6							7	6	6						
4	19-May							7	6	7							7	6	7
	7-Jun				7	7	7							7	6	7			
	6-Jul	6	6	5							7	7	5						

F.5.2 Ground-end insulator section

Table F-56: A summary of wettability classifications for HTV-SR 44, ground-end section

Hydrophobicity classification for HTV-SR 44: Ground-end Section																			
Test cycle	Date	SEA SIDE									LAND SIDE								
		AC			DC+			DC-			AC			DC+			DC-		
		Shed top	Shed bottom	Sheath	Shed top	Shed bottom	Sheath	Shed top	Shed bottom	Sheath	Shed top	Shed bottom	Sheath	Shed top	Shed bottom	Sheath	Shed top	Shed bottom	Sheath
1	10-Feb							4	2	7							4	2	2
	21-Feb				6	4	6							6	6	3			
	3-Mar	6	3	7							5	4	4						
2	11-Mar							7	4	7							7	6	5
	24-Mar				7	6	5							6	6	5			
	5-Apr	7	3	7							5	5	3						
3	13-Apr							7	4	7							7	5	6
	19-Apr				7	6	6							7	7	7			
	4-May	7	4	6							7	7	5						
4	19-May							7	4	7							7	6	7
	7-Jun				7	7	7							7	7	7			
	6-Jul	7	6	7							7	7	4						

F.6 Wettability classifications for high temperature vulcanized, silicone rubber insulators with a unified specific creepage length of 29 mm/kV –HTV-SR 29

F.6.1 Live-end insulator section

Table F-57: A summary of wettability classifications for HTV-SR 29, live-end section

Hydrophobicity classification for HTV-SR 29: Live-end Section																			
Test cycle	Date	SEA SIDE									LAND SIDE								
		AC			DC+			DC-			AC			DC+			DC-		
		Shed top	Shed bottom	Sheath	Shed top	Shed bottom	Sheath	Shed top	Shed bottom	Sheath	Shed top	Shed bottom	Sheath	Shed top	Shed bottom	Sheath	Shed top	Shed bottom	Sheath
1	10-Feb							6	2	7							6	3	3
	21-Feb				3	4	7							5	4	7			
	3-Mar	6	4	5							6	4	3						
2	11-Mar							6	5	7							5	5	6
	24-Mar				6	6	7							7	6	6			
	5-Apr	7	4	7							7	5	4						
3	13-Apr							6	6	7							7	7	7
	19-Apr				6	6	7							7	7	7			
	4-May	7	5	7							7	5	6						
4	19-May							7	7	7							7	7	7
	7-Jun				6	6	6							7	6	7			
	6-Jul	5	6	7							7	7	5						

F.6.2 Ground-end insulator section

Table F-58: A summary of wettability classifications for HTV-SR 29, ground-end section

Hydrophobicity classification for HTV-SR 29: Ground-end Section																			
Test cycle	Date	SEA SIDE									LAND SIDE								
		AC			DC+			DC-			AC			DC+			DC-		
		Shed top	Shed bottom	Sheath	Shed top	Shed bottom	Sheath	Shed top	Shed bottom	Sheath	Shed top	Shed bottom	Sheath	Shed top	Shed bottom	Sheath	Shed top	Shed bottom	Sheath
1	10-Feb							4	2	7							3	2	2
	21-Feb				7	5	7							4	4	3			
	3-Mar	5	4	7							5	4	4						
2	11-Mar							6	5	7							5	5	7
	24-Mar				7	7	7							7	7	6			
	5-Apr	7	4	6							7	3	5						
3	13-Apr							7	6	7							7	6	6
	19-Apr				7	6	6							7	7	6			
	4-May	6	5	7							7	6	5						
4	19-May							7	6	7							7	6	7
	7-Jun				7	6	7							7	6	7			
	6-Jul	6	7	6							7	7	4						